Modulation of antigen-specific CD8 T cell responses by the skin commensal *Staphylococcus epidermidis*

DISSERTATION ZUR ERLANGUNG DES

DOKTORGRADES DER NATURWISSENSCHAFTEN (DR. RER. NAT.)

DER FAKULTÄT FÜR BIOLOGIE UND VORKLINISCHE MEDIZIN

DER UNIVERSITÄT REGENSBURG

vorgelegt von

Benedikt Franz Ludwig Nerb

aus

Regensburg

im Jahr

2024

Das Promotionsgesuch wurde eingereicht am:

Die Arbeit wurde angeleitet von:

Prof. Dr. Uwe Ritter und Prof. Dr. Markus Feuerer

Unterschrift:

Table of contents

Abstract

As the outermost barrier of the body, the skin protects us from harmful environmental influences, microorganisms and dehydration. The skin is colonised by countless microorganisms such as viruses, fungi and bacteria, which form the so-called skin microbiome. The immune system of the skin and the microbiome are in constant interaction with each other. Maintaining skin homeostasis requires a finely balanced immune system to prevent the spread of pathogens while simultaneously tolerating harmless commensals to avoid chronic immune responses. The bacterium *Staphylococcus epidermidis (S. epidermidis)* is one of the most frequently isolated representatives of the human skin microbiome. *S. epidermidis* is usually considered a commensal, but can also cause serious infections under certain circumstances. Interestingly, hardly any immune response is induced during these infections.

This thesis therefore investigated how and whether *S. epidermidis* can regulate immune responses. In particular, an antigen-specific immune response involving CD8 T cells and antigen-presenting cells was investigated, as these cells make up a large proportion of the immune cells of the epidermis and are essential for an early control of infections. Bone marrow-derived dendritic cells (BMDCs) and OT-I CD8 T cells were used in a co-culture system. The presentation of the processed ovalbumin (OVA) protein by BMDCs triggers antigen-specific proliferation of the OT-I CD8 T cells. By adding *S. epidermidis* to the co-cultures, its effect on the activation and proliferation of OT-I CD8 T cells was investigated. *S. epidermidis* suppressed the proliferation of antigen-specific OT-I CD8 T cells. This suppression was dependent on the concentration of contacting bacteria. We could show that interferon γ (IFNγ) and nitric oxide (NO) were the critical molecules in this regulatory mechanism. Our data suggest that the OT-I CD8 T cells directly recognise *S. epidermidis* via pattern recognition receptors (PRRs). This activation together with the OVA antigen-specific activation through the T cell receptor (TCR) induced an early release of IFNγ by the memory fraction of OT-I CD8 T cells within hours. In addition, by the use of $IFN\gamma^{-/-}$ and $IFN\gamma R^{-/-}$ BMDCs in co-cultures, BMDCs could be excluded as source of IFNγ and identified as the target of IFNγ. The early IFNγ in turn induced the release of NO by BMDCs, which ultimately suppressed the proliferation of the entire OT-I CD8 T cell pool, including the naive fraction. The critical role of NO in the suppression of OT-I CD8 T cells was validated by co-culture experiments with $iNOS^{-/-}$ BMDCs. Interestingly, this mechanism seems to be triggered by the direct recognition of *S. epidermidis* by memory CD8 T cells. RNA analyses of proliferating and resting OT-I CD8 T cells were used to assess the possible expression of PRRs and to characterise the transcriptome of the suppressed OT-I CD8 T cells.

The here described suppressive mechanism could play a role in maintaining skin homeostasis by the immune system, but could also be involved in immune evasion of *S. epidermidis* due to the suppression of CD8 T cells.

Zusammenfassung

Als äußerste Barriere unseres Körpers schützt uns die Haut vor schädlichen Umwelteinflüssen, Mikroorganismen und Austrocknung. Die Haut wird von unzähligen Mikroorganismen wie Viren, Pilzen und Bakterien besiedelt, die das sogenannte Hautmikrobiom bilden. Das Immunsystem der Haut und das Mikrobiom stehen in ständiger Interaktion miteinander. Die Aufrechterhaltung der Hauthomöostase erfordert dabei ein fein balanciertes Immunsystem um die Ausbreitung von Pathogenen zu verhindern, während Kommensalen toleriert werden müssen um chronische Immunreaktionen zu vermeiden. Das Bakterium *Staphylococcus epidermidis* (*S. epidermidis*) ist einer der am häufigsten isolierten Vertreter des menschlichen Hautmikrobioms. Normalerweise wird *S. epidermidis* als Kommensale eingeordnet, kann aber unter bestimmten Umständen auch schwere Infektionen verursachen. Interessanterweise wird bei diesen Infektionen kaum eine Immunreaktion ausgelöst.

In dieser Arbeit wurde daher untersucht, wie und ob *S. epidermidis* Immunantworten regulieren kann. Insbesondere wurde eine antigenspezifische Immunantwort unter Beteiligung von CD8-T-Zellen und antigenpräsentierenden Zellen untersucht, da diese Zellen einen Großteil der epidermalen Immunzellen ausmachen und für eine frühe Kontrolle von Infektionen essentiell sind. Dendritische Zellen aus Knochenmark (BMDCs) und OT-I CD8 T-Zellen wurden in einem Kokultur-System verwendet. Die Präsentation des prozessierten Ovalbumin (OVA)-Proteins durch BMDCs löst die antigenspezifische Proliferation der OT-I CD8 T-Zellen aus. Durch Zugabe von *S. epidermidis* zu den Kokulturen wurde dessen Wirkung auf die Aktivierung und Proliferation von OT-I CD8 T-Zellen untersucht. *S. epidermidis* unterdrückte die Proliferation von antigenspezifischen OT-I CD8 T-Zellen. Diese Suppression war abhängig von der Konzentration der kontaktierenden Bakterien. Wir konnten zeigen, dass Interferon γ (IFNγ) und Stickstoffmonoxid (NO) die entscheidenden Moleküle in diesem Regulationsmechanismus sind. Unsere Daten deuten darauf hin, dass OT-I CD8 T-Zellen *S. epidermidis* direkt über Mustererkennungsrezeptoren (PRRs) erkennen. Diese Aktivierung führte zusammen mit der OVA antigenspezifischen Aktivierung über den T-Zell-Rezeptor innerhalb von Stunden zu einer frühen Freisetzung von IFNγ durch die Fraktion der OT-I CD8 T-Gedächtniszellen. Durch die Verwendung von IFNγ$^{-/-}$ und IFNγR$^{-/-}$ BMDCs in den Kokulturen konnten BMDCs als Quelle von IFNγ ausgeschlossen und als Ziel von IFNγ identifiziert werden. Das frühe IFNγ wiederum induzierte die Freisetzung von NO durch BMDCs, was letztlich die Proliferation des gesamten OT-I CD8 T-Zell Pools, einschließlich der naiven Fraktion, unterdrückte. Die entscheidende Rolle von NO bei der Unterdrückung von OT-I CD8 T-Zellen wurde durch Kokultur-Experimente mit iNOS$^{-/-}$ BMDCs bestätigt. Interessanterweise scheint dieser Mechanismus durch die direkte Erkennung von *S. epidermidis* durch CD8 T-Gedächtniszellen ausgelöst zu werden. RNA-Analysen von proliferierenden und nicht-proliferierenden OT-I CD8 T-Zellen wurden verwendet,

um die mögliche Expression von PRRs zu bewerten und das Transkriptom der unterdrückten OT-I CD8 T-Zellen zu charakterisieren.

Der hier beschriebene Mechanismus könnte eine Rolle bei der Aufrechterhaltung der Homöostase der Haut durch das Immunsystem spielen, könnte aber auch in der Immunevasion von *S. epidermidis* durch die Unterdrückung von CD8-T-Zellen beteiligt sein.

1 Introduction

1.1 The skin: protective barrier to the environment and home to the skin microbiome

The human skin is the largest organ of the body and the outermost protective barrier towards the environment. Adding up the flat surface of the skin and its appendage infoldings such as hair follicles and sebaceous glands, results in an area of approximately 25 - 30 m^2 (Gallo 2017; Nakatsuji et al. 2013; Sfriso et al. 2020). The skin consists of three specialised layers with distinct characteristics to maintain health and to protect the host from the environment and pathogens. These are the epidermis, dermis and the hypodermis or subcutaneous adipose tissue (Mohamed and Hargest 2022). The epidermis can be further subdivided into the stratum corneum, stratum granulosum, stratum spinosum and stratum basale (Smythe and Wilkinson 2023). Important tasks of the epidermis are the prevention of water loss and physical protection against damaging environmental influences (Baroni et al. 2012). Collagen and elastin fibres, which form an extracellular matrix, comprise the vast majority of dermal tissue. The dermal compartment contains blood and lymph vessels, sensory nerves, sweat and sebaceous glands, hair follicles and various types of immune cells. Therefore, the dermis contributes to thermoregulation, elasticity, perception and immune regulation. Fat cells are the main cell type in the hypodermis, which is involved in thermoregulation and serves as an energy reservoir. Moreover, the hypodermis harbours immune cells (Alliliche et al. 2023; Rutter 2000; Mohamed and Hargest 2022; Kabashima et al. 2019). The three main layers of the skin fulfil different tasks to ensure the skin's barrier functions. These barriers are categorised according to their function as microbiome, chemical, physical and immune barriers (Eyerich et al. 2018). An overview of the skin layers and barriers and the localization of the microbiome and selected cells is shown in Figure 1.

1.1.1 The immune barrier

From the inside of the body, protection begins with the immune barrier, which extends from the hypodermis through the dermis to parts of the epidermis (Eyerich et al. 2018; Kabashima et al. 2019). The skin therefore represents an important immunological interface in which both innate and adaptive immunity take place to maintain homeostasis (Sfriso et al. 2020; Eyerich et al. 2018). In addition to the main cell type, the keratinocytes, the epidermis also contains immune cells. These include specialised antigen-presenting cells (APC) of the skin, the Langerhans cells (LCs), but also T cells such as γδ T cells, CD8+ resident memory T cells (T_{RM}) and CD4+ T helper cells (T_H) (Kabashima et al. 2019; Nestle et al. 2009). Due to the expression of pattern recognition receptors (PRRs), keratinocytes are part of the innate immunity of the skin. After antigen

encounter, they express cytokines of the tumor necrosis factor (TNF) and interleukin-(IL)-1 family or chemokines and thereby contribute to immune cell recruitment (Lebre et al. 2007; Kabashima et al. 2019). Keratinocytes produce antimicrobial peptides (AMPs), which are an evolutionary conserved cell defence mechanism and an early defence that bacteria and viruses encounter after entering the body. They act under homeostatic as well as inflammatory conditions and can directly eliminate microorganisms or inhibit their growth (Nestle et al. 2009; Belkaid and Segre 2014). CD4+ and CD8+ skin-resident T_{RM} cells are located around hair follicles and are responsible together with dendritic cells (DCs) for a secondary immune response. Moreover, CD4+ regulatory T cells (T_{reg}) that are important in the regulation of immune responses can be found in the epidermis. Various immune cell types such as DCs, macrophages, mast cells, γδ T cells and innate lymphoid cells (ILCs) reside in the dermis. Mainly T cells, B cells and macrophages reside in the hypodermis (Kabashima et al. 2019).

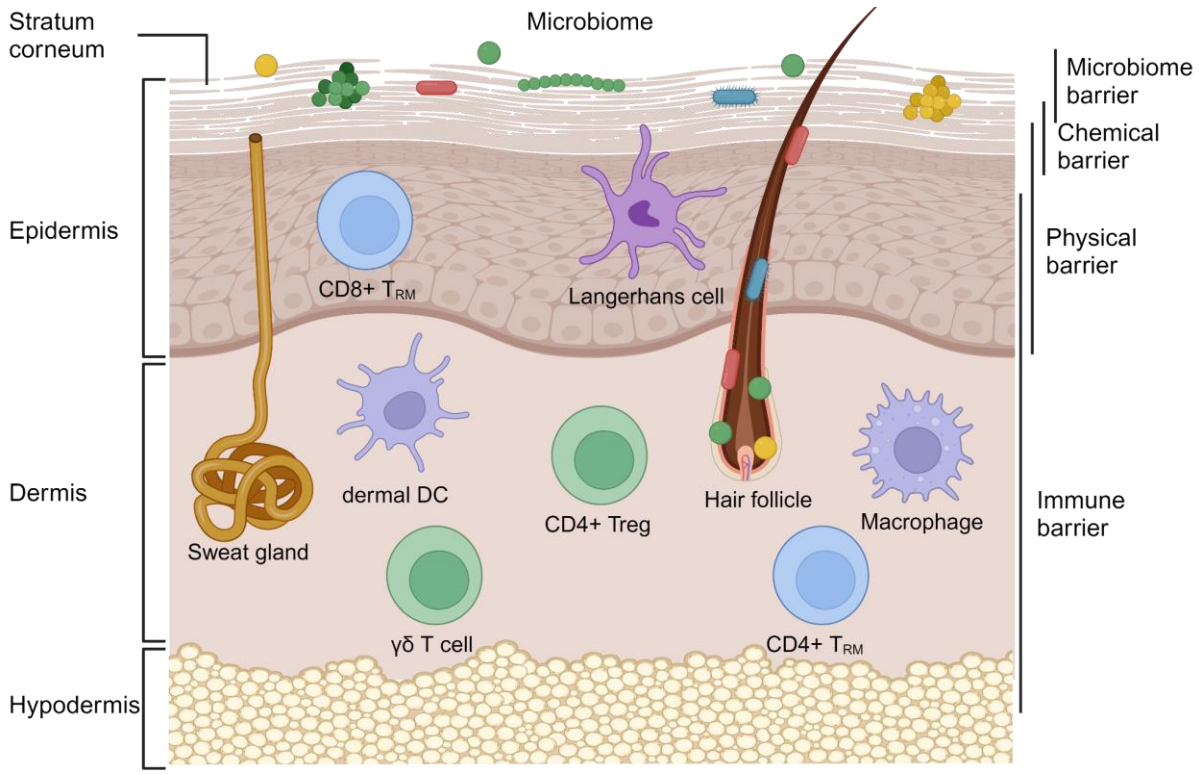

Figure 1: Structure, barriers and immune cells of the skin.

Schematic illustration of the main skin layers and the associated microbiome, chemical, physical and immune barriers. The localization of selected immune cells is assigned to the respective skin layers. Langerhans cells and CD8+ T_{RM} cells reside in the epidermis, whereas dermal DCs, CD4+ T_{RM} cells, CD4 T_{reg} cells, γδ T cells and macrophages are located in the dermis. The colonization of the stratum corneum and hair follicles by the microbiome is shown. Created with BioRender.com and adapted according to Eyerich et al. 2018 and C. Zhang et al. 2022.

1.1.2 The physical barrier

The physical barrier encompasses the epidermis with the stratum corneum and the connection of cells by tight junctions. Corneocytes, which are terminally differentiated keratinocytes that moved from the epidermis, build the stratum corneum. Directly underneath lies the stratum granulosum, which is composed of keratinocytes that are closely connected via tight junctions. This forms an efficient barrier to keep harmful stressors and pathogens out and avoids water loss by preventing the ingress and egress of water and water-soluble substances (Eyerich et al. 2018; Matsui and Amagai 2015; Egawa and Kabashima 2016; Kabashima et al. 2019).

1.1.3 The chemical barrier

Next, the skin provides a chemical barrier, which overlaps with the physical barrier. The chemical barrier consists of compounds that keep the moisture and of epidermal lipids and fatty acids that contribute to the acidic pH of the skin surface (Eyerich et al. 2018). Keratinocytes in the stratum corneum supports the acidic pH and its preservation by the expression of lipids and acids (Coates et al. 2019; H. J. Lee and Kim 2022). Due to free fatty acids, a low pH thereby inhibits the growth of pathogens, but not commensals. As one example, sapienic acid inhibits the colonization and growth of *Staphylococcus aureus* (*S. aureus*) but not the growth of commensals such as *S. epidermidis* and *Corynebacterium* (Coates et al. 2019; Moran, Alorabi, and Horsburgh 2017; H. J. Lee and Kim 2022).

1.1.4 The microbiome barrier

The real outermost layer on top of the physical and chemical barrier of the skin is the microbiome barrier, which completes and closes off the protective wall (Eyerich et al. 2018). The skin microbiome with its diverse microbiota is closely related with the other barriers and the included non-immune and immune cells (H. J. Lee and Kim 2022; Sanford and Gallo 2013). Consequently, the immune barrier gets in contact with the microbiome barrier and faces commensals as well as pathogens. However, a difficult task of the skin's immune system is to maintain a balance between protecting the body against pathogens and coexisting with skin commensals (Belkaid and Tamoutounour 2016).

The skin microbiome consists of bacteria but also of fungi, viruses and archaea (Grice et al. 2009; Erin Chen, Fischbach, and Belkaid 2018). As the outermost layer of the skin, the stratum corneum is colonised by the microbiome, but also the skin appendages up to the dermis and hypodermis harbour microbes (Lunjani et al. 2021; Dréno et al. 2016). In numbers, 10^4 to 10^6 bacteria per cm^2 of skin colonise our body. *Actinobacteria, Firmicutes, Proteobacteria and Bacteroidetes* dominate among the 18 phyla with over 200 identified genera (Smythe and Wilkinson 2023).
The specific composition of the skin microbiota of an individual is presumed to be initialised already in the foetus and to be further formed from birth (Rojas et al. 2022; Stinson et al. 2019). The type of birth, the mother's microbiome and the post-natal environment are just some of the

many factors that determine the initial composition of the microbiome and lead to rapid colonisation within the first year (Bäckhed et al. 2015; Kong and Segre 2017). Important tasks are attributed to the microbiome. These include the promotion of immune system development and the induction of immune tolerance (Sfriso et al. 2020; Scharschmidt et al. 2015; Scharschmidt et al. 2017). The composition of the microbiome is not fixed at all once it has been established. Many studies have shown that it changes over time. For example, increased hormone and sebum production during puberty leads to a change in the skin microbiome (J. Park et al. 2022; Coates et al. 2019). However, not only time but also the topography of the body affects the representatives of the microbiome. In fact, the cutaneous microbial composition is relatively homogenous throughout the body but varies greatly between distinct sebaceous, moist and dry skin sites. Further, host factors such as sex and age but also environmental circumstances as climate and hygiene influence the microbiome composition (Coates et al. 2019; Grice and Segre 2011; Grice et al. 2009; Oh et al. 2016). Acidic areas such as around the sebaceous glands are mainly colonised by bacteria that can withstand low pH values. *Cutibacterium* and *Propionibacterium*, but above all *Staphylococcus* can be found here. Moist skin areas are mainly colonised by *Staphylococcus* and *Cornyebacterium*. Dry areas are home to a wide variety of bacteria, including *Cutibacterium* and *Flavobacteria* as frequent representatives (Grice et al. 2009; Smythe and Wilkinson 2023; Nakamura et al. 2021).

The core of the skin microbiome is presumed to be relative constant and formed by resident microorganisms. A smaller proportion consists of transient microorganisms that only last for hours or days. A general distinction is made in the microbiome between commensals and pathogens. Most members of the microbiome are assumed to belong to the commensals, which co-exist with the host and are neutral but often even beneficial for the host. In contrast, pathogens as well as opportunistic bacteria can cause serious diseases and infections. Some of them only become pathogenic under certain conditions. They need to express special virulence factors that allow them adhesion, invasion and immune evasion. This is the case, for example, with *S. aureus* or *C. albicans*, which account for the majority of skin infections (Belkaid and Tamoutounour 2016; Dréno et al. 2016). Commensals can protect the host in a variety of ways, including the support of the other three skin barriers and their functions. Simply the presence of commensal bacteria shields the host through direct competition with potential pathogens for the available space (Smythe and Wilkinson 2023). However, the positive influence of commensals by microbe-microbe interactions go beyond mere competition for resources and space. For example, the coagulase negative *Staphylococcus* (CoNS) strains *S. hominis* and *S. lugdunensis* produce antibiotics or AMPs against *S. aureus* to prevent colonization of this pathogen (Zipperer et al. 2016; H. J. Lee and Kim 2022; Bitschar et al. 2019; Nakatsuji et al. 2017). Other CoNS strains even block the accessory gene regulator (agr) gene of *S. aureus*, which plays an important role in quorum sensing and skin colonization (Williams et al. 2019), or secrete proteases that directly prevent biofilm formation of *S. aureus* (H. J. Lee and Kim 2022).

Furthermore, the microbiome contributes to the chemical barrier by the secretion of lipids and acids (H. J. Lee and Kim 2022; Dréno et al. 2016). *C. acnes* and *Corynebacterium* mainly colonise sebaceous areas where they hydrolyse free fatty acids and thus help to establish the acidic pH value. This contributes to the expression of one of the most common AMPs in humans, beta-defensin 2 (H. J. Lee and Kim 2022; Bomar et al. 2016).

Nevertheless, the protective barriers of the skin not only impedes the colonisation for pathogens. The skin is also a rough habitat for commensal representatives of the microbiome due to many challenges such as epithelial turnover, pH value and osmotic stress. Because of this, commensals have developed numerous adaptations that enable them to colonise the skin. One of the most important adaptations is the expression of specific proteins such as adhesins on their cell surface, allowing the attachment to matrix proteins of the skin. *S. epidermidis* expresses 18 genes encoding binding proteins, that support surface attachment (Gill et al. 2005; Sfriso et al. 2020). Another possibility to adhere is the formation of a biofilm, which is normally not permitted under the homeostatic conditions of the skin. Indeed, biofilm formation is usually associated with diseases and infections (Donlan and Costerton 2002; Sfriso et al. 2020). Many other factors allow bacteria to survive on the skin, but these are mostly associated with virulence (Sfriso 2020).

A study of Nakatsuji et al. showed that bacteria of the microbiome like *S. epidermidis* and *Pseudomonas spp*. are not only located on the stratum corneum on top of human skin, but also in deeper layers. Microbial components routinely penetrate the epidermal layer and are therefore visible for immune cells of the skin appendages and even in subcutaneous areas such as the dermis (Nakatsuji et al. 2013). This means that the immune cells located in these layers are in contact to the microbiome, even if the skin is intact. This strongly intertwined network contributes in various ways to the immune homeostasis of the skin. Nevertheless, the interaction with the microbiome and its composition is therefore subject to a fine balance. This balance can easily be upset in the event of dysbiosis and a shifted microbiome composition resulting in skin diseases such as psoriasis or atopic dermatitis, which is in most cases caused by a greatly increased presence of *S. aureus* (Kong et al. 2012). After barrier disruption, even commensals such as *S. epidermidis* can turn into opportunistic pathogens due to siege of the resource-rich tissue and blood circulation in combination with high reproduction and spread (Sfriso et al. 2020). The special relationship of microbiome and skin immunity with its fragile equilibrium is described in more detail in the following chapter.

1.2 Skin immunity: crosstalk of skin immune cells and microbiome

As already mentioned above, next to keratinocytes, the main cell type of the skin are various immune cell types. They colonise the cutaneous region in order to build a first immunological protective wall far from being just a mechanical barrier (Nestle et al. 2009; Pasparakis, Haase, and Nestle 2014). A constant interchange of epithelial cells, immune cells and microbiome influences skin immunity and the maintenance of homeostasis is dependent on finely regulated interactions between them (Pasparakis, Haase, and Nestle 2014). On the one hand, the microbiome exerts a direct protective function due to microbe-microbe interactions and competition with pathogens. On the other hand, the microbiome also shapes the innate and adaptive immune responses of the skin due to the interaction with the host cells (Prescott et al. 2017; Quaresma 2019). The microbiome does not only cause inflammatory reactions, but also induce tolerance mechanisms and signals that support immune defence (Abdallah, Mijouin, and Pichon 2017; Scharschmidt et al. 2015; Scharschmidt et al. 2017). A symbiotic relationship between skin immunity and commensal microbes has developed to tolerate commensals while pathogens are controlled (Coates et al. 2019).

In general, immunity is divided into the innate and adaptive arms. Although these take on very specific and different tasks, they are by no means isolated mechanisms. They are closely interlinked and complement each other. The maintenance of skin homeostasis and the induction of inflammation to eliminate pathogens depend on the balance and interaction of the innate and adaptive immune system with all its components. Imbalance or disruption of this system usually leads to pathological inflammatory processes, diseases or autoimmune disorders. The innate immunity reacts rather broadly to conserved foreign and microbial structures, which are known as pathogen-associated molecular patterns (PAMPs). PAMPs are structures found exclusively on microbes and not expressed on host cells. Lipopolysaccharide (LPS), lipoteichoic acid (LTA) and peptidoglycan (PGN) are common PAMPs of gram-negative or gram-positive bacteria. Innate immune responses can be called up immediately and are continually present. This is made possible by a broad selection of germ-line encoded PRRs expressed on the innate immune cells. PRRs are classified into five main families consisting of Toll-like receptors (TLRs), Nod-like receptors (NLRs), absent in melanoma-2-like receptors (ALRs), c-type lectin receptors (CLRs) and RIG-I-like receptors (RLRs) (Abdallah, Mijouin, and Pichon 2017; Coligan and Vogel 2008; Cavaillon 2017; Li and Wu 2021).

The adaptive immune response is much more specialised and antigen-specific, but also comes into action at a later stage as it requires some time to be set up. If the innate immunity is unable to eliminate pathogens, it is only a matter of time before the adaptive immune system intervenes. However, the extent and function of the adaptive immune system depends on the innate immune response. The link between the two systems is mediated by APCs, in particular LCs and DC

subsets in the case of the skin. B and T cells are the main cell types of the adaptive immunity. The presentation of antigens to these cells or sometimes direct interaction with the antigen are essential for their activation. Another unique component of the adaptive immune response is the establishment of an immune memory in the form of memory cells. This enables the establishment of a constantly growing basis for rapid but pathogen-specific adaptive immune responses in the event of a second or multiple encounters (Abdallah, Mijouin, and Pichon 2017; Coligan and Vogel 2008; Cavaillon 2017; Li and Wu 2021).

In this chapter, only a few representatives of the cells and mechanisms that contribute to skin immunity and homeostasis and their interaction with the microbiome are introduced, as a detailed consideration of all components is not possible due to their sheer amount. Especially, the interaction of the microbiome with the innate immune response, the APCs of the skin that link innate and adaptive immunity, the involvement of dermal T cells in the adaptive immune response and the concept of inducible skin-associated lymphoid tissue (iSALT) will be examined in more detail.

1.2.1 Innate immunity

After barrier disruption of the skin by physical or chemical stressors, the innate immunity is the first line of defence acting immediately or within hours facing microbial invaders (Coates et al. 2019; Paludan et al. 2021). Besides the chemical and physical components created by the skin barriers, the innate immunity is composed of humoral and cell-mediated components. Lysozymes, AMPs, natural antibodies, cytokines, acute phase proteins and the complement system are all part of the humoral response system. The cell-mediated side is composed of immune as well as non-immune cells, which contribute to the innate immune response of the skin (Riera Romo, Pérez-Martínez, and Castillo Ferrer 2016).

The immune cell department of the innate immunity includes myeloid phagocytic cells such as DCs and macrophages as well as leukocytes as natural killer cells or γδ T cells (Coates, Blanchard, and MacLeod 2018). Under steady-state conditions, the myeloid cells are involved in phagocytosis of debris, promotion of tolerance and maintenance of skin homeostasis. However, APCs of the myeloid cell compartment such as LCs and DCs are localized in the epidermis and dermis and react directly to inflammatory signals and link the innate with the adaptive immune response by antigen presentation (A. V. Nguyen and Soulika 2019). In addition, myeloid cells in the skin induce inflammation by production of pro-inflammatory cytokines and contribute to the elimination of pathogens in example by phagocytosis and the secretion of NO (Ono and Kabashima 2015; Nestle et al. 2009).

In this study, special attention will be paid to the antigen-presenting DCs as they link the innate and adaptive immunity and express several PRRs such as TLRs to recognize bacterial antigens (Riera Romo, Pérez-Martínez, and Castillo Ferrer 2016; Abdallah, Mijouin, and Pichon 2017). They are therefore described in more detail in the following section.

1.2.2 Dendritic cells: linking innate and adaptive immunity

Antigens that breach the physical barrier of the stratum corneum are captured and processed by dermal APCs, which than normally migrate into skin-draining lymph nodes. The peptides resulting from the processing are then presented to naive T cells via MHC class I and II molecules together with co-stimulatory signals and cytokines to induce the adaptive immune response (Steinbrink and Raker 2016). Thus, dermal DC subsets and epidermal LCs are essential immune sentinels that connect innate with adaptive immunity (Ruddle 2020; Dress, Wong, and Ginhoux 2018). However, in skin, APCs are an important component of the iSALT concept, which is described in more detail together with adaptive immunity in chapter 1.2.3 (Ono and Kabashima 2015).

The skin harbours many different DC subsets, each of which can trigger unique immune responses, some of which also overlap in their functions, and can usually be assigned to specific regions of the skin. The function of a particular DC subtype in the antimicrobial immune response is always highly dependent on the pathogen, the location and the type of infection (Belkaid and Tamoutounour 2016). Under steady-state conditions, APCs consist of epidermal LCs and dermal DCs (dDC). The dDCs can be further subdivided into conventional DC1 (cDC1), cDC2, plasmacytoid DCs (pDCs) and monocyte-derived DCs (moDCs). cDC1 show strong cross-presentation capabilities whereas cDC2 are known to induce T_H2 immune responses (Honda, Egawa, and Kabashima 2019; Belkaid and Tamoutounour 2016; Ruddle 2020; Guilliams et al. 2016; Schlitzer, McGovern, and Ginhoux 2015). Moreover, cDC1 are presumed to control the development of commensal-specific dermal CD8+ T cells and therefore are involved in the homeostasis between the microbiome and immune cells. pDCs appear in the skin exclusively under inflammatory conditions, and mainly produce huge levels of type I interferons upon activation, in example via TLRs (Nestle et al. 2009; A. V. Nguyen and Soulika 2019; Naik et al. 2015a).

It is assumed that professional APCs, especially LCs, of the skin can extend their dendrites outward beyond the tight junctions to collect surface samples of the outer regions which are heavily colonised by the microbiome, such as hair follicles, even when the skin barrier is intact. However, it is also possible that antigenic or microbial products of a certain size can passively diffuse through the epithelial barrier, especially in regions such as the hair follicles where cell adhesion is weaker and the stratum corneum is missing (Kabashima et al. 2019; Kubo et al. 2009; Hansen and Lehr 2014; Zheng, Liwinski, and Elinav 2020). As LCs reside in the epidermis, they primarily encounter antigens of the microbiome upon barrier disruption (Nestle et al. 2009). In their antigen-presenting role, they activate CD4+ and CD8+ T cells. They were shown to favourably induce T_{H2} and T_{H17} differentiation, but they are also involved in cross-presentation of antigens. However, the ability of cross-presentation seems to be mainly carried out by dermal CD103+ cDC1 (Pasparakis, Haase, and Nestle 2014; Del Rio et al. 2010; Bedoui et al. 2009). LCs are assumed to be involved in initiation of cell-mediated immunity and inflammation, but they

are also suppressors of inflammation and can establish tolerance, too (Steinbrink and Raker 2016; A. V. Nguyen and Soulika 2019; Matejuk 2018; Nestle et al. 2009). The respective function of the LCs appears to take different paths depending on the pathogenic condition (Ruddle 2020).

Antigens that reach the dermis are likely captured by the dDC compartment (Kabashima et al. 2019). Dermal langerin+ CD103+ DCs are estimated to be the main cell type presenting exogenous antigens to CD8+ T cells via cross-presentation (Nestle et al. 2009). Upon activation, dDCs produce cytokines and chemokines that promote inflammation. dDCs that produce TNF and inducible nitric oxide synthase (iNOS), were used to be designated as TIP (TNF- and iNOS-producing) DCs and can be induced in skin. They seem to be influenced in immune responses and also in dysregulations of the skin such as psoriasis (Serbina et al. 2003; Nestle et al. 2009). It is also known, that LCs and dDCs are further able to initiate immune tolerance to antigens, in example by promoting T_{reg} cells (Tordesillas et al. 2018; A. V. Nguyen and Soulika 2019).

There is a wide range of evidence on how the interaction of dDCs and the microbiome influences immunity. One example is the induction of a specific IL-17A-producing CD8+ T cell subtype by CD103+ DCs as well as CD11b+ DCs in response to *S. epidermidis*. This CD8+ T cell subtype was observed to support innate barrier immunity and to reduce pathogen invasion (Naik et al. 2015a). LCs are for example necessary to mediate an inflammatory response of γδ T cells and CD4+ T cells in *S. aureus* infections. They further promoted the accumulation of T_{reg} cells, and self-regulating CD4+ T cells in *L. major* skin infection models (Belkaid and Tamoutounour 2016; Brewig et al. 2013). The importance of cross-presentation of antigens by CD103+ DCs to activate CD8+ T cells to control the microbiome has been demonstrated in HSV-1 infections (Bedoui et al. 2009). That different microbes can have opposing effects on the same skin disease via activation of dDCs could be shown in the treatment of atopic dermatitis. Treatment with the bacterium *Vitreoscilla filiformi*, found in thermal waters, induced secretion of IL-10, an anti-inflammatory cytokine, by DCs leading to the activation of T_{reg} cells and control of atopic dermatitis inflammation. Regarding skin inhabitants, specific *C. acnes* strains of healthy individuals also induced the expression of IL-10, whereas strains of patients induced IFNγ and IL-17 secretion (Rojas et al. 2022).

1.2.3 Adaptive immunity

The second line of defence is provided by the adaptive immune system. In contrast to the innate immune system, this is a highly specific reaction to distinct antigens. The main cells involved in adaptive immunity are the lymphocytes, more specifically the B and T cells. The general function of B cells is the production of antigen-specific antibodies after antigen-encounter. This leads to complement activation as well as the opsonisation of the antigen-connected organism, which than is neutralized in further steps. Another function of activated B cells is the priming of T_H cells into a T_H2 type (Chaplin 2010; Abdallah, Mijouin, and Pichon 2017). However, the number of B cells in skin is relatively low and their function in skin immunity is still not well understood. Recently, it

has been shown that B cells are involved in both skin homeostasis and disease (Lerman, Mitchell, and Richardson 2021; E. G. Lee and Oh 2024).

The ability of B cells as well as T cells to react specifically to pathogen-derived antigens is essential for the generation of an adaptive immune response. During the development of T cells, the acquisition of a diverse T cell receptor (TCR) repertoire ensures that a discrete TCR variant exists for every conceivable antigen from every organism (Chaplin 2010; Abdallah, Mijouin, and Pichon 2017). This is achieved by the so-called TCR gene rearrangement during T cell development. T cell activation is not only triggered by the binding of the MHC-antigen peptide complexes to the TCR, but also requires additional signals. A second signal is transmitted by the binding of co-stimulatory molecules of the APCs such as CD80 and CD86 to the CD28 molecule which is expressed on T cells. Cytokine signalling serves as a third signal (Cox, Harrington, and Zajac 2011; Abdallah, Mijouin, and Pichon 2017; Murphy and Weaver 2018).

The human skin harbours about $2x10^{10}$ T cells, which is more than twice as in the circulating blood. The T cells are mainly located in the dermis, but also to a lesser extent in the epidermis and hypodermis (Nestle et al. 2009; C. Zhang et al. 2022). T cells can be subdivided in two main subpopulations. On the one hand, the CD4+ T cells, which in turn can be divided into different subtypes of T_H cells and T_{reg} cells. On the other hand, the CD8+ T cells which can also be divided in subtypes including cytotoxic T cells. CD4+ T cells recognise antigens that are presented via MHC class II and perform a wide variety of tasks in the context of adaptive immunity. These include the recruitment of other immune cells using cytokines to combat various pathogens, but also the regulation of the immune response (Abdallah, Mijouin, and Pichon 2017; Koh et al. 2023). Of the CD4+ T cells, 10-30 % in humans and 20-60 % in mice are Tregs, but also different CD4+ T_H such as T_H1, T_H2, T_H17 and T_H22 are found during inflammation (C. Zhang et al. 2022; Nestle et al. 2009). The CD8+ T cell recognition of antigens is restricted to presentation via MHC class I molecules, as the CD8 molecule interacts specifically with the α3 domain of the MHC class I molecule (Chaplin 2010). Normally, endogenous cytosolic proteins or peptide fragments are presented via MHC class I molecules. However, this would not allow the priming of CD8+ T cells against antigens from extracellular pathogens or representatives of the microbiome. To overcome this problem, DCs are able to present phagocytised exogenous antigens via MHC class I by means of the mechanism of cross-presentation (Abdallah, Mijouin, and Pichon 2017; Murphy and Weaver 2018). CD8+ T cells' main function is the induction of target cell apoptosis via cytokines and cytotoxic components. Also innate-like T cells such as γδ T cells and NKT cells are present in the skin and are often involved in immunoregulation (Nestle et al. 2009).

Some effector T cells remain in the target tissue after infiltration and become T_{RM}. In skin, this subtype can be distinguished from other T cells by the expression of markers such as CD103, CD69, CD44 and CD49a. In case of the skin, it is assumed that they persist there for up to over a year (Mackay et al. 2012; Gebhardt et al. 2011; Ruddle 2020; Konjar et al. 2022). This is different

from the circulating central memory T cells, which retreat into the lymphoid organs and are only recruited back into the skin after the induction of signals such as cytokines (Steinbrink and Raker 2016; Hirai, Whitley, and Kaplan 2020). There are both CD4+ and CD8+ T_{RM} cells, but these show different preferences for their localisation in the skin. CD4+ T_{RM} cells tend to reside in the dermis whereas CD8+ T_{RM} cells are more likely to be found in the epidermis (Mueller et al. 2013). It is suspected that T_{RM} cells are antigen-specific sensors in the skin inducing rapid responses to infections. Their cytokines can activate the attending innate immunity and maturation of DCs (Ruddle 2020). CD8+ T_{RM} cells of the epidermis even adopt a dendritic-like morphology, which makes it possible to scan many cells simultaneously to identify pathogens (Belkaid and Tamoutounour 2016).

Most studies investigating the relationship between the skin microbiome and T cells focussed on the function of CD4+ T cell subsets. It was shown that T_{reg} cells are involved in the establishment of tolerance to commensals in the early neonatal period. However, the effector function of CD4+ T cells is also influenced by the microbiome. Interestingly, the same bacterium can result in different outcomes for T cell functions. *S. aureus*-derived toxin A induces T_{H17} response, whereas *S. aureus*-derived LTA potentially induces T cell anergy (Maseda, Manfredo-Vieira, and Payne 2023). Furthermore, exposure of a new commensals to murine skin can induce specific CD4+ and CD8+ T cell responses in the absence of barrier breach. In this context, adaptive immune responses can occur without any form of inflammation, resulting in a process that was referred as homeostatic immunity (Belkaid and Tamoutounour 2016). One example are the already mentioned, *S. epidermidis*-specific IL-17A producing CD8+T cells that promote the production of AMPs by keratinocytes (Naik et al. 2015a).

The way in which dermal CD8+ T cells are involved in skin immunity and interaction with the microbiome is explained separately in the following section, as they are in focus of this thesis.

1.2.4 CD8+ T cells of the skin

In general, T_{RM} cells make up a large proportion of CD8 T cells in the skin, enabling a rapid and local immune response without egression to secondary lymphoid sites (C. Zhang et al. 2022; Nestle et al. 2009). Memory CD8+ αβ T cells are the largest subpopulation in the epidermis and are often in the direct vicinity of LCs (Nestle et al. 2009; Lerman, Mitchell, and Richardson 2021; Quaresma 2019).

The main activity of CD8+ T cells is characterised by their cytotoxic activity against tumour cells and cells infected with intracellular pathogens, such as viruses, bacteria and parasites. However, regulatory CD8+ T cells, which control the immune response, also exist. Their activity is restricted to the expression of short peptide fragments via MHC class I molecules (Chaplin 2010). CD8+ T cells can be divided into different subtypes. The first CD8+ T cell subtype generally produce TNF, IFNγ and lymphotoxin alpha in response to antigen stimulation. There is also a CD8+ T cell

subtype (with expression of IL-18receptor) that produces IL-17 in combination with IFNγ (Annunziato, Romagnani, and Romagnani 2015). Another type is able to produce cytokines such as IL-4, IL-5 and IL-13. It was shown that resident memory T cells were activated by dDCs, leading to a local proliferation of antigen specific memory CD8+ T cells and supporting protection from pathogens (Wakim et al. 2008; Nestle et al. 2009).

As already mentioned, skin immunity is closely interwoven to the skin microbiome and functions of the two barriers interlock and promote each other. If one consider the interaction with adaptive immunity, a beneficial support of the microbiome can be observed in many cases. However, it must be mentioned that the influence of the microbiome on innate immunity also has an impact here, as adaptive immunity is dependent on innate immunity. In general, skin-resident commensals are able to control the balance of effector and regulatory T cells (Zheng, Liwinski, and Elinav 2020). Colonisation of germ-free mice with *S. epidermidis* shows, that the skin commensal induced T_H17 cells but also an increase in the frequency of IFNγ/IL-17-producing CD8+ T cells in the epidermis. In particular, the commensal-specific IL-17A+ CD8+ T cells contribute to improved barrier immunity and prevent the entry of pathogens (Naik et al. 2012; Naik et al. 2015b; Y. J. Park and Lee 2018). Moreover, it was demonstrated that they express genes associated with tissue repair and immunomodulatory functions (Linehan et al. 2018; Nakatsuji, Cheng, and Gallo 2021).

Barrier disruption of the skin by injuries can lead to microbial dysbiosis. Pathogenic bacteria such as *S. aureus* can invade the skin proliferate and cause inflammation. Once there, they modulate the adaptive immune response of the skin. *S. aureus* alpha toxin for example prevents cytotoxic killing by CD8+ T cells in the skin (Y. Zhang et al. 2022; Blümel et al. 2020; Kobayashi et al. 2015).

1.2.5 The inducible skin-associated lymphoid tissue

In general, the lymphoid organs can be divided into primary and secondary lymphoid organs. Primary lymphoid organs include the thymus and bone marrow in which, for example, naive T cells are produced. T cell priming takes place in secondary lymphoid organs such as the spleen and lymph nodes. For priming, skin-derived APCs present processed antigens to the T cells. Primed T cells then migrate to the periphery into the non-lymphoid organs, which are considered to be the main sites of effector functions of immune cells. After renewed antigen contact, however, antigen can be presented in the skin itself, in example to tissue-standing memory T cells, which leads to inflammation. In the 1980s, Streilin and others introduced the concept of the skin-associated lymphoid tissue (SALT) (Egawa and Kabashima 2011; Clark 2010; Wayne Streilein 1983). The SALT is assumed to serve as a tertiary lymphoid structure, enabling the induction of adaptive immune response without the migration of cells to and from secondary lymphoid structures such as skin-draining lymph nodes (Honda, Egawa, and Kabashima 2019). This makes the skin not just a simple barrier but also a component of the immune system.

After the discovery of dDC clusters in models of contact dermatitis, this concept was further developed and the term inducible skin-associated lymphoid tissue (iSALT) was created. The permanent presence of the SALT is more of a conceptual description, whereas for the iSALT real structures around postcapillary venules could be detected which were induced after various immunogenic stimulations. As a result of the detection of DC and T cell clusters in various skin-related diseases, it has been further suggested that activation of T cells occurs in the iSALT clusters in skin (Honda and Kabashima 2016; Honda, Egawa, and Kabashima 2019; Kabashima et al. 2019). These inducible leukocyte-clusters of dDCs, T cells and other skin-associated cells are necessary for efficient activation of T cells in the skin and are formed during cutaneous adaptive immune responses. It is not assumed that the iSALT is present under homeostatic condition but forms rapidly upon inflammation. This tertiary lymphoid structure is similar to others found in diverse peripheral regions such as the lung or gut. Whether the priming of naive T cells also takes place there has not yet been clarified (Ono and Kabashima 2015; Kogame, Kabashima, and Egawa 2021; Honda, Egawa, and Kabashima 2019). However, it is proposed that the iSALT is an efficient site for antigen presentation. The local interaction between skin-resident APCs and skin-resident T_{RM} cells allows a specific and effective T cell effector response, but also regulatory T cell activation, which was shown to be independent of additional extravasation of T cells from the peripheral blood under certain conditions (Steinbrink and Raker 2016). The network of cells in the iSALT thus makes the skin a complex immunological organ that can react to external influences by means of innate and adaptive immunity. Nevertheless, as observed in other organs, misdirected reactions of complexes like the iSALT or its immune cells against harmless exogenous or endogenous antigens can lead to allergic reactions or autoimmune diseases in the skin. Thus, the iSALT plays an important role in maintaining a balance between targeted immune response and tolerance induction (Quaresma 2019; Kabashima et al. 2019; Steinbrink and Raker 2016).

1.2.6 Immune regulation and tolerance

It is not always necessary and useful to induce an immune response against every microorganism. Immune responses are always associated with the consumption of resources and can also have a detrimental effect on the organism, such as chronic inflammations. In addition, once an immune response has been triggered, it must be controlled and stopped as soon as the pathogen has been eliminated. This is where immune tolerance and T_{reg} cells come into play (Paludan et al. 2021; Scharschmidt 2017). In addition to their role as initiators of inflammation, DCs are also significantly involved in the mediation of tolerance. The type of DC function is strongly dependent on surrounding factors such as cytokines, cell type and the type of microorganism with which they interact (Scheib et al. 2022).

The skin contains one of the highest frequencies of T_{reg} cells in the entire body. They are mainly found in the dermis and in skin appendages where they get in regular contact with the skin

microbiome (Quaresma 2019; Belkaid and Harrison 2017; Suffia et al. 2006). High numbers of activated T_{reg} cells in the skin of neonate mice suggest that early in life contact with the representatives of the skin microbiome is necessary to establish tolerance to them (Belkaid and Harrison 2017; Scharschmidt 2017; Eyerich et al. 2018). In the second week of life of neonate mice, high levels of CTLA-4 and ICOS, which are known mediators of tolerance, are detected on T_{reg} cells during the invasion of the skin (Y. J. Park and Lee 2018). However, it is not exactly known yet how these mechanisms work. It is assumed that selected microbes can still induce tolerance at a later stage. For example, *V. filiformis* was able to accumulate T_{reg} cells and *S. epidermidis* induced the expression of DC-derived IL-10 (Volz et al. 2014; Laborel-Préneron et al. 2015; Belkaid and Harrison 2017). Pathogens such as *S. aureus* also exhibit the ability to suppress immune responses. In mouse studies, *S. aureus* induced the expression of IL-10 and PD-L1 accompanied by downregulation of HLA-DR and CD86 on monocytes via TLR2, affecting their T cell-stimulatory capacity (Wang, Roderiquez, and Norcross 2012). *S. aureus*-derived protein A induced human T_{reg} cells due to soluble factors of MoDCs, but independent of antigen presentation (Uebele et al. 2020). Further, CD4+ T cell proliferation and IFNγ secretion was suppressed due to co-stimulation with anti-CD3/CD28 beads and *S. aureus* LTA in murine and human T cells (Kaesler et al. 2016). It therefore appears to be situation-dependent whether tolerance is established on the part of the immune cells or is actively induced by bacteria.

It has to be considered that immune tolerance is not favourable in every case. Tolerance towards normally harmless and even beneficial commensals such as *S. epidermidis* can result in severe infections as soon as the commensals change into a pathogenic phenotype or get inside the body. A better understanding of how tolerance to commensals is induced could help to break this tolerance again in infections with opportunistic representatives. *S. epidermidis* is an ideal candidate for such an investigation, as explained in more detail in the following chapter.

1.3 *S. epidermidis*: a skin commensal in health and disease

S. epidermidis is one of the most frequently isolated bacteria of almost all areas of the human skin, whit a strong preference for moist regions, and becomes a lifelong member of the human skin microbiome (J. Y. H. Lee et al. 2018; Severn and Horswill 2022; Brescó et al. 2017). *S. epidermidis* can also be detected on murine skin, albeit in low quantities (Battaglia and Garrett-Sinha 2023; Belheouane et al. 2020). *S. epidermidis* is a gram-positive, non-motile and facultative anaerobic bacterium. Among the staphylococci, it can be assigned to the group of coagulase-negative staphylococci (Chabi and Momtaz 2019).

Many studies have shown the benefits of *S. epidermidis* as a commensal of the microbiome. It is involved in wound healing, prevents the colonization of the skin by pathogenic bacteria and supports the maintenance of homeostasis. Recently it has been proven that *S. epidermidis* is

involved in skin diseases and infections, too. It is one of the most common causes of implant-associated infections and its ability to form biofilms and acquire antibiotic resistances makes a treatment difficult. In fact, three nearly pan-resistant strains are known nowadays. Treatment poses major challenges due to the many resistances and the fact that immune tolerance to this bacterium is being established in early life further exacerbates the issue (Severn and Horswill 2022; J. Y. H. Lee et al. 2018). Many different strains of *S. epidermidis* exist, sharing a core genome, which accounts for about 80 % of all genes. The remaining 20 % are variable individual genes and thus each strain have a unique phenotype. Strain diversity spreads within and between hosts. In order to be able to live as a commensal on the skin, *S. epidermidis* must have some adaptations also known as virulence factors. Probably the most important is the expression of several adhesion molecules and cell wall-anchored proteins, which enable adhesion to components of the stratum corneum and the extracellular matrix (Conlan et al. 2012; Severn and Horswill 2022; Foster 2020).

The already mentioned early acquired immune tolerance to bacteria, such as *S. epidermidis*, through the induction of commensal-specific T_{reg} cells, is also necessary to enable the bacteria to live as a commensal on the skin (Leech et al. 2019; Scharschmidt et al. 2015). *S. epidermidis*, even appears to contribute to attracting T_{reg} cells and thus promoting the establishment of immune tolerance by inducing the C-C motif chemokine ligand (CCL) 20 on foetal skin (Scharschmidt et al. 2017; Severn and Horswill 2022). As part of the commensal lifestyle, *S. epidermidis* has many advantages for the host. The presence of *S. epidermidis* can hinder or prevent colonisation by pathogenic organisms such as *S. aureus*, one of the most common causes of skin diseases. Responsible for this are *S. epidermidis*-derived bacteriocytic substances such as phenol soluble modulins (PSMs) γ and δ but also the stimulation of keratinocytes and innate immune cells for the production of AMPs. Further, the release of serine proteases by *S. epidermidis* can impair the biofilm formation of *S. aureus* (Lunjani et al. 2021; Cogen et al. 2010; Severn and Horswill 2022). In adulthood, *S. epidermidis* improves the immunity of the skin barrier by influencing DC-T cell interactions. It has been shown that DCs induce IL-17A CD8+ T cells after contact with *S. epidermidis*, which impede the colonisation of pathogens. LTA, a major component of the cell surface of *S. epidermidis* can induce IL-10 balanced phenotypes in DCs (Naik et al. 2015a; Volz et al. 2018; Severn and Horswill 2022). Furthermore, various studies have shown that *S. epidermidis* supports and accelerates wound healing. This was achieved by various *S. epidermidis*-induced mechanisms such as the expression of C-X-C motif chemokine ligand (CXCL) 10, specific CD8+ T cells or *S. epidermidis*-derived trace amines. Attenuated expression of TNF and IL-6 by LTA of certain *S. epidermidis* strains also improved wound healing (Severn and Horswill 2022).

Despite its various beneficial contributions to skin health and homeostasis during asymptomatically skin colonisation, *S. epidermidis* can be the cause of serious infections, which

can be challenging to treat. Changes in the quantity of *S. epidermidis* are associated with skin diseases such as atopic dermatitis or rosacea. Moreover, *S. epidermidis* accounts to a large part of all medical device-related infections and nosocomial blood infections in patients and leads to its classification as an opportunistic pathogen. As *S. epidermidis* is one of the main representatives of the skin microbiome, such implants often allow entry and infection. The ability to form biofilms often leads to infections becoming chronic and an ever-widening spectrum of antibiotic resistance is making it increasingly difficult to treat such infections (Widerström 2016; Otto 2009; Brescó et al. 2017; Severn and Horswill 2022). It is assumed that *S. epidermidis* strains isolated from infections are a subgroup of those from the skin and that these are genetically different. In one study, 61 genes were identified that contained infection-associated genetic elements and are correlated with pathogenicity traits (Méric et al. 2018; Y. J. Park, Kim, and Lee 2019). Studies by the group of Du et al. also suggest that inter-species exchange of resistance, virulence and colonization factors between *S. epidermidis* and other close relatives such as *S. aureus* is possible. The basis for this is the presence of the accessory genetic element *tarlJLM*, which leads to the expression of an *S. aureus*-type wall teichoic acid (WTA) in *S. epidermidis* and makes DNA exchange possible (Du et al. 2021). Horizontal gene transfer between *S. aureus* and *S. epidermidis* has been demonstrated for other genetic elements such as SCC*mec* and ACME, but also the intraspecific gene transfer seems to be quite high (Severn and Horswill 2022).

Compared to strains known to be predominantly pathogenic such as *S. aureus*, *S. epidermidis* carries only a few virulence factors. In addition, many of these appear to play a role both in its commensal life and in infection. Lacking most of the aggressive virulence factors as known for *S. aureus*, the formation of biofilms mainly contributes to the pathogenic phenotype of *S. epidermidis* (Le, Park, and Otto 2018). As already mentioned this allows the bacteria to attach to implants and thus causes chronic infections (Otto 2009; Foster 2020). Removal of the affected implants is usually the last resort to get the infection under control. Biofilms are agglomerations of bacteria surrounded by a self-produced extracellular matrix of proteins, polysaccharides and extracellular (Brescó et al. 2017; T. H. Nguyen, Park, and Otto 2017; Otto 2008). The biofilm protects the bacterium from antibiotics and immune reactions such as complement, opsonisation, AMPs and phagocytosis (Schilcher and Horswill 2020; Le, Park, and Otto 2018; Brescó et al. 2017). Many studies indicate that the immune response to biofilm-associated infections is weakened and ineffective. Biofilms inhibit the phagocytosis capabilities of macrophages and the immune system is urged to produce anti-inflammatory cytokines, while the production of pro-inflammatory cytokines is reduced (Spiliopoulou et al. 2012; T. H. Nguyen, Park, and Otto 2017). In the worst case, bacteraemia due to a device-related infection can even lead to sepsis. Immunocompromised patients and premature neonates are particularly susceptible to this. However, the immune response to bloodstream infections is different from tissue-associated biofilm infections. In particular, the stimulation of innate immune cells, primarily neutrophils, via TLR2 appears to be important in the fight against sepsis. However, *S. epidermidis* has some

methods of immune evasion such as the PSM-mec (Cheung and Otto 2010; T. H. Nguyen, Park, and Otto 2017). PSMδ has been observed to be cytolytic to human neutrophils. Biofilm-derived *S. epidermidis* can survive efficiently in macrophages after phagocytosis. The polysaccharide intercellular adhesin, a biofilm component, even reduced the phagocytosis of *S. epidermidis* by macrophages and appears to prevent neutrophil activity (Le, Park, and Otto 2018; Spiliopoulou et al. 2012; Vuong et al. 2004). Many strains of *S. epidermidis* already carry a high level of antibiotic resistance, which is constantly increasing. In isolates from hospital infections, all examined strains of *S. epidermidis* carried at least three antibiotic resistances and the spectrum ranged up to multi-drug resistance to 7 antibiotics in approximately 17 % of the samples (Chabi and Momtaz 2019). The study by Lee et al. showed that almost pan-resistant strains such as ST2 and ST23 are also spreading globally, posing an ever-increasing threat in the form of possible incurable infections (J. Y. H. Lee et al. 2018).

Taken together, *S. epidermidis* has several ways to escape the immune system and create a low inflammatory profile. Immune evasion mechanisms and the influence of *S. epidermidis* on the immune system have not yet been investigated in as much detail as for primarily pathogenic bacteria such as *S. aureus*. However, the increasing number of infections with multi-resistant strains of *S. epidermidis* and the virulence factors considered make a more detailed investigation well worthwhile.

1.4 IFNγ and NO in the context of T cell proliferation

1.4.1 IFNγ

Interferons area a broad family of cell signalling molecules, which are crucially involved in innate and adaptive immunity. They are induced in response to infection and stimulate the expression of interferon stimulatory genes. IFNs consist of three main types dependent on the receptor usage. Type I interferons such as IFNα and IFNβ are important in anti-viral immunity. The type II interferon IFNγ stimulates macrophages and recruits leukocytes. Type III interferons are involved in immune responses at mucosal surfaces (Coligan and Vogel 2008; Ding et al. 2022).

IFNγ is mainly produced by T cells and NK cells upon induction via TCR or other cytokines. Recent reports also show that other cell types such as B cells, DCs and macrophages can express IFNγ (Negishi, Taniguchi, and Yanai 2018). IFNγ binds to the IFNγ receptor (IFNγR), which is a tetramer of two IFNγR-1 and IFNγR-2 heterodimers, resulting in Janus kinase (JAK) and signal transducers and activators of transcription (STAT) signalling. This often results in the activation of IFNγ response genes such as IFN regulatory factor (IRF) 1 and IRF8. This can contribute to the regulation of genes in conjunction with other transcription factors, including iNOS (Ozato, Tailor, and Kubota 2007; Tamura et al. 2008; Negishi, Taniguchi, and Yanai 2018). The IFNγR is expressed on a wide range of cell types, including macrophages and DCs. The IFNγ signalling

coordinates immune regulation, cell proliferation and anti-microbial effects (Ding et al. 2022; Kak, Raza, and Tiwari 2018). Further, IFNγ can enhance antigen presentation by APCs and boost the secretion of reactive nitrogen intermediates. IFNγ is also essential in the control of many infections such as mycobacteria or viral infections. Protective effects supporting anti-bacterial immune responses against *S. aureus* can be mediated by IFNγ, too (Kak, Raza, and Tiwari 2018).

1.4.2 NO

The diatomic gas NO can be produced by mammalian cells from L-arginine and molecular oxides and its production is catalysed by NO synthases (NOS). There are three different isoforms of NOS, eNOS (endothelial), nNOS (neuronal) and iNOS/NOS2, which differs substantially from the other two constitutive NOSs regarding regulation and output of NO. iNOS is induced e.g. in immune cells after stimulation with bacterial components or with pro-inflammatory cytokines, such as IFNγ, and leads to high levels of NO. More precisely, NOS converts L-arginine, NAPD and molecular oxide into NO, NADP+ and L-citruline (Thwe and Amiel 2018; Aktan 2004; Lundberg and Weitzberg 2022). NO is relatively unstable and is quickly oxidised to more stable nitrate and nitrite and thus inactivated. Nitrate is the dominant end product. However, the two oxidation products can be reduced back to NO. NO can also react with superoxide to form peroxynitrite (Lundberg and Weitzberg 2022).

Murine BMDCs and dermal DCs as well as iDCs (inflammatory DCs) were shown to express iNOS in response to LPS stimulation, resulting in NO release. After its release, NO can act on the producing cell itself or on neighbouring cells by diffusion. The uncharged state and lipophilic nature of NO enables direct diffusion through the cell membrane. Once inside a cell, NO normally activates soluble guanylyl cyclase, which ultimately regulates many physiological processes in a series of reactions(Lundberg and Weitzberg 2022). There is evidence for positive stimulation of immune responses, but many studies also show an inhibitory function of NO on DCs and T cells. Furthermore, NO acts not only on the DCs themselves but also on nearby cells and bystander cells. It has been shown that DC-derived NO attenuates the proliferation of T cells (Thwe and Amiel 2018; Bogdan 2015; Lundberg and Weitzberg 2022). However, it appears that CD8 T cells are more sensitive to DC-derived NO than CD4 T cells. Thus, significantly lower levels of NO were sufficient to inhibit proliferation in CD8 T cells than in CD4 T cells (Hoffman et al. 2002).

As part of the immune defence, NO prevents bacterial growth and inhibits viruses, but it also has an anti-inflammatory effect. For example, iNOS activity promotes the recruitment of granulocytes in *S. aureus* infections of the lung to support the defence, whereas iNOS-induced granulocyte accumulation was detrimental in infections with mycobacterium. In turn, bacteria such as *Salmonella* have developed defence mechanisms to prevent iNOS induction, e.g. by suppressing IFNγ-induced STAT1 signalling (Lundberg and Weitzberg 2022; Thwe and Amiel 2018). *M. tuberculosis* can convert NO into nitrite to avoid being killed. Other bacteria go one step further, using NO to increase their chances of survival and even expressing their own bacterial NOS.

Alternatively, specific genes are activated in response to NO detection and induce detoxification mechanisms (Bogdan 2015).

iNOS activity can therefore be beneficial or harmful to both the host and the bacteria. However, “the overall role of iNOS in inflammation is still very unclear, and its impact on pathophysiological processes likely depend on the timing and duration of iNOS induction” (Lundberg and Weitzberg 2022) and, despite years of research in this area, further studies are needed to complete the picture.

1.5 Objective

The skin's immune system is in close contact with the dermal microbiome. This finely regulated interaction ensures the maintenance of skin homeostasis while at the same time preventing infections caused by pathogens. However, how the dermal immune system distinguishes commensals from pathogens is still not completely elucidated yet. What is clear, is that the immune system also reacts to the commensals of the skin microbiome, but does not trigger chronic inflammation. Some studies have already investigated possibilities how tolerance to commensals can be mediated either by the immune system or by the bacteria. However, many aspects still need to be clarified in this mediation of tolerance. Ultimately, a shift in the microbiome composition or a misdirected immune response can also lead to infection by opportunistic commensals and to diseases.

The aim of this study is to investigate whether commensals such as *S. epidermidis* can influence an antigen-specific adaptive immune response of CD8 T cells and which mechanisms are involved. Since the skin, especially the epidermis, harbours many CD8 T cells, the influence of *S. epidermidis* on the interaction of dendritic cells and CD8 T cells is the focus of this study. For this purpose, co-cultures of BMDCs and OT-I CD8 T cells were prepared in which OT-I CD8 T cell proliferation can be induced by stimulation with ovalbumin (OVA). *S. epidermidis* was added in different concentrations and its influence on OVA-specific OT-I CD8 T cell proliferation as well as on BMDC maturation was investigated in more detail. The expression of cytokines in the presence of *S. epidermidis* was also analysed. After a suppressive effect of *S. epidermidis* on the OVA-induced proliferation of OT-I CD8 T cells was observed, the next step was to unravel the underlying mechanism. In addition, it was investigated whether *S. epidermidis* is able to directly influence OT-I CD8 T cells

The study contributes to a better understanding of why commensals are not generally combated. By revealing the relevant mechanisms for a suppressed T cell proliferation, its modulation can be used to influence T cell responses. This could be relevant for adjuvant immunotherapies to initiate the control of infections by restoring T cell activity or to prevent T cell exhaustion. The knowledge could also be used to suppress CD8 T cells in autoimmune diseases

2 Material and Methods

2.1 Mice and husbandry

All mice used for the generation of BMDCs and isolation of T cells are listed in Table 1. C57BL/6J wild type, C57BL/6N wild type mice, IFNγR$^{-/-}$ and IFNγ$^{-/-}$ mice were used to isolate femora and tibiae for generating BMDCs for stimulation and co-culture experiments, and RNAseq analysis. For the generation of BMDCs from (Myeloid differentiation primary response 88) MyD88$^{-/-}$, (TIR domain-containing adaptor protein inducing interferon beta) TRIF$^{-/-}$, iNOS$^{-/-}$ and Arg1$^{-/-}$ knockout mice and CD11c-DTR mice, femora and tibiae were isolated by the respective institute and sent on wet ice with over night transport. In CD11c-DTR mice, the expression of the diphtheria toxin receptor (DTR) is directed by the CD11c promotor (*Itgax*), therefore all CD11c+ cells express the DTR (Dennis et al. 2002). Administration of diphtheria toxin (DT) induces the depletion of such CD11c+ dendritic cell populations. Cells of the IFNγ$^{-/-}$ mice are no longer able to produce IFNγ, whereas cells from the IFNγR$^{-/-}$ mice lack the cognate receptor for IFNγ and therefore can no longer be triggered by the cytokine. In the case of MyD88$^{-/-}$ and TRIF$^{-/-}$ mice, the deficiency for MyD88 and TRIF, two important adaptor proteins in TLR signalling, allows to investigate TLR-dependent mechanisms in experiments (Sameer and Nissar 2021). iNOS and arginase 1 are both involved in the regulation of the arginine metabolism and respective knock out mice are used in this study to examine the influence of NO within the co-culture system (Rath et al. 2014).
OT-I mice were used to isolate CD8+ T cells. CD45.1, the congenic marker of CD45.2, was crossed into the OT-I mouse line. This allows distinguishing the CD45.1-expressing OT-I CD8 T cells from CD45.2-expressing wild type mice, which were used for BMDC generation. This is especially useful in co-cultures. CD8 T cells from OT-I mice express a transgenic TCR that specifically recognizes chicken ovalbumin peptide residues 257-264 ($OVA_{257-264}$) in the context of $H2K^b$ when presented by MHC class I. Stimulation with the appropriate OVA peptide (SIINFEKL) or the entire OVA protein, when processed and presented by APCs, induce an antigen-specific adaptive immune response that leads to the proliferation of the OT-I CD8 T cells.

Animals were bred and kept under specific pathogen-free (SPF) conditions in the central animal laboratories (ZTL) of the University medical centre of Regensburg. Mice had unlimited access to sterilised water and food. Cages were filled with sterile bedding and contained enrichment. The relative humidity in the ZTL facilities was between 45-65 % at an average temperature of 22 ± 2 °C with a dark-light cycle of 12 h.

Table 1: Origin and designation of mice used in this study.

Name/Strain	Origin
C57BL/6JRj wild type	Janvier Labs (Le Genest Saint Isle, France) or in-house breeding
C57BL/6NRj wild type	Janvier Labs (Le Genest Saint Isle, France) or in-house breeding
B6.Tg(TcraTcrb)1100Mjb x B6.SJL-Ptprc^{a} Pepc^{b}/BoyJ (Referred to as "OT-I")	In-house breeding
B6.FVB-Tg$^{(Itgax-DTR/EGFP)57Lan}$/J (Referred to as "CD11c-DTR")	Femora and tibiae were kindly provided by Diana Dudziak from the Department of Dermatology of the University Hospital Erlangen
B6.129S7-Ifngr1^{tm1Agt}/J (Referred to as "IFNγR$^{-/-}$")	In-house breeding; AG Edinger, Central animal laboratories (ZTL) at the University Hospital Regensburg
B6.129S7-Ifng^{tm1Ts}/J (Referred to as "IFNγ$^{-/-}$")	In-house breeding; AG Poeck, Central animal laboratories (ZTL) at the University Hospital Regensburg
C57BL/6J-Tekcre Arg1 flox (Referred to as "Arg1$^{-/-}$")	Femora and tibiae were kindly provided by Ulrike Schleicher/Christian Bogdan from the Institute for Clinical Microbiology, Immunology and Hygiene of the University Hospital Erlangen
C57BL/6- INOS-/- x Arg B6 TCre/flox (Referred to as "iNOS$^{-/-}$")	Femora and tibiae were kindly provided by Ulrike Schleicher/Christian Bogdan from the Institute for Clinical Microbiology, Immunology and Hygiene of the University Hospital Erlangen
B6.129P2-Myd88^{tm1Aki} (Referred to as "MyD88$^{-/-}$")	Femora and tibiae were kindly provided by Annett Ziegler/Ulrich Kalinke from the TWINCORE Hannover
C57BL/6J-Ticam1^{Lps2} (Referred to as "TRIF$^{-/-}$")	Femora and tibiae were kindly provided by Annett Ziegler/Ulrich Kalinke from the TWINCORE Hannover

2.2 Material

2.2.1 Bacterial strains

Detailed information about the used bacterial strains are written in Table 2.

Table 2: Bacterial strains used for immune cell stimulation.

Name	Strain details	Source	Used inactivation protocols
***S. epidermidis* 614**	*Staphylococcus epidermidis* EStaSa614 (B11-10.12.0163)	IMHR	Heat-inactivation; UV-attenuation
***S. epidermidis* 617**	*Staphylococcus epidermidis* EStaSa617 (B11-10.26.022)	IMHR	Heat-inactivation
***S. epidermidis* 618**	*Staphylococcus epidermidis* EStaSa618 (B11-10.26.0067)	IMHR	Heat-inactivation
***S. epidermidis* 912**	*Staphylococcus epidermidis* EStaSa1370 (NIHLM040)	BEI Resources HM-912	Heat-inactivation
***S. epidermidis* 918**	*Staphylococcus epidermidis* EStaSa1369 (NIH05001)	BEI Resources HM-918	Heat-inactivation
***L. rhamnosus* 473**	*Lactobacillus rhamnosus* EStaSa473 (B09-10.28.0163)	IMHR	UV-attenuation

IMHR = Institute of Clinical Microbiology and Hygiene at the University Hospital Regensburg

2.2.2 Cell culture media and buffers

Table 3: Composition of cell culture media and buffers.

Medium/Solution	Ingredients
Cell culture medium	500 ml RPMI 1640 medium 50 ml FCS (10 %; Sigma) heat-inactivated 5 ml Pen/Strep (1%; final conc.: 100 U/ml) 500 µl β-Mercaptoethanol (final conc.: 50 µM)
FACS buffer	2 l PBS 40 ml FCS (2%, Sigma)
Immature cell culture medium	500 ml RPMI 1640 medium 50 ml FCS (10 %; PAN) heat-inactivated 5 ml Pen/Strep (1%; final conc.: 100 U/ml) 500 µl β-Mercaptoethanol (final conc.: 50 µM)
MACS buffer	2 l PBS 10 g BSA (0.5 %) 8 ml EDTA 0.5 M (final conc.: 2 mM)

2.2.3 Chemicals, reagents and stimuli

Table 4: Chemicals, reagents and stimuli used in this study.

Name	Manufacturer	Catalogue number
ACK Lysing Buffer	Gibco	A1049201
BD Bacto™ Dehydrated Agar	Fisher Scientific	BD 214010
BD Horizon™ Brilliant Stain Buffer Plus	BD Biosciences	566385
BD OptEIA™ TMB Substrate Reagent Set	BD Biosciences	555214
BD™ Difco™ Lactobacilli MRS Broth	Fisher Scientific	BD 288130
Bovine serum albumin (BSA)	Sigma-Aldrich	A4503
Bovine serum albumin (BSA)	PanReac AppliChem	A1391
Bovine serum albumin (BSA)	Sigma-Aldrich	A9418-10G
Diphtheria Toxin, Unnicked, Corynebacterium diphtheriae - Calbiochem	Sigma-Aldrich	322326
DPBS (Dulbecco's Phosphate buffered saline)	Gibco	14190-094

Continuation of Table 4.

Name	Manufacturer	Catalogue number
eBioscience™ Foxp3 / Transcription Factor Staining Buffer Set	Invitrogen	00-5523-00
Ethanol ≥96 %, denatured	Carl Roth	T171.4
FcR Blocking Reagent, mouse	Miltenyi Biotec	130-092-575
FCS (Fetal Calf Serum)	PAN Biotech	P30-8500
FCS (Fetal Calf Serum)	Sigma-Aldrich	F7524
GM-CSF/CSF2 Protein, Mouse, Recombinant	Sino Biological	51048-MNAH
IL-2 (PROLEUKIN® S; 1 x 10^6 units/ml)	Novartis	CLB-P-476-750-11240
Normal saline (NaCl)	G-Biosciences	786-560
$OVA_{257-264}$ peptide fragment (SIINFEKL)	ANASPEC	AS-60193-1
Penicillin/Streptomycin (10.000 U/ml) (Referred to as “Pen/Strep“)	Sigma-Aldrich	P0781
Penicillin/Streptomycin (10.000 U/ml) (Referred to as “Pen/Strep“)	Gibco	15140-122
ProClin™ 300	Sigma-Aldrich	48912-U
Recombinant Murine IFN-γ	Peprotech	315-05-20UG
RLT Plus Buffer	Qiagen	1053393
RPMI 1640 Medium	Gibco	21875-034
Streptavidin-R-Phycoerythrin (ver 7), 1 mg	Agilent	PJRS301-1
SYTO™9 green fluorescent nucleic acid stain	Thermo Fisher Scientific /Invitrogen	S34854
TheraPEAK ACK Lysing Buffer	Lonza	LONBP10-548E
Thermo Scientific™ Columbia Blood Agar with Sheep Blood Medium	Thermo Scientific	PB5039A
Titriplex III	Merck	1.08418
Trypan Blue (0.5% in PBS)	Sigma-Aldrich	T6146-5g
Trypsin-EDTA 10x (1x in PBS)	Sigma-Aldrich	T4174
Tryptic Soy Broth	Merck Millipore	1.05459.5000

Continuation of Table 4.

Name	Manufacturer	Catalogue number
Türk's solution	Sigma-Aldrich	1092770100
TWEEN® 20	Sigma-Aldrich	P1379
UltraPure™ 0,5 M EDTA, pH 8,0	Invitrogen	15575020
UltraPure™ 0,5 M EDTA, pH 8,0	Invitrogen	15575020
β-Mercaptoethanol (50 mM)	Gibco	31350-010

2.2.4 Analysis and Labelling Kits

The used kits are listed in Table 5. The Alexa Fluor™ 647 Protein Labeling Kit was used to label the LTA antibody (Invitrogen; MA1-40134) for flow cytometry. CellTrace™ Violet Cell Proliferation Kit and Vybrant™ CFDA SE Cell Tracer Kit were used to label OT-I CD8 T cells in order to track proliferation in flow cytometry. The Mouse IFN-gamma DuoSet ELISA and the Nitrite assay kit (Griess Reagent) were used to detect IFNγ or NO levels in cell culture supernatants.

Table 5: List of used Kits.

Name	Manufacturer	Catalogue number
Alexa Fluor™ 647 Protein Labeling Kit	Thermo Fisher Scientific / Invitrogen	A20173
CellTrace™ Violet Cell Proliferation Kit (Referred to as “CTV“)	Thermo Fisher Scientific / Invitrogen	C34557
Mouse IFN-gamma DuoSet ELISA	R&D Systems	DY485
Nitrite assay kit (Griess Reagent)	Merck	MAK367-1KT
Vybrant™ CFDA SE Cell Tracer Kit (Referred to as “CFSE“)	Thermo Fisher Scientific / Invitrogen	V12883

2.2.5 Beads

Beads used for compensation in flow cytometry, stimulation of OT-I CD8 T cells, for MACS purification of OT-I CD8 T cells or for Luminex assay are listed in Table 6.

Table 6: List of stimulation, compensation, separation and Luminex beads.

Name	Manufacturer	Catalogue number
Anti-Biotin MicroBeads UltraPure	Miltenyi Biotec	130-105-637
OneComp eBeads™ Compensation Beads	Thermo Fisher Scientific /Invitrogen	01-1111-42
SeroMAP™ Microspheres	DiaSorin	L100-S048-04, L100-S089-04, L100-S005-04, L100-S036-04, L100-S027-04, L100-S052-04
Treg expansion Kit, mouse (anti-CD3/CD28 beads)	Miltenyi Biotec	130-095-925
UltraComp eBeads™ Plus Compensation Beads	Thermo Fisher Scientific /Invitrogen	01-3333-42

2.2.6 Antibodies

Antibodies or Kits that were used for flow cytometry analysis are listed in Table 7. Table 8 lists the neutralizing antibodies which were used to inhibit cytokines in cell cultures. All neutralizing antibodies were used in a working concentration of 20 µg/ml. Antibodies used for MACS isolation of specific cell populations are registered in Table 9.

Table 7: Antibodies used for flow cytometry analysis.

Antigen	Fluorochrome	Clone	Isotype	Reactivity	Manufacturer	Catalogue number
Annexin V	AF647	IRF4.3E4			Life Technologies	1678857
Biotin	APC/Cy7				BioLegend	405208
CD11b	BUV395	M1/70	Rat IgG2b κ	M	BD Biosciences	563553
CD11b	PerCP/Cy5.5	M1/70	Rat IgG2b κ	M,H	BioLegend	101228
CD11b	AF488	M1/70	Rat IgG2b κ	M,H	BioLegend	101217
CD11b	BV605	M1/70	Rat IgG2b κ	M,H	Biolegend	101237/ 101257
CD11b	BV605	M1/70	Rat IgG2b κ	M,H	Biolegend	101237/ 101257

Continuation of Table 7.

Antigen	Fluorochrome	Clone	Isotype	Reactivity	Manufacturer	Catalogue number
CD11c	PE/Dazzle 594	N418	Armenian Hamster IgG	M	BioLegend	117348
CD11c	PB	N418	Armenian Hamster IgG	M	BioLegend	117321/ 117322
CD11c	BUV496	HL3	Armenian Hamster IgG1, λ2	M	BD Biosciences	750483
CD11c	PE-CF594	N418	Armenian Hamster IgG2	M	BD Biosciences	565591
CD19	APC	6D5	Rat IgG2a, κ	M	BioLegend	115512
CD19	PE/Cy7	6D5	Rat IgG2a, κ	M	BioLegend	115520
CD197 (CCR7)	PE	4B12	IgG2a, κ	R	BioLegend	120105
CD274 (PD-L1)	BUV737	MIH5	IgG2a, λ, Rat SD	M	BD Biosciences	741877
CD3	BV711	145-2C11	Arm. Hamster IgG	M	BioLegend	100241
CD4	BV785	RM4-5	Rat IgG2a κ	M	BioLegend	100552
CD4	BUV395	GK1.5	Rat IgG2b κ	M	BD Biosciences	563790
CD4	PE/Cy7	RM4-5	Rat IgG2a, κ	M	BioLegend	100528
CD4	BV421	RM4-5	Rat IgG2a, κ	M	BioLegend	100544
CD40	PB	3/23	Rat IgG2a, κ	M	BioLegend	124626
CD44	BV605	IM7	Rat IgG2b κ	M	BioLegend	103047
CD45.1	BUV737	A20 (RUO)	Mouse A.SW IgG2a, κ	M	BD Biosciences	612811
CD45.1	BV605	A20	Mouse (A.SW) IgG2a κ	M	BioLegend	110738
CD45.2	PerCP/Cy5.5	104	Mouse (SJL) IgG2a κ	M	BioLegend	109828
CD45.2	AF647	104	Mouse (SJL) IgG2a κ	M	BioLegend	109818
CD62L	APC	MEL-14	Rat IgG2a, κ	M	BioLegend	104412
CD80	AF647	16-10A1	Arm. Hamster IgG	M	BioLegend	104718
CD85k (ILT3)	AF647	H1.1	Arm. Hamster IgG	M	BioLegend	144906
CD86	PE/Cy7	GL-1	Rat IgG2a, κ	M	BioLegend	105014
CD86	FITC	GL-1	Rat IgG2a, κ	M	BioLegend	105005/ 105006

Continuation of Table 7.

Antigen	Fluorochrome	Clone	Isotype	Reactivity	Manufacturer	Catalogue number
CD86	BUV805	GL1	Rat LOU, also known as Louvain, LOU/C, LOU/M IgG2a, κ	M	BD Biosciences	741946
CD8a	BV605	53-6.7	Rat IgG2a κ	M	BioLegend	100744
CD8a	BV421	53-6.7	Rat IgG2a, κ	M	BioLegend	100738
eBioscience™ Fixable Viability Dye eFlour 506	eFlour 506				Invitrogen	65-0866-14
eBioscience™ Fixable Viability Dye eFlour 780	eFlour 780				Invitrogen	65-0865-14
I-A/I-E (MHC II)	PE	M5/114.15.2	Rat IgG2b κ	M	BioLegend	107607
I-A/I-E (MHC II)	AF700	M5/114.15.2	Rat IgG2b κ	M	BioLegend	107622
I-A/I-E (MHC II)	AF488	M5/114.15.2	Rat IgG2b κ	M	BioLegend	107616
Lipoteichoic Acid (LTA); labelled with Alexa Fluor™ 647 Protein Labeling Kit	AF647	55	Mouse IgG3	Bacteria	Invitrogen	MA1-40134
MHC Class I (H2Db)	PE/Cy7	KH95	Mouse (BALB/c) IgG2b, κ	M	BioLegend	111515/ 111516

Table 8: Neutralizing antibodies and isotype controls.

Isotype	Manufacturer	Catalogue number
Armenian Hamster IgG Isotype Control (eBio299Arm), Functional Grade, eBioscience™	Invitrogen	16-4888-85
Rat IgG1 kappa Isotype Control (eBRG1), Functional Grade, eBioscience™	Invitrogen	16-4301-85
IFN gamma Monoclonal Antibody (XMG1.2), Functional Grade, eBioscience™	Invitrogen	16-7311-85
TNF alpha Monoclonal Antibody (TN3-19.12), Functional Grade, eBioscience™	Invitrogen	16-7423-85

Table 9: Antibodies used for MACS cell isolation.

Antigen	Fluorochrome	Clone	Isotype	Reactivity	Manufacturer	Catalogue number
CD11b	Biotin	M1/70	Rat IgG2b κ	M,H	BioLegend	101204
CD11c	Biotin	N418	Arm. Hamster IgG	M	BioLegend	117304
CD19	Biotin	6D5	Rat IgG2a, κ	M	BioLegend	115504
CD4	Biotin	RM4-5	Rat IgG2a, κ	M	BioLegend	100508
CD45R/B220	Biotin	RA3-6B2	Rat IgG2a, κ	M,H	BioLegend	103204
CD8a	Biotin	53-6.7	Rat IgG2a, κ	M	BioLegend	100704
Ter-119	Biotin	TER-119	Rat IgG2b κ	M	BioLegend	116203/116204

Table 10: Antibodies used for Luminex assay.

Parameter	Manufacturer	Catalogue number Kit	Catalogue number capture antibody	Catalogue number detection antibody
mu CCL2	BD Biosciences		551217	554444
mu CXCL10	Peprotech	900-M153		
mu IL10	BD Biosciences (BD OptEIA)	555252		
mu IL12p40	BD Biosciences		551219	554476
mu IL6	R&D Systems	DY406	MAB406	BAF406
mu TNFα	BD Biosciences (BD OptEIA)	558534		

2.2.7 Consumable materials

Table 11: List of consumable materials.

Material	Manufacturer	Catalogue number
1.5 ml tube	Sarstedt	72.690.001
15 ml tube	Sarstedt	62.554.502
40 µM cell strainer	Sarstedt	83.3945.040
50 ml tube	Sarstedt	62.547.254
6-well cell culture plate, flat bottom	Greiner	657160
70 µM cell strainer	Sarstedt	83.3945.070
96-well cell culture plate, flat bottom	Greiner	655 180
96-well cell culture plate, round bottom	Corning	3799
96-well cell culture plate, V bottom	Sarstedt	83.3926
Adhesive film (Acetate foil for microtest)	Sarstedt	82.1586
Cannula, 27G (ø 0,40 x 20 mm)	Braun	4657705
Clear Flat-Bottom Immuno Nonsterile 96-Well Plates (Maxisorp Nunc-immuno plate)	Thermo Scientific	442404
DNA LoBind Tube 1.5 ml	Eppendorf	0030 108,051
FACS filter, mesh made of polyamide (41µm)	Labomedic	2183468DCCC
FACS tube, 5 ml	Sarstedt	55.1579.002
Fast-Read counting chambers	Kisker biotech	390497
Filter tip PP, 0 - 20 µl	Nerbe plus	06-622-5300
Filter tip PP, 0 - 200 µl	Nerbe plus	06-662-5300
Filter tip PP, 0.1 - 10 µl	Nerbe plus	06-613-5300
Filter tip PP, 100 - 1250 µl	Nerbe plus	06-695-5300
LS columns	Miltenyi Biotec	130-042-401
Petri dish, 92 x 16 mm	Sarstedt	82.1473
Pre-Separation filter, 30 µm	Miltenyi Biotec	130-041-407
SafeSeal tube 0.5 ml	Sarstedt	72.704
Serological pipette, 10 ml	Sarstedt	86.1254.001
Serological pipette, 2 ml	Sarstedt	86.1252.001
Serological pipette, 25 ml	Sarstedt	86.1685.001
Serological pipette, 5 ml	Sarstedt	86.1253.001
Syringe, 2 ml (BD Discardit II)	BD Biosciences	300928
Syringe, 5 ml (BD Discardit II)	BD Biosciences	309050

2.2.8 Devices

Table 12: List of devices.

Device	Manufacturer
Anoxomat	Mart Microbiology
BD FACSAria™ Fusion high throughput cell sorter	BD Biosciences
BD FACSCelesta™ cell analyzer	BD Biosciences
BD FACSymphony™ A5 (SORP) cell analyzer	BD Biosciences
BD™ High Throughput Sampler (HTS)	BD Biosciences
Biometra TS1 ThermoShaker	Analytik Jena
Centrifuge 5417R	Eppendorf
Centrifuge 5424R	Eppendorf
Heracell™ 240i CO2 Incubator	Thermo Scientific
Heraeus Multifuge X3 FR centrifuge	Thermo Scientific
HeraSafe™ 2030i 1.2 Class II Biological Safety Cabinet	Thermo Scientific
HeraSafe™ KS 12 Class II Biological Safety Cabinet	Thermo Scientifi
Luminex 100 System	Luminex Corporation (meanwhile DiaSorin)
MACS™ Multistand	Miltenyi Biotec
ProteinSimple imager	AlphaImager HP
QuadroMACS™ Separator	Miltenyi Biotec
SmartSpecPlus spectrophotometer	Bio-Rad
Stratalinker 1800 Agilent Genomics	Stratagene
TECAN Spark 10M	Tecan Trading AG

2.2.9 Software

Table 13: List of used software.

Software	Manufacturer
BioRender	BioRender
FACSDiva™ (v9.1 for Windows)	BD Biosciences
FlowJo™ (v10.10.0 for Windows)	BD Biosciences
GraphPad Prism 10 (v10.1.1 for Windows)	GraphPad Software
Microsoft Office Standard 2016	Microsoft
R version 4.3.3 (2024-02-29)	R Core Team (2024); _R: A Language and Environment for Statistical Computing_. R Foundation for Statistical Computing, Vienna, Austria.

2.3 Methods

2.3.1 Preparation of heat-inactivated bacteria lysates and UV-attenuated bacteria

Heat-inactivated bacterial lysates and UV-attenuated suspensions were prepared and provided by the Institute of Clinical Microbiology and Hygiene at the University Hospital Regensburg (IMHR). Information on the respective preparation protocol is described below.

Preparation of heat-inactivated bacterial lysates:
Pre-cultures were first grown for the production of the respective heat-inactivated bacterial lysates. 100 µl of the pre-culture was inoculated into 200 ml TSB medium in a 1 l Erlenmeyer flask. The cultures were incubated at 37 °C, 210 rpm on a shaker for 24 hours. After incubation, they were transferred to 15 ml centrifuge tubes and centrifuged at 4 °C, 4500 rpm (5000 g) for 15 min. Pellets of the TSB cultures were resuspended in 10 ml PBS. Subsequently, the optical density $(OD)_{600}$ was measured to determine the cell count and to adjust the bacteria to $5x10^9$ cells/ml. For heat inactivation, the suspensions were heated for 15 min at 95°C on a thermal shaker. To check for inactivation of bacteria, 100 µl of each heat-inactivated bacterial lysate was plated onto TSB plates and incubated overnight at 37 °C. If no growth was detected, the heat-inactivated bacterial lysates could be used for experiments. The heat-inactivated bacterial lysates were aliquoted at 1 ml each and stored at -80 °C.

In the course of the thesis, a second method for bacterial inactivation could be established at the IMHR. UV-irradiation of bacteria ensures that they are no longer capable of replication. An advantage of this method is that bacteria are not lysed and denatured as for the preparation of heat-inactivated bacterial lysates. As UV-attenuated bacteria are expected to be more physiologic than the heat-inactivated bacterial lysates, from this point on only UV-attenuated bacteria were used in the experiments. However, before changing the protocol, it was ensured that both heat-inactivated bacterial lysate and UV-attenuated bacteria behaved the same way in the experiments with regard to the activation of BMDCs and the influence on OT-I CD8 T cell proliferation.

Preparation of UV-attenuated bacteria:
Bacteria were pre-cultured on plates. *S. epidermidis* was grown on Columbia Blood Agar with Sheep Blood Medium plates for one day at 37 °C. To culture *L. rhamnosus*, plates were prepared by adding 15 g agar to 1 l MRS medium. *L. rhamnosus* was grown for two days at 37 °C in an anaerobic jar using an anoxomat system that sets 6 % O2 saturation.
For overnight cultures, a single colony of each bacterium was picked and inoculated in the respective medium. *S. epidermidis* was cultured in 25-150 ml LB medium in a 250 ml baffle flask and incubated at 37 °C, 215 rpm for 24 h on a shaker. In the case of *L. rhamnosus*, the single colony was inoculated into 50 ml MRS medium and incubated for two days at 37 °C without shaking. After incubation, the cultures were centrifuged at 4 °C, 4500 rpm (5000 g) for 10 min. The pellet was resuspended in 10 ml PBS and the whole procedure was repeated two more times.

The concentration of the bacterial suspensions were adjusted to $5x10^9$ CFU/ml using OD_{600} measurement in a SmartSpecPlus spectrophotometer. An OD_{600} of 1 corresponds to $1 x 10^9$ CFU/ml *S. epidermidis* or $1 x 10^8$ CFU/ml *L. rhamnosus*. The suspensions were then irradiated with UV light (302 nm) for 4 h in a ProteinSimple imager. During the project, the UV irradiation source was changed to the Stratalinker 1800 Agilent Genomics, where UV irradiation could be reduced to 10 min. 50 µl of the UV-attenuated bacterial suspensions were plated onto TSB plates (*S. epidermidis*) or Columbia Blood Agar with Sheep Blood Medium plates (*L. rhamnosus*) and incubated overnight at 37 °C. If this growth control showed no bacterial growth, the UV-attenuated bacteria were used in the experiments. The UV-attenuated bacteria were stored at 4 °C until successful irradiation was confirmed. The production of UV-attenuated bacteria was always timed to have as fresh as possible suspensions for experiments and new UV-attenuated bacteria were produced for each experiment.

2.3.2 SYTO™ 9 labelling of bacteria

For RNAseq analysis of BMDCs it was important to differentiate between BMDCs that have phagocytised bacteria and those that have not. For this purpose, live bacteria were labelled with SYTO 9, a green fluorescent nucleic acid stain. It can be used to stain RNA and DNA in Gram-positive and Gram-negative bacteria. The dye shows a very low intrinsic fluorescence when not bound to nucleic acids, but largely enhanced fluorescence upon binding. The SYTO 9 dye has an absorption maximum at 485/486 nm and an emission maximum at 498/501 nm and can be detected in the “FITC-channel” in the used cytometers.

Live *S. epidermidis* and *L. rhamnosus* were cultured as already described in chapter 2.3.1. After incubation, the bacterial suspensions were centrifuged at 4 °C, 4500 rpm (5000 g) for 15 min. The pellet was resuspended in 15 ml NaCl and the whole procedure was repeated two more times. OD_{600} measurement was used to set the bacterial suspensions to a concentration of $1x10^8$ CFU/ml. The washing is important to avoid medium residues and resuspension in NaCl is required, as phosphate-containing buffers can disturb the staining.

Prior usage, the SYTO 9 dye was warmed to room temperature (RT). 1 ml of the adjusted bacterial suspension was stained with 10 µM SYTO 9 (2 µl of 5 mM stock solution) and incubated 15 min at RT in the dark. Afterwards, the bacteria were washed twice with cell culture medium (centrifugation at RT, maximum speed for 5 min) to remove unbound SYTO 9. Then SYTO 9-stained bacteria were resuspended in 1 ml cell culture medium and were used for stimulation.

2.3.3 Preparation of control media of UV-attenuated *S. epidermidis* suspensions

To exclude the possibility that contaminants from bacterial culture media, metabolic products or secreted factors during bacterial culture are responsible for the suppression of OT-I CD8 T cell proliferation, supernatants and media were collected during the production process of UV-attenuated *S. epidermidis* described in chapter 2.3.1. Supernatants were collected at different

steps of the protocol. Supernatants and media used as controls are described in Table 14.

Table 14: Control supernatants and media from UV-attenuated *S. epidermidis* preparation.

Control	Collection step
Sterile LB medium (Referred to as "LB")	Aliquot of sterile LB medium used to set up bacterial culture
***S. epidermidis* culture supernatant** (Referred to as "LB-S")	Supernatant from *S. epidermidis* growth culture collected after first centrifugation step
Washing PBS (Referred to as "PBS-S")	Supernatant PBS collected after second centrifugation of the two washing steps during production
***UV-attenuated S. epidermidis* suspension PBS** (Referred to as "PBS-UV")	An aliquot of a stored ready to use UV-attenuated *S. epidermidis* suspension was centrifuged again directly prior usage and the supernatant was collected and used

For experiments, the controls were treated as they were a UV-attenuated *S. epidermidis* suspension and therefore they were diluted in exactly the same way as it was done for the generation of the respective CFU concentrations from a UV-attenuated *S. epidermidis* suspension.

2.3.4 Bone marrow-derived dendritic cell generation

As only limited numbers of DCs can be isolated from murine organs, BMDCs were used in this study. They were generated from murine bone marrow cells using granulocyte-macrophage colony-stimulating factor (GM-CSF) and were used as APCs. BMDCs are thought to be genetically and functionally most similar to inflammatory DCs. In vivo, these are DCs that are characterised by TNFα and iNOS production and are involved in inflammation (Xu et al. 2007; Thwe and Amiel 2018). BMDCs are able to present exogenous antigens to CD8+ T cells. The so-called cross-presentation plays an important role in the induction of anti-tumour responses or pathogenic infections that do not directly infect DCs but are only present extracellularly (Datta et al. 2003). The used protocol for the generation of bone marrow-derived dendritic cells from Lutz et al. allows the production of mature and immature BMDCs in large numbers (Lutz et al. 1999). The protocol was adopted with a few adaptions and is described in the following.

Mice were sacrificed by cervical dislocation. Femora and tibiae of the hind legs were removed and freed from surrounding tissue. The following workflow was performed in a biological safety cabinet under sterile conditions. Intact bones were soaked in 70 % ethanol for two minutes for disinfection and dried at air. For each biological replicate, a separate 50 ml tube was pre-filled

with 5 ml RPMI 1640 medium. Next, both epiphyses of the bone were cut and the bone marrow was flushed into a prepared 50 ml tube, using 5 ml RPMI 1640 medium in a 5 ml syringe fitted with a 27G cannula. Cell clusters were disintegrated by pipetting and cell number was counted using Türk's solution and a fast-read counting chamber. 2 x 10^6 bone marrow cells were transferred into bacterial petri dishes and filled up with immature cell culture medium or cell culture medium to 10 ml, supplemented with 20 ng/ml recombinant murine granulocyte-macrophage colony-stimulating factor (rmGM-CSF). Cells were incubated at 37 °C and 5 % CO_2.

On day 3, 10 ml of the respective medium supplemented with 20 ng/ml rmGM-CSF were added to the cultures. On days 6 and 8 (if not already used on day 8), 10 ml of the cell culture supernatant was carefully collected and centrifuged at 500 g, 5 min, RT. The supernatant was discarded, the remaining cell pellet was resuspended in 10 ml of the respective medium (supplemented with 20 ng/ml rmGM-CSF) and transferred back into the original petri dish. On day 10 (if not used on that day), the medium was changed as described for days 6 and 8, with the exception, that the concentration of rmGM-CSF within the fresh medium was reduced to 10 ng/ml.

The BMDCs could be used for experiments from day 8 on. For this purpose, the non-adherent BMDCs were flushed out of the petri dishes and thus separated from the adherent bone marrow-derived macrophages (BMDMs). They were then centrifuged (500 g, 5 min, RT), resuspended in cell medium, counted with Trypan Blue solution and adjusted to the required concentration.

The use of cell culture medium or immature cell culture medium to generate BMDCs resulted in BMDCs with different expression levels of maturation markers such as CD86 and MHC class II. Therefore, BMDCs generated with "immature cell culture medium" are referred to as "immature BMDCs" and those generated with "cell culture medium" are referred to as "mature BMDCs". The mature BMDCs showed a higher expression of maturation-associated markers than the immature BMDCs.

The term "BMDC" always refers to the "mature BMDCs" generated with standard cell culture medium. If BMDCs were used that were generated with "immature cell culture medium", this is explicitly indicated by the designation "immature BMDCs". This designation applies to the entire study.

2.3.5 Isolation of OT-I CD8 T cells from lymphoid tissues using magnetic cell separation

Before OT-I CD8 T cells from lymphatic organs can be used for the experiments, they must first be isolated and purified in order to separate them from other cell types present in these organs. Only in this way, observations in experiments can be clearly assigned to the OT-I CD8 T cells used. Magnetic cell separation (MACS) and fluorescence-activated cell sorting (FACS) are established methods to purify different T cell populations. From here on, OT-I CD8+ T cells are referred to as OT-I T cells in the methods chapter.

First, mice were sacrificed by cervical dislocation and spleens and mesenteric as well as inguinal lymph nodes were isolated under aseptic conditions in the animal facilities and transferred into a tube containing cold PBS. From now on, lymphatic organs and resulting cell suspensions were kept on ice between working steps and handled in a biological safety cabinet under sterile conditions. A 40 µm cell strainer was put on a 50 ml tube and moistened with 4 ml cold PBS. Organs were rubbed trough the cell strainer using the plunger of a 2 ml syringe. The cell strainer was rinsed with 5 ml cold PBS, shortly rubbed again, and rinsed with another 5 ml of cold PBS. The cell suspensions were centrifuged at 700 g, 4 °C for 3 min and the supernatant was discarded. Next, the remaining cell pellet was resuspended in 2 ml RT-warmed ammoniochloride-potassium (ACK)-lysis buffer and incubated for 2 min at RT. To stop lysis, 9 ml PBS (containing 5 % FCS) were added and cell suspensions were centrifuged (700 g, 4 °C, 3 min). The supernatant was discarded. The cell pellet was resuspended in 5 ml cold FACS buffer, flushed trough a new 4 µm cell strainer into a new 50 ml tube, and the cell strainer was rinsed with 5 ml cold FACS buffer. After an additional centrifugation step, the cell pellet was resuspended in 250 µl antibody mix (FACS buffer plus 2.5 µl of each biotin-conjugated antibody), transferred into a 1.5 ml tube and incubated on ice for 20 min. The antibody mix depends on the desired cell population to be separated and a detailed list of the mixes is given in Table 15. The antibody mixes were designed for untouched MACS. All unnecessary cells were actively labelled with antibodies and only the population of interest, in this study the OT-I T cells, was not labelled with antibodies. This is to prevent the cells from being stimulated by antibody binding prior to the experiment. In the later course of the isolation (see below), all unwanted and antibody-labelled cell types were caught by the magnet and only the cell population of interest ran through the column and is then collected in the flow-through.

After incubation, the cell suspensions were washed (centrifugation at 1000 g, 4 °C, 2 min followed by discarding the supernatant and resuspending the pellet in the respective buffer) two times with 1 ml FACS buffer to remove unbound antibodies. Following the second wash step, the pellet was resuspended in 900 µl MACS buffer (see Table 3) and 100 µl anti-biotin micro beads, which couple to the biotin-conjugated antibodies. Cells were incubated for 20 min on ice. Afterwards, cells were washed two times with 1 ml MACS buffer, followed by resuspension in 1 ml cold MACS buffer. A LS MACS column was fixed on a manual MACS magnetic separator and equilibrated with 2 ml cold MACS buffer. Subsequently a new 15 ml tube was placed under the column to collect the flow-through and the cell suspension was transferred onto the column. Then, the column was rinsed three times with 3 ml cold MACS buffer to increase the cell yield. The OT-I cell population was now in the flow-through in the 15 ml tube, while all other unwanted cells were still retained in the magnet.

The OT-I T cell population was purified from other contaminating cell types and could subsequently be used for experiments, CFSE and CTV labelling (chapter 2.3.6) or further separation into subtypes by FACS sorting (chapter 2.3.9).

Table 15: Antibody mixes used for MACS of OT-I T cells.

Population of interest and intended use	Used antibodies
OT-I T cells for further FACS sorting	B220-biotin, CD4-biotin, CD11b-biotin, CD19-biotin, Terr-119-biotin
OT-I T cells for cell culture	CD4-biotin, CD11b-biotin, CD11c-biotin, CD19-biotin

2.3.6 CFSE and CTV labelling

In order to trace OT-I T cell proliferation, the OT-I T cells were labelled with either CellTrace™ Violet Cell Proliferation Kit (CTV) or Vybrant™ CFDA SE Cell Tracer Kit (CFSE). These cell tracer dyes pass the plasma membrane and diffuse into cells where they are cleaved by intracellular esterases. Afterwards they bind covalently to intracellular amines resulting in stable fluorescent signals. During cell division, the dye and therefore the fluorescence intensity is halved between the daughter cells and can be distinguished from the previous generation by its weaker intensity. This allows up to ten divisions to be traced.

After the final centrifugation of OT-I T cell isolation (see chapter 2.3.5), the cell pellet is resuspended in 5 ml (for CFSE labelling) or 2.5 ml (for CTV labelling) PBS, which has been pre-warmed to 37 °C. In the case of CFSE labelling, 5 ml PBS, containing 1 µM CFSE (1 µl from 10 mM stock) are added to the cell suspension. For CTV labelling, 2.5 ml PBS, containing 5 µM CTV (5 µl from 5 mM stock) are added. Immediately afterwards, the suspension was briefly vortexed and incubated for 10 min at 37 °C, 5 % CO_2 in the dark. After incubation, cells were centrifuged (700 g, 3 min, RT) and the supernatant was discarded. To quench unconjugated reagent, the cell pellet was resuspended in 10 ml warm cell culture medium and incubated at 37 °C, 5 % CO_2 for 30 min. Following a further centrifugation step, the cells were resuspended in cell culture medium and were ready for further use.

2.3.7 OVA-specific co-culture systems

In order to investigate the possible influence of commensals such as *S. epidermidis* on antigen-specific immune responses, co-culture systems of OVA-specific OT-I T cells and BMDCs were used. OT-I T cells express a transgenic TCR that recognises a specific peptide sequence of OVA when presented by the MHC class I molecule H-2Kb, resulting in OT-I T cell activation and proliferation. The transgenic TCR specifically binds the peptide sequence $OVA_{257-264}$ (SIINFEKL) and consists of the variable region 2 of the α-chain (Va2) and the variable region 5 of the β-chain (Vb5) (Hogquist et al. 1994; Pritchard et al. 2016; Nakagawa et al. 2022).

WT or KO BMDCs (see 2.3.4) were co-cultured with OT-I T cells. The added OVA protein (100 µg/ml) is taken up, processed and presented by the BMDCS. Alternatively, the appropriate peptide SIINFEKL was used for stimulation. Unless otherwise stated, 20,000 BMDCs were co-

cultured with 200,000 OT-I T cells in 200 µl cell culture medium, containing 20 units/ml IL-2. Dependent on the experiment, different concentrations of *S. epidermidis* or *L. rhamnosus*, stimuli or inhibitory antibodies were added to the co-culture. The co-cultures were incubated at 37 °C, 5 % CO_2.

As read-out, the proliferation of labelled OT-I T cells (see chapter 2.3.6) or analysis of the supernatant for cytokines (see chapter 2.3.10) were used. In other experiments, OT-I T cells were sorted for proliferating and non-proliferating cells after 3 days of co-culture and were used for RNAseq analysis (see chapter 2.3.13).

2.3.8 Flow cytometry analysis

Flow cytometry (FACS™, Fluorescence Activated Cell Sorting) is a laser-based analysis technique to measure characteristics and function of a single cell. It enables a rapid analysis of the visible light scatter, to determine cell size granularity, as well as multiple fluorescent parameters. Flow cytometry is widely applied in the field of biomedical research such as in immunology (McKinnon 2018).

In this thesis, flow cytometry was used to identify cell types and quantify their state of activation and to trace proliferation of OT-I T cells. This was achieved by utilising the ability of flow cytometers to simultaneously analyse several parameters of cells in mixed populations. Immunophenotyping uses fluorochrome-conjugated antibodies that target specific antigens on the cell surface as well as intracellularly to antigens, transcription factors and cytokines. Cell populations can thus be identified using specific lineage markers, usually CD markers. Further characterisation is possible using activation markers (e.g. CD86) or antigen-specific markers (e.g. MHC class II). The use of CFSE or CTV (see chapter 2.3.6) allows to trace cell proliferation. The configurations and laser settings of the used flow cytometers BD FACSSymphony™ A5 and the BD FACSCelesta™ are listed in Table 16 and Table 17 respectively. The FACS DIVA software was used during analyses, to set the devices and acquisition settings and to control the measurement process. Samples were acquired using the tube mode of the FACS devices. If a large number of samples had to be measured, the BD™ High Throughput Sampler (HTS) connected to the FACSSymphony™ A5 was used. The HTS settings for the acquisition were set as shown in Table 18.

Table 16: Instrument configuration of the BD FACSCelesta™.

Laser	LP Filter	BP Filter	Fluorochromes
405 nm (violet)	-	450-40	BV421, Pacific Blue, DAPI
	505	525-50	BV510
	595	610-20	BV605
	655	670-30	BV650
	690	710-50	BV711
488nm (blue)	502	530-30	FITC, GFP, CFSE, AF488
	550	575-25	PE
	670	695-40	PerCP, PerCP-Cy5.5
	750	780-60	PE-Cy7
633 nm (red)	-	670-30	APC, AF647
	690	730-45	AF700
	755	780-60	APC-Cy7, APC-H7, APC-eF780, APC-Fire750

Compensation:

A major issue of the acquisition of a multicolour sample in flow cytometry is the physical overlap among the emission spectra of used fluorochromes, also known as spillover. This arises when the emission of one fluorochrome is sensed in a detector that is related to another fluorochrome. This can result in false positive signals and misinterpretation. Acquired signals from single colour controls and unstained controls for each fluorochrome in all detectors, are used to perform compensation. This single stain controls can either be run with cells or compensation beads. The information is then used by the FACSDiva™ software to mathematically remove the fluorescence spillover of any fluorochrome from all detectors where it is detected incorrectly. The compensation therefore ensures accurate measurement with multicolour panels (Biosciences 2009). UltraComp eBeads Plus were used for complex compensations with many colours or UV fluorochromes. Otherwise, the compensation was carried out with OneComp eBeads (compare Table 6). For this purpose, one drop of the compensation beads (or 200,000 cells) were stained for 20 min at 4 °C in 100 µl FACS buffer with the same concentration of antibody/fluorochrome as was to be used in the experiment. Individual stainings for all antibodies/fluorochromes used in a staining panel were prepared in this way. The compensation beads were then centrifuged at 1000 g, 2 min, 4 °C and resuspended in 200 µl FACS buffer. Unstained controls were included for subsequent exclusion of auto fluorescence. Using the measured single stain controls, the FACSDiva™ software automatically calculated the compensation, which was then applied to the respective experiment.

Table 17: Instrument configuration of the BD FACSSymphony™ A5.

Laser	LP Filter	BP Filter	Fluorochromes
355 nm (UV)	-	379-28	BUV395
	410	450-50	DAPI
	490	515-30	BUV496
	550	580-20	BUV563
	595	605-20	BUV615-P
	630	670-25	BUV661
	690	735-30	BUV737
	770	810-40	BUV805
405 nm (violet)	410	431-28	BV421, Pacific Blue, DAPI
	505	525-50	BV480, BV510
	550	586-15	BV570
	595	605-40	BV605
	635	677-20	BV650
	685	710-50	BV711
	735	750-30	BV750-P
	770	810-40	BV786
488nm (blue)	505	530-30	FITC, GFP, CFSE, AF488, BB515
	600	610-20	BB630-P
	635	670-30	PerCP
	685	710-50	PerCP-Cy5.5
	735	750-30	BB575-P
	770	810-40	BB790-P
561nm (yellow-green)	570	586-15	PE
	600	610-20	PE-TR, PE-Dazzle594, PE-eF610, AF594
	635	670-30	PE-Cy5
	685	710-50	PE-Cy5.5
	750	780-60	PE-Cy7
633 nm (red)	-	670-30	APC, AF647
	690	730-45	AF700
	750	780-60	APC-Cy7, APC-H7, APC-eF780, APC-Fire750

Table 18: HTS parameter settings

Parameter	Setting
Throughput Mode	Standard
Sample Flow Rate (µl/sec)	2.5
Sample Volume (µl)	80
Mixing Volume (µl)	60
Mixing Speed (µl/sec)	200
Number of Mixes	4
Wash Volume (µl)	200
Enable BLR	activated
BLR Period	150

Surface antibody staining:

All incubation steps during staining for surface markers were performed on ice or at 4 °C and whenever possible direct exposure of the fluorochromes to light was avoided. All centrifugation wash steps ran at 1000 g, 2 min, 4 °C.

In order to stain surface markers, the cells of interest were resuspended in 100 µl FACS buffer and transferred into a 96-well V bottom plate. In the case of primary cell suspensions from tissues or if cell suspensions contained myeloid cells, an FcR block was performed first. For this purpose, the cell pellet was taken up in 100 µl FcR blocking buffer (FcR blocking reagent diluted 1:1000 in FACS buffer) following a centrifugation step and incubated for 10 min. The pellet was then centrifuged and resuspended in 50 µl of antibody mix and incubated for 20 min. The dilutions of the individual antibodies were titrated in advance. If several BV- or BUV-conjugated antibodies were used, 10 µl brilliant stain buffer was added to the antibody mix. After incubation, the cells were washed to remove unbound antibodies. Cells were taken up in 100 µl FACS buffer and for the measurement in tube mode the samples were transferred directly before the measurement via a filter mesh into a FACS tube. If a large number of samples had to be measured at once, the samples were left in 96-well V-bottom plates and measured using the HTS.

2.3.9 Fluorescence activated cell sorting

In some experiments, very pure populations of specific cell types needed to be isolated from cell suspensions either for subsequent usage in cell culture or for RNAseq analysis. The BD FACSAria™ Fusion high throughput cell sorter is a flow cytometer equipped with a cell sorter.

The configurations and laser settings are listed in

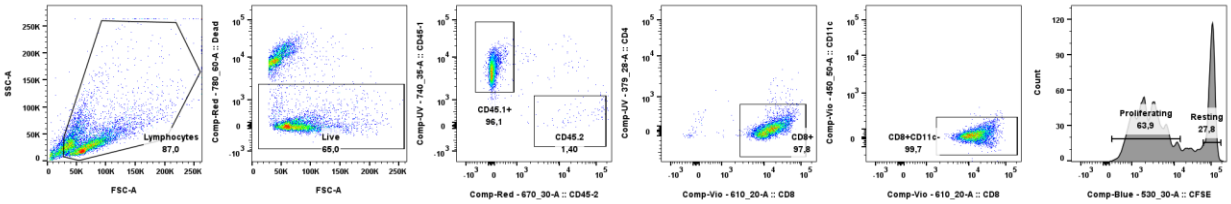

Figure 2: Representative gating strategy for the sort of proliferating and resting OT-I T cells from co-cultures with BMDCs, OVA protein and different concentrations of *S. epidermidis*.

The sorting strategy that was used to isolate proliferating and resting OT-I T cells from co-cultures for RNAseq analysis is depicted. This is a retrospective gating that recreates the gating used in the sort.

Table 19. With this device it is possible to identify certain cell types by fluorescence staining as already described in section 2.3.8 and to sort them with very high purity from a cell suspension. In the FACS cell sorting process, the cells are analysed for physical criteria and fluorescence intensity. Downstream the sample interrogation, the flow stream is converted into fine droplets by a vibration mechanism. Each droplet gets charged electrically when formed and carries exactly one cell due to their size. If the desired cell population is identified, the trajectory of the cell droplet can be directed into a sample tube by applying an electric pulse in an electric field.

For the sort of OT-I T cells a 70 µM nozzle and for the sort of BMDCs a 100 µM nozzle was used. Cells were sorted at 4 °C into 1.5 ml LoBind tubes, prefilled with an appropriate buffer. In this thesis, cell sorting was used to get highly pure populations of OT-I T cells and to subdivide OT-I T cells into naive and memory subtypes. Naive OT-I T cells were sorted for CD4- CD8+ CD62L+/- CD44+. Memory OT-I T cells were sorted for CD4- CD8+ CD62L+ CD44-. These subpopulations were then used in co-culture experiments. For RNAseq analysis (chapter 2.3.13), OT-I T cells were sorted from co-cultures as shown in Figure 2. First, debris was excluded by the SSC-A and FSC-A signal, followed by selection of live cells. Next, CD45.1+ OT-I T cells were discriminated from CD45.2+ BMDCs within the co-culture. CD45.1+ cells were further gated on CD4- CD8+ OT-I T cells. OT-I T cells that were still connected to BMDCs were excluded by the CD11c signal. The CFSE profile was used to distinguish between proliferating (from the third CFSE peak onwards) and resting OT-I T cells (highest CFSE peak).

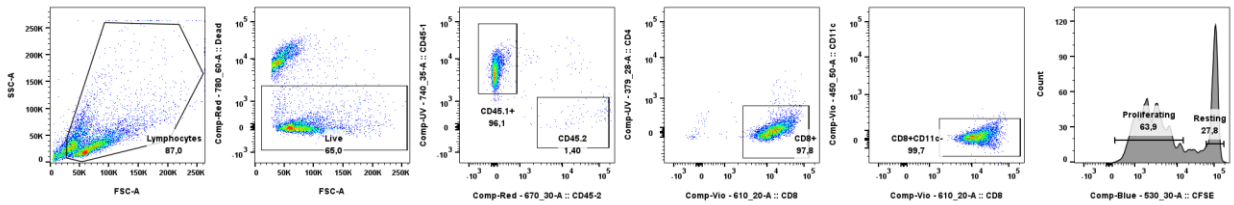

Figure 2: Representative gating strategy for the sort of proliferating and resting OT-I T cells from co-cultures with BMDCs, OVA protein and different concentrations of *S. epidermidis*.

The sorting strategy that was used to isolate proliferating and resting OT-I T cells from co-cultures for RNAseq analysis is depicted. This is a retrospective gating that recreates the gating used in the sort.

Table 19: Instrument configuration of the BD FACSAria™ Fusion.

Laser	LP Filter	BP Filter	Fluorochromes
355 nm (UV)	-	379-28	BUV395
	450	515-30	DAPI , BUV496
	690	740-35	BUV737
405 nm (violet)	-	450-50	BV421, Pacific Blue, DAPI
	505	525-50	BV480, BV510
	595	610-20	BV605
	630	660-20	BV650
	690	710-50	BV711
	750	780-60	BV786
488nm (blue)	502	530-30	FITC, GFP, CFSE, AF488, BB515
	655	695-40	PerCP, PerCP-Cy5.5
561nm (yellow-green)	-	586-15	PE
	600	610-20	PE-TR, PE-Dazzle594, PE-eF610, AF594
	630	670-14	PE-Cy5
	735	780-60	PE-Cy7
633 nm (red)	-	670-30	APC, AF647
	690	730-45	AF700
	755	780-60	APC-Cy7, APC-H7, APC-eF780, APC-Fire750

In order to isolate BMDCs for RNAseq analysis (chapter 2.3.14) that have incorporated SYTO9-labelled bacteria, the following strategy was used (Figure 3). After size exclusion of debris by FSC-A, live cells were identified as DAPI-. Next, the cells were delimited using the SSC-A FSC-A signal followed by gating on CD11c+ cells. SYTO9+ and LTA- fluorescence signals were used to discriminate BMDCs that have incorporated bacteria (SYTO9+ LTA-) from those that have bacteria bound to their surface (SYTO9+/- LTA+). Therefore, BMDCs that had taken up bacteria were determined as SYTO9+ LTA-. In unstimulated controls, SYTO9- LTA- cells were sorted. Cells were sorted into 1.5 ml LoBind tubes containing 700 µl RLT+ buffer.

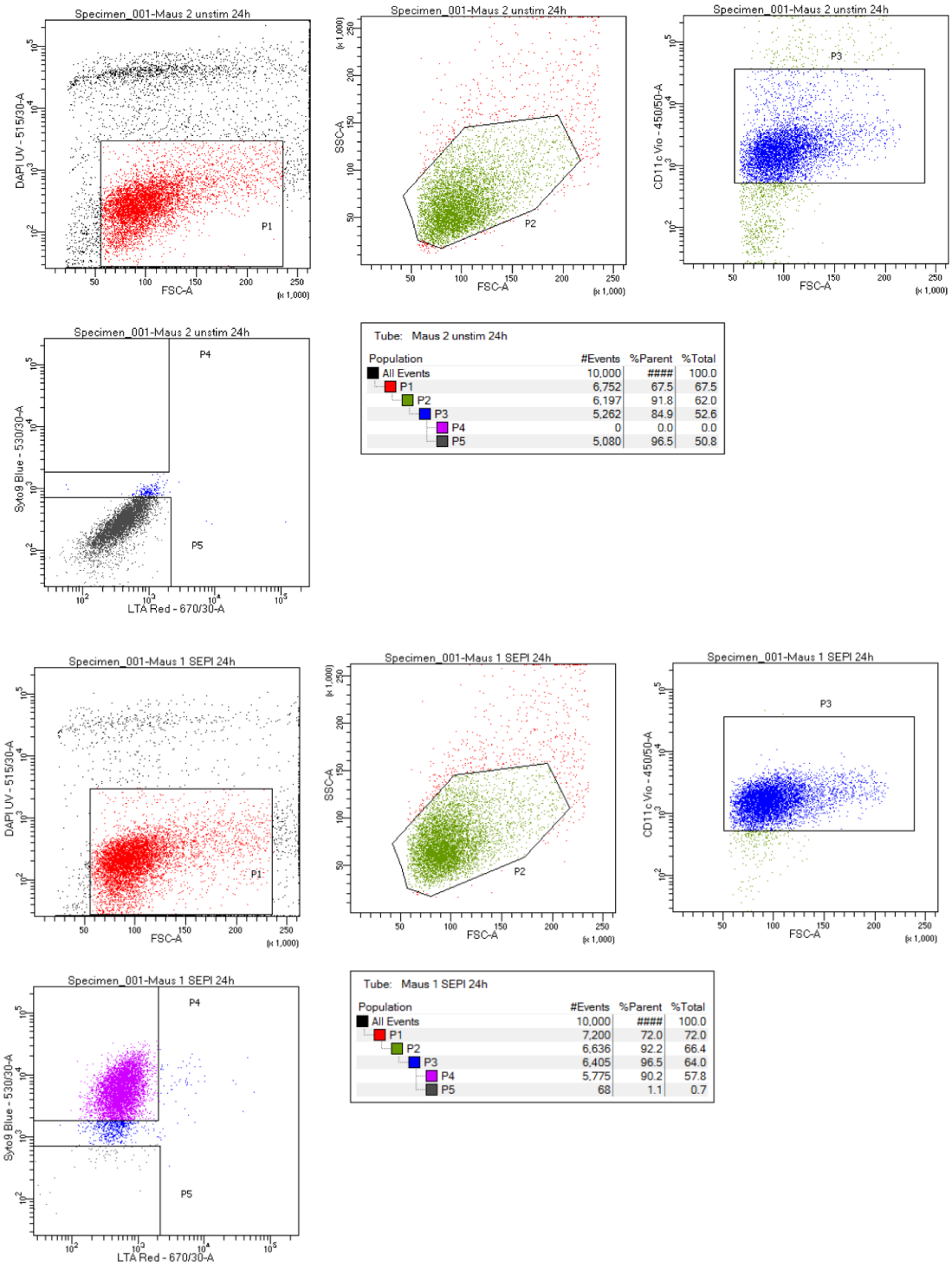

Figure 3: Representative gating strategy for the sort of BMDCs that have internalised *S. epidermidis* but did not have *S. epidermidis* bound to their surface and unstimulated BMDCs.

In the upper half of the picture, the gating is applied to an unstimulated BMDC sample sorted on SYTO9- LTA- cells after 24 h incubation. In the lower half of the picture, the gating is applied to a BMDC sample that was incubated with *S. epidermidis* for 24 h, sorting SYTO9+ LTA- cells. Files were kindly provided by the FACS Core facility, that performed the sort.

2.3.10 ELISA for the detection of IFNγ

ELISA was used to detect IFNγ levels in cell culture supernatants. With a few exceptions, the ELISAs were performed as specified by the manufacturer. The prescribed volume for coating

antibody, detection antibody, samples, standard, streptavidin-HRP and substrate solution was halved from 100 µl to 50 µl. The volume of the stop solution was adjusted from 50 µl to 25 µl. A brief overview of the protocol is described below.

For preparation, a 96-well Maxisorp Nunc-immuno plate was filled with 50 µl/well capture antibody (diluted to working concentration in PBS), sealed with an adhesive strip and incubated overnight at RT. The next day, the wells were emptied and washed three times with 400 µl wash buffer (0.05% Tween 20 in PBS). The plates were then blocked with 300 µl/well reagent diluent (1 % BSA in PBS) for 1 h at RT. After washing 3 times, 50 µl sample (undiluted or diluted in reagent diluent) and standard were added to the wells. The plate was sealed and incubated for 2 h at RT. The standard series was prepared as prescribed in the LOT-specific instructions. A seven-point standard curve using 2-fold serial dilutions is recommended. After incubation, wells were washed again three times and 50 µl/well detection antibody was added. The plate was sealed with a new adhesive strip and incubated for 2 h at RT. After washing three times, 50 µl/well streptavidin-HRP was added and plates were incubated for 20 min at RT, protected from light. Washing was performed three times before adding 50 µl/well TMB-substrate solution (1 part reagent A plus 1 part reagent B; BD OptEIA™ TMB Substrate Reagent Set). Plates were incubate again at RT and were protected from light. As soon as the standard series showed a clear coloration with gradations, the reaction was stopped with 25 µl/well stop solution (2N H_2SO_4). Immediately afterwards, the OD_{450} was determined with the TECAN Spark M10 reader. The wavelength correction was set to 540 nm.

2.3.11 Griess Reagent for nitrite detection

The nitrite assay kit (Griess reagent) was used to detect nitrite levels in cell culture supernatants. Nitrite is a relative stable product of the NOS reaction and allows conclusions to be drawn about the production level and presence of immunomodulatory NO (Bogdan 2001). In the Griess assay, nitrite is reduced to NO by Griess reagent I, which then reacts with Griess reagent II to a stable product. This product can be detected by measuring the OD_{540} to estimate nitrite levels in supernatants (see manufacturer's data sheet).

The assay was performed according to the manufacturer's protocol. Only the volumes of samples and therefore reagents used were halved in order to save samples for other analyses. All reagents were warmed to RT prior use. The nitrite standard was prepared as described by the manufacturer. The dilutions for the standard curve were selected as follows and prepared from the standard and diluted in nitrite assay buffer: 0.25, 0.5, 1, 2, 4, 6, 8 nmol/well nitrite. 50 µl sample or standard per well were transferred to a 96-well Maxisorp Nunc-immuno plate. Next, 5 µl of Griess reagent I followed by 5 µl of Griess reagent II were added to each well. Finally, 40 µl Nitrite assay buffer was added. After 10 min incubation at RT, nitrite levels were measured on the TECAN reader at OD_{540}. Nitrite concentrations in µM were calculated using the OD_{540} as specified by the manufacturer in the data sheet.

2.3.12 Luminex assay for multiple cytokine detection

The Luminex assay enables simultaneous detection of several cytokines within one sample by coupling them to fluorochrome-labelled microsphere beads (see Table 6). Sigrid Buelow, Martina Toelge and Lisa Zeller at the IMHR kindly carried out the measurements. The method is briefly described below.

To quantify the protein levels of IL-6, IL-10, IL-12p40, CCL2, CXCL10 and TNFα in cell culture supernatants of BMDCs after incubation with *S. epidermidis*, cytokine-specific antibodies were coupled to the fluorochrome-labelled beads according to the manufacturer's specifications. 50 µl of sample were added to the beads followed by incubation overnight at 4 °C. After 2 wash steps with wash buffer (0.4 % BSA, 0.05 % tween, 0.1 % Proclin, 1 mM Titriplex in PBS; pH – 7.4), 50 µl of biotinylated antibody mix was added and plates were incubated for 1 h at RT. After two wash steps, 50 µl streptavidin-phycoerythrin were added followed by incubation for 30 min at RT. Beads were washed 3 more times and filled up with 125 µl wash buffer. Finally, fluorescence analysis was performed in the Luminex 100 device (Diasorin; Austin, TX, USA). For quantification the LiquiChip Analyzer Software (Qiagen, Hilden, Germany) was used.

2.3.13 BulkRNAseq of OT-I T cells

In the co-cultures, proliferating and resting (non-proliferating) OT-I T cells could be detected depending on the type of stimulation and bacterial concentration used. In order to identify possible transcriptome differences between the conditions, a bulkRNAseq analysis was performed.

For this purpose, co-cultures of OT-I T cells, BMDCs and OVA protein were prepared (as described in chapter 2.3.7) and exposed to 1, 10 and 100 CFU/BMDC UV-attenuated *S. epidermidis* strain 614. OT-I T cells were labelled with CFSE before co-culture (see chapter 2.3.6). 72 h after incubation of the co-culture, the cell suspensions were sorted for proliferating and resting live CD45.1+ CD8+ OT-I T cells as described in chapter 2.3.9. The cells were sorted directly into 1.5 ml DNA LoBind tubes containing 350 µl RLT+ buffer. Where possible, a total of 25,000 cells per condition were sorted. The samples were then stored at -80 °C until transfer to the NGS Core facility. Sequencing and data preparation was performed by the NGS Core Facility as follows in the next section (protocol written by NGS Core).

Total RNA was isolated using the Qiagen RNeasy Micro Kit, and RNA was eluted in 14 µL RNase-free water. RNA quality was assessed using the Tapestation system 4200 and High-Sensitivity RNA screentape (Agilent). 7 µl of the RNA including spike-ins from Lexogen (SIRV-Set 3) for normalization were used for generating RNA-seq libraries using the SMART-seq Stranded Kit from Takara. Indexed libraries were pooled in an equimolar ratio and single-end sequenced on an Illumina NextSeq 2000 machine with a NextSeq 2000 P3 Kit (50 cycles). Quality control and read mapping to the mouse reference genome (GRCm38, gencode, release23) was performed using the SnakePipes analysis pipeline (v2.5.1). Mapping was performed using STAR, and gene counts are based on featureCounts. Quality control of the count matrix and differential expression

gene calling was performed with DESeq2. Gene counts were imported and prefiltered with edgeR:filterByExpr, and the false discovery rate (FDR) was set to 0.05. gene ontology analysis was performed with genes upregulated with a log2 fold change > 1 and FDR < 0.05 using goseq. Gene set enrichment analysis was performed using fgsea. Plots were created with ggplot2 and EnhancedVolcano (51).

Bioinformatic analysis were performed in collaboration with Nicoals Strieder from the NGS Core and Bernd Daller from the IMHR.

2.3.14 BulkRNAseq of BMDCs

BulkRNAseq analysis were performed to investigate the influence of *S. epidermidis* on the transcriptome of BMDCs. Immature BMDCs were generated as described in chapter 2.3.4 using immature cell culture medium. On day 8 of generation, immature BMDCs were harvested and 1 x 10^5 cells/well were seeded in a 96-well cell culture plate. Replicates of 24 wells of each BMDC donor were seeded to be able to combine them for the sorting and thus increase the cell yield. Live *S. epidermidis* was labelled with SYTO 9 (described in chapter 2.3.2). BMDCs were incubated with 10 CFU/BMDC *S. epidermidis* for 4 h and 24 h. After incubation, BMDCs were harvested, washed 3 times with FACS buffer and stained and sorted as described in the section for the sort of BMDCs for RNAseq analysis in chapter 2.3.9. The cells were sorted directly into 1.5 ml DNA LoBind tubes containing 350 µl RLT+ buffer. Where possible, a total of 50,000 cells per condition were sorted. The samples were then stored at -80 °C until transfer to the NGS Core facility. Sequencing and data preparation was performed by the NGS Core Facility. The used protocol of the NGS Core was identical to the one already described in chapter 2.3.13 for OT-I T cells.

Bioinformatic analysis were performed in collaboration with Nicoals Strieder from the NGS Core and Bernd Daller from the IMHR.

2.4 Statistics

The results in this thesis are shown as mean ± SEM (standard error of mean). GraphPad Prism was used to generate and display graphs and to perform statistical analyses. The statistical test used in each case is indicated separately in the results section. Differences with a p value < 0.05 were considered significant. The exact p value of the individual comparisons is indicated in the graph. Unless stated otherwise, no p value was mapped for non-significant comparisons.

3 Results

3.1 Antibiotic resistance profile and genome analysis of *S. epidermidis*

Five strains of *S. epidermidis* have been selected in this study to treat BMDCs and co-cultures of BMDCs and OT-I T cells. We investigated whether different isolates behave similarly or differently regarding their influence on the mentioned cells. Strains 614, 617 and 618 are clinical isolates from Regensburg from the IMHR. Strain 912 is an isolate from a healthy donor and strain 918 was isolated from a patient suffering from chronic infections.
As antibiotic resistance is a serious problem in *S. epidermidis* infections, Andreas Hiergeist (IMHR) prepared an antibiogram of each strain (see Figure 4) (Severn and Horswill 2022). Strains 614 and 617 were sensitive to almost all antibiotics tested except Ceftazidim. In contrast, strains 912 and 918 already showed resistance to most antibiotics and were only susceptible to Vancomycin, Teicoplanin, Linezolid, Daptomycin, Tigecycline, Fosfomycin and Fusidic acid. Compared to the sensitive strains 614 and 617, strain 618 already shows a high level of resistance. However, compared to strains 912 and 918, strain 618 is sensitive to four additional antibiotics. It therefore is an intermediate between the other four strains.

The pan genome analysis represents a matrix that maps the presence and absence of the predicted genes. Green areas indicate the presence and white areas the absence of genes. Analysis of the used *S. epidermidis* strains revealed that a large proportion of the genome is identical between the different strains (Figure 5), indicated by the green regions. However, they also differed in many gene areas due to the different presence and absence of genes and had an individual genome.

	614	617	618	912	918
Amoxicillin/Clavulanic Acid	S	S	R	R	R
Ampicillin o. Amoxicillin	NA	NA	R	R	R
Piperacillin/Tazobactam	S	S	R	R	R
Piperacillin	NA	NA	R	R	R
Piperacillin/Sulbactam	NA	NA	R	R	R
Flucloxacillin	S	S	R	R	R
Cefazolin	S	S	R	R	R
Cefuroxim i.v.	S	S	R	R	R
Ceftriaxon o. Cefotaxim	S	S	R	R	R
Cefotaxim o. Ceftriaxon	S	S	R	R	R
Ceftazidim	R	R	R	R	R
Cefepim	S	S	R	R	R
Imipenem	S	S	R	R	R
Meropenem	S	S	R	R	R
Vancomycin	S	S	S	S	S
Teicoplanin	S	S	S	S	S
Linezolid	S	S	S	S	S
Ciprofloxacin	S	S	R	R	R
Moxifloxacin	S	S	R	R	R
Cotrimoxazol	S	S	S	R	R
Makrolide	S	S	R	R	R
Clindamycin	S	S	R	R	R
Tetracycline	S	S	S	R	R
Gentamicin	S	S	S	R	R
Rifampicin	X	X	X	R	R
Daptomycin	S	S	S	S	S
Tigecyclin	S	S	S	S	S
Fosfomycin	S	S	S	S	S
Fusidinsäure	S	S	S	S	S
Mezlocillin	NA	NA	R	R	R
Ticarcillin/Clavulanic Acid	NA	NA	R	R	R

Figure 4: Antibiogram of the five *S. epidermidis* strains used.

Antimicrobial susceptibility testing (AST) was performed at the IMHR as part of a diagnostic process accredited by DIN EN ISO 15189, utilizing a BD Phoenix™ M50 instrument (Becton Dickinson, Heidelberg, Germany). The evaluation of antibiotic susceptibility followed the guidelines established by the European Committee for the Study of Antimicrobial Susceptibility (EUCAST). The level of antibiotic resistance of the respective strain to the specified antibiotics is labelled with letters. It indicates the lowest antibiotic concentration that prevents visible bacterial growth and is referred to as the minimum inhibitory concentration (MIC). NA = not analysed; S = sensitive; R = resistant; X = resistance classification not possible. Picture kindly provided by Andreas Hiergeist (IMHR).

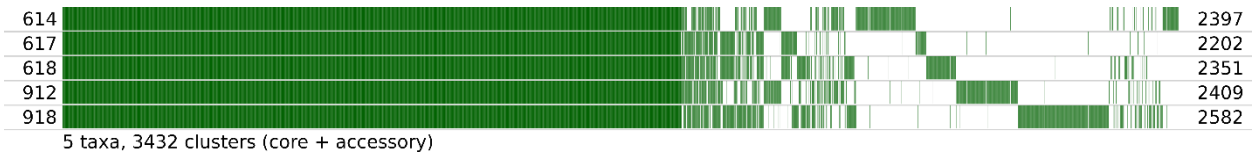

Figure 5: Pan genome analysis of the five *S. epidermidis* strains used.

The graphs shown represent a gene presence/absence matrix. This means that the strains are compared in terms of the presence and absence of the predicted genes. The analyses were carried out by Andreas Hiergeist at the IMHR. The procedure is summarised below: For the five strains, a "short reads" genome sequencing IonTorrent GeneStudio S5 Plus and a "long reads" genome sequencing MinION (Oxford Nanopore) were performed. A hybrid assembly for short and long reads was performed using unicycler (v 0.5.0). Prokka (v 1.14.5) was used to annotate the genomes and roary (v 3.11.2) was used for pan genome analysis. Picture kindly provided by Andreas Hiergeist (IMHR).

3.2 Activation of BMDCs upon contact with *S. epidermidis*

As already mentioned in the methods section 2.3.4, BMDCs with different maturation levels were generated, depending on the used medium during the generation process. The term "BMDC" always refers to the "mature BMDCs" generated with cell culture medium. If BMDCs were generated with "immature cell culture medium", resulting in lower expression of maturation-associated markers such as CD86 or MHC class II, this is explicitly indicated by the designation "immature BMDCs". This designation applies to the entire study.

It is well known, that DCs are sentinels of the immune system, patrol the tissue and recognise foreign substances as well as bacteria (Merad et al. 2013; Helft et al. 2015). Therefore, whether and in what manner *S. epidermidis* influences the generated BMDCs and whether the heat-inactivated *S. epidermidis* lysates used may have a toxic effect on the cells was investigated. For this, heat-inactivated lysates of the already introduced five *S. epidermidis* strains were added to BMDC cultures at defined concentrations, ranging from 0.1 to 1000 (Colony forming units) CFU/BMDC in logarithmic steps. Equivalent volumes of PBS in relation to the respective volume of heat-inactivated *S. epidermidis* lysate used served as controls. PBS controls are labelled with the CFU/BMDC information to which the volume was adjusted, although they did not contain any bacteria. After 24 h incubation, BMDCs were analysed by FACS and gated on CD11b+ CD11c+ cells followed by gating on live cells (Figure 6A). The percentage of live cells among all CD11b+ CD11c+ cells was used as an indicator to study if *S. epidermidis* influences the viability of BMDCs. The viability of immature BMDCs was unaffected by *S. epidermidis* (Figure 6B), whereas mature BMDCs had a lower frequency of live cells for higher concentrations of *S. epidermidis* (Figure 6C). 1000 CFU/BMDC reduced the frequency of live BMDCs slightly but significantly for all strains. At 1000 CFU/BMDC, an average of 23 % fewer living cells were detected than in the respective PBS control. Strains 912 and 918 already reduced viability at 100 CFU/BMDC, compared to the low *S. epidermidis* concentration of 0.1 CFU/BMDC.

Comparing the *S. epidermidis* strains with the respective PBS controls there was no significance for all strains regarding immature BMDCs. Viability of mature BMDCs stimulated with 1000 CFU/BMDC *S. epidermidis* were lower than in the related PBS control (Graphs not shown; $p < 0.001$; Two-way ANOVA with Dunnett’s multiple comparisons test).

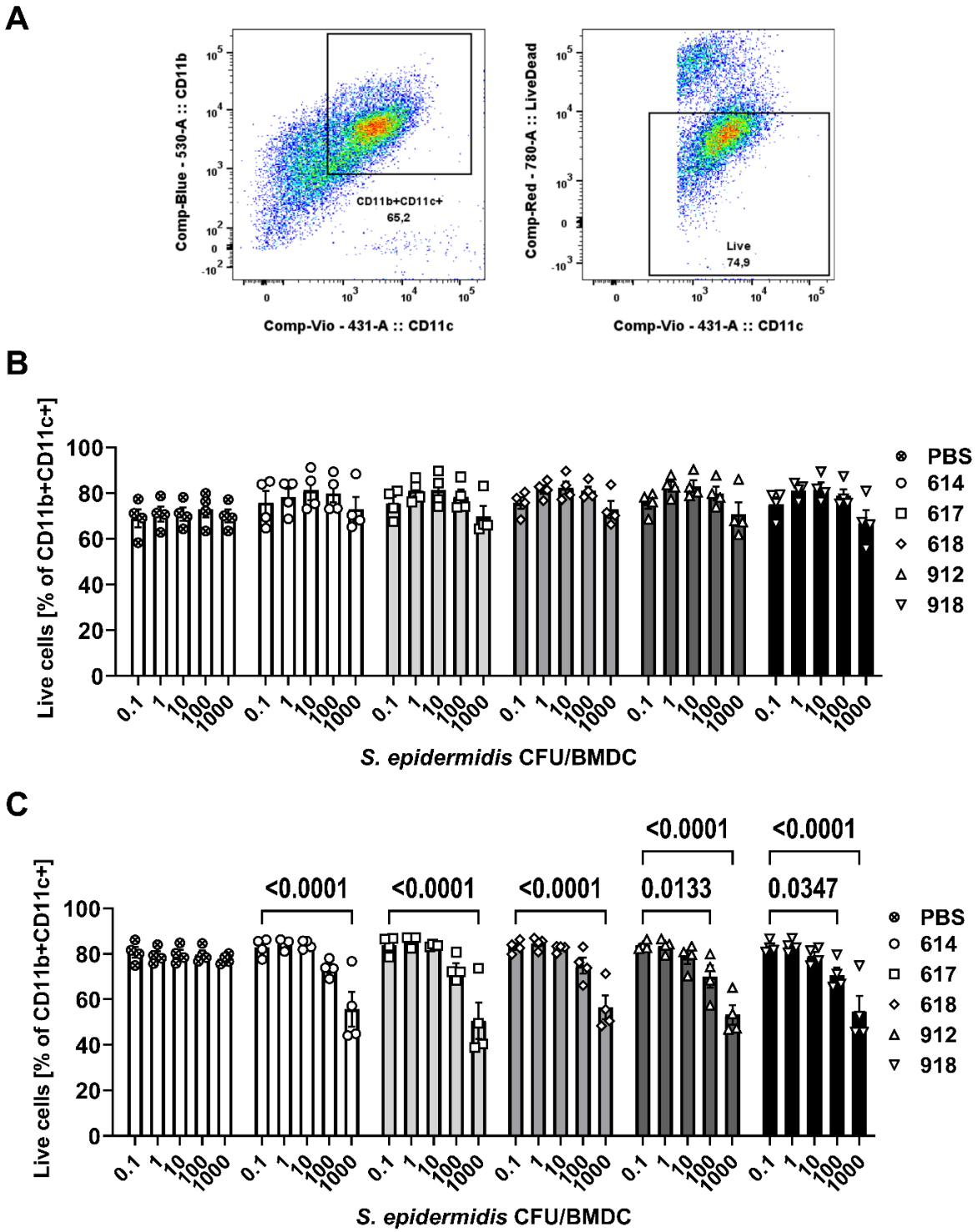

Figure 6: Percentage of live BMDCs after exposure to *S. epidermidis*.

At day 8 of generation, 100.000 mature as well as immature BMDCs/well were exposed to heat-inactivated *S. epidermidis* lysate for 24 h. Heat-inactivated lysates of five *S. epidermidis* strains (614, 617, 618, 912, 918) were used at the indicated concentrations. Equivalent volumes of PBS in relation to the respective volume of heat-inactivated *S. epidermidis* lysates used served as a control. These PBS controls are labelled in the graph with the same CFU information as used for the heat-inactivated *S. epidermidis* lysates, but did not contain any bacteria. **(A)** Exemplary gating used for the analysis of BMDCs. **(B)** The frequency of live cells among CD11b+CD11c+ cells is depicted for immature BMDCs generated with immature cell culture medium. 0.1 *S. epidermidis* CFU/BMDC of each group (*S. epidermidis* strain or PBS control) was compared to the other *S. epidermidis* concentrations of the respective group. **(C)** The frequency of live cells among CD11b+CD11c+ cells is depicted for BMDCs generated with cell culture medium. 0.1 *S. epidermidis* CFU/BMDC of each group (*S. epidermidis* strain or PBS control) was compared to the other *S. epidermidis* concentrations of the respective group.
Bars represent means ± SEM of n = 4. Biological replicates are illustrated in symbols. Ordinary two-way ANOVA with Dunnett's multiple comparisons test was performed to obtain p values. Only p values < 0.05 are shown.

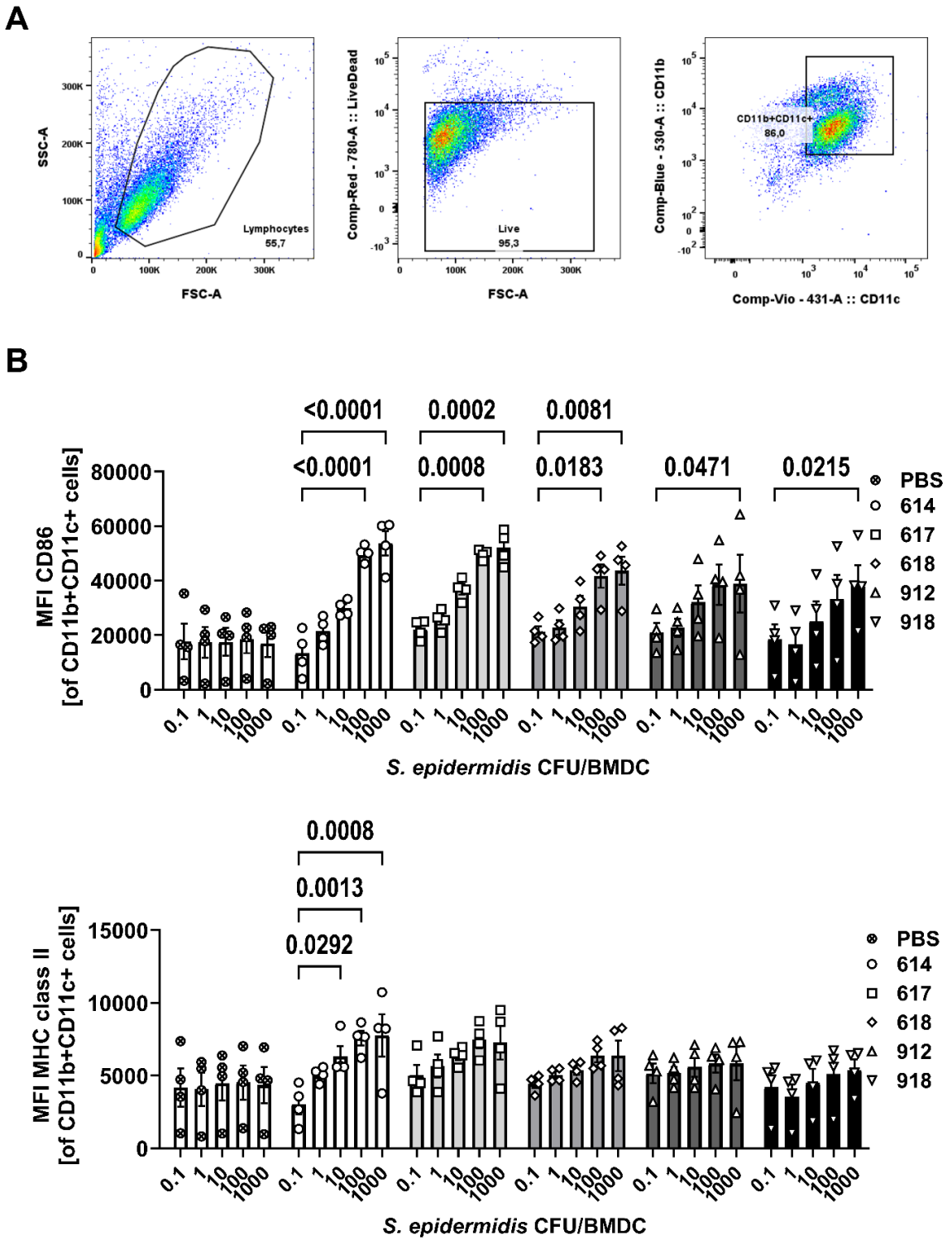

Figure 7: CD86 and MHC class II expression levels of BMDCs exposed to heat-inactivated *S. epidermidis* lysates.

At day 8 of generation, 100.000 BMDCs/well, generated with cell culture medium, were exposed to heat-inactivated *S. epidermidis* lysate for 24 h. Heat-inactivated lysates of five *S. epidermidis* strains (614, 617, 618, 912, 918) were used at the indicated concentrations. Equivalent volumes of PBS in relation to the respective volume of heat-inactivated *S. epidermidis* lysate used served as a control. These PBS controls are labelled in the graph with the same CFU information as used for the heat-inactivated *S. epidermidis* lysates, but did not contain any bacteria. **(A)** Exemplary gating used for the analysis of BMDCs. **(B)** CD86 and MHC class II expression of BMDCs generated with cell culture medium, was analysed by FACS. The median fluorescence intensities (MFI) for both markers among live CD11b+CD11c+ cells are depicted for. 0.1 *S. epidermidis* CFU/BMDC of each group (*S. epidermidis* strain or PBS control) was compared to the other *S. epidermidis* concentrations of the respective group.
Bars represent means ± SEM of n = 4. Biological replicates are illustrated in symbols. Ordinary two-way ANOVA with Dunnett's multiple comparisons test was performed to obtain p values. Only p values < 0.05 are shown.

After contact and uptake of foreign antigens, DCs can mature and migrate into lymphoid organs to present these antigens to other immune cells. This maturation can be monitored by the expression of markers such as MHC class II or CD86 (Alloatti et al. 2016). Mature BMDCs, generated with cell culture medium, were exposed to heat-inactivated *S. epidermidis* lysates for 24 h to investigate whether the lysate can enhance expression of the markers CD86 and MHC class II. For the analysis, cells were first identified via size (SSC-A, FSC-A lymphocytes) followed by gating on live cells and CD11b+ CD11c+ BMDCs (see Figure 7A). The median fluorescence intensity (MFI) for the expression of CD86 and MHC class II is shown in Figure 7B for five different strains and the PBS control. Compared to the low *S. epidermidis* concentration of 0.1 CFU/BMDC, the expression of CD86 was significantly increased at 1000 CFU/BMDC stimulation for all strains used. 100 CFU/BMDC increased the marker expression for strains 614, 617 and 618. A comparison of the CD86 expression after incubation with *S. epidermidis* with the related PBS controls showed a significant increase starting from 10 CFU/BMDC for strain 617, starting from 100 CFU/BMDC for strains 614, 618 and 912 and for strain 918 at 1000 CFU/BMDC (Graphs not shown; Two-way ANOVA with Dunnett's multiple comparisons test). Expression of MHC class II was only notably increased for 10, 100 and 1000 CFU/BMDC of strain 614, compared to 0.1 CFU/BMDC. Compared to the respective PBS control, MHC class II expression was higher only for strain 614 at 100 CFU/BMDC (Statistics not shown; Two-way ANOVA with Dunnett's multiple comparisons test).

Another way to monitor the reactivity of BMDCs to *S. epidermidis* is the expression of cytokines. After contact with bacteria, DCs can release cytokines such as TNFα and IL-6 and chemokines like CCL2 and CXCL10. However, the pattern of cytokines and chemokines depends on the subtype of DC and the respective stimulus (Alloatti et al. 2016; Jensen and Gad 2010). Luminex analyses were used to examine the supernatants of immature BMDCs after 24 h incubation with heat-inactivated *S. epidermidis* strain 614 for the expression of IL-6, IL-10, IL-12p40, CCL2, CXCL10 and TNFα (Figure 8). Compared to BMDCs without bacterial contact, stimulation with 1000 *S. epidermidis* CFU/BMDC increased the secretion of IL-10, IL12-p4, CCL2 and TNFα. Secretion of IL-6 and CXCL10 were significantly elevated for 100 and 1000 CFU/BMDC.

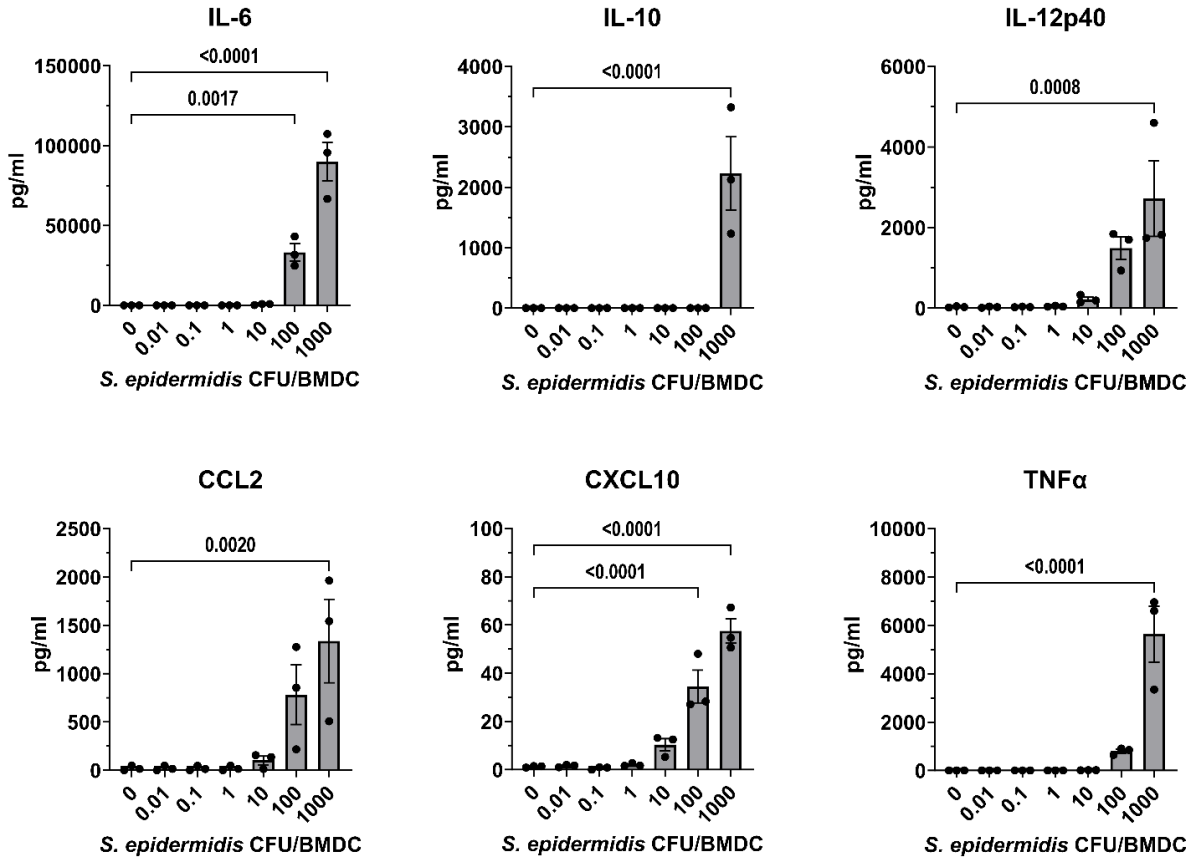

Figure 8: Cytokine expression of BMDCs after exposure to *S. epidermidis*.

At day 8 of generation (generated with immature cell culture medium), 200.000 immature BMDCs/well were incubated with heat-inactivated *S. epidermidis* lysate (strain 614) at the indicated concentrations for 24 h. Expression of IL-6, IL-10, IL-12p40, CCL2, CXCL10 and TNFα was analysed in the supernatants by Luminex measurements. Measurement and data processing was kindly carried out by Sigrid Buelow, Martina Toelge and Lisa Zeller (IMHR) Bars represent means ± SEM of n = 3 independent experiments. Replicates are illustrated in symbols. Ordinary one-way ANOVA with Dunnett's multiple comparisons test was performed to obtain p values. Only p values < 0.05 are shown.

Further, bulk RNA sequencing (RNAseq) analysis was performed of immature BMDCs that were incubated with SYTO9-labelled live *S. epidermidis* for 4 h and 24 h to analyse the influence of *S. epidermidis* on the gene expression of BMDCs. The sort was restricted to BMDCs that internalised *S. epidermidis*. Gating is explained in more detail in the methods section 2.3.9. In short, live BMDCs that had internalised bacteria (SYTO9+) but had not bound bacteria to the surface (LTA-) were identified. As BMDCs with a positive signal for LTA (derived from *S. epidermidis*) also show a signal for SYTO9, but internalisation cannot be confirmed with certainty, these cells were excluded from the analysis. BMDCs that have internalised *S. epidermidis* should not show a signal for LTA, as the antibody does not penetrate the cells.

In Figure 9, a principal component analysis (PCA) plot of the analysed samples is shown, indicating the similarity between samples depending on the treatment time PC1 (48.54 %) and the PBS or *S. epidermidis* treatment PC2 (19.88 %). Analysed replicates cluster for the respective treatment and time point. The 4 h and 24 h clusters and thus the gene expression differed significantly between the PBS and *S. epidermidis* treatment. Regarding the specific time points,

the *S. epidermidis*-exposed samples show significantly different gene expression compared to the respective PBS samples.

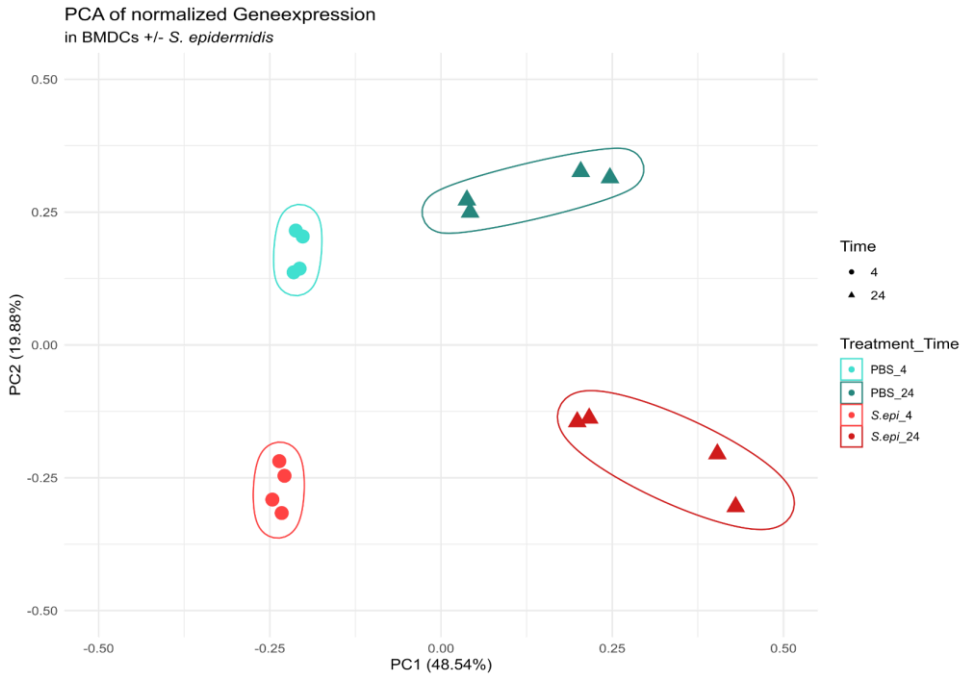

Figure 9: Differential gene expression profiling of BMDC by principal component analysis upon *S. epidermidis* exposure.

Differential Gene expression profiling of immature BMDCs by principal component analysis (PCA). This PCA plot gives an overview over the transcriptional response of BMDCs exposed to *S. epidermidis* (*S. epi*). PC1 (48.54 %) segregates samples based on the treatment time, while PC2 (19.88 %) separates according to the treatment with PBS or *S. epidermidis*, indicating distinct expression profiles induced by bacterial challenge. Symbols represent individual samples across different treatments and time points, with shape encoding treatment time and colour denoting treatment type.
Analysis and graphical illustration by Bernd Daller (IMHR).

Volcano plots visualize the differentially expressed genes between *S. epidermidis*- and PBS-treated BMDCs for 4 h and 24 h respectively (Figure 10). We observed that after 4 h about 2400 genes are differentially expressed between *S. epidermidis* and PBS treatment and after 24 h about 2000 genes are differentially expressed. At the 4 h time point, many of the upregulated genes can be assigned to a response to bacterial stimuli or symbionts according to GO term assignment. These include genes for cytokines such as Tnf, Il12b, Ccl4, Cxcl3 and Cxcl10, but also Nfkb-associated genes or genes coding for PRRs, such as Tlr2. After 24 h, genes that are upregulated are for example involved in response to symbionts and viruses and can be assigned to the innate immune response.

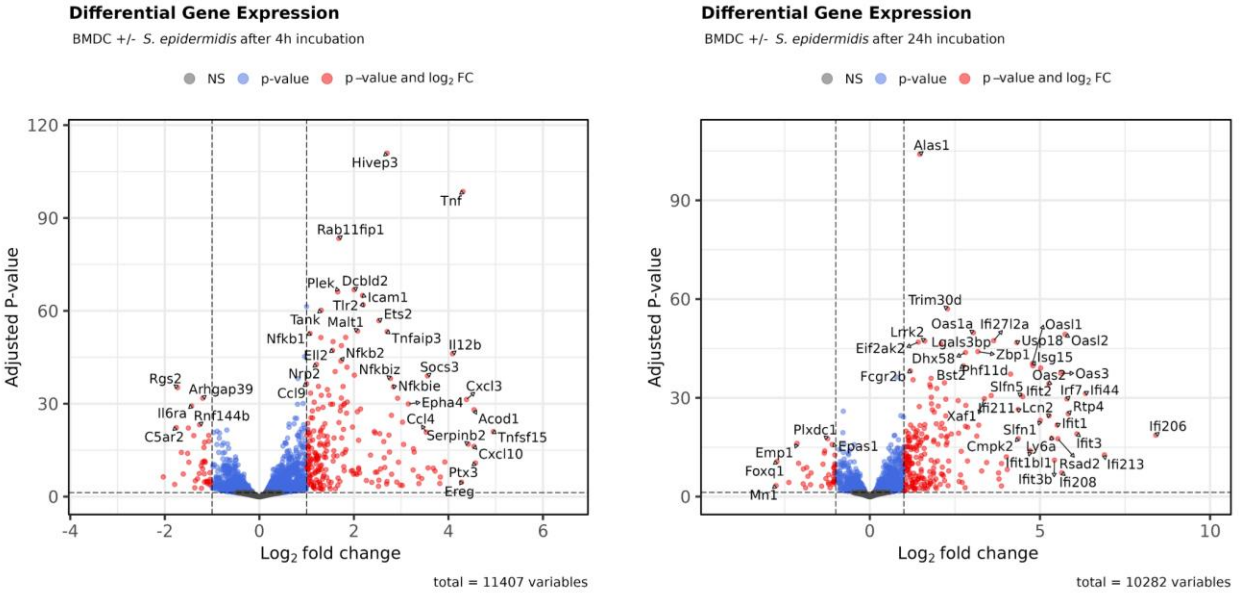

Figure 10: Volcano plot of differential gene expression of BMDCs harbouring *S. epidermidis* and BMDCs without *S. epidermidis* contact.

Immature BMDCs were incubated with live *S. epidermidis* for 4 h and 24 h or remained untreated. BMDCs were then used for bulk RNAseq analysis. Each point represents the average value of one transcript in 3 replicate experiments. Significance is determined by an FDR-adjusted p-value threshold of 0.05, indicated by a dashed light grey horizontal line. Differentially expressed (DE) genes were selected based on a log2 fold change ≥1 or ≤−1, depicted as red points and demarcated by dashed grey vertical lines.
Analysis and graphical illustration by Bernd Daller (IMHR).

Figure 11 shows the transcripts per million (TPM) of selected genes. The adjusted p values for the comparisons of the TPMs of the expressed genes between *S. epidermidis*-treated and PBS-treated BMDCs after 4 h and 24 h incubation are listed in Table 20. The genes associated with the cytokines analysed in Figure 8 in Luminex as well as the TPMs of the genes coding for the co-stimulatory markers CD80 and CD86 are shown. The TPMs of Ccl2 as well as CD80 and CD86 are slightly increased after 4 h *S. epidermidis* incubation compared to the PBS control, albeit without significance. For Cxcl10, Il12b, TNF and Il6, TPMs are significantly increased due to *S. epidermidis* exposure after 4 h. In the case of Il12b, Ccl2 and Cxcl10 a significant increase due to *S. epidermidis* exposure compared to PBS was detected after 24 h. Cd80 expression was elevated by *S. epidermidis* after 24 h, but without significance. Il10 does not appear to be induced, as the TPM values are very low.

In summary, we observed that *S. epidermidis* influenced the phenotype of BMDCs. The bacterium increased the expression of maturation-associated markers and induced the secretion of cytokines. At the transcriptional level, incubation of BMDCs with *S. epidermidis* also led to differential expression of genes.

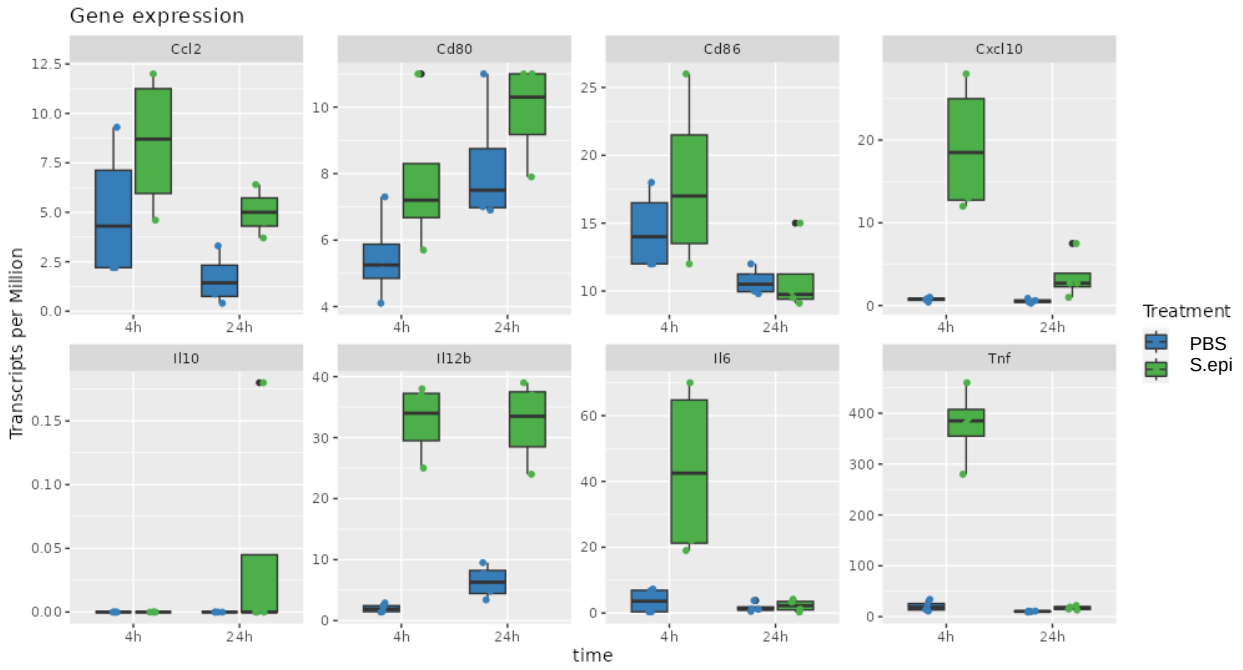

Figure 11: Gene expression in transcripts per million (TPM) of a selection of genes from RNAseq analyses of BMDCs incubated with *S. epidermidis* or PBS.

TPM values were mapped from RNAseq analyses of immature BMDCs that were incubated with live *S. epidermidis* or PBS for 4 h and 24 h. TPMs of the genes associated with the cytokine measurements in the Luminex assay as well as the genes coding for the co-stimulatory molecules CD80 and CD86 are shown. Blue boxes represent the control group of BMDCs incubated with PBS. Green boxes represent the BMDCs that were incubated with *S. epidermidis* (S.epi). The incubation time is indicated on the x-axis. Significance is determined by an FDR-adjusted p-value threshold of 0.05. Significance is not displayed in the figure, but is shown in Table 20.Sequencing by NGS core facility. Analyses and app programming for visualisation by Bernd Daller (IMHR).

Table 20: Adjusted p values for TPMs of expressed genes of BMDCs incubated with *S. epidermidis* (S.epi) compared to BMDCs incubated with PBS after for 4 h and 24 h incubation.

		Ccl2	Cd80	Cd86	Cxcl10	Il10	Il12b	Il6	Tnf
S.epi vs. PBS	4 h	ns	ns	ns	8.310 E-12	ns	5.080 E-10	1.649 E-06	8.51 E-19
	24 h	0.015	ns	ns	0.006	ns	0.001	ns	ns

3.3 *S. epidermidis* suppressed the antigen-specific proliferation of OT-I T cells

After the observation that *S. epidermidis* influenced cytokine and gene expression of BMDCs, the following experiments were designed to analyse whether *S. epidermidis* influences the induction or ongoing of an antigen-specific immune response. For this purpose, BMDCs were co-cultured with CFSE-labelled OT-I CD8+ T cells. As described in the material and methods section 2.3.7, these OT-I T cells are specifically activated by the peptide sequence SIINFEKL of the OVA protein when presented by the MHC class I molecule. From here on, these OT-I CD8+ T cells are referred to as OT-I T cells. After uptake and processing of the OVA protein, BMDCs present peptide sequences, which trigger antigen-specific proliferation in the OT-I T cells. Proliferation of OT-I T cells was analysed after 72 h incubation by FACS using the CFSE profile. A potential influence of *S. epidermidis* can be determined by an altered OT-I T cell proliferation (Figure 12).

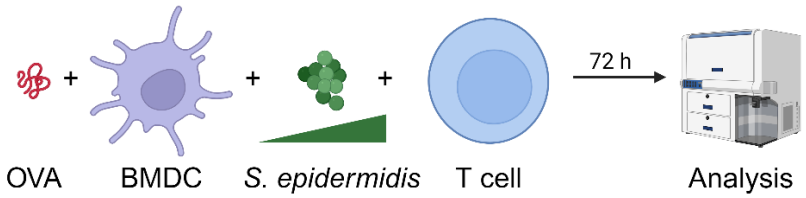

Figure 12: Experimental setup: Co-culture of BMDCs and OT-I T cells stimulated with OVA protein and exposed to *S. epidermidis*.

In co-culture experiments, BMDCs were cultured together with CFSE-labelled OT-I T cells. OVA protein (100 µg/ml) stimulation induced proliferation of OVA-specific OT-I T cells. In addition, co-cultures were exposed to different concentrations of *S. epidermidis*. After 72 h of incubation, the proliferation of OT-I T cells was analysed by the CFSE profile, which was detected using FACS. Created with BioRender.com.

All co-culture conditions contained 100 µg/ml OVA protein and the indicated CFU/BMDC of *S. epidermidis* strain 614. Since the different *S. epidermidis* strains influenced BMDCs to the same extent only strain 614 was used in the following experiments. The CFU used to indicate the quantity of *S. epidermidis* were based on the cell count of the BMDCs, unless otherwise indicated. In the case of pure OT-I T cell cultures, CFU of *S. epidermidis* were based on the T cell counts. Only the condition labelled with “unstim.” (unstimulated) contained neither OVA protein nor bacteria and served as negative control. The 0 CFU/BMDC *S. epidermidis* condition only contained OVA protein and served as positive control for the induction of OT-I T cell proliferation. Unless explicitly stated otherwise, these terms and descriptions of the conditions also applies to all subsequent experiments in this thesis.

The influence of *S. epidermidis* on the proliferation of OT-I T cells on co-cultures is shown in Figure 13. To analyse OT-I T cell proliferation, acquired cells were identified by size (SSC-A and FSC-A) and gated on live CD45.2- cells to exclude BMDCs. Next, CD8+ T cells were gated in a CD4/CD8 plot. Potential contaminating BMDCs that could still be bound to OT-I T cells were excluded by the CD11c signal. The CFSE profile of the remaining CD8+ CD11c- T cells was used to read out counts of proliferating OT-I T cells and their frequency among all OT-I T cells (Figure 13A). The counts and the frequencies of proliferating OT-I T cells are depicted in Figure 13B. The positive control 0 *S. epidermidis* CFU/BMDC was compared to all other concentrations and the unstimulated condition. In comparison to the unstimulated condition, the addition of OVA alone increased the counts and frequencies of proliferating OT-I T cells. Compared to 0 CFU/BMDC (OVA only), *S. epidermidis* reduced the counts and frequencies of proliferating OT-I T cells at a concentration of 100 and 1000 CFU/BMDC. The counts of proliferating OT-I T cells were higher at 10000 CFU/BMDC *S. epidermidis* than at 0 CFU/BMDC.

In short, the addition of *S. epidermidis* to co-cultures consisting of BMDCs, OT-I T cells and OVA protein reduced the proliferation of OT-I T cells depending on the CFU used.

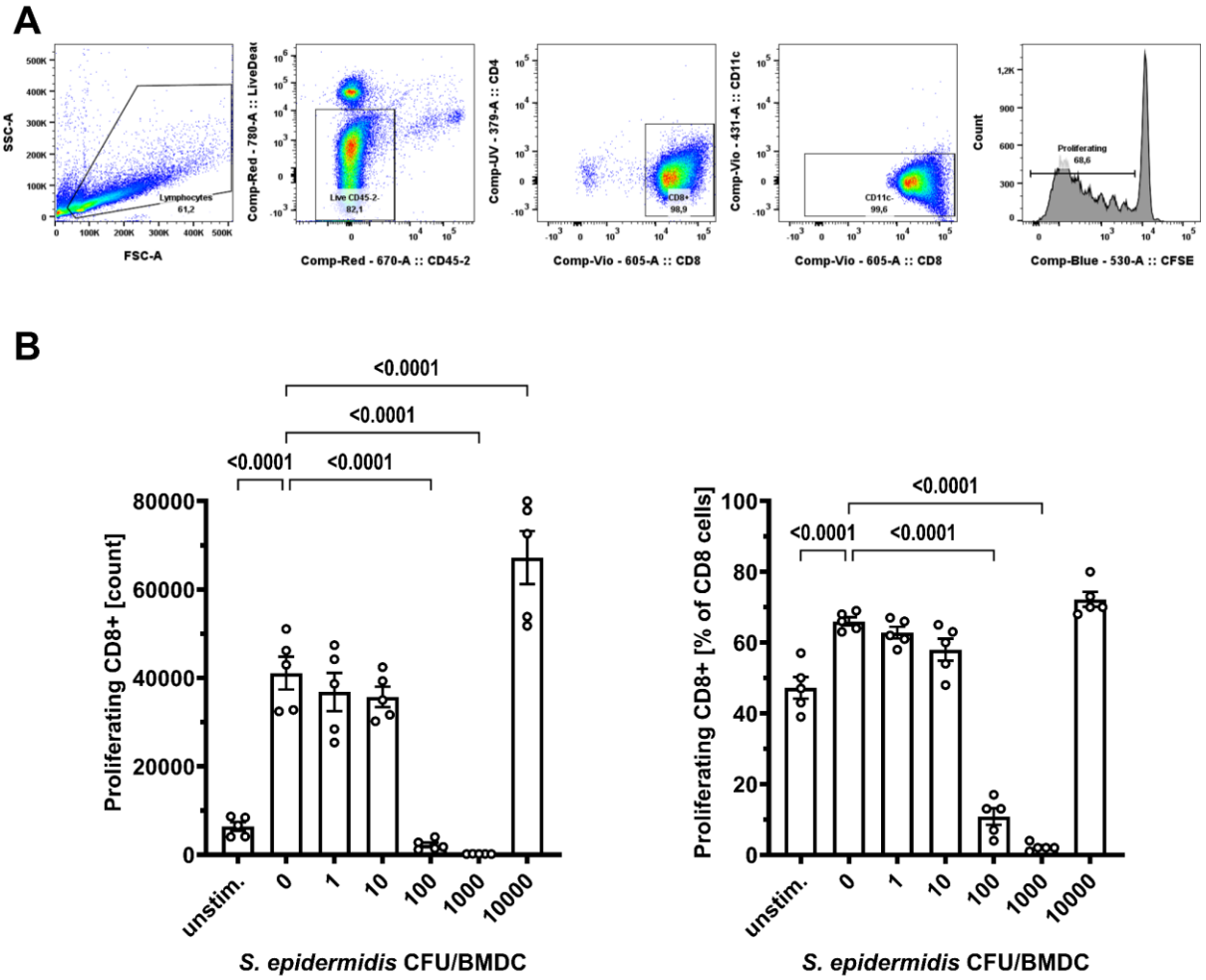

Figure 13: Proliferation of OT-I T cells in co-culture with BMDCs and stimulated with OVA protein and exposed to *S epidermidis*.

Co-cultures of BMDCs and OT-I T cells were stimulated with OVA protein and exposed to UV-attenuated *S. epidermidis*. OT-I T cell proliferation was analysed by detection of the CFSE intensity in FACS after 72 h of incubation. **(A)** Representative dot plots of the gating strategy after FACS analysis. **(B)** Counts of proliferating OT-I T cells and their frequencies among all OT-I T cells were compared to the respective 0 *S. epidermidis* CFU/BMDC condition.
Bars represent means ± SEM of n = 5 BMDC donors. Replicates are illustrated in symbols. Ordinary one-way ANOVA with Dunnett's multiple comparisons test was performed to obtain p values. Only p values < 0.05 are shown.

3.4 Similar immunomodulatory potential of heat-inactivated *S. epidermidis* and UV-attenuated *S. epidermidis*

At the beginning of the study, it was not possible to produce bacteria incapable of replication using UV irradiation. Therefore, heat-inactivated *S. epidermidis* lysate was used. During the study, a new protocol was established that enables the inactivation of bacteria by UV irradiation. We assume that UV-irradiated bacteria still have an intact cell morphology and, in contrast to the lysates, are not completely denatured. This state is considered to be more physiological, which is why the production process was changed from this point onwards. Since the production method of the bacteria was changed from heat-inactivated lysates to UV-attenuated bacteria, we investigated whether they behave similarly in order to ensure the comparability of the data. On the one hand, we analysed whether they equally induce BMDC maturation. On the other hand, suppressing potential of both production methods on antigen-specific proliferation of OT-I T cells in co-cultures was compared.

BMDCs were either incubated with heat-inactivated (HI) or UV-attenuated (UV) *S. epidermidis* for 24 h (Figure 14). The expression of MHC class II, CD86, PD-L1, and CD40, some markers known to be upregulated after activation, was acquired using FACS (Saito et al. 2020; Lutz et al. 1999; Dudek et al. 2013). The maturation of BMDCs, indicated by an upregulated CD86 and MHC class II expression was induced by the presence of *S. epidermidis* in a dose-dependent manner. There was no difference between the usages of HI or UV *S. epidermidis*, when comparing same CFU/BMDC conditions. In addition, the MFIs for the expression CD86 and MHC class II did not differ between the two *S. epidermidis* products. However, they appear slightly more elevated for stimulation with UV-attenuated *S. epidermidis* than with heat-killed *S. epidermidis* at the concentration of 100 CFU/BMDC. Looking at the expression of the markers PD-L1 and ILT3, stimulation with HI as well as UV *S. epidermidis* increased the MFIs to the same extent. Compared to the respective 0 CFU/BMDC, the PD-L1 expression of 50 and 100 CFU/BMDC were increased for UV *S. epidermidis.* For HI stimulation, 100 CFU/BMDC increased the PD-L1 expression. Only the MFI of CD40 was different between HI and UV *S. epidermidis* for the stimulation with 50 and 100 CFU/BMDC. This was because 50 and 100 CFU/BMDC UV *S. epidermidis* increased the expression of CD40 compared to 0 CFU/BMDC, whereas no increase was observed for HI *S. epidermidis*.

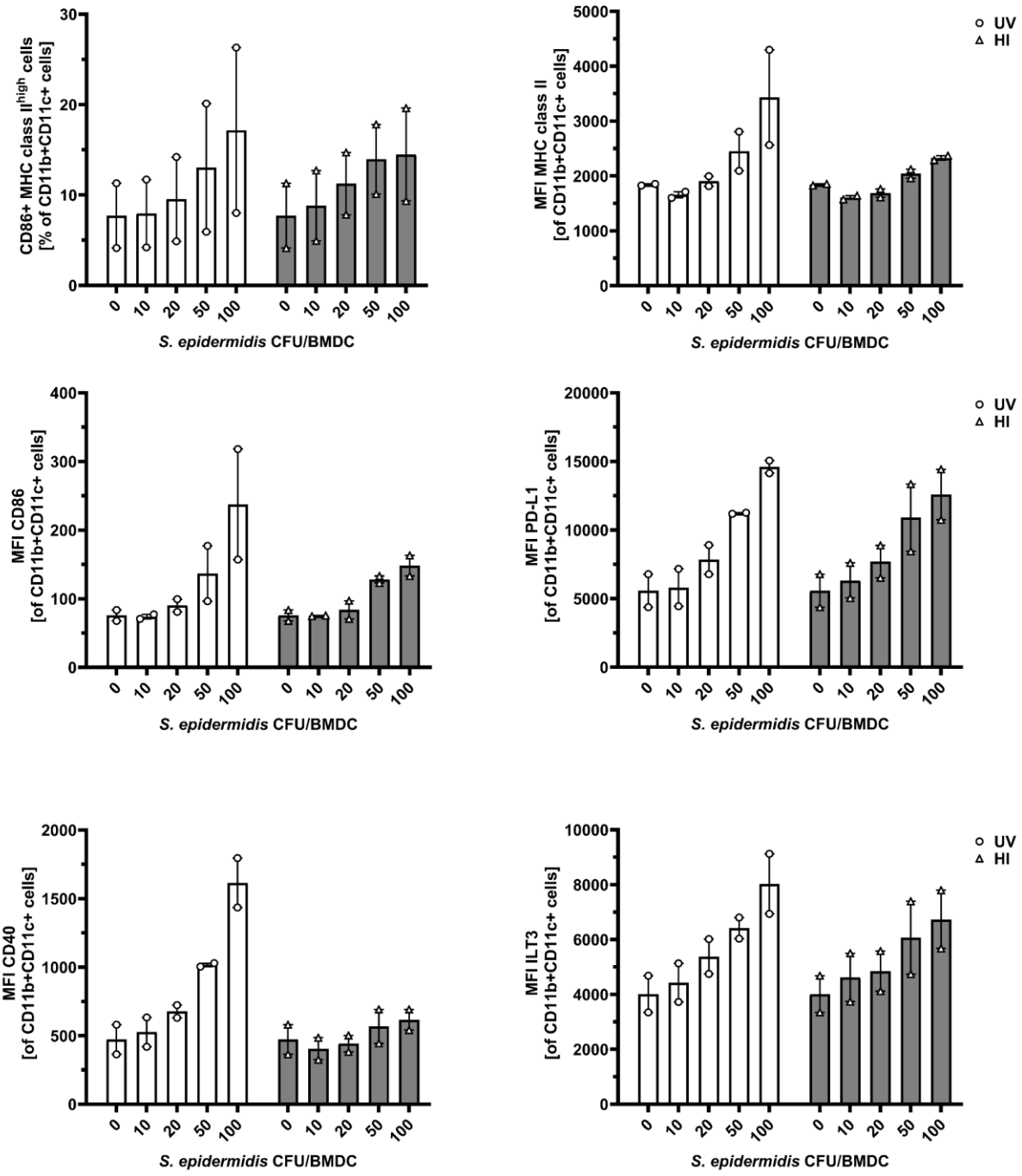

Figure 14: Surface marker expression of BMDCs incubated with heat-inactivated or UV-attenuated *S. epidermidis*.

At day 8 of generation (using immature cell culture medium), 100.000 immature BMDCs/well were incubated with heat-inactivated or UV-attenuated *S. epidermidis* (strain 614) at the indicated concentrations for 24 h. Percentage of matured BMDCs, defined as CD86+MHC class II^{high}, as well as the MFIs of inhibitory markers such as PD-L1 and ILT3 and the MFI of activation markers CD86, MHC class II and CD40 are depicted.
Bars represent means ± SEM of n = 2 BMDC donors. Replicates are illustrated in symbols.

The two production methods of *S. epidermidis* were also compared for their suppressive capacity in the co-culture assay. For this purpose, OT-I T cells were co-cultured with BMDCs and stimulated with OVA protein and either HI or UV *S. epidermidis* was added in increasing concentrations (Figure 15). It was observed, that HI and UV *S. epidermidis* suppressed the counts and frequencies of proliferating OT-I T cells to an almost identical extent. Comparing the counts and frequencies of related CFU/BMDC between the two products, no major differences were observed.

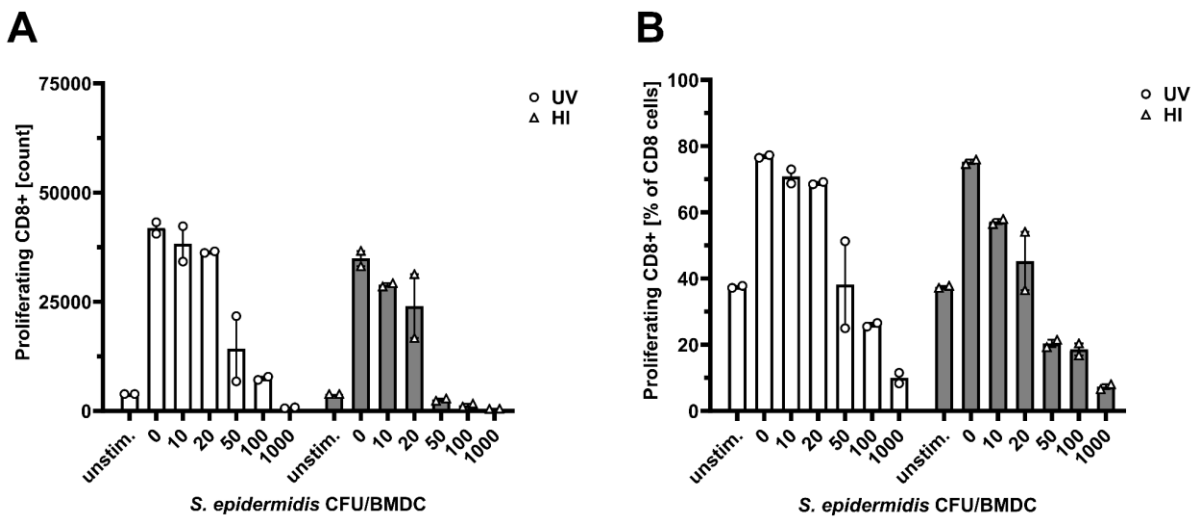

Figure 15: Comparison of the OT-I T cell proliferation in co-culture with BMDCs and stimulated with OVA protein and exposed to either UV-attenuated or heat-inactivated *S. epidermidis*.

Co-cultures of BMDCs and OT-I T cells were stimulated with OVA protein and exposed to heat-inactivated (HI) or UV-attenuated (UV) *S. epidermidis* strain 614 at the indicated concentrations. OT-I T cell proliferation was analysed by detection of the CFSE intensity in FACS after 72 h of incubation. **(A)** Counts and **(B)** frequencies of proliferating OT-I T cells are depicted.
Bars represent means ± SEM of n = 2 BMDC donors. Replicates are illustrated in symbols.

3.5 The suppression of OT-I T cells is caused by *S. epidermidis* itself and not by metabolic products or contaminations

Control experiments were conducted to exclude the possibility that contaminations, being carried over from the production of UV-attenuated *S. epidermidis,* or metabolic products of the *S. epidermidis* growth culture reduced the OT-I T cell proliferation. An overview of the experimental setup is illustrated in Figure 16. Supernatants and media controls were removed at various times in the course of the production of UV-attenuated *S. epidermidis* and also underwent UV-irradiation. These controls then replaced *S. epidermidis* in the co-cultures, which were performed as explained above (see Figure 12 and associated explanation).

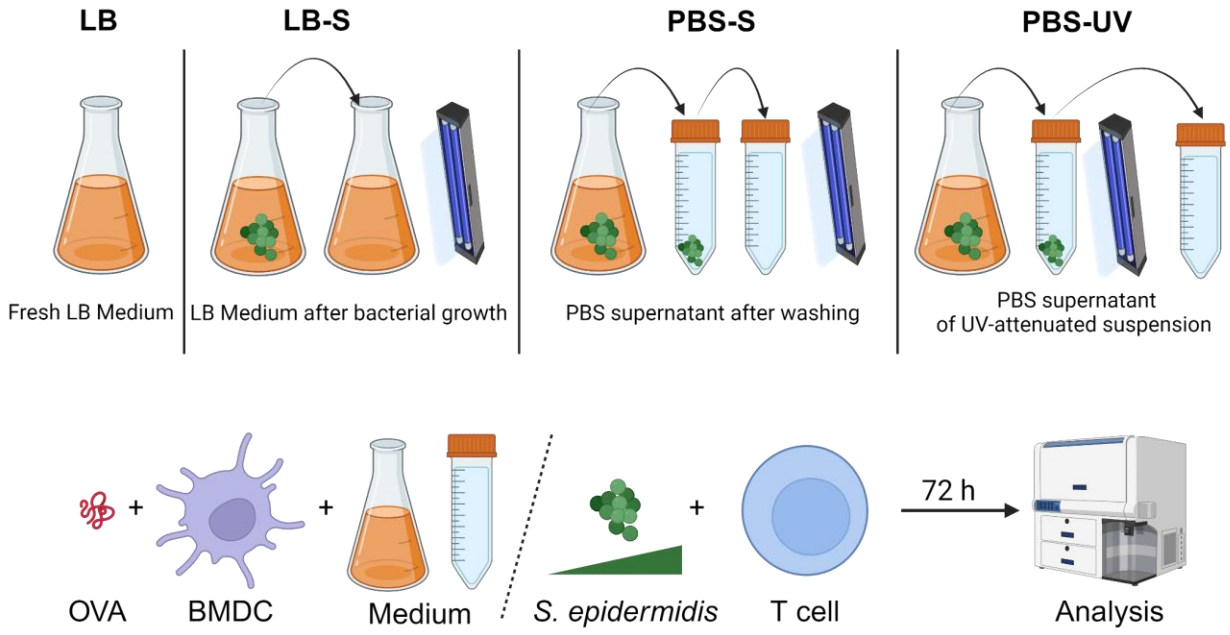

Figure 16: Experimental setup: Extraction of media controls during *S. epidermidis* production, used to replace *S. epidermidis* in the co-cultures.

The different media controls which replaced *S. epidermidis* in the co-cultures of BMDCs and OT-I T cells were extracted at different steps during the production of UV-attenuated *S. epidermidis*. An aliquot of LB medium (LB) was separated before being used for culturing *S. epidermidis*. After centrifugation of the *S. epidermidis* growth suspension, supernatant culture medium was collected, defined as LB-S. PBS supernatant was collected during washing steps of *S. epidermidis* (PBS-S). LB-S and PBS-S underwent the same UV-attenuation process as the *S. epidermidis* suspension. Prior usage of the UV-attenuated *S. epidermidis*, an aliquot of the stock was centrifuged and the supernatant served as last control (PBS-UV). Co-cultures where then stimulated with OVA and incubated with UV-attenuated *S. epidermidis* or the media controls for 72 h, followed by proliferation analysis of OT-I T cells.
Created with BioRender.com.

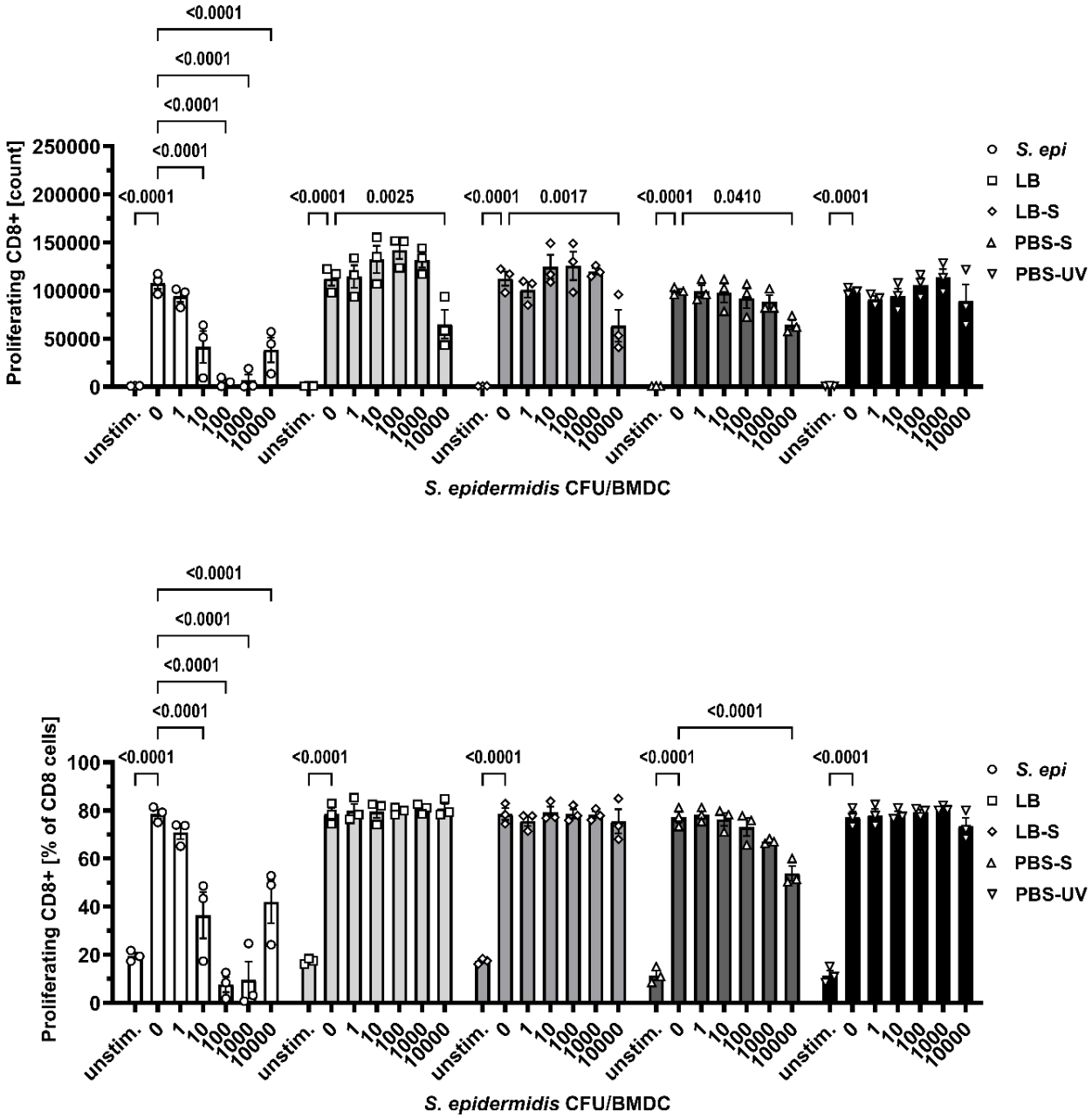

Figure 17: Proliferation of OT-I T cells in co-cultures with BMDCs, OVA protein and *S. epidermidis* or media controls.

Co-cultures of BMDCs and OT-I T cells were stimulated with OVA protein and incubated with UV-attenuated *S. epidermidis* strain 614 (*S. epi*) or media controls at the indicated concentrations. Equivalent volumes of the media controls in relation to the respective volume of UV-attenuated *S. epidermidis* used served as controls. These media controls are labelled in the graph with the same designations as used for the UV-attenuated *S. epidermidis*, but did not contain any bacteria. OT-I T cell proliferation was analysed by detection of the CFSE profile in FACS after 72 h of incubation. Counts and frequencies of proliferating OT-I T cells are depicted. Within groups, counts or frequencies of each *S. epidermidis* CFU/BMDC concentration were compared to the respective 0 *S. epidermidis* CFU/BMDC concentration.
Bars represent means ± SEM of n = 3 BMDC donors. Replicates are illustrated in symbols. Ordinary two-way ANOVA with Dunnett's multiple comparisons test was performed to obtain p values. Only p values < 0.05 are shown.

Counts and frequencies of proliferating OT-I T cells within co-cultures incubated with UV-attenuated *S. epidermidis* or the media controls are displayed in Figure 17. The OVA-specific proliferation of OT-I T cells was induced in all co-culture groups. This is recognisable by the fact that the counts and frequencies of proliferating OT-I T cells in the 0 CFU/BMDC condition, which contains only OVA, are significantly increased compared to the unstimulated control. *S. epidermidis* significantly reduced the antigen-specific proliferation of OT-I T cells, when compared to the 0 CFU/BMDC condition. This was observed for the count and frequency parameter. Looking at the media controls, the counts of proliferating OT-I T cells generally did not drop in cell numbers compared to the OVA control (0 CFU/BMDC). Only in LB, LB-S and PBS-S co-cultures the stimulation with the volume equivalent for 10000 CFU/BMDC markedly reduced the counts. For the frequencies of proliferating OT-I T cells in the media controls, only the equivalent for 10000 CFU/BMDC of the PBS-S control was significantly decreased by approximately 20 per cent compared to 0 CFU/BMDC.

P values from the comparison of the specific *S. epidermidis* CFU/BMDC concentrations with their related volume equivalents in the media controls are delineated in Table 21 (Ordinary two-way ANOVA with Dunnett's multiple comparisons test). Counts as well as frequencies of 10, 100, and 1000 CFU/BMDC equivalents were significantly higher in the control groups than in *S. epidermidis*. Regarding the 10000 CFU/BMDC stimulation, counts of the PBS-UV and frequencies at all conditions of the media controls except the one of PBS-S were significantly higher than the respective *S. epidermidis* condition.

Taken together, the addition of UV-attenuated *S. epidermidis* but not the media controls reduced the OT-I T cell proliferation in co-cultures in general. Only the medium controls for the 10000 *S. epidermidis* CFU/BMDC condition showed a slight reduction in OT-I T cell proliferation.

Table 21: P values for the comparison of the media controls against *S. epi* for the respective *S. epidermidis* CFU/BMDC concentration.

Proliferating CD8+ [count]							
	unstim.	**0**	**1**	**10**	**100**	**1000**	**10000**
***S. epi* vs. LB**	ns	ns	ns	<0.0001	<0.0001	<0.0001	ns
***S. epi* vs. LB-S**	ns	ns	ns	<0.0001	<0.0001	<0.0001	ns
***S. epi* vs. PBS-S**	ns	ns	ns	0.0002	<0.0001	<0.0001	ns
***S. epi* vs. PBS-UV**	ns	ns	ns	0.0005	<0.0001	<0.0001	0.0007

Proliferating CD8+ [% of CD8]							
	unstim.	**0**	**1**	**10**	**100**	**1000**	**10000**
***S. epi* vs. LB**	ns	ns	ns	<0.0001	<0.0001	<0.0001	<0.0001
***S. epi* vs. LB-S**	ns	ns	ns	<0.0001	<0.0001	<0.0001	<0.0001
***S. epi* vs. PBS-S**	ns	ns	ns	<0.0001	<0.0001	<0.0001	ns
***S. epi* vs. PBS-UV**	ns	ns	ns	<0.0001	<0.0001	<0.0001	<0.0001

3.6 *S. epidermidis* failed to suppress OT-I T cell proliferation induced by anti-CD3/CD28 beads in absence of BMDCs

To investigate if *S. epidermidis* directly influences the proliferation of OT-I T cells, pure cultures of CFSE-labelled OT-I T cells were stimulated with anti-CD3/C28 beads, which induce proliferation in a MHC class I-independent way, and were exposed to different concentrations of *S. epidermidis*. After 72 h, the proliferation was analysed by the CFSE profile (Figure 18).

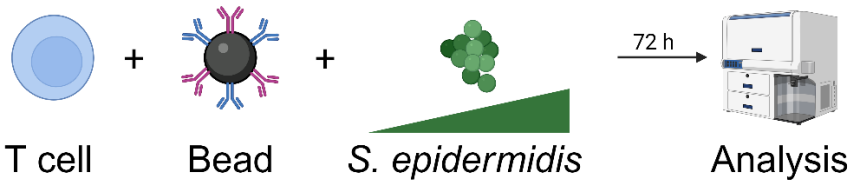

Figure 18: Experimental setup: OT-I T cell cultures stimulated with anti-CD3/CD28 beads and exposed to *S. epidermidis*.

CFSE-labelled OT-I T cells are stimulated with anti-CD3/CD28 beads to induced proliferation and were exposed to *S. epidermidis*. After 72 h incubation, the proliferation is analysed by the CFSE profile using FACS. Created with Biorender.com.

Depicted in Figure 19, the stimulation with anti-CD3/CD28 (indicated by the 0 *S. epidermidis* CFU/T cell label, which only contained beads in the well) induced the proliferation of OT-I T cells compared to unstimulated controls. Unlike previously observed in co-cultures with BMDCs, the addition of *S. epidermidis* did not reduce counts or frequencies of proliferating OT-I T cells. In contrast, counts of 100 CFU/T cell *S. epidermidis*-stimulated OT-I T cells were even higher than in the 0 CFU/T cell control.

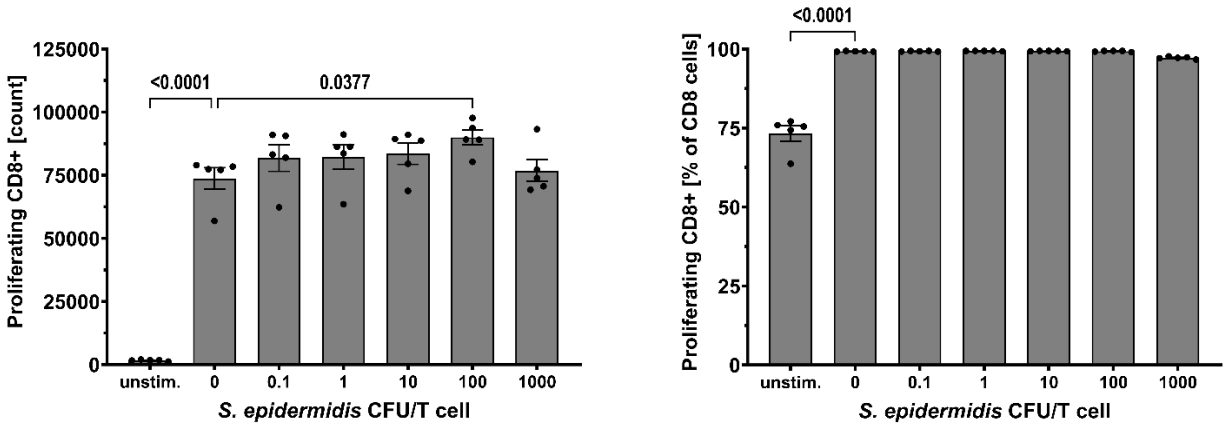

Figure 19: Proliferation of OT-I T cells stimulated with anti-CD3/CD28 beads and exposed to *S. epidermidis*.

100.000 OT-I T cells per well were stimulated with anti-CD3/CD28 beads, in a ratio of 1:1, and were exposed to different concentrations of UV-attenuated *S. epidermidis* strain 614 for 72 h. Proliferation was analysed by detection of the CFSE intensity in FACS. The counts of proliferating OT-I T cells and their percentages among all OT-I T cells were compared to the respective 0 *S. epidermidis* CFU/T cell condition.
Bars represent means ± SEM of n = 5 OT-I T cell donor mice. Biological replicates are illustrated in symbols. Ordinary one-way ANOVA with Dunnett's multiple comparisons test was performed to obtain p values. Only p values < 0.05 are shown.

3.7 The presence of BMDCs is crucial for the suppression of OT-I T cell proliferation

OT-I T cell proliferation was not suppressed in experiments where OT-I T cells were stimulated with anti-CD3/CD28 beads and exposed to UV-attenuated *S. epidermidis* in the absence of BMDCs (cf. chapter 3.6). Therefore, in the following we investigated whether the presence of BMDCs is necessary to suppress an antigen-specific OT-I T cell proliferation during *S. epidermidis* exposure.

3.7.1 Stimulation of OT-I T cells with anti-CD3/CD28 beads in presence of BMDCs and *S. epidermidis*

In the first experiment, the experimental setup from chapter 3.6 was adopted, with the difference that BMDCs were now added to the OT-I T cell/bead culture (see Figure 20). Therefore, the *S. epidermidis* concentration was now determined in relation to the BMDC number again. However, it was still a MHC class I-independent activation of the OT-I T cell proliferation by anti-CD3/CD28 beads, as no OVA protein was present in this co-culture.

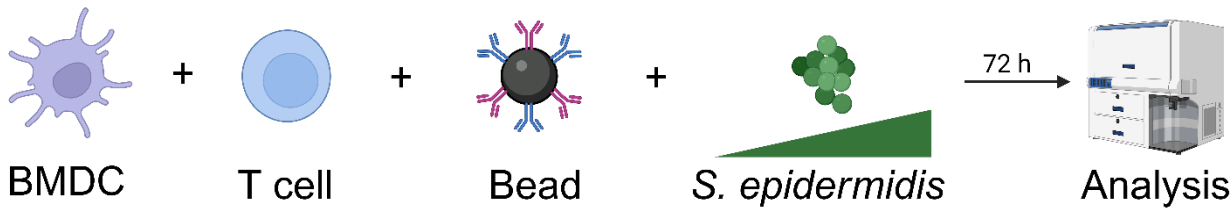

Figure 20: Experimental setup: Co-culture of BMDCs and OT-I T cells stimulated with anti-CD3/CD28 beads in the presence of *S. epidermidis*.

CFSE-labelled OT-I T cells were co-cultured with BMDCs and different concentrations of *S. epidermidis*. Anti-CD3/CD28 beads were added to induce proliferation of OT-I T cells. After 72 h of incubation, the proliferation of OT-I T cells was analysed by the CFSE profile, which was detected using FACS. Created with BioRender.com.

Looking at the counts of proliferating OT-I T cells, we observed that beads alone (0 CFU/BMDC) did not stimulate proliferation as strongly as this was the case in Figure 19. In comparison to 0 CFU/BMDC, the addition of 10 and 10000 CFU/BMDC actually increased proliferation. 100 or 1000 *S. epidermidis* CFU/BMDC obviously reduced the counts, but the statistics showed no significance for this. Referred to the percentages of proliferating OT-I T cells, significantly more cells proliferated due to the addition of beads than without any stimulus. Compared to 0 CFU/BMDC, the concentrations 100 and 1000 CFU/BMDC of *S. epidermidis* significantly reduced the frequency of proliferating OT-I T cells. A weak but significant reduction in the frequency of proliferating OTI T cells was also analysed for 10000 CFU/BMDC.

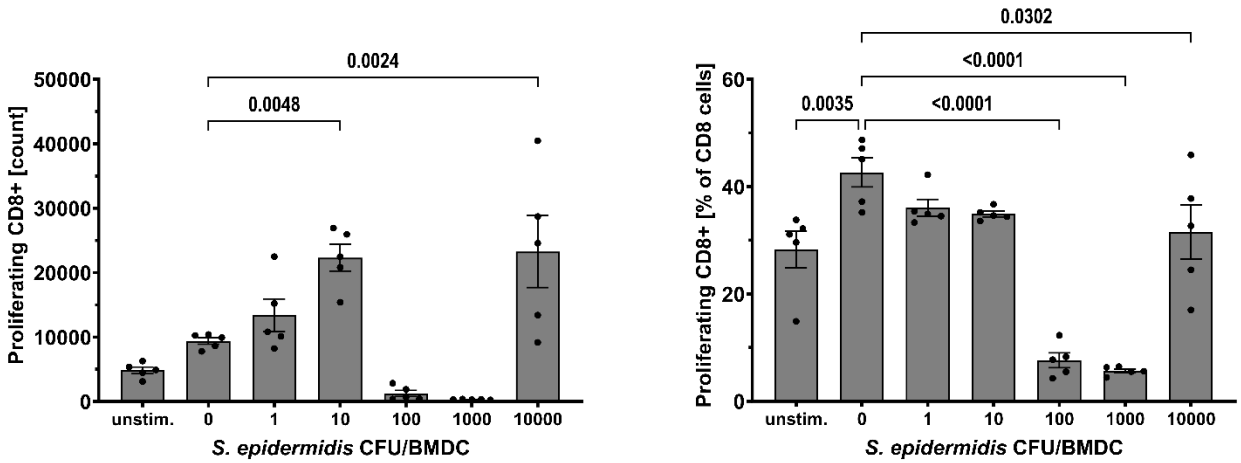

Figure 21: Proliferation of OT-I T cells co-cultured with BMDCs and *S. epidermidis* and stimulated with anti-CD3/CD28 beads.

Co-cultures of BMDCs and OT-I T cells were stimulated with anti-CD3/CD28 in the presence of heat-inactivated *S. epidermidis* strain 614 at the indicated concentrations. OT-I T cell proliferation was analysed by detection of the CFSE intensity in FACS after 72 h of incubation. Counts and frequencies of proliferating OT-I T cells were compared to the 0 *S. epidermidis* CFU/BMDC condition.
Bars represent means ± SEM of n = 5 BMDC donors. Replicates are illustrated in symbols. Ordinary one-way ANOVA with Dunnett's multiple comparisons test was performed to obtain p values. Only p values < 0.05 are shown.

3.7.2 Stimulation of OT-I T cells with the $OVA_{257-264}$ peptide SIINFEKL in presence of BMDCs and *S. epidermidis*

In another investigation, only OT-I T cells were exposed to *S. epidermidis* and stimulated with the $OVA_{257-264}$ peptide SIINFEKL (Figure 22). This highly affine peptide can induce proliferation of OT-I T cells in absence of antigen-presenting cells. A second culture additionally contained BMDCs. In both cultures, stimulation with the $OVA_{257-264}$ peptide (0 *S. epidermidis* CFU/T cell) substantially induced proliferation of OT-I T cells compared to the unstimulated condition. In the absence of BMDCs, *S. epidermidis* had no negative effect on OT-I T cell proliferation. There was even the tendency for 10 and 100 CFU/BMDC to enhance proliferation. In contrast, the addition of *S. epidermidis* significantly dampened the proliferation compared to 0 CFU/T cell at all concentrations used, when BMDCs were present.

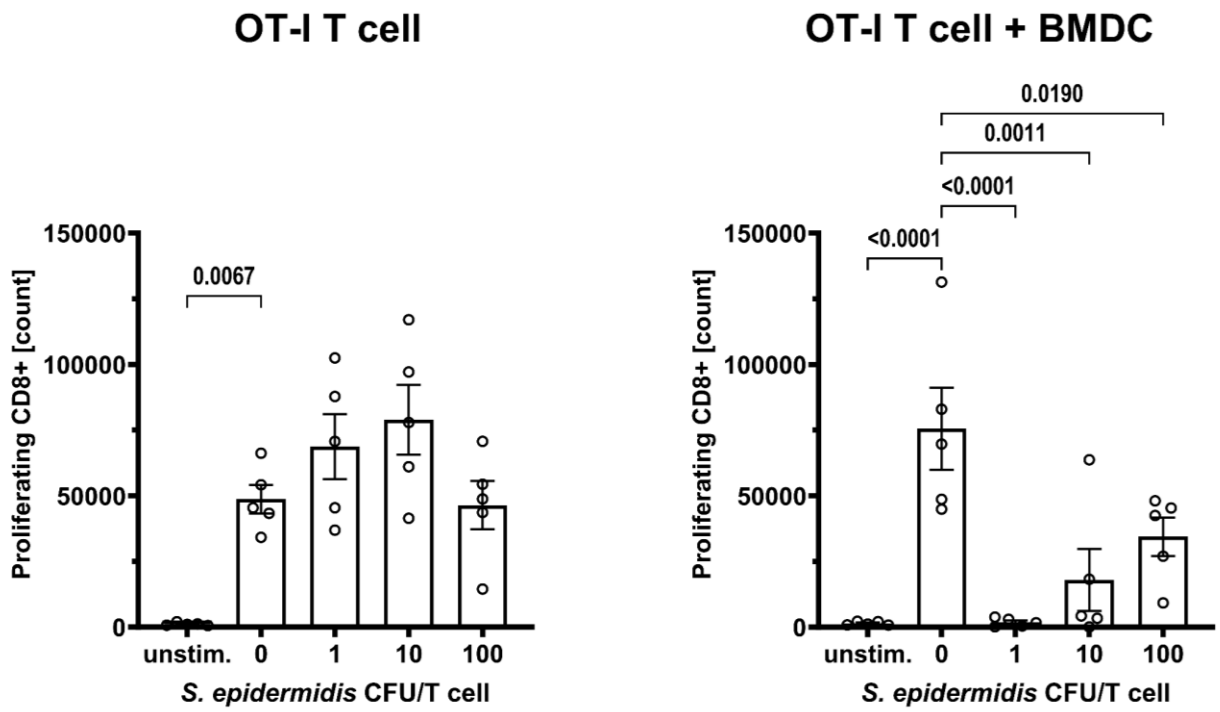

Figure 22: Proliferation of OT-I T cells that were stimulated with $OVA_{257-264}$ (SIINFEKL) and exposed to *S. epidermidis* in the absence and presence of BMDCs.

Pure OT-I T cell cultures (left graph) or co-cultures of OT-I T cells with BMDCs (right graph) were stimulated with 1 nM $OVA_{257-264}$ peptide and exposed to heat-inactivated *S. epidermidis* lysate strain 614 at the indicated concentrations. The pure OT-I T cell culture was stimulated with the same CFU of *S. epidermidis* lysate as the co-culture. OT-I T cell proliferation was analysed by detection of the CFSE profile in FACS after 72 h of incubation. Counts of proliferating OT-I T cells are graphed and the 0 *S. epidermidis* CFU/T cell concentration was compared to the other concentrations.

Bars represent means ± SEM of n = 5 BMDC donors. Replicates are illustrated in symbols. Ordinary one-way ANOVA with Dunnett's multiple comparisons test was performed to obtain p values. Only p values < 0.05 are shown.

3.7.3 The depletion of CD11c-DTR BMDCs during co-culture mitigated the *S. epidermidis*-induced suppression of OT-I T cell proliferation

Another approach to investigate the necessity of BMDCs for the suppression of OT-I T cell proliferation was to remove the BMDCs in a co-culture after a certain period of time (Figure 23). For this purpose, BMDCs were generated from the bone marrow of CD11c-DTR mice. The special feature of these mice is that all cells expressing CD11c co-express the diphtheria toxin receptor (DTR) (Dennis et al. 2002). The addition of diphtheria toxin (DT) then leads to the depletion of CD11c positive cells. This method allows the depletion of BMDCs, as they express CD11c, in the co-cultures at a defined point in time. The co-cultures consisted of OT-I T cells and either WT BMDCs or CD11c-DTR BMDCs and were stimulated with OVA protein and incubated with UV-attenuated *S. epidermidis*. After 24 h, DT was administrated to deplete CD11c-DTR BMDCs. This time point was chosen to allow the initial activation of OT-I T cells by OVA-presenting BMDCs before their depletion. After a further 48 h of incubation, OT-I T cell proliferation was analysed by the CFSE profile.

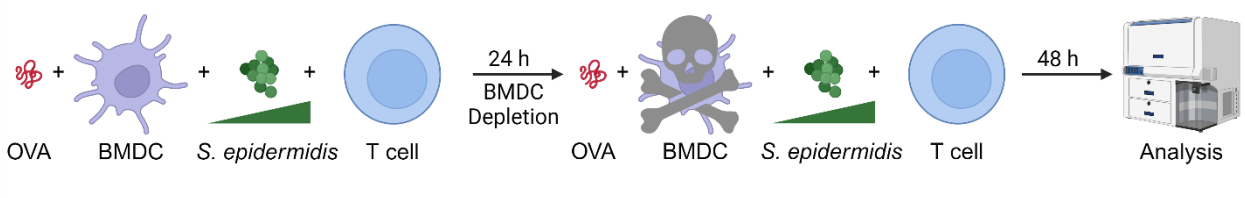

Figure 23: Experimental setup: Co-culture of OT-I T cells and CD11c-DTR BMDCs stimulated with OVA protein and exposed to *S. epidermidis*.

BMDCs were generated from WT and CD11c-DTR mice and were co-cultured with CFSE-labelled OT-I T cells. OVA protein stimulation induced proliferation of OVA-specific OT-I T cells. *S. epidermidis* was added at different concentrations to the co-cultures. Diphtheria toxin (DT) was administrated to the co-cultures after 24 h and incubation was continued. After another 48 h of incubation, the proliferation of OT-I T cells was analysed by the CTV profile, which was detected using FACS. Created with BioRender.com.

Firstly, it was investigated whether the generated WT and CD11c-DTR BMDCs are similar in maturation and whether DT depletes the CD11c-DTR BMDCs (Figure 24). BMDCs were treated 24 h with DT or remained untreated, followed by FACS analysis for viability and MHC class II as well as CD86 expression. Exemplary dot plots for the gating are depicted in Figure 24A. Cell debris was excluded by size in the FSC-A channel followed by the determination of live cell percentages. Live cells were gated on CD11b+ cells, and CD86 and MHC class II expression levels defined maturity. Viability of WT BMDCs was not affected by DT administration, but it clearly reduced the percentage of live CD11c-DTR BMDCs compared to the unstimulated ones (Figure 24B). We were able to deplete about 93 % of BMDCs. Approximately 7 % of the CD11c-DTR BMDCs remained alive. It was noticeable that around 10 % more living cells were measured in the DT-untreated WT BMDCs than in the respective CD11c-DTR BMDCs. The percentage of

mature BMDCs was comparable for both types. DT did not affect the maturation status of WT-BMDCs. CD11c-DTR BMDCs that were treated with DT and were still alive showed a lower proportion of mature cells than unstimulated BMDCs.

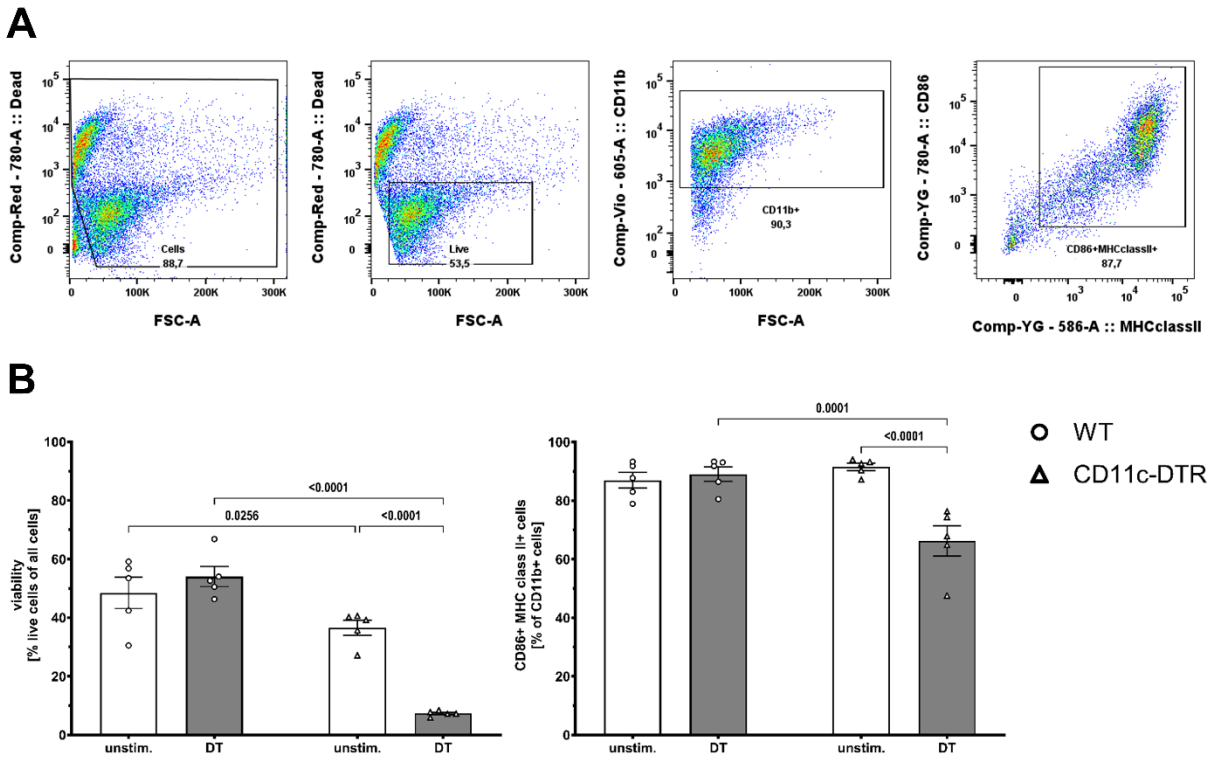

Figure 24: Comparison of WT and CD11c-DTR BMDCs.

BMDCs generated from WT and CD11c-DTR mice were examined to see if they had a comparable phenotype before they were used in the co-cultures. Moreover, depletion efficiency of CD11c-DTR BMDCs by DT was controlled. **(A)** Representative dot plots of the gating strategy after FACS analysis (WT BMDCs without DT treatment). **(B)** Viability and maturation state of untreated and 24 h DT-treated BMDCs.
Bars represent means ± SEM of n = 5 BMDC donor mice for each genotype. Replicates are illustrated in symbols. Empty bars represent untreated BMDCs whereas grey bars represent DT-treated ones. Circles represent WT BMDCs and triangles represent CD11c-DTR BMDCs. Ordinary two-way ANOVA with uncorrected Fisher's LSD test was performed to obtain p values. Only p values < 0.05 are shown.

In the following, we investigated how the depletion of BMDCs in co-cultures with OT-I T cell affects the suppressive effect of *S. epidermidis* on the OT-I T cell proliferation. Counts and frequencies of proliferating OT-I T cells within co-cultures are presented in Figure 25A for WT BMDCs and in Figure 25B for CD11c-DTR BMDCs. Compared to 0 CFU/BMDC, significantly lower counts and frequencies of proliferating OT-I T cells were detected in unstimulated as well as 10, 100 and 1000 *S. epidermidis* CFU/BMDC conditions (statistics not shown; $p < 0.0001$; Two-way ANOVA with Dunnett's multiple comparisons test) in WT BMDC co-cultures, irrespective of DT treatment. Moreover, there were no statistical differences between co-cultures with and without DT for related CFU/BMDC *S. epidermidis* concentrations (Figure 25A).

The counts and frequencies of OT-I T cells were also reduced in the CD11c-DTR BMDC co-cultures without DT treatment (Figure 25B). The unstimulated condition and the addition of 10,

100, 1000 *S. epidermidis* CFU/BMDC resulted in significantly less OT-I T cell proliferation than the 0 CFU/BMDC condition (statistics not shown; $p < 0.0001$; Two-way ANOVA with Dunnett's multiple comparisons test). However, when CD11c-DTR BMDC co-cultures were treated with DT after 24 h, OT-I T cell proliferation was significantly lower in the unstimulated condition than in the OVA control (0 CFU/BMDC) (statistics not shown; $p < 0.0001$; Two-way ANOVA with Dunnett's multiple comparisons test). A comparison of the related co-culture conditions between the CD11c-DTR co-cultures with and without DT treatment revealed differences in OT-I T cell proliferation. For 100 CFU/BMDC, the OT-I T cell counts in the DT-treated co-culture were significantly higher than in the control (without DT). At 10 and 1000 CFU/BMDC, more counts of proliferating OT-I T cells were also detectable in DT-treated than DT-untreated CD11c-DTR BMDC co-cultures, but without statistical significance. Looking at the frequencies of proliferating OT-I T cells, the conditions 10, 100, 1000 CFU/BMDC showed significantly higher percentages in the DT-treated co-cultures than in the respective counterparts of untreated co-cultures.

Considering the three experiments in this chapter, we observed that OT-I T cell proliferation is only suppressed by *S. epidermidis* in the presence of BMDCs. In experiments of the sections 3.7.1 and 3.7.2, *S. epidermidis* failed to suppress the proliferation of OT-I T cells, which was induced by stimulation with either anti-CD3/CD28 beads or the $OVA_{257-264}$ peptide SIINFEKL, in the absence of BMDCs. The co-culture with BMDCs under otherwise constant conditions resulted in a suppressed OT-I T cell proliferation when *S. epidermidis* was added. In section 3.7.3, the depletion of BMDCs after 24 h still allowed the initialisation of the OT-I T cell proliferation, but the suppression of OT-I T cell proliferation due to the presence of *S. epidermidis* was attenuated.

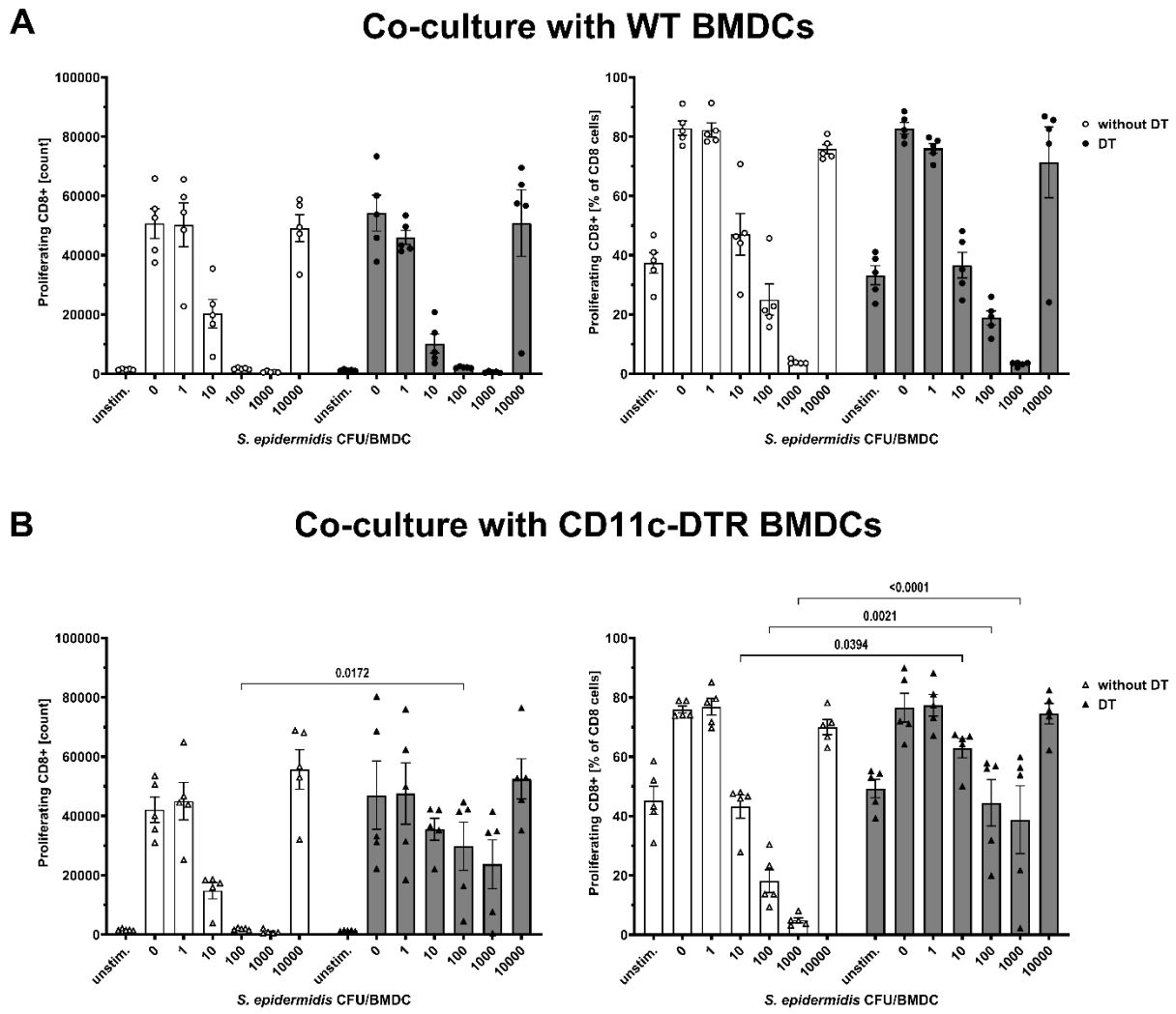

Figure 25: Proliferation of OT-I T cells in co-cultures with WT or CD11c-DTR BMDCs and OVA protein and exposure to *S. epidermidis*.

Co-cultures of CTV-labelled OT-I T cells with BMDCs, generated from WT or CD11c-DTR mice, were stimulated with OVA and UV-attenuated *S. epidermidis* strain 614. DT was administrated to the co-culture after 24 h to deplete CD11c-DTR BMDCs. OT-I T cell proliferation was analysed by detection of the CTV intensity in FACS. Counts of proliferating OT-I T cells and their percentage among all OT-I T cells are depicted for co-cultures without DT and with DT administration. The influence of DT administration and thereby potential BMDC depletion on OT-I T cell proliferation is displayed for co-cultures with **(A)** WT BMDCs and **(B)** CD11c-DTR BMDCs, comparing the proliferation between "DT" and "without DT" for each condition.
Bars represent means ± SEM of n = 5 BMDC donor mice for each genotype. Replicates are illustrated in symbols. Empty bars and triangles represent co-cultures without DT administration whereas grey bars and filled triangles represent co-cultures with DT administration. Ordinary two-way ANOVA with Šídák's multiple comparisons test was performed to obtain p values. Only p values < 0.05 are shown.

3.8 Involvement of soluble, heat-sensitive molecules in the suppression of OT-I T cell proliferation

The previous experiments showed that antigen-specific OT-I T cell proliferation was attenuated by the simultaneous presence of BMDCs and *S. epidermidis*. A direct influence of *S. epidermidis* on OT-I T cell proliferation was excluded and the antigen presentation of BMDCs did not seem to be involved. In the following, we investigated whether *S. epidermidis*-induced expression of molecules or cytokines by OT-I T cells or BMDCs during incubation of the co-cultures could be the cause of the suppression.

The experimental setup is outlined in Figure 26. First, supernatants were generated in a culture/co-culture #1. These were either i) pure BMDC cultures or ii) pure anti-CD3/CD28-stimulated OT-I T cell cultures or iii) OVA-stimulated co-cultures of BMDCs and OT-I T cells. All three cultures were exposed to different concentrations of *S. epidermidis*. After 72 h, the supernatants were harvested and residual cells and bacteria were removed by centrifugation. These supernatants were then used to stimulate a fresh co-culture #2 consisting of BMDCs, CFSE-labelled OT-I T cells and OVA protein. Thus, the supernatants replaced *S. epidermidis*. After 72 h, the proliferation of the OT-I T cells was analysed using the CFSE profile. The aim of this experiment was to determine whether soluble factors such as cytokines are involved in the suppression and whether BMDCs or OT-I T cells are their potential source. If soluble factors are responsible for OT-I T cell suppression, this should be transferable through the supernatants.

Before the use of the supernatants, the OT-I T cell proliferation of co-culture #1 was analysed to verify that the co-cultures and *S. epidermidis* functioned as usual. The addition of OVA (0 CFU/BMDC) clearly induced OT-I T cell proliferation compared to the unstimulated condition, as indicated by the increased counts and frequencies. Addition of 10, 100 and 1000 *S. epidermidis* CFU/BMDC suppressed this induced OT-I T cell proliferation again, as already observed in previous experiments (Figure 27A). Figure 27B shows the counts and frequencies of proliferating OT-I T cells from co-cultures #2. Addition of the supernatants of the pure BMDC culture #1 did not decrease the counts of proliferating OT-I T cells for any of the conditions. However, compared to the OVA control the percentage of OT-I T cells in proliferation was reduced by approximately 20 % from 100 CFU/BMDC on. Next, the counts of OT-I T cells in co-culture #2 treated with supernatants from the bead-stimulated pure OT-I T cell cultures are considered. The counts of proliferating OT-I T cells were decreased, although not significant, in correlation with the in culture #1 used *S. epidermidis* CFU/BMDC concentration. However, supernatants from *S. epidermidis*-treated OT-I T cell cultures #1 significantly decreased the percentage of proliferating OT-I T cells in co-culture #2 from 10 CFU/BMDC on. The higher the *S. epidermidis* concentration was in culture #1, the more the supernatants reduced the proliferation in co-culture #2. Finally, the proliferation of OT-I T cells in co-culture #2 that were treated with supernatants from BMDC and

OT-I T cell co-cultures #1 is considered. Here, the strongest suppression by supernatants was detected. Compared to the OVA control (0 CFU/BMDC), the counts were significantly lower from 100 CFU/BMDC due to supernatants. The frequencies also showed a clear suppression of OT-I T cell proliferation. Starting from 10 CFU/BMDC supernatant condition, the frequencies were lower than in the OVA control (0 CFU/BMDC).

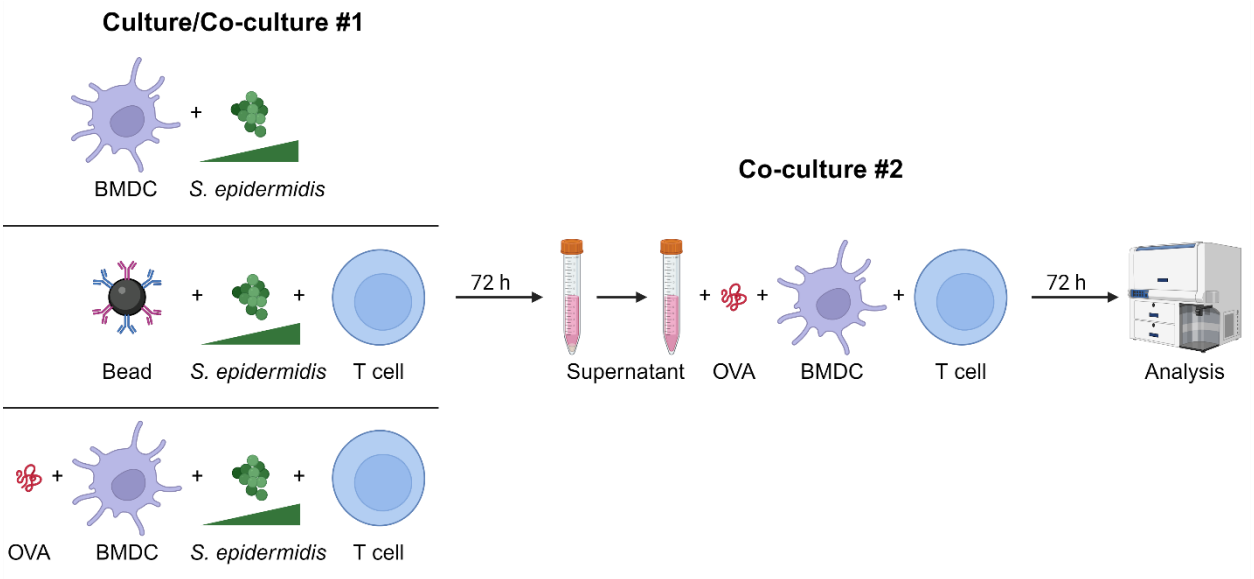

Figure 26: Experimental setup: Replacement of *S. epidermidis* in co-cultures by supernatants harvested from *S. epidermidis*-exposed cultures/co-cultures.

Three different kinds of cultures/co-cultures were set up to generate supernatants. In the first culture, pure BMDC cultures were incubated with UV-attenuated *S. epidermidis.* The second culture, consisting of OT-I T cells, was stimulated with anti-CD3/CD28 beads and exposed to UV-attenuated *S. epidermidis*. The last culture was a co-culture of BMDCs and OT-I T cells and was stimulated with OVA protein and exposed to UV-attenuated *S. epidermidis*. The three cultures were incubated for 72 h each and then the supernatant was removed and cleaned of cell and bacterial residues by centrifugation. These supernatants were then added to fresh co-cultures consisting of BMDCs, CFSE-labelled OT-I T cells and OVA protein. The supernatants replaced *S. epidermidis*. After 72 h, the proliferation of OT-I T cells was analysed by the CFSE profile, which was detected using FACS. Created with BioRender.com.

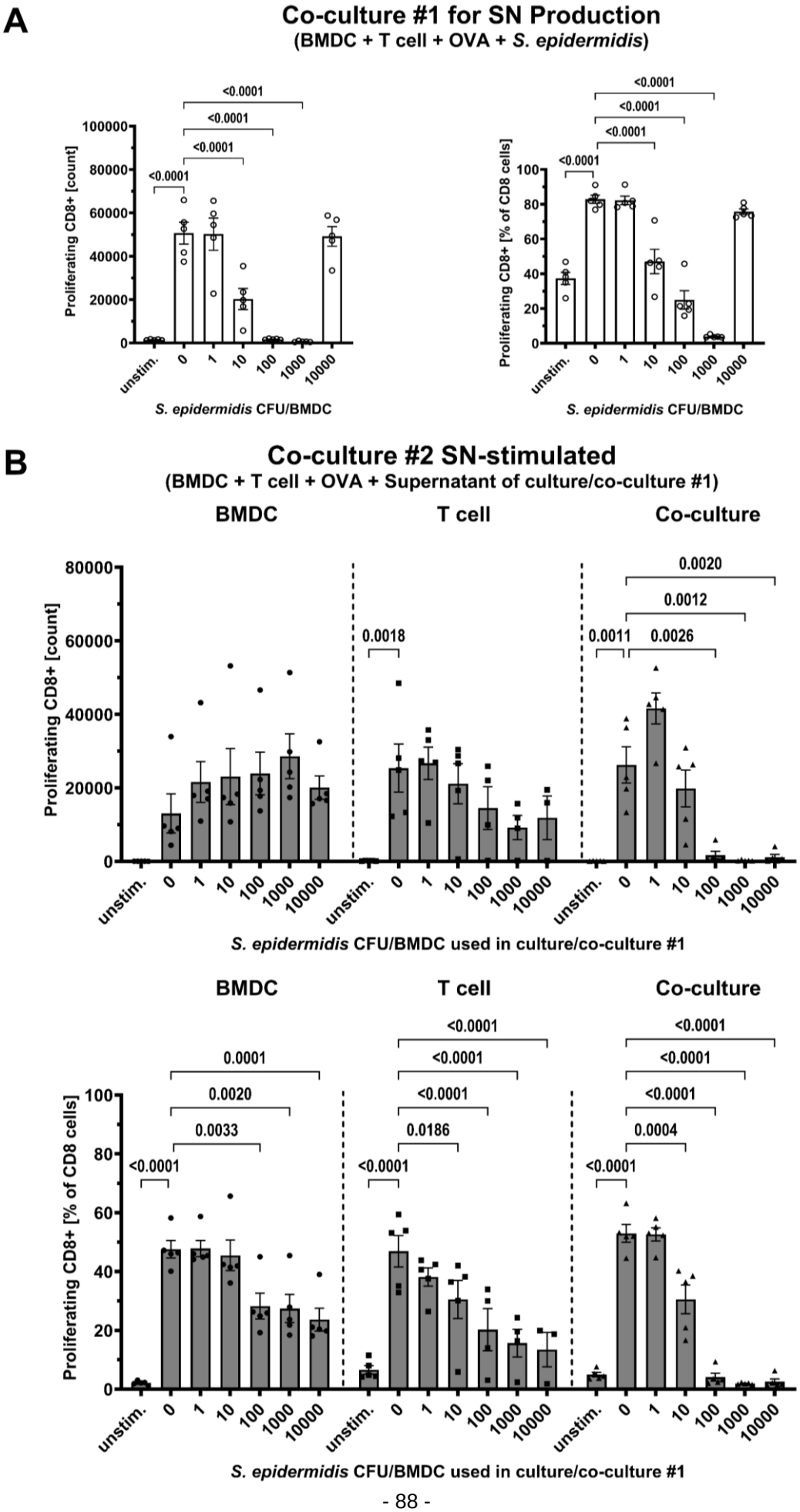
A
Co-culture #1 for SN Production
(BMDC + T cell + OVA + S. epidermidis)
Proliferating CD8+ [count]
Proliferating CD8+ [% of CD8 cells]
<0.0001
unstim.
0
1
10
100
1000
10000
S. epidermidis CFU/BMDC
B
Co-culture #2 SN-stimulated
(BMDC + T cell + OVA + Supernatant of culture/co-culture #1)
BMDC
T cell
Co-culture
0.0018
0.0011
0.0026
0.0012
0.0020
0.0001
0.0033
0.0186
0.0004
S. epidermidis CFU/BMDC used in culture/co-culture #1

Figure 27: Proliferation of OT-I T cells in co-cultures that were treated with supernatants of *S. epidermidis*-treated pure BMDC cultures, OT-I T cell/Bead cultures or BMDC OT-I T cell co-cultures.

BMDC cultures, OT-I T cell / bead cultures as well as co-cultures of BMDCs, OT-I T cells and OVA protein were exposed to different concentrations of UV-attenuated *S. epidermidis* strain 614 for 72 h. Supernatants of these cultures / co-cultures #1 were added to fresh co-cultures #2 of BMDCs, OT-I T cells, and OVA protein. OT-I T cell proliferation was analysed by detection of the CFSE intensity in FACS after 72 h of incubation. **(A)** Counts and frequencies of proliferating OT-I T cells were compared to the respective 0 *S. epidermidis* CFU/BMDC value in the co-culture #1 used for supernatant production. **(B)** Counts and frequencies of proliferating OT-I T cells were compared to the respective 0 *S. epidermidis* CFU/BMDC value in a fresh co-culture, treated with supernatants instead of *S. epidermidis*. The type of original culture / co-culture #1 whose supernatant was used to stimulate co-culture #2 is indicated above the respective graph group as "BMDC", "T cell" or "Co-culture". The co-culture #2 medium contained 50 % supernatant from culture / co-culture #1. The x-axis indicates the CFU/BMDC *S. epidermidis* that were used in culture / co-culture # 1 to generate the supernatants. No *S. epidermidis* was used in the depicted co-culture #2.
Bars represent means ± SEM of n = 5 BMDC or OT-I T cell donor mice. One of two independent repetitions for this experiment is displayed here. Replicates are illustrated in symbols. Ordinary two-way ANOVA with Dunnett's multiple comparisons test was performed to obtain p values. Only p values < 0.05 are shown.

If the factors transferred with the supernatant that suppressed proliferation in fresh co-cultures are cytokines, it should be possible to neutralise the effect by heat inactivation. For this purpose, selected supernatants were heat-inactivated after collection. The supernatants from co-culture #1 with 100 and 1000 *S. epidermidis* CFU/BMDC treatment were selected, as the strongest suppression of OT-I T cell proliferation was usually observed here. Subsequently, their influence on OT-I T cell proliferation in co-cultures was compared with supernatants that were not heat-inactivated (Figure 28). Shown in Figure 28A, the counts and frequencies of proliferating OT-I T cells were significantly reduced compared to the OVA control (CFU/BMDC) when 100 and 1000 CFU/BMDC unheated supernatants were used. In contrast, the use of heat-inactivated supernatants did not reduce the counts. Only the addition of heat-inactivated 1000 CFU/BMDC supernatant slightly reduced the frequency of proliferating OT-I T cells. A direct comparison of unheated and heat-inactivated supernatants showed that the OT-I T cell count for 1000 CFU/BMDC after treatment with unheated supernatants was significantly lower than for heat-inactivated supernatants (Figure 28B). The frequency of proliferating OT-I T cells was also significantly lower after stimulation with unheated supernatant than with heat-inactivated supernatant.

In brief, we observed that the transfer of supernatants from pure BMDC or OT-I T cell cultures or co-cultures, which were exposed to *S. epidermidis*, into a new co-culture affected the proliferation of OT-I T cells to different extents. The suppression of OT-I T cell proliferation was strongest with supernatants from co-cultures. However, supernatants from *S. epidermidis*-treated OT-I T cell cultures also reduced the proliferation of OT-I T cells in co-culture #2. Finally, we were able to show that heat inactivation abolished the suppressive effect of transferred supernatants.

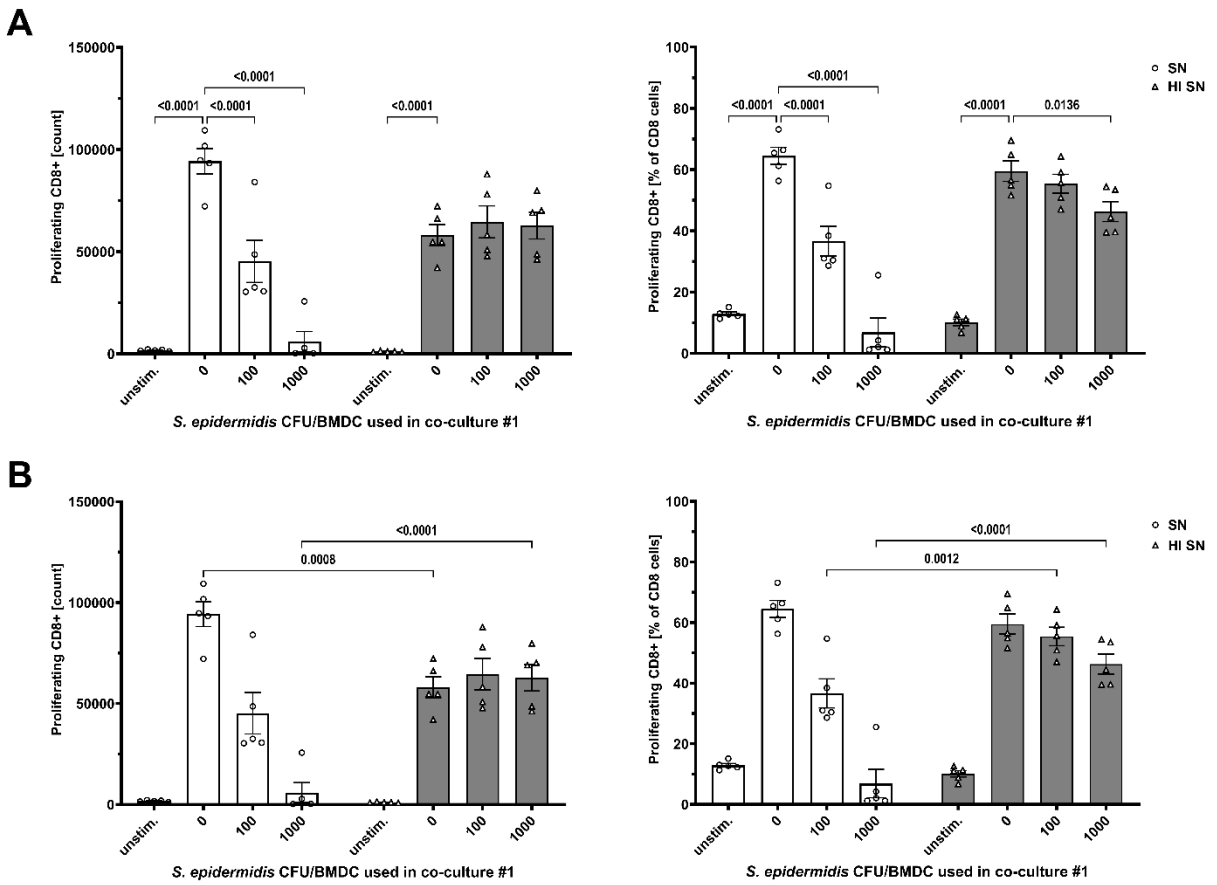

Figure 28: Proliferation of OT-I T cells in co-cultures, treated with unheated and heat-inactivated supernatant from *S. epidermidis*-treated co-cultures.

Supernatants generated from co-cultures of BMDCs and OT-I T cells stimulated with OVA protein and treated with UV-attenuated *S. epidermidis* strain 614 were collected after 72 h and were heat inactivated (HI SN) or remained unheated (SN). Fresh co-cultures of BMDCs and CFSE-labelled OT-I T cells were stimulated with OVA and the supernatants. **(A)** Counts of proliferating OT-I T cells and their frequencies among all OT-I T cells were compared to the respective 0 *S. epidermidis* CFU/BMDC concentration. **(B)** Counts and frequencies of proliferating OT-I T cells was also compared between the unheated and heat-inactivated supernatants for each concentration. The x-axis indicates the CFU/BMDC *S. epidermidis* that were used as treatment in co-culture #1 to generate the supernatants. No *S. epidermidis* was used in co-culture #2.
Bars represent means ± SEM of n = 5 BMDC donor mice in co-culture #1. Replicates are illustrated in symbols. Ordinary two-way ANOVA was performed to obtain p values. Dunnett's multiple comparisons test was applied for the comparison of 0 *S. epidermidis* CFU/BMDC to the other concentrations. Šidák's multiple comparisons test was applied to compare SI HN and SN conditions. Only p values < 0.05 are shown.

3.9 IFNγ is crucial in the suppression of OT-I T cells

3.9.1 Neutralisation of IFNγ restored OT-I T cell proliferation

In the previous section, the transfer of supernatants from 72 h incubated co-cultures into fresh co-cultures inhibited OT-I T cell proliferation. One possibility is that cytokines from the previous culture are transferred within the supernatants, which then influence the OT-I T cells or BMDCs. To investigate this hypothesis, neutralising antibodies were added to standard co-cultures in the subsequent experiment (Figure 29). In particular, the cytokines IFNγ and TNFα should be neutralised, as it has already been shown in the literature that they can have an influence on T cell proliferation (Bhat et al. 2017; Refaeli et al. 2002; Bertrand et al. 2016). After 72 h, the proliferation of the OT-I T cells was analysed using the CFSE profile to reveal possible effects of cytokine neutralisation.

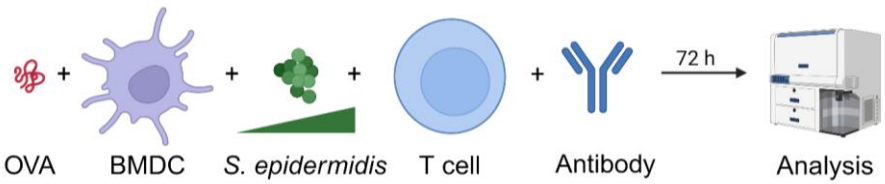

Figure 29: Experimental setup: Neutralisation of IFNγ and TNFα in co-cultures of BMDCs and OT-I T cells stimulated with OVA protein and exposed to *S. epidermidis*.

BMDCs were co-cultured with CFSE-labelled OT-I T cells. OVA protein was added to induce proliferation of OVA-specific OT-I T cells. In addition, neutralising antibodies against IFNγ or TNFα and different concentrations of *S. epidermidis* were added to the co-cultures. After 72 h of incubation, the proliferation of OT-I T cells was analysed by the CFSE profile, which was detected using FACS. Created with BioRender.com.

The treatment of co-cultures with anti-TNFα is shown in Figure 30. The counts of proliferating OT-I T cells of the unstimulated condition (unstim.) and each *S. epidermidis* concentration were compared to the respective 0 CFU/BMDC condition within each group. In every group, OVA stimulation alone (0 CFU/BMDC) resulted in higher OT-I T cell counts compared to unstimulated co-cultures. Moreover, 10, 100 and 1000 *S. epidermidis* CFU/BMDC reduced the counts of proliferating OT-I T cells irrespective of the anti-TNFα treatment (Figure 30A). Comparing the proliferation of OT-I T cells between the Isotype control (Iso-TNFα) and the anti-TNFα group, in the 0 and 1 CFU/BMDC condition more counts were detected in the anti-TNFα than in the Iso-TNFα group (Figure 30B).

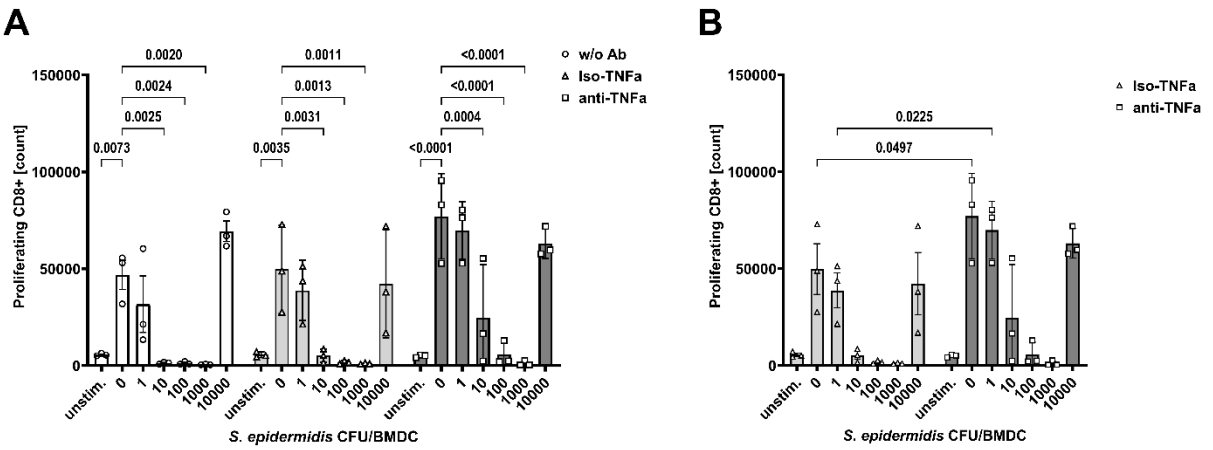

Figure 30: Counts of proliferating OT-I T cells in co-cultures treated with neutralising anti-TNFα antibody.

Co-cultures of CFSE-labelled OT-I T cells with BMDCs were stimulated with OVA protein and exposed to UV-attenuated *S. epidermidis* strain 614. Moreover, neutralising anti-TNFα (anti-TNFα) or an appropriate isotype control (Iso-TNFα) was added to the co-cultures or they remained without antibody treatment (w/o Ab). OT-I T cell proliferation was analysed by detection of the CFSE profile in FACS after 72 h of incubation. **(A)** Counts of proliferating OT-I T cells compared to the respective 0 *S. epidermidis* CFU/BMDC concentration within a group are depicted. **(B)** Counts of proliferating OT-I T cells in co-cultures with neutralising anti-TNFα were compared to the ones in co-cultures containing the isotype for the related stimulation conditions.
Bars represent means ± SEM of n = 3 BMDC donor mice. Replicates are illustrated in symbols. Ordinary two-way ANOVA was performed to obtain p values. Dunnett's multiple comparisons test was applied for the comparison of 0 *S. epidermidis* CFU/BMDC to the other concentrations within a group. Tukey's multiple comparisons test was applied to compare the related *S. epidermidis* CFU/BMDC conditions between anti-TNFα and Iso-TNFα groups. Only p values < 0.05 are shown.

Next, a neutralising antibody against IFNγ was tested to investigate if IFNγ is involved in the suppression of OT-I T cells. The treatment of co-cultures with anti-IFNγ or the isotype control (Iso-IFNγ) is shown in Figure 31. OVA stimulation (cf. 0 CFU/BMDC) clearly induced the proliferation of OT-I T cells, as can be seen from the increased counts when compared with the unstimulated condition. Incubation with 10, 100 or 1000 *S. epidermidis* CFU/BMDC significantly suppressed this induced proliferation in the w/o Ab and the Iso-IFNγ treatment group. Interestingly, in the anti-IFNγ treatment group, no such suppression was observed for the mentioned concentrations of *S. epidermidis*. On the contrary, the counts of proliferating OT-I T cells were even higher in the 100 CFU/BMDC condition than in the 0 CFU/BMDC condition. Also the concentrations 10 and 1000 CFU/BMDC showed elevated counts of proliferating cells, albeit without significance (Figure 31A). The reversal of a *S. epidermidis*-induced suppression of OT-I T cell proliferation by anti-IFNγ treatment becomes even clearer when comparing the two groups Iso-IFNγ and anti-IFNγ (Figure 31B). Here, the OT-I T cell counts were significantly higher in the anti-IFNγ than in the Iso-IFNγ group for all stimulation conditions, except the unstimulated one.

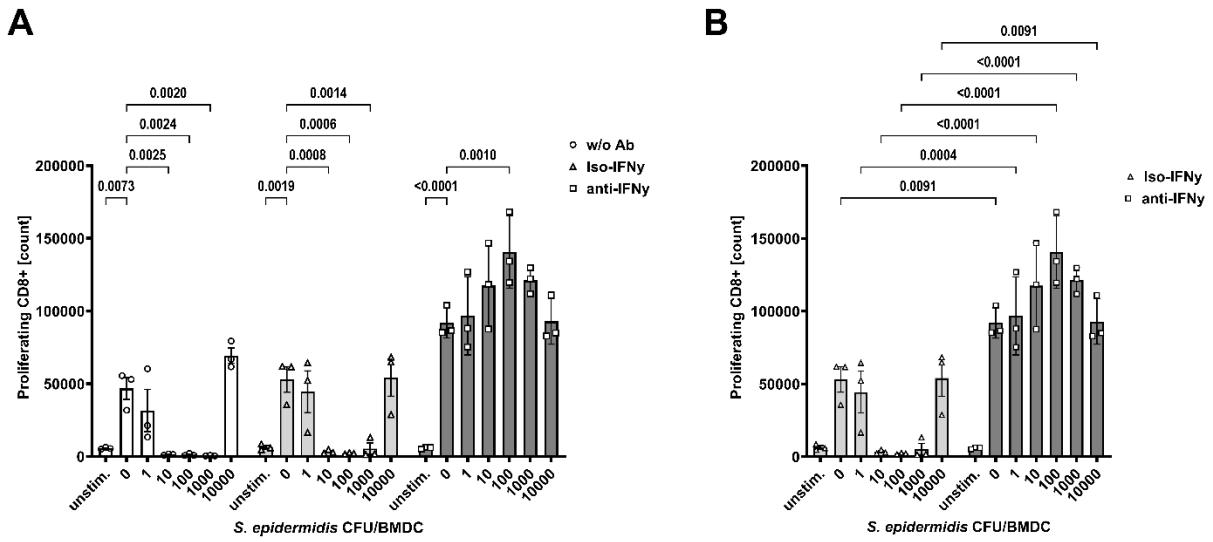

Figure 31: Counts of proliferating OT-I T cells in co-cultures treated with neutralising anti-IFNγ antibody.

Co-cultures of CFSE-labelled OT-I T cells with BMDCs were stimulated with OVA protein and exposed to UV-attenuated *S. epidermidis* strain 614. Moreover, neutralising anti-IFNγ (anti-IFNγ) or an appropriate isotype control (Iso-IFNγ) was added to the co-cultures or they remained without antibody treatment (w/o Ab). OT-I T cell proliferation was analysed by detection of the CFSE profile in FACS after 72 h of incubation. **(A)** Counts of proliferating OT-I T cells compared to the respective 0 *S. epidermidis* CFU/BMDC concentration within a group are depicted. **(B)** Counts of proliferating OT-I T cells in co-cultures with neutralising anti-IFNγ were compared to the ones in co-cultures containing the isotype control for the related stimulation conditions.
Bars represent means ± SEM of n = 3 BMDC donor mice. Replicates are illustrated in symbols. Ordinary two-way ANOVA was performed to obtain p values. Dunnett's multiple comparisons test was applied for the comparison of 0 *S. epidermidis* CFU/BMDC to the other concentrations within a group. Tukey's multiple comparisons test was applied to compare the related *S. epidermidis* CFU/BMDC conditions between anti-IFNγ and Iso-IFNγ groups. Only p values < 0.05 are shown.

3.9.2 IFNγ stimulation of co-cultures suppressed the OVA-specific OT-I T cell proliferation

In the previous section, we identified that neutralisation of IFNγ in the co-cultures restored OT-I T cell proliferation. In the following, we examined whether the addition of recombinant murine IFNγ (rmIFNγ) can lead to the suppression of OT-I T cell proliferation. For this purpose, co-cultures are stimulated with OVA protein. In addition, they were treated with increasing concentrations of rmIFNγ or remained untreated (see Figure 32). The counts and frequencies of proliferating OT-I T cells are illustrated in Figure 32. Stimulation with OVA alone (cf. 0 ng/ml) resulted in more proliferating OT-I T cells when compared to the unstimulated condition. Counts as well as frequencies were significantly increased. rmIFNγ reduced this proliferation again and resulted in significantly fewer counts as well as frequencies of proliferating OT-I T cells from a concentration of 10 ng/ml rmIFNγ onwards when compared to the OVA control (cf. 0 ng/ml).

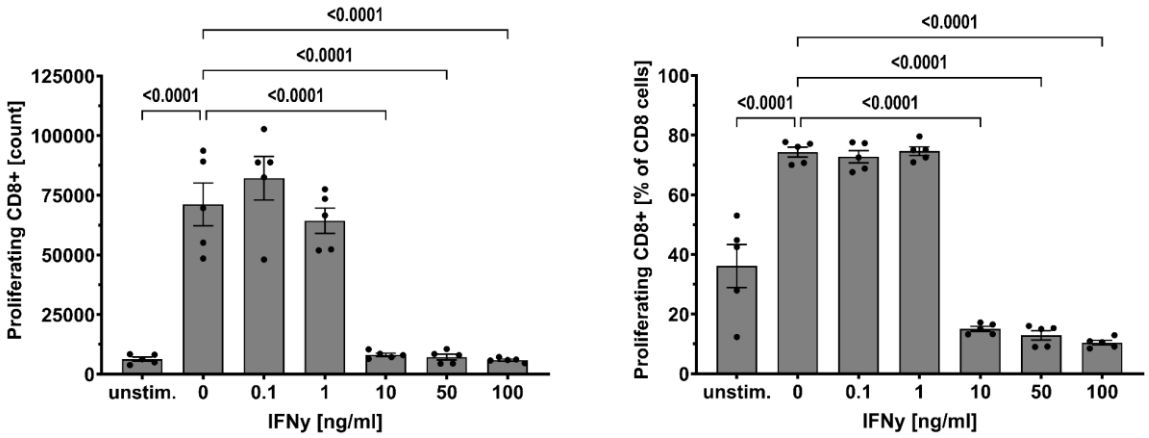

Figure 32: Counts and frequencies of proliferating OT-I T cells in co-cultures of OT-I T cells and BMDCs treated with rmIFNγ.

Co-cultures of BMDCs and OT-I T cells were stimulated with OVA protein and treated with ranging concentrations of recombinant murine IFNγ (rmIFNγ). OT-I T cell proliferation was analysed by detection of the CFSE intensity in FACS after 72 h of incubation. Counts and frequencies of proliferating OT-I T cells were compared to the respective 0 ng/ml IFNγ (OVA stimulus only) condition.
Bars represent means ± SEM of n = 5 BMDC donors. Replicates are illustrated in symbols. Ordinary one-way ANOVA with Dunnett's multiple comparisons test was performed to obtain p values. Only p values < 0.05 are shown.

3.9.3 BMDCs as target of the IFNγ signalling within the cascade of OT-I T cell suppression

Having identified IFNγ as a potential candidate responsible for OT-I T cell suppression, we investigated whether the BMDCs are influenced by IFNγ or whether they even possibly secrete IFNγ. For this purpose, co-cultures of BMDCs and CFSE-labelled OT-I T cells were stimulated with OVA protein and incubated with *S. epidermidis* as already described in Figure 12. BMDCs were generated from WT, IFNγR$^{-/-}$ and IFNγ$^{-/-}$ mice to investigate a potential link between BMDCs and IFNγ.

Before setting up co-cultures with BMDCs of the different knockout (KO) mice, they were compared to WT BMDCs in viability, CD11b/CD11c expression and the expression of maturation and activation markers (Figure 33). Exemplary dot plots for the gating are depicted in Figure 33A. Cell debris was excluded by size gating (SSC-A, FSC-A) followed by the determination of the viable cell population. Live cells were gated on CD11b+CD11c+ cells. MFIs for the expression of different markers were extracted from this population. Moreover, for the evaluation of the maturation state a gate was put on CD86+ MHC class II+ cells. Results of the analysis are depicted in Figure 33B. Overall, we detected that the BMDCs are very similar in terms of maturation and viability, except for small differences. The percentage of live IFNγ$^{-/-}$ BMDCs was slightly higher than in the WT BMDCs. In the IFNγR$^{-/-}$ BMDCs, the MHC class II expression and thus also the percentage of CD86+ MHC class II+ cells was slightly lower than in the WT BMDCs.

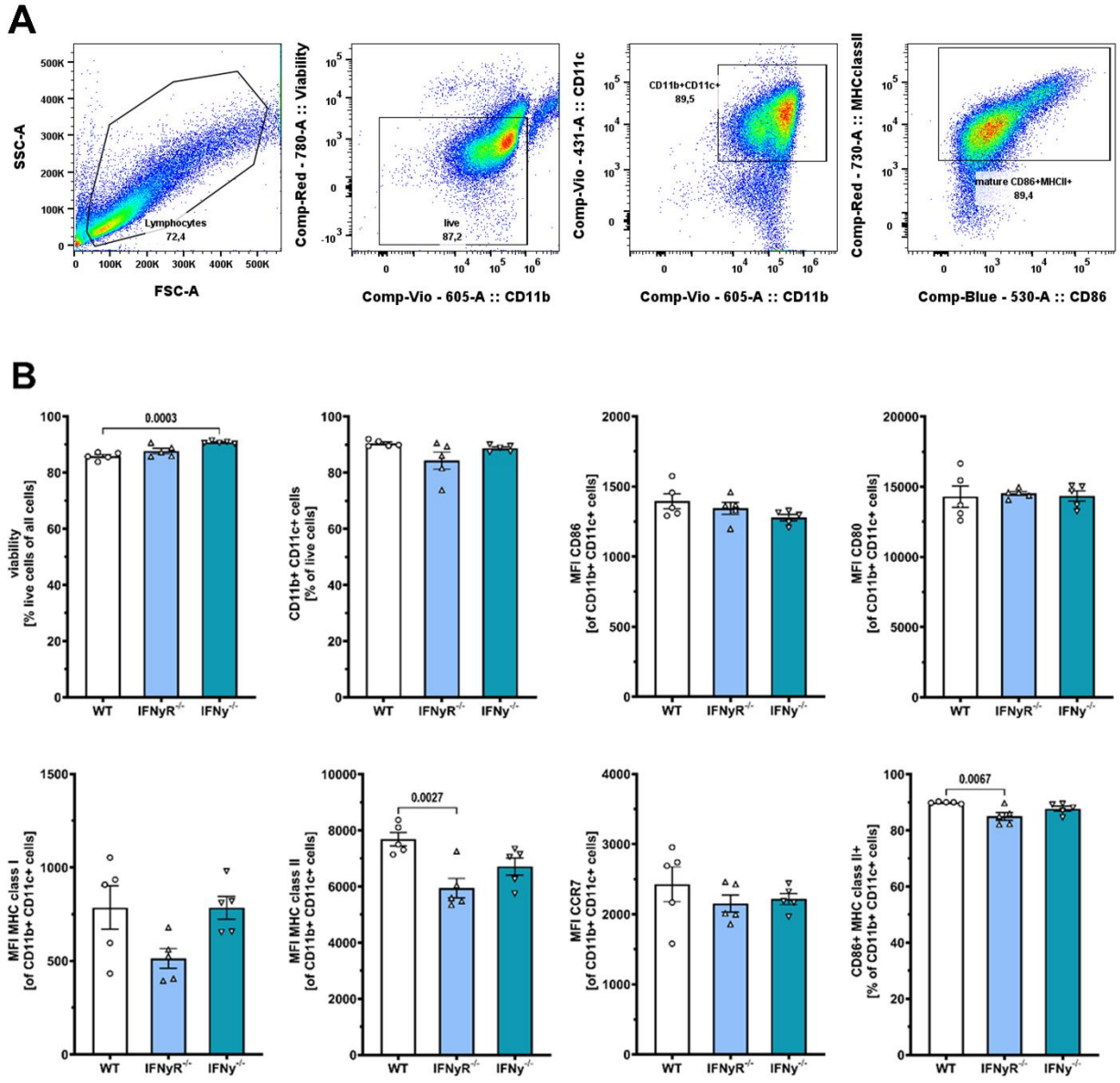

Figure 33: Comparison of IFNγR$^{-/-}$ BMDCs and IFNγ$^{-/-}$ BMDCs with WT BMDCs.

Day 9 BMDCs generated from WT, IFNγR$^{-/-}$ and IFNγ$^{-/-}$ mice were examined to see if they had a comparable phenotype before they were used in the co-cultures. **(A)** Representative dot plots of the gating strategy after FACS analysis (unstimulated WT BMDCs). **(B)** Viability, maturation state (CD86+ MHC class II+) and MFI of CD80, CD86, MHC class I, MHC class II and CCR7 expression of unstimulated BMDCs.
Bars represent means ± SEM of n = 5 BMDC donor mice for each genotype. Biological replicates are illustrated in symbols. Ordinary two-way ANOVA with Dunnett's multiple comparisons test was performed to obtain p values. Only p values < 0.05 are shown.

In the following, these WT, IFNγ$^{-/-}$, and IFNγR$^{-/-}$ BMDCs were used in co-cultures with OT-I T cells, OVA protein and UV-attenuated *S. epidermidis* to determine if BMDCs are involved in a IFNγ-mediated suppression of OT-I T cells. Counts and frequencies of proliferating OT-I T cells in co-culture with the different BMDC mutants are illustrated in Figure 34. Compared to the unstimulated condition, counts and frequencies of OT-I T cells were increased due to OVA stimulation in all co-cultures, irrespective of the used BMDC type. *S. epidermidis* reduced the proliferation again in the WT BMDC co-culture, which served as quality control. Counts and frequencies were significantly lower for 10, 100 and 1000 CFU/BMDC stimulation than for 0 CFU/BMDC. Additionally, the counts of 10000 CFU/BMDC stimulation were also markedly reduced. A similar suppression of OT-I T cell proliferation by addition of *S. epidermidis* was also observed in co-cultures with IFNγ$^{-/-}$ BMDCs. Compared to 0 CFU/BMDC, stimulation with 10, 100 and 1000 CFU/BMDC reduced the OT-I T cell counts. Same concentrations plus the 1 CFU/BMDC concentration showed reduced frequencies of proliferating OT-I T cells when compared to 0 CFU/BMDC.

A different picture emerged in the co-cultures that were set up with IFNγR$^{-/-}$ BMDCs. Frequencies of proliferating OT-I T cells were not reduced after exposure to *S. epidermidis*. The counts also did not decrease in comparison with the 0 CFU/BMDC proliferation control. In contrast, concentrations of 100 and 1000 *S. epidermidis* CFU/BMDC increased the counts considerably. The comparisons of the counts and frequencies of proliferating OT-I T cells between the KO BMDC co-cultures and the WT control were calculated for related conditions (Ordinary two-way ANOVA with Dunnett's multiple comparisons test). However, they were not presented graphically but are listed in Table 22. The main observation was that the suppression of OT-I T cell proliferation was abolished in counts and frequencies at 10, 100 and 1000 CFU/BMDC in the IFNγR$^{-/-}$ BMDC co-cultures, but not the IFNγ$^{-/-}$ BMDC co-cultures compared to the WT BMDC co-cultures.

Table 22: P values for the comparison of the WT BMDC co-cultures with the IFNγR$^{-/-}$ and IFNγ$^{-/-}$ BMDC co-cultures for the related *S. epidermidis* CFU/BMDC concentration.

Proliferating CD8+ [count]							
	unstim.	**0**	**1**	**10**	**100**	**1000**	**10000**
WT vs. IFNγR$^{-/-}$	ns	<0.0001	0.0003	<0.0001	<0.0001	<0.0001	ns
WT vs. IFNγ$^{-/-}$	ns	0.0021	<0.0001	ns	ns	ns	0.0414
Proliferating CD8+ [% of CD8]							
	unstim.	**0**	**1**	**10**	**100**	**1000**	**10000**
WT vs. IFNγR$^{-/-}$	ns	ns	ns	<0.0001	<0.0001	<0.0001	0.0011
WT vs. IFNγ$^{-/-}$	ns	ns	0.008	ns	ns	ns	ns

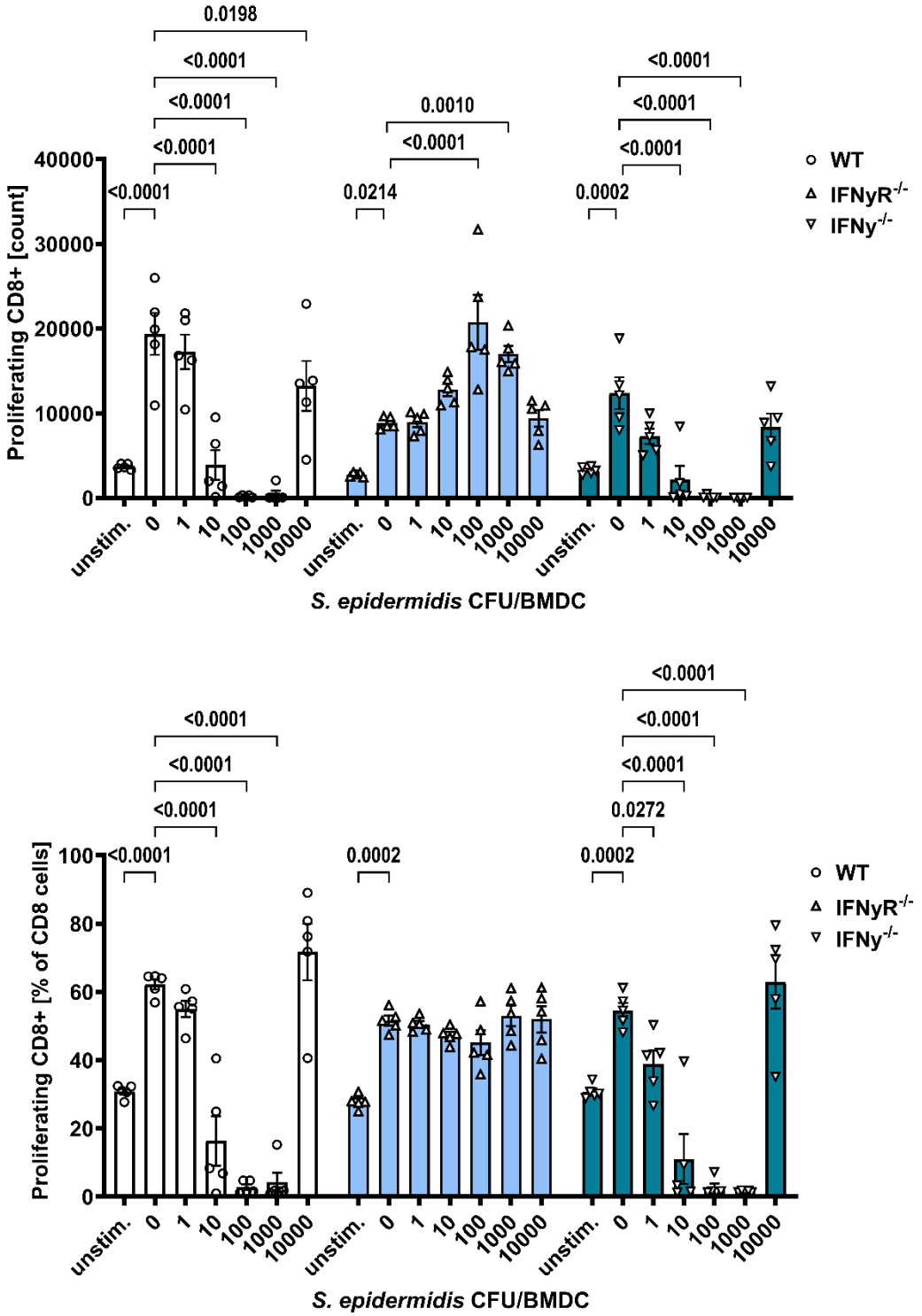

Figure 34: Proliferation of OT-I T cells in co-culture with BMDCs, generated from WT, IFNγR$^{-/-}$ or IFNγ$^{-/-}$ mice.

Co-cultures of CFSE-labelled OT-I T cells with BMDCs, generated from WT, IFNγR$^{-/-}$ or IFNγ$^{-/-}$ mice, were stimulated with OVA protein and treated with UV-attenuated *S. epidermidis* strain 614. OT-I T cell proliferation was analysed by detection of the CFSE intensity in FACS after 72 h of incubation. Counts of proliferating OT-I T cells and their frequencies among all OT-I T cells were compared to the respective 0 *S. epidermidis* CFU/BMDC value within a BMDC mutant.
Bars represent means ± SEM of n = 5 BMDC donor mice for each genotype. Replicates are illustrated in symbols. Ordinary two-way ANOVA with Dunnett's multiple comparisons test was performed to obtain p values. Only p values < 0.05 are shown.

To ensure that the OT-I T cell proliferation in IFNγR$^{-/-}$ BMDC co-cultures was restored due to absence of IFNγ signalling in the BMDCs and not due to lacking IFNγ, the IFNγ cytokine levels of the co-culture supernatants were determined (Figure 35). The measurements showed similar IFNγ levels in all three co-cultures. With increasing *S. epidermidis* concentrations, the amount of secreted IFNγ in the co-cultures increased. Compared to 0 CFU/BMDC, this was significant from 100 CFU/BMDC for WT and IFNγR$^{-/-}$ and from 1000 CFU/BMDC for IFNγ$^{-/-}$. The comparison of the IFNγ level of the KO BMDC co-cultures with the WT was calculated but is not shown. With one exception there were no differences. Only the IFNγ level at 10000 CFU/BMDC was lower in the IFNγR$^{-/-}$ co-culture than in the WT ($p < 0.001$; Ordinary two-way ANOVA with Dunnett's multiple comparisons test).

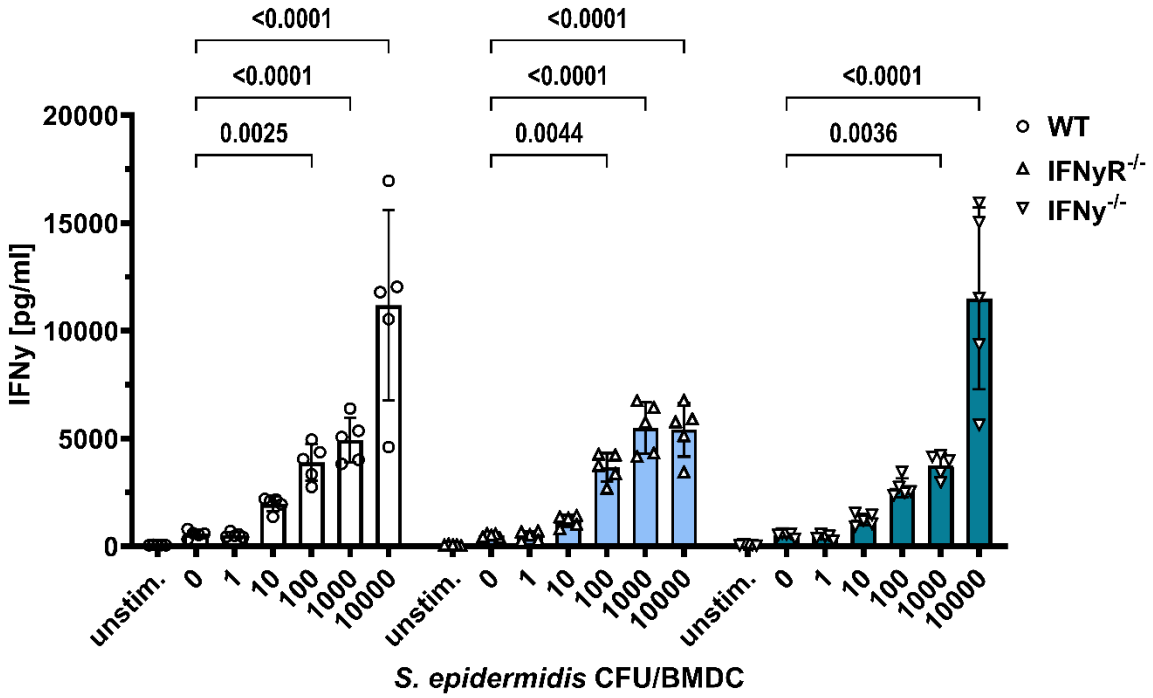

Figure 35: IFNγ levels in co-cultures of OT-I T cells and BMDCs, generated from WT, IFNγR$^{-/-}$ or IFNγ$^{-/-}$ mice.

Co-cultures of CFSE-labelled OT-I T cells with BMDCs, generated from WT, IFNγR$^{-/-}$ or IFNγ$^{-/-}$ mice, were stimulated with OVA protein and treated with UV-attenuated *S. epidermidis* strain 614. Supernatants were collected after 72 h of incubation. IFNγ levels in supernatants of the co-cultures were compared to the respective 0 *S. epidermidis* CFU/BMDC value within each mutant.
Bars represent means ± SEM of n = 5 BMDC donor mice for each genotype. Replicates are illustrated in symbols. Ordinary two-way ANOVA with Dunnett's multiple comparisons test was performed to obtain p values. Only p values < 0.05 are shown.

To summarise chapter 3.9, the blockade of IFNγ by a neutralising antibody and the addition of rmIFNγ in co-cultures showed that IFNγ is critical in mediating the suppression of OT-I T cells. Furthermore, the experiments with IFNγR$^{-/-}$ BMDCs showed that BMDCs as a target of IFNγ are significantly involved in the suppression of OT-I T cells. In addition, BMDCs could be excluded as the responsible source for IFNγ by the use of IFNγ$^{-/-}$ BMDCs in co-cultures.

3.10 Suppression of OT-I T-cell proliferation by BMDC-derived NO

It has already been worked out above that the presence of BMDCs is necessary for a *S. epidermidis*-mediated suppression of an antigen-specific OT-I T cell proliferation. IFNγ-induced signalling in BMDCs was identified to be involved in this suppression cascade. One possible response of BMDCs to IFNγ signalling could be the expression of NO. There is already evidence that this molecule can have a dampening effect on the proliferation of cells (Bogdan 2015; Thwe and Amiel 2018). Subsequently, different approaches were used to investigate whether NO could be involved in the suppression of the antigen-specific OT-I T cell proliferation in this study. The Griess reagent was used to draw conclusions about NO activity. This allows the detection of accumulated, relatively stable nitrite, which is formed by oxidation of the short-lived NO (Lundberg and Weitzberg 2022).

3.10.1 Induction of NO expression in BMDCs due to activation of IFNγR by IFNγ

The addition of rmIFNγ to co-cultures of BMDCs and OT-I T cells, reduced the proliferation of OT-I T cells (see section 3.9.2). Supernatants of these co-cultures were analysed for nitrite levels to investigate the hypothesis, that NO could be involved in the cascade of OT-I T cell suppression. The detected nitrite levels in the supernatants of rmIFNγ-stimulated co-cultures are shown in Figure 36. Nitrite levels were relatively low in unstimulated and OVA-stimulated co-cultures. Addition of rmIFNγ resulted in significantly higher amounts of nitrite after treatment with 10, 50 and 100 ng/ml rmIFNγ in comparison to the 0 ng/ml condition.

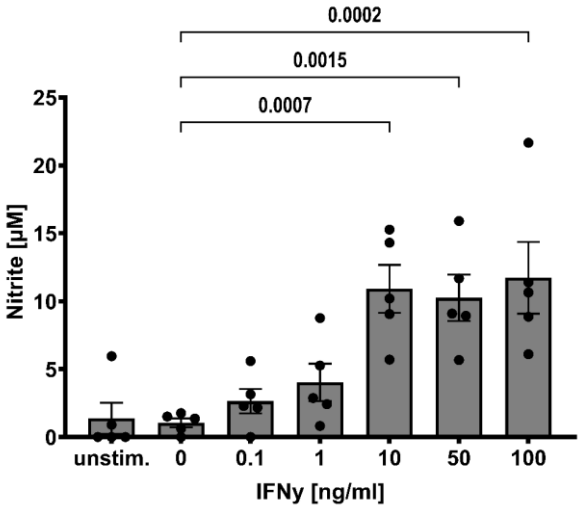

Figure 36: Nitrite levels in co-cultures of OT-I T cells and BMDCs stimulated with OVA and treated with rmIFNγ.

Co-cultures of BMDCs and OT-I T cells were stimulated with OVA protein and treated with ranging concentrations of recombinant murine IFNγ (rmIFNγ). Supernatants were collected for nitrite analysis after 72 h. Nitrite levels in supernatants of the co-cultures were compared to the respective 0 ng/ml IFNγ (OVA stimulus only) condition.
Bars represent means ± SEM of n = 5 BMDC donors. Replicates are illustrated in symbols. Ordinary one-way ANOVA with Dunnett's multiple comparisons test was performed to obtain p values. Only p values < 0.05 are shown.

IFNγ was already detected in the supernatants of the IFNγR$^{-/-}$ and IFNγ$^{-/-}$ BMDC co-cultures (see section 3.9.3). However, we noticed that there was no suppression of OT-I T cell proliferation in the co-cultures with IFNγR$^{-/-}$ BMDCs. To investigate the involvement of NO, the nitrite levels in these co-cultures were analysed (Figure 37). For the co-cultures with WT and IFNγ$^{-/-}$ BMDCs, significantly higher nitrite levels were measured after stimulation with 10, 100, 1000, 10000 *S. epidermidis* CFU/BMDC compared to 0 CFU/BMDC stimulation. The nitrite level peaked at 1000 CFU/BMDC. In contrast, no significant increase of nitrite was observed after addition of *S. epidermidis* in the co-cultures with IFNγR$^{-/-}$ BMDCs. Comparison of the nitrite levels of KO BMDCs with the WT control for related conditions showed no differences between IFNγ$^{-/-}$ and WT BMDC co-cultures. 10, 100, 1000 and 10000 CFU/BMDC were significantly lower in the IFNγR$^{-/-}$ BMDC co-culture than in the WT BMDC co-culture (statistics not shown; p = 0.001 for 10 CFU/BMDC; p < 0.0001 for 100, 1000 and 10000 CFU/BMDC; Ordinary two-way ANOVA with Dunnett's multiple comparisons test).

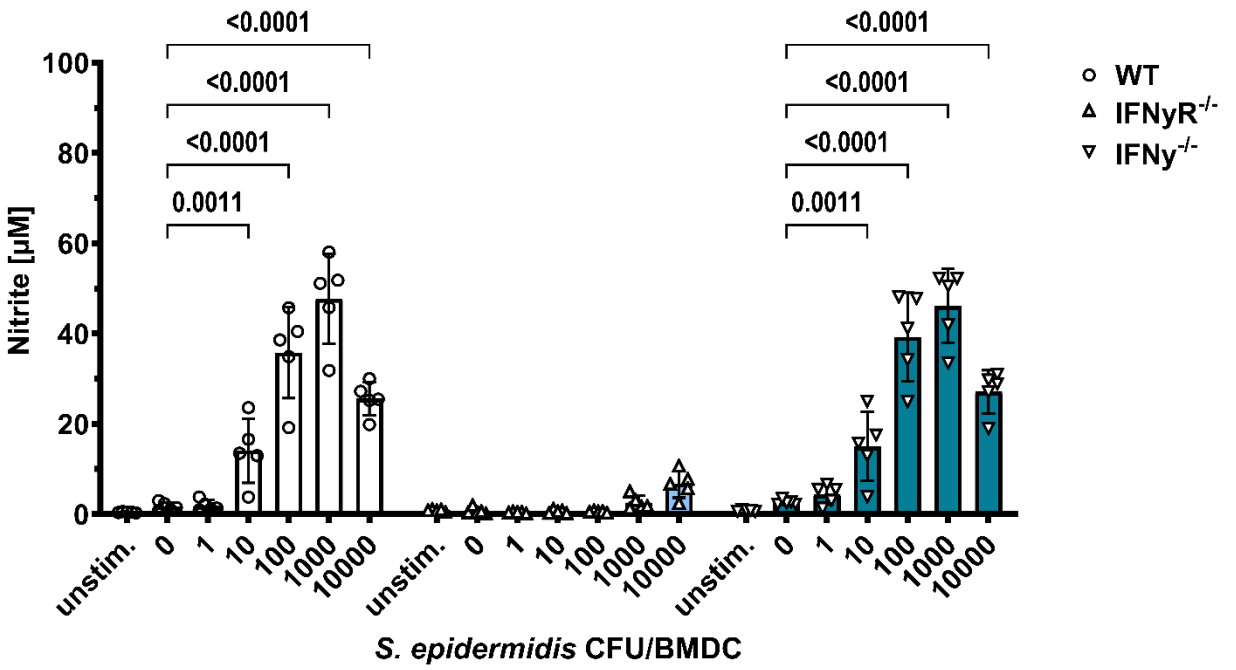

Figure 37: Nitrite levels in co-cultures of OT-I T cells and BMDCs, generated from WT, IFNγR$^{-/-}$ or IFNγ$^{-/-}$ mice.

Co-cultures of OT-I T cells with BMDCs, generated from WT, IFNγR$^{-/-}$ or IFNγ$^{-/-}$ mice, were stimulated with OVA protein and treated with UV-attenuated *S. epidermidis* strain 614. Supernatants were collected after 72 h of incubation. Nitrite levels in supernatants of the co-cultures were compared to the respective 0 *S. epidermidis* CFU/BMDC value within each group.
Bars represent means ± SEM of n = 5 BMDC donor mice for each genotype. Replicates are illustrated in symbols. Ordinary two-way ANOVA with Dunnett's multiple comparisons test was performed to obtain p values. Only p values < 0.05 are shown.

3.10.2 iNOS deficiency in BMDCs abrogated the suppression of OT-I T cell proliferation

In this part, co-cultures of BMDCs and CFSE-labelled OT-I T cells were stimulated with OVA protein and exposed to *S. epidermidis* (as already described in Figure 12). BMDCs, generated from WT, iNOS$^{-/-}$ and Arg1$^{-/-}$ mice, were used to validate whether NO is involved in the suppression of OT-I T cell proliferation and whether BMDCs are the source of NO.

Before setting up co-cultures with the different BMDC genotypes, they were analysed for similarity in viability, CD11b/CD11c expression and the expression of maturity and activation makers (Figure 38). The gating was identical to the one already explained in Figure 33A. Viability as well as frequencies of CD11b+ CD11c+ BMDCs were relatively similar between the BMDC mutants, despite significant statistic. MFIs of CD80, CD86, and MHC class II as well as frequency of CD86+ MHC class + BMDCs were lower in iNOS$^{-/-}$ BMDCs than in WT BMDCs. Expression level of the MHC class I and MHC class II were lower for Arg1$^{-/-}$ BMDCs than in the WT BMDCs.

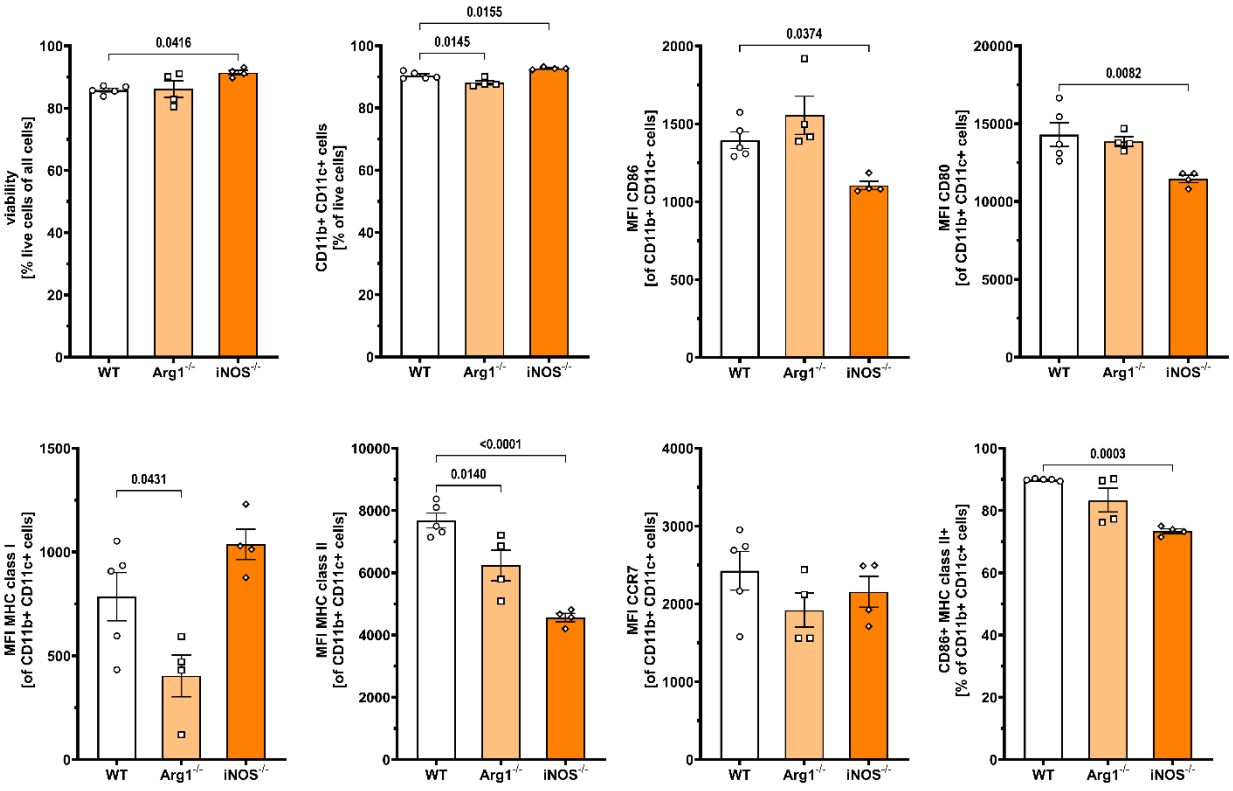

Figure 38: Comparison of iNOS$^{-/-}$ and Arg1$^{-/-}$ BMDCs with WT BMDCs.

Day 9 BMDCs generated from WT, iNOS$^{-/-}$ and Arg1$^{-/-}$ mice were examined to see if they had a comparable phenotype before they were used in the co-cultures. Viability, maturation state (CD86+ MHC class II+) and MFI of CD80, CD86, MHC class I, MHC class II and CCR7 expression of unstimulated BMDCs.
Bars represent means ± SEM of n = 5 BMDC donor mice for each genotype. Biological replicates are illustrated in symbols. Ordinary two-way ANOVA with Dunnett's multiple comparisons test was performed to obtain p values. Only p values < 0.05 are shown.

Despite slight differences in marker expression, all BMDCs should be able to activate OT-I T cells. Therefore, they were used in the following co-culture experiments to investigate whether BMDC-derived NO affects OT-I T cell proliferation. Counts and frequencies of proliferating OT-I T cells in co-culture with the three BMDC mutants are depicted in Figure 39. Compared to the unstimulated condition, counts and frequencies of proliferating OT-I T cells were increased by OVA stimulation for all BMDC types. Addition of *S. epidermidis* reduced the proliferation in the WT BMDC as well as the Arg1$^{-/-}$ BMDC co-culture. For WT co-cultures, counts and frequencies were significantly lower at 10, 100 and 1000 CFU/BMDC than at 0 CFU/BMDC. For the 10000 CFU/BMDC stimulation, counts were lower whereas the frequency was higher than the OVA-control. In Arg1$^{-/-}$ co-cultures, the 100 and 1000 *S. epidermidis* CFU/BMDC reduced the counts and frequencies of proliferating OT-I T cells compared to 0 CFU/BMDC. For the frequencies, additionally the 10 CFU/BMDC condition was reduced for this genotype. In contrast to the Arg1$^{-/-}$ and WT BMDC co-cultures, the counts and frequency for proliferating OT-I T cells of the iNOS$^{-/-}$ BMDC co-culture were decreased only at 10000 *S. epidermidis* CFU/BMDC compared to the corresponding OVA control. Even higher counts were detected at 10 and 100 *S. epidermidis* CFU/BMDC than in the 0 CFU/BMDC condition.

The comparisons of the counts and frequencies of proliferating OT-I T cells between the KO BMDC co-cultures and the WT control were calculated for identical conditions (Ordinary two-way ANOVA with Dunnett's multiple comparisons test). They were not presented graphically but are listed in Table 23. The most important observations are the comparison at a concentration of 100 and 1000 *S. epidermidis* CFU/BMDC, as the strongest suppression was usually observed here in the WT BMDC co-culture. For these concentrations, the counts and frequencies of proliferating OT-I T cells of the iNOS$^{-/-}$ co-cultures were significantly higher than for the WT. However, no difference was observed between Arg1$^{-/-}$ and the WT at these concentrations, except for frequencies at 10 CFU/BMDC. Here, the frequency of proliferating OT-I T cells was higher in the Arg1$^{-/-}$ BMDC co-culture than in the WT BMDC co-culture.

Table 23: P values for the comparison of the WT BMDC co-cultures with the iNOS$^{-/-}$ and Arg1$^{-/-}$ BMDC co-cultures for the related *S. epidermidis* CFU/BMDC concentration.

Proliferating CD8+ [count]							
	unstim.	**0**	**1**	**10**	**100**	**1000**	**10000**
WT vs. Arg1$^{-/-}$	ns	<0.0001	<0.0001	ns	ns	ns	0.0001
WT vs. iNOS$^{-/-}$	ns	0.0009	ns	<0.0001	<0.0001	<0.0001	<0.0001
Proliferating CD8+ [% of CD8]							
	unstim.	**0**	**1**	**10**	**100**	**1000**	**10000**
WT vs. Arg1$^{-/-}$	ns	0.0102	ns	<0.0001	ns	ns	<0.0001
WT vs. iNOS$^{-/-}$	ns	ns	ns	<0.0001	<0.0001	<0.0001	<0.0001

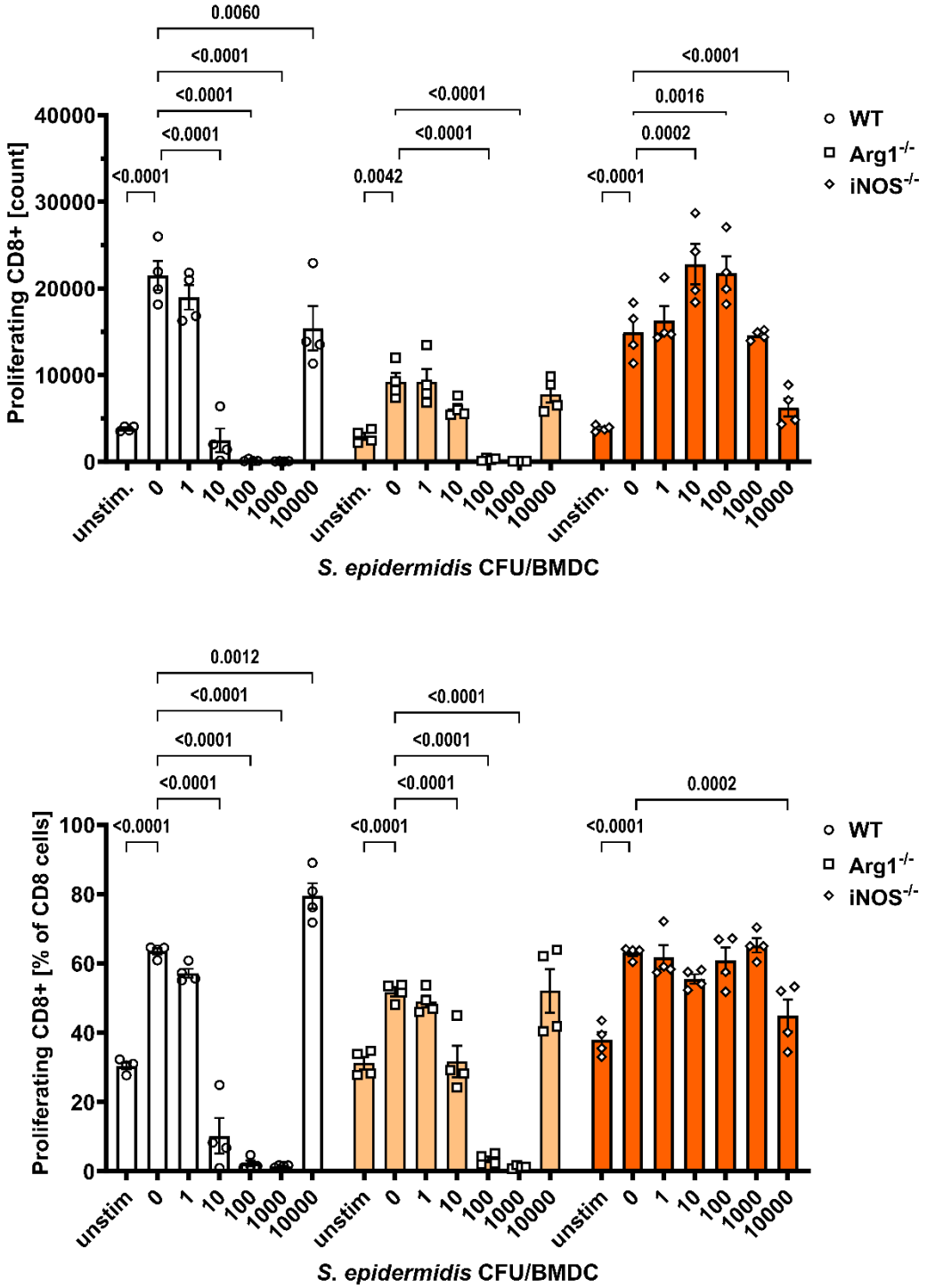

Figure 39: Proliferation of OT-I T cells in co-culture with BMDCs, generated from WT, iNOS$^{-/-}$ or Arg1$^{-/-}$ mice.

Co-cultures of CFSE-labelled OT-I T cells with BMDCs, generated from WT, iNOS$^{-/-}$ or Arg1$^{-/-}$ mice, were stimulated with OVA protein and exposed to UV-attenuated *S. epidermidis* strain 614. OT-I T cell proliferation was analysed by detection of the CFSE intensity in FACS after 72 h of incubation. Counts of proliferating OT-I T cells and their frequencies among all OT-I T cells were compared to the respective 0 *S. epidermidis* CFU/BMDC value within the respective co-culture.
Bars represent means ± SEM of n = 4 BMDC donor mice for each genotype. Replicates are illustrated in symbols. Ordinary two-way ANOVA with Dunnett's multiple comparisons test was performed to obtain p values. Only p values < 0.05 are shown.

In addition, the IFNγ and nitrite levels were also measured in the supernatants of these co-cultures. In the co-cultures of all three BMDC mutants, a similar trend was observed as in the IFNγR$^{-/-}$ and IFNγ$^{-/-}$ co-cultures (see chapters 3.9.3 and 3.10.1). With increasing concentrations of *S. epidermidis*, the IFNγ level also increased (Figure 40). For the WT and iNOS$^{-/-}$ co-cultures, IFNγ was significantly increased compared to the 0 CFU/BMDC condition for 100, 1000 and 10000 CFU/BMDC. For Arg1$^{-/-}$ this was only true for 1000 and 10000 CFU/BMDC. Regarding nitrite, *S. epidermidis*-treated co-cultures with WT and Arg1$^{-/-}$ BMDCs contained higher levels than their respective 0 CFU/BMDC control (Figure 41). This finding was significant for both, Arg1$^{-/-}$ and WT BMDCs, at 100, 1000 and 10000 CFU/BMDC. Additionally, the nitrite level was significantly higher at 10 CFU/BMDC in the WT co-culture. No nitrite could be detected in the iNOS$^{-/-}$ BMDC co-cultures.

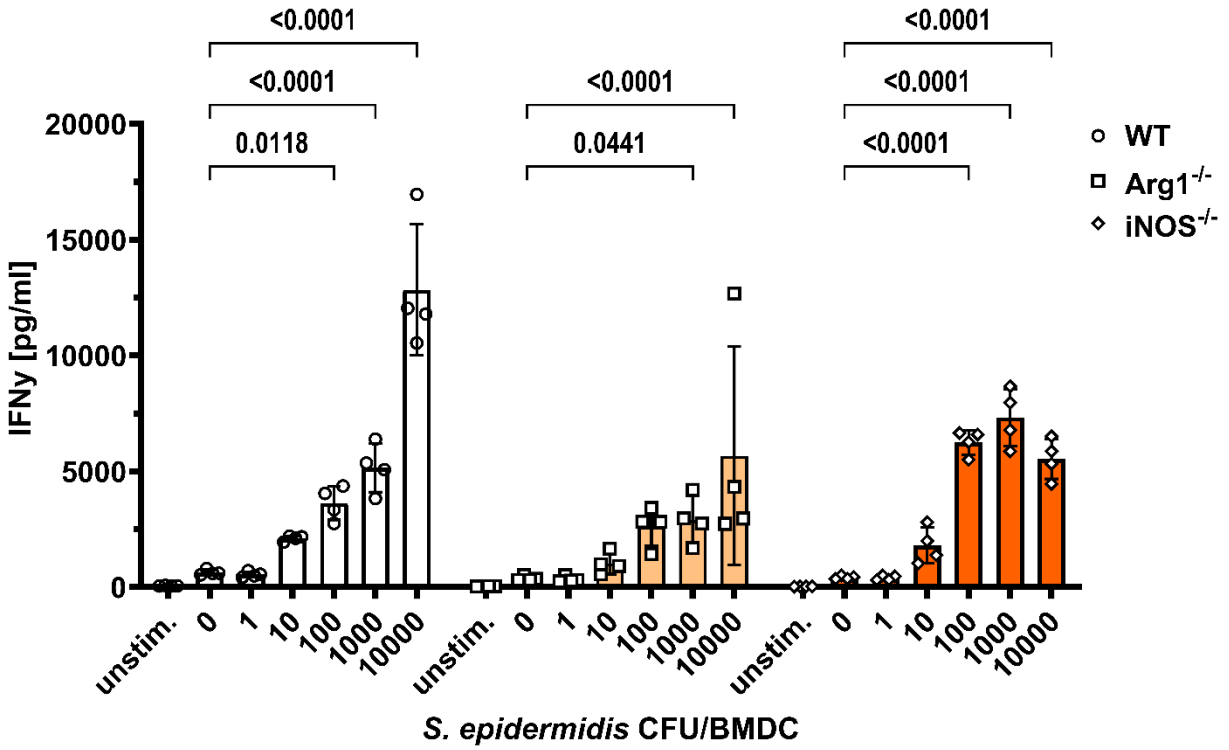

Figure 40: IFNγ levels in co-cultures of OT-I T cells and BMDCs, generated from WT, Arg1$^{-/-}$ or iNOS$^{-/-}$ mice.

Co-cultures of OT-I T cells with BMDCs, generated from WT, Arg1$^{-/-}$ or iNOS$^{-/-}$ mice, were stimulated with OVA protein and treated with UV-attenuated *S. epidermidis* strain 614. Supernatants were collected after 72 h of incubation. IFNγ levels in supernatants of the co-cultures were compared to the respective 0 *S. epidermidis* CFU/BMDC value within each group.
Bars represent means ± SEM of n = 4 BMDC donor mice for each genotype. Replicates are illustrated in symbols. Ordinary two-way ANOVA with Dunnett's multiple comparisons test was performed to obtain p values. Only p values < 0.05 are shown.

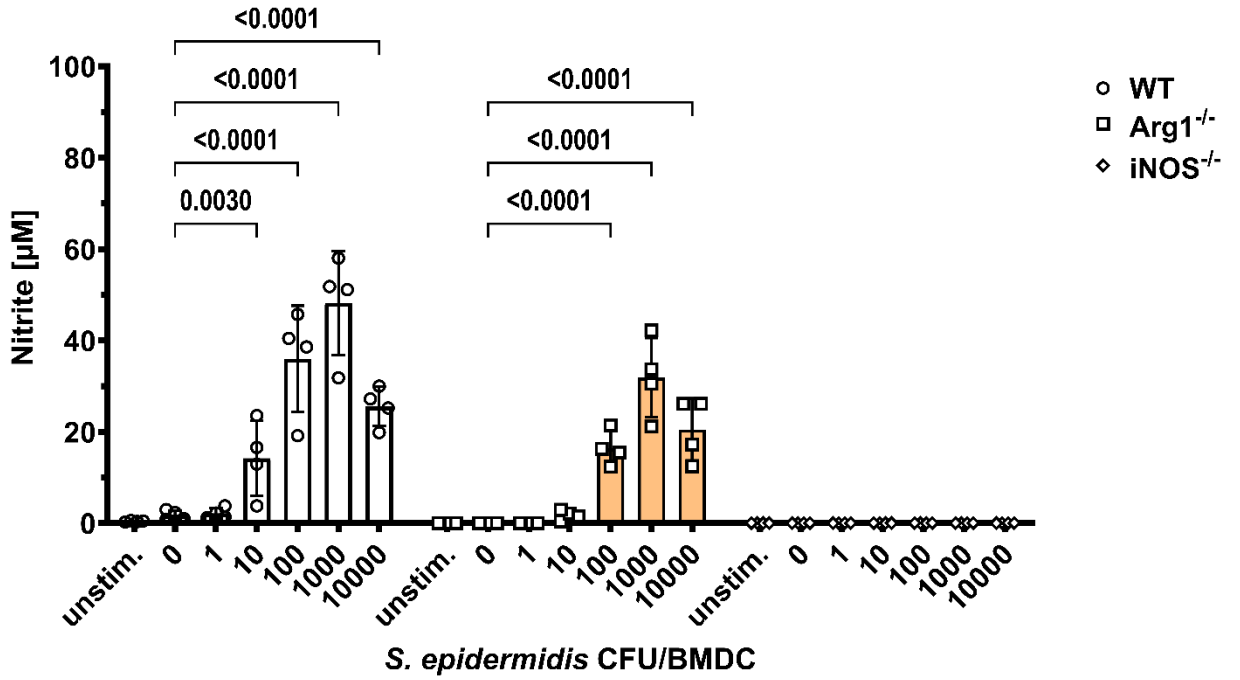

Figure 41: Nitrite levels in co-cultures of OT-I T cells and BMDCs, generated from WT, Arg1$^{-/-}$ or iNOS$^{-/-}$ mice.

Co-cultures of CFSE-labelled OT-I T cells with BMDCs, generated from WT, Arg1$^{-/-}$ or iNOS$^{-/-}$ mice, were stimulated with OVA protein and treated with UV-attenuated *S. epidermidis* strain 614. Supernatants were collected after 72 h of incubation. Nitrite levels in supernatants of the co-cultures were compared to the respective 0 *S. epidermidis* CFU/BMDC value within each group.
Bars represent means ± SEM of n = 4 BMDC donor mice for each genotype. Replicates are illustrated in symbols. Ordinary two-way ANOVA with Dunnett's multiple comparisons test was performed to obtain p values. Only p values < 0.05 are shown.

3.10.3 Temporally shifted expression of nitrite and IFNγ in co-cultures of BMDCs and OT-I T cells

In the following experiment (Figure 42), the temporal relationship between the expression of IFNγ and NO (measured as nitrite) was investigated. Co-cultures were set up as already described (cf. Figure 12) and nitrite as well as IFNγ levels were analysed after 6 h, 14 h, 24 h and 48 h of incubation. This may indicate a potential dependence on each other and the sequence within the suppressive signalling chain.

Low concentrations of IFNγ, ranging from 30 to 200 pg/ml were already detected after 6 h of incubation for all conditions except the unstimulated one (Figure 42A). The IFNγ levels further raised over time. Compared to the respective 0 CFU/BMDC stimulation, 100 and 1000 *S. epidermidis* CFU/BMDC at 24 h and additionally 10000 CFU/BMDC at 48 h enhanced the expression of IFNγ. Treatment with 1000 CFU/BMDC resulted in the highest IFNγ values in each co-culture at time points of 24 h and 48 h.

The measured nitrite levels are graphed in Figure 42B. Very low nitrite values (< 2 µM) were measured after 14 h at the earliest at 1000 and 10000 *S. epidermidis* CFU/BMDC. After 24 h, the expression was clearly detectable at these two *S. epidermidis* concentrations. After 48 h, nitrite expression could be analysed at all conditions except the unstimulated condition. Similar to IFNγ, more nitrite was released at higher *S. epidermidis* concentrations. At 100, 1000 and 10000 *S. epidermidis* CFU/BMDC there was significantly more nitrite than in the 0 CFU/BMDC control. Figure 42C shows the expression of IFNγ and nitrite over time for 1000 *S. epidermidis* CFU/BMDC, which shows the highest induction potential. IFNγ started to be expressed prior to nitrite production with an estimated difference of 8 h.

To summarize Chapter 3.10, by adding rmIFNγ, we found that NO is released as a consequence of IFNγ signalling. By using iNOS$^{-/-}$ BMDCs, we identified the BMDCs as the source of NO in our co-cultures. A temporal dissection showed that NO is released later than IFNγ.

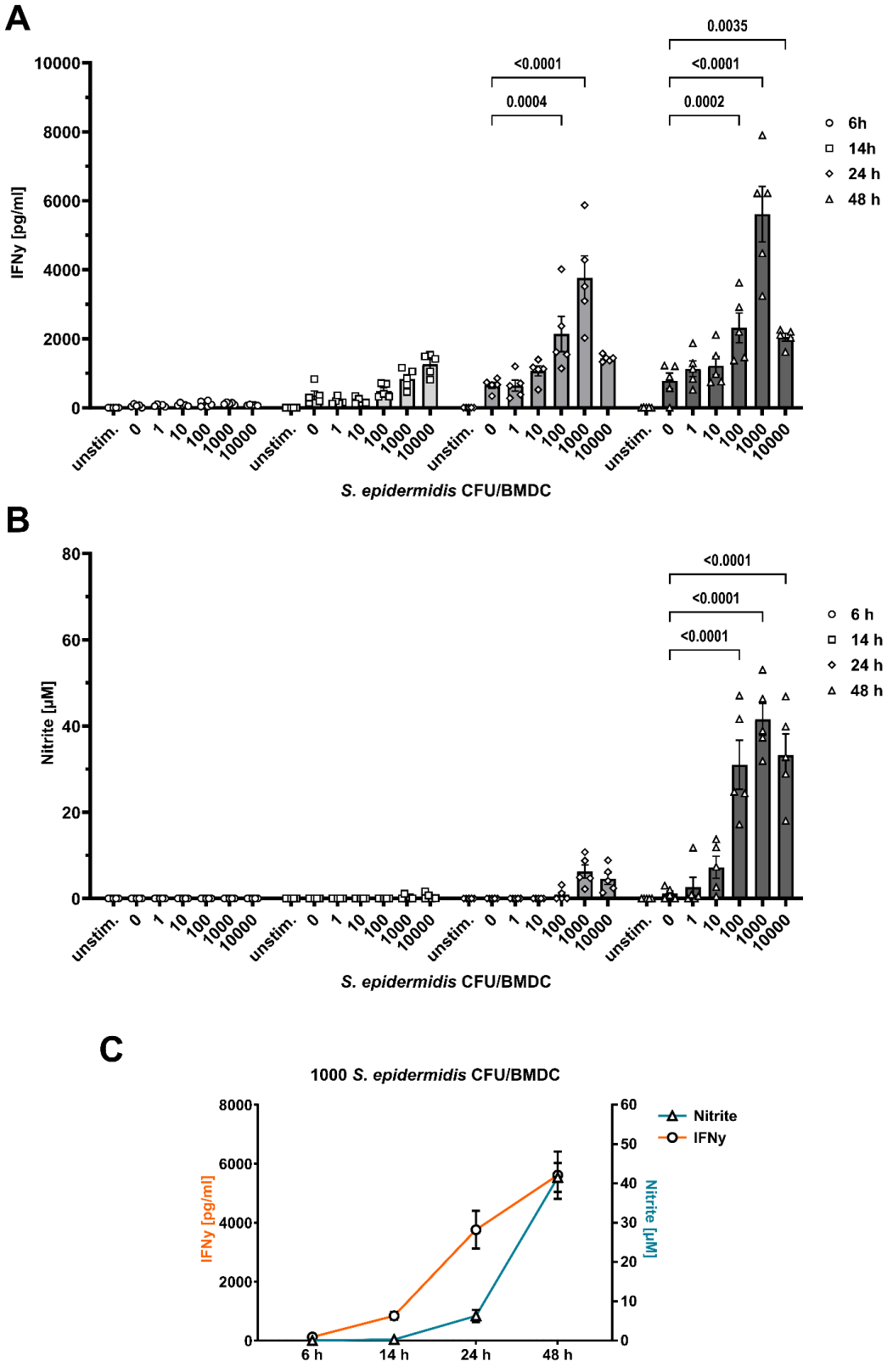

Figure 42: Temporal resolution of IFNγ and nitrite expression in co-cultures of OT-I T cells, BMDCs, OVA and *S. epidermidis*.

Co-cultures of OT-I T cells with BMDCs were stimulated with OVA protein and exposed to UV-attenuated *S. epidermidis* strain 614. Supernatants were collected after 6 h, 14 h, 24 h and 48 h of incubation. **(A)** IFNγ and **(B)** nitrite levels in supernatants of the co-cultures were compared to the respective 0 *S. epidermidis* CFU/BMDC value at each time point. **(C)** The expression of IFNγ and nitrite in co-cultures after incubation with 1000 *S. epidermidis* CFU/BMDC is shown over the time course from 6 h to 48 h.
Bars represent means ± SEM of n = 5 BMDC donor mice. Replicates are illustrated in symbols. Ordinary two-way ANOVA with Dunnett's multiple comparisons test was performed to obtain p values. Only p values < 0.05 are shown.

3.11 *S. epidermidis*-induced increase in IFNγ expression by memory OT-I T cells contributes to a suppressed OT-I T cell proliferation

Previous data showed that the presence of *S. epidermidis* can suppress OT-I T-cell proliferation in co-cultures of BMDCs and OT-I T cells. In addition, our investigations revealed that *S. epidermidis* does not directly suppress OT-I T cell proliferation, that BMDCs play a crucial role in this suppression and that IFNγ and NO are both involved. Using different KO BMDCs in co-cultures, BMDCs were identified as sensor of IFNγ, and as source of NO. The deficiency for the IFNγ gene in BMDCs had no influence on the suppressed OT-I T cell proliferation and IFNγ was still detectable in this $IFN\gamma^{-/-}$ BMDC co-cultures, which excludes BMDCs as the source of IFNγ. As a consequence, only OT-I T cells remain as a source of IFNγ, which was tested in the following experiment. Furthermore, it needed to be clarified whether OT-I T cells can sense *S. epidermidis* and whether IFNγ secretion is related to such potential sensing.

First, we investigated if *S. epidermidis* has an influence on the IFNγ expression of OT-I T cells (Figure 43). Therefore, OT-I T cells were stimulated with anti-CD3/CD28 beads or remained unstimulated and *S. epidermidis* was added in different concentrations (cf. experimental setup in Figure 18). After 72 h, bead stimulation resulted in higher IFNγ levels than in the unstimulated controls. Addition of *S. epidermidis* to the bead stimulus increased the levels of IFNγ at all concentrations except for 1000 CFU/T cell. This increase was highest at 1 and 10 CFU/T cell. The IFNγ levels for this concentration were significantly higher than in the 0 CFU/T cell control, which only contained beads. In OT-I T cell cultures without beads, the detected IFNγ concentrations were almost 0 pg/ml and addition of *S. epidermidis* did not increase them significantly.

The experiment depicted in Figure 45, investigated whether naive or memory OT-I T cells are the source of IFNγ. For this purpose, OT-I T cells were separated into naive and memory OT-I T cells by FACS sorting prior to culture. Figure 44 shows the gating strategy used for the sort of naive and memory OT-I T cells as well as an example for reanalysis of both populations. Cells were gated on size (SSC-A and FSC-A) and single cells. Next CD4-CD8+ out of live cells were chosen. In the last gating step, naive (CD44- CD62L+) OT-I T cells were distinguished from memory (CD44+) OT-I T cells using CD62L and CD44 signals.
The OT-I T cells were then stimulated with beads and incubated with *S. epidermidis* as described above. As shown in Figure 42, IFNγ expression can be detected in co-cultures after only a few hours, supernatants from the OT-I T cell cultures used here were analysed after 24 h of incubation. Naive OT-I T cells did not secrete any IFNγ. In contrast, IFNγ was measured in cultures of memory OT-I T cells, but only when stimulated with both beads and *S. epidermidis*. The highest concentration was detected for the treatment with 10 *S. epidermidis* CFU/T cell.

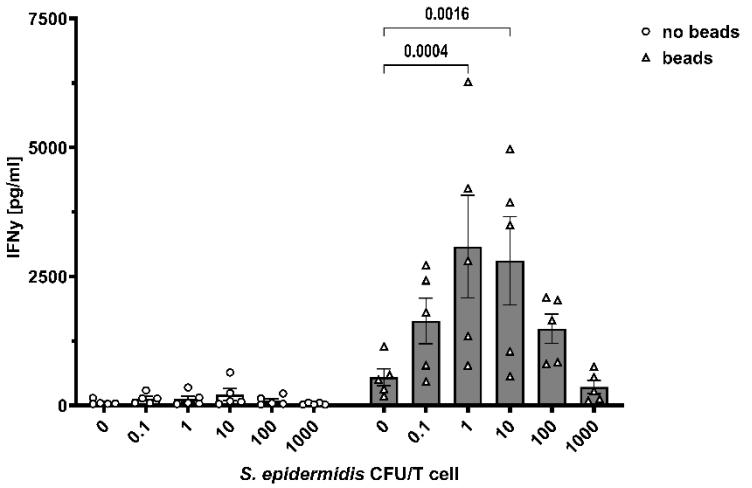

Figure 43: IFNγ expression of OT-I T cells stimulated with anti-CD3/CD28 beads and exposed to *S. epidermidis*.

OT-I T cells were stimulated with anti-CD3/CD28 beads and exposed to UV-attenuated *S. epidermidis* strain 614. One OT-I T cell culture was treated only with UV-attenuated *S. epidermidis* at different concentrations whereas the other culture was stimulated additionally with anti-CD3/CD28 beads. Supernatants were collected after 72 h of incubation. IFNγ levels in supernatants of the cultures were compared to the respective 0 *S. epidermidis* CFU/BMDC value within each group.
Bars represent means ± SEM of n = 5 OT-I T cell donor mice. Replicates are illustrated in symbols. Ordinary two-way ANOVA with Dunnett's multiple comparisons test was performed to obtain p values. Only p values < 0.05 are shown.

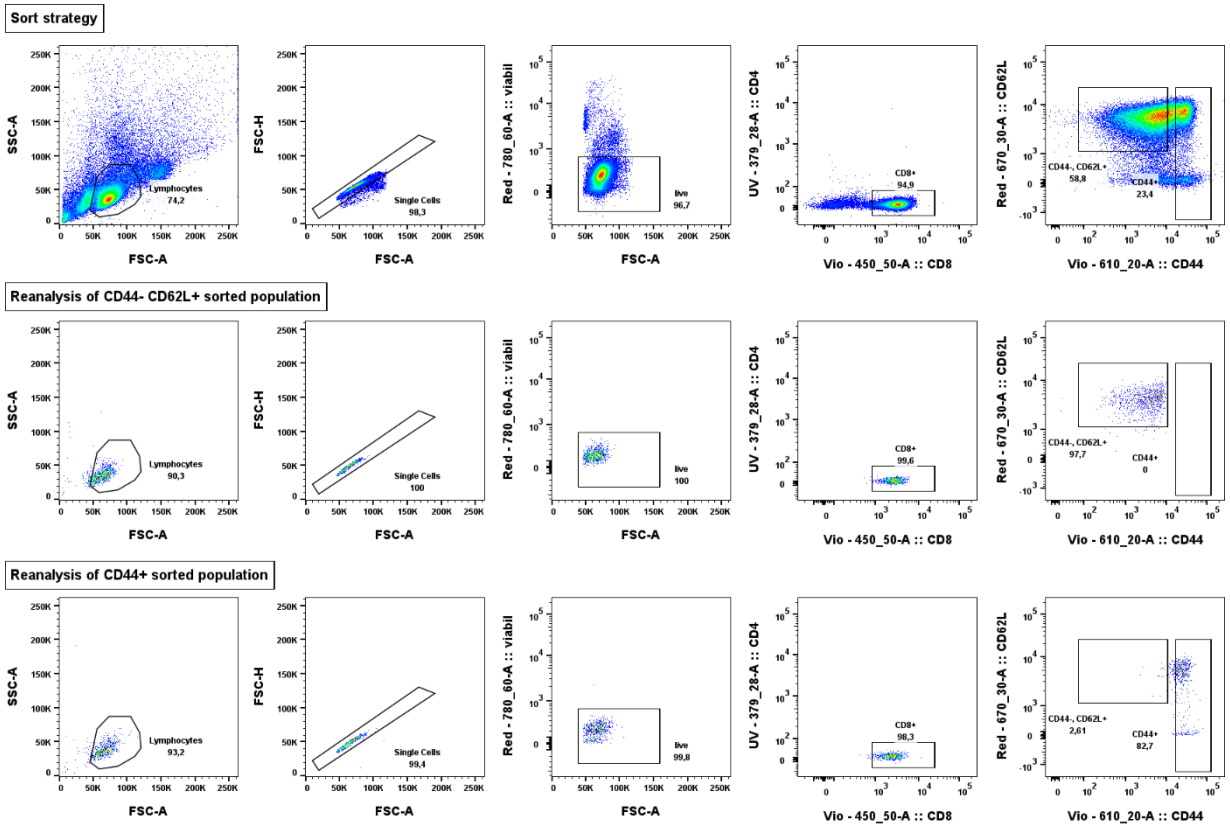

Figure 44: Sort strategy and reanalyses of naive and memory OT-I T cells.

Representative dot plots for the FACS sorting strategy to isolate naive (CD44- CD62L+) OT-I T cells and memory (CD44+) OT-I T cells from OT-I mice spleens and lymph nodes are depicted in the first line. Second and third line of dot plots represent the reanalysis control for naive and memory OT-I T cells respectively.

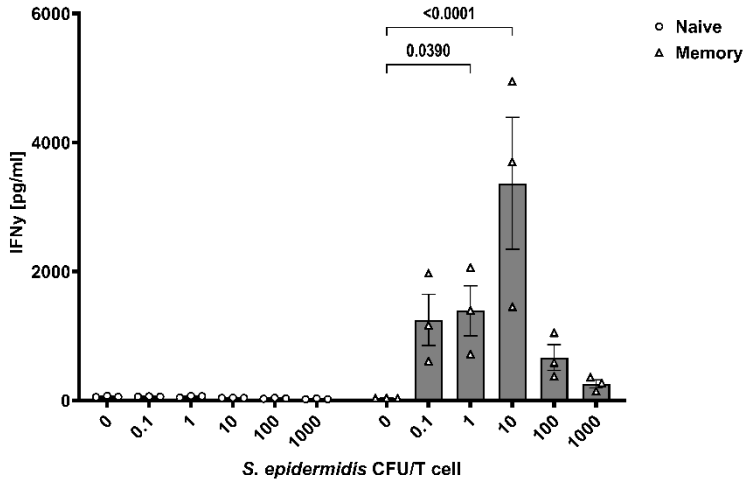

Figure 45: IFNγ expression of naive and memory OT-I T cells stimulated with anti-CD3/CD28 beads and incubated with *S. epidermidis*.

100.000 naive or memory OT-I T cells were stimulated with anti-CD3/CD28 beads and incubated with UV-attenuated *S. epidermidis* strain 614. Supernatants were collected after 24 h of incubation. IFNγ levels in supernatants of the cultures were compared to the respective 0 *S. epidermidis* CFU/BMDC value within each group.
Bars represent means ± SEM of n = 3 OT-I T cell donor mice. Replicates are illustrated in symbols. Ordinary two-way ANOVA with Dunnett's multiple comparisons test was performed to obtain p values. Only p values < 0.05 are shown.

As memory OT-I T cells were identified as the source of the early IFNγ, also co-cultures of BMDCs with naive or memory OT-I T cells were set up. These co-cultures were then stimulated with OVA protein and exposed to *S. epidermidis.* The OT-I T cell proliferation was analysed by the CFSE profile after 72 h incubation. In addition to the co-cultures with naive and memory OT-I T cells, a control co-culture with unseparated OT-I T cells, referred to as pool, was used. Counts and frequencies of proliferating OT-I T cells in these co-cultures are shown in Figure 46. OVA stimulation induced OT-I T cell proliferation in all three groups (Figure 46A). Even if it was not tested significant for the memory group, increased counts can be observed in the 0 *S. epidermidis* CFU/BMDC when compared to the unstimulated condition. The comparison of the OT-I T cell counts after *S. epidermidis* exposure with the respective 0 CFU/BMDC control in each group showed that *S. epidermidis* significantly reduced OT-I T cell proliferation in the pool and memory group (Figure 46B). This was dependent on the *S. epidermidis* concentration used with the strongest suppression at 100 and 1000 CFU/BMDC. In the naive OT-I T cell group, no such suppression was detected. In comparison to 0 CFU/BMDC, the counts were lowered at 1000 CFU/BMDC, but no significance could be calculated. Regarding the concentration 100 and 1000 CFU/BMDC where the suppression can be noticed usually, frequencies in the memory OT-I T cell co-culture were lower than in the naive group (Figure 46C).

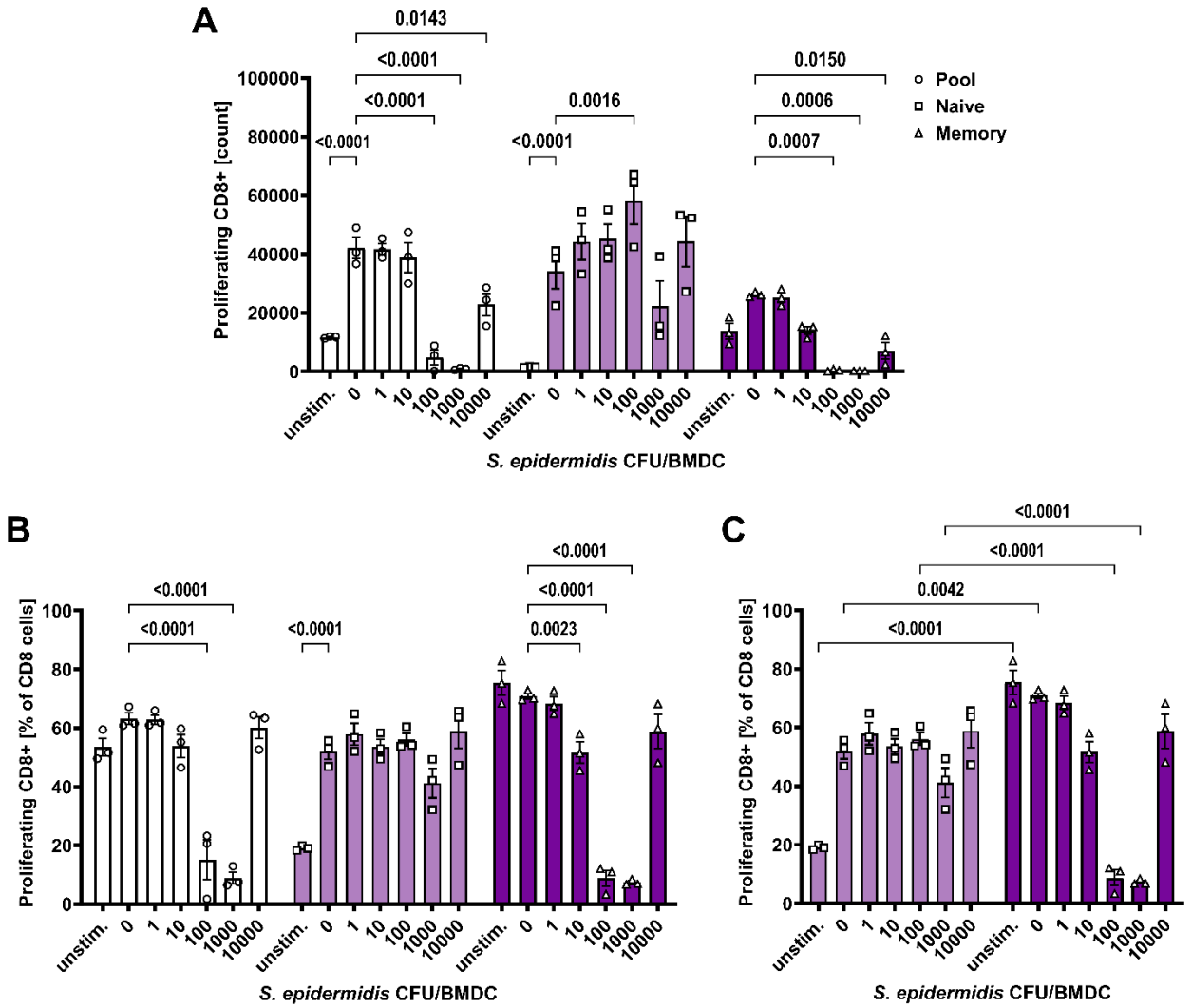

Figure 46: Proliferation of naive and memory OT-I T cells in co-culture with BMDCs and stimulated with OVA and exposed to UV-attenuated *S. epidermidis*.

Co-cultures of BMDCs with 200.000 naive or 100.000 memory OT-I T cells or a pool of 200.000 unseparated OT-I T cells were stimulated with OVA protein and exposed to UV-attenuated *S. epidermidis* strain 614. OT-I T cell proliferation was analysed by detection of the CFSE intensity in FACS after 72 h of incubation. **(A)** Counts of proliferating OT-I T cells were compared to the respective 0 *S. epidermidis* CFU/BMDC value within a group. **(B)** Frequencies of proliferating OT-I T cells among all OT-I T cells were compared to the respective 0 *S. epidermidis* CFU/BMDC value within a group. **(C)** The frequencies of proliferating OT-I T cells were compared between co-cultures with naive and memory OT-I T cells for related concentrations of *S. epidermidis*.
Bars represent means ± SEM of n = 3 BMDC donor mice for each genotype. Replicates are illustrated in symbols. Ordinary two-way ANOVA with Dunnett's multiple comparisons test (A and B) or with Šidák's multiple comparisons test (C) was performed to obtain p values. Only p values < 0.05 are shown.

In brief, we could identify memory OT-I T cells as the source of IFNγ and that addition of *S. epidermidis* to a proliferation-inducing stimulus such as beads can increase the amount of secreted IFNγ. Interestingly, no suppression was observed in co-cultures with only naive OT-I T cells.

3.12 Transcriptome analysis of OT-I T cells

RNAseq analysis were performed for OT-I T cells following co-culture incubation to study the influence of the *S. epidermidis*-induced signalling cascade of IFNγ and NO on OT-I T cell transcriptome. As shown in Figure 47, the addition of *S. epidermidis* reduced the percentage of proliferating OT-I T cells in co-cultures. Therefore, we decided to sort proliferating as well as resting OT-I T cells for RNAseq analysis. On the on hand, differences in of *S. epidermidis*-exposed resting and proliferating OT-I T cells could be analysed. On the other hand, the transcriptome profile of proliferating OT-I T cells could be compared in dependence of the *S. epidermidis* concentration used. The detailed gating for the sort is already described in section 2.3.9 in Figure 2. Proliferating and resting OT-I T cells were separated 72 h after co-culture with BMDCs. Within these co-cultures, they were incubated with different concentrations of *S. epidermidis*. The PCA plot of the analysed samples is shown in Figure 48. The analysis showed a clear difference between proliferating and resting OT-I T cells, indicated by the PC1 axis. In resting and proliferating OT-I T cells, *S. epidermidis*-treated cells clustered relatively close together with large overlaps. Proliferating and resting OT-I T cells that were stimulated only with OVA but not incubated with *S. epidermidis* (0 CFU/BMDC) were separated slightly from the respective *S. epidermidis*-treated groups. In the 0 CFU/BMDC samples of proliferating OT-I T cells, however, the cluster was more spread and one sample of the group overlapped with the *S. epidermidis*-treated clusters.

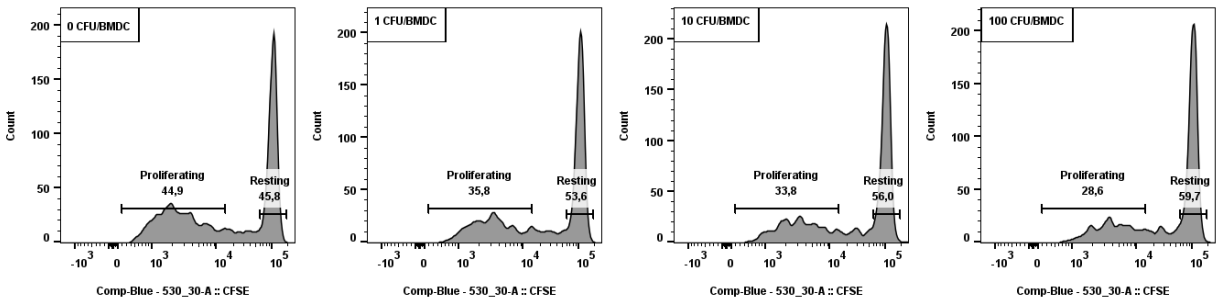

Figure 47: Representative CFSE plots of the sort for proliferating and resting OT-I T cells.

OT-I T cells were co-cultured with BMDCs and different concentrations of *S. epidermidis* and were stimulated with OVA protein. After 72 h of incubation, OT-I T cells were sorted and separated into proliferating and resting OT-I T cells by their CFSE profile. The sorted cells were used for RNAseq analysis. Gates indicate the percentage of the proliferating and resting population respectively.

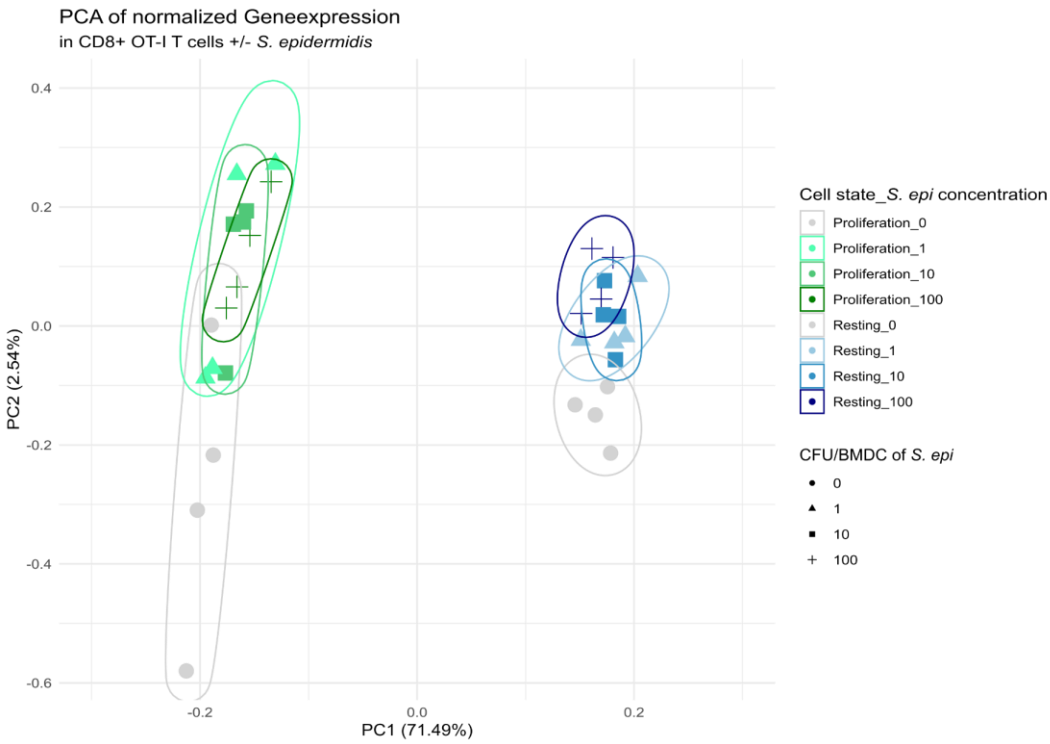

Figure 48: Differential gene expression profiling of OT-I T Cells by principal component analysis upon *S. epidermidis* exposure.

The PCA plot visualizes the global gene expression changes in OT-I T cells under resting and proliferative states when challenged with varying concentrations of *S. epidermidis*, quantified in CFU/BMDC. Principal component 1 (PC1), capturing 71.49 % of the total variance, discriminating between the proliferative and resting states. Principal component 2 (PC2) accounts for 2.54 % of the variance. Each symbol represents an individual biological replicate, with the symbol shape indicating the specific CFU/BMDC concentration (0, 1, 10, 100) and the colour designating the cell state under a particular bacterial load.
Analysis and graphical illustration by Bernd Daller (IMHR).

With regard to the expression of PRRs, varying read counts could be detected in the sequencing data for some PRRs, depending on the receptor gene (Figure 49).

In the proliferating OT-I T cells, TPM values for the Cd6 and Nod1 genes were detected in the range of 50 to 130. The TPMs for the Tlr1 and Tlr6 genes were around 15, while TPMs for the Tlr2 and Nod2 genes were hardly present. TPMs of genes such as Cd6, Tlr1 and Nod1 were slightly higher in *S. epidermidis*-treated samples than in the corresponding untreated controls, albeit not significant. Comparing the TPMs of proliferating and resting OT-I T cells, the TPM values of the proliferating OT-I T cells were significantly higher for Cd6 and Nod1 than in the resting OT-I T cells, whereas TPMs of Tlr1 and Tlr6 were significantly higher in the resting than in the proliferating OT-I T cells at the corresponding *S. epidermidis* concentrations. There were no noticeable differences in the low expressed genes Tlr2 and Nod2 between conditions with and without *S. epidermidis*.

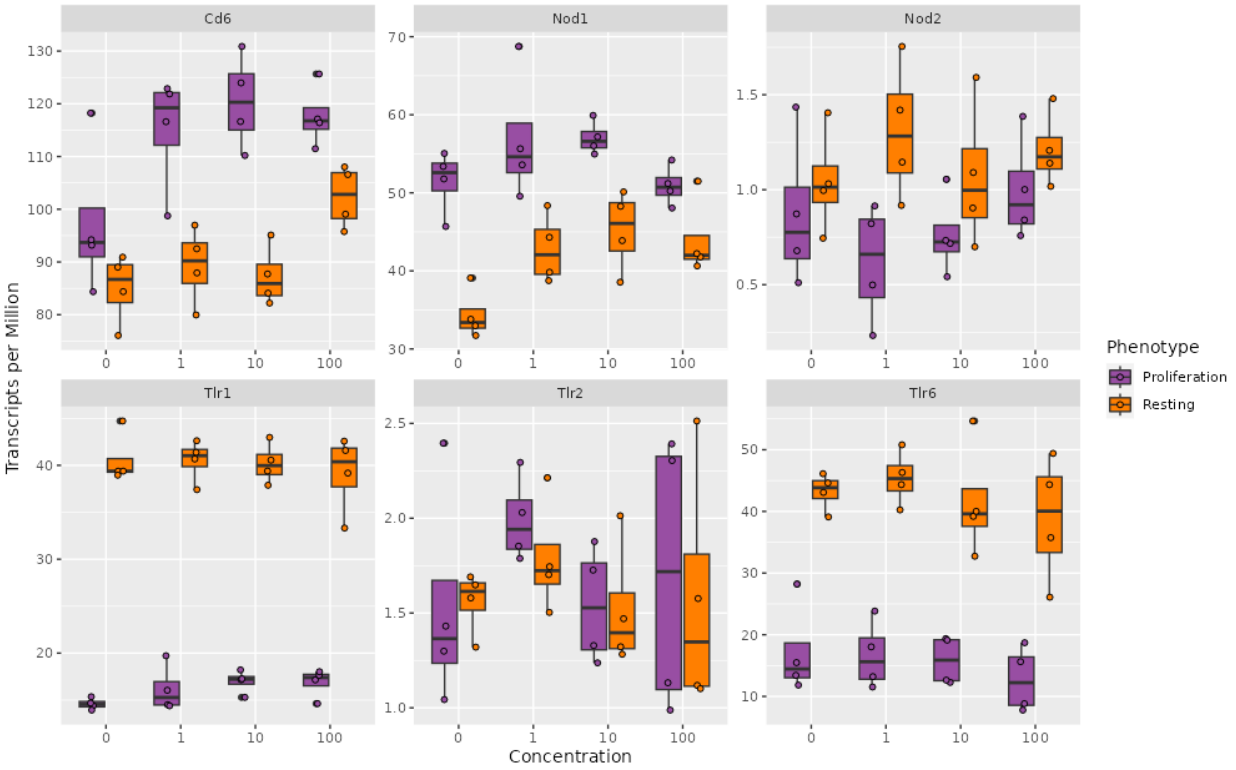

Figure 49: Gene expression in transcripts per million (TPM) of a selection of pattern recognition receptor-associated genes from RNAseq analyses of proliferating and resting OT-I T cells.

TPM values were mapped from RNAseq analyses of proliferating as well as resting OT-I T cells for selected genes. OT-I T cells were incubated with BMDCs, OVA and the indicated concentration of *S. epidermidis* CFU/BMDC (concentration; x-axis) for 72 h. Proliferating (CFSE low) and resting (CFSE high) OT-I T cells were sorted, dependent on the CFSE intensity, and used for bulk RNAseq analysis. Sequencing by NGS core facility and analyses and app programming by Bernd Daller (IMHR).

In Figure 50, TPM values for selected genes that are associated with T cell exhaustion are depicted for proliferating and resting OT-I T cells. TPMs of Cblb, Entpd1, Eomes and Lag3 were higher in proliferating than in resting OT-I T cells. It was the other way around with the genes Foxo1 and Tcf7. For the genes Cblb, Entpd1, Eomes and Tcf7, treatment with *S. epidermidis* increased the TPMs of proliferating OT-I T cells compared to the 0 CFU/BMDC condition.

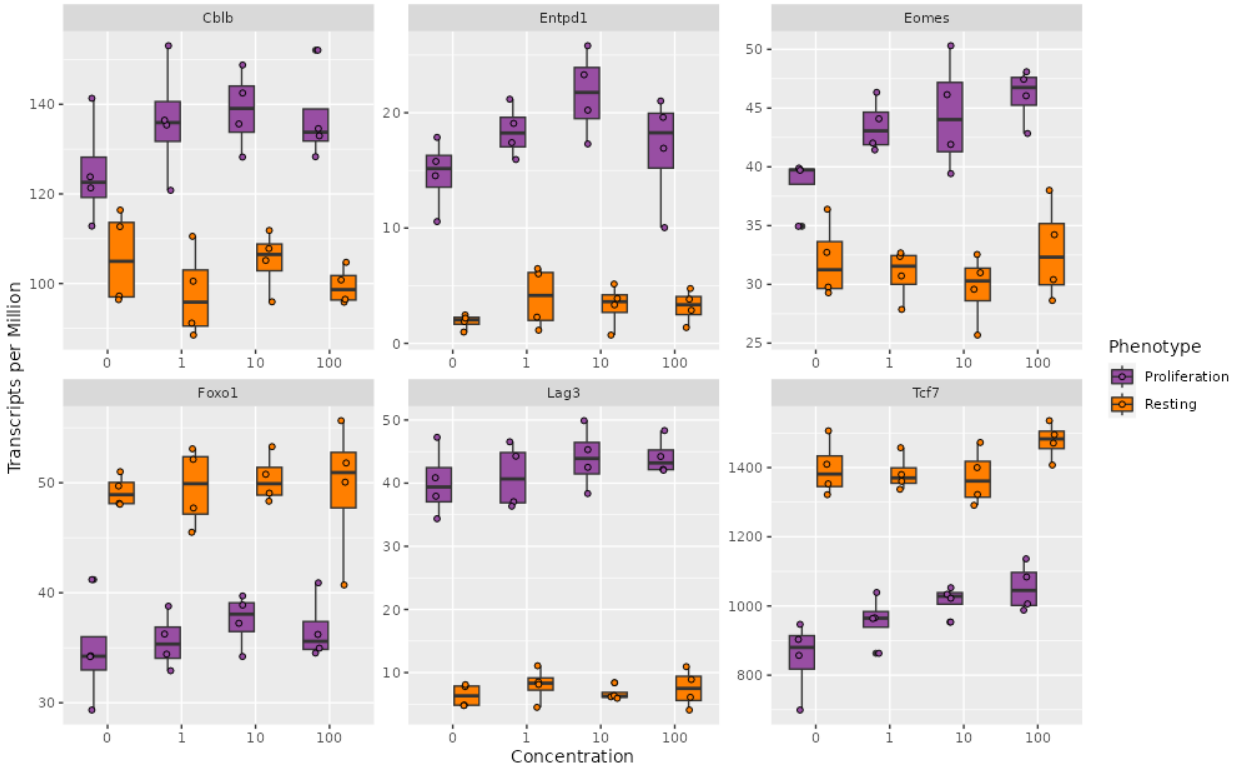

Figure 50: Gene expression in transcripts per million (TPM) of a selection of T cell exhaustion-associated genes from RNAseq analyses of proliferating and resting OT-I T cells.

TPM values were mapped from RNAseq analyses of proliferating as well as resting OT-I T cells for selected genes that are associated with exhaustion in T cells. OT-I T cells were incubated with BMDCs, OVA and the indicated concentration of *S. epidermidis* CFU/BMDC (x-axis) for 72 h. Proliferating (CFSE low) and resting (CFSE high) OT-I T cells were sorted, dependent on the CFSE intensity, and used for bulk RNAseq analysis. Sequencing by NGS core facility and analyses and app programming by Bernd Daller (IMHR).

3.13 TLR activation of BMDCs by *S. epidermidis* is not crucial for mediating the suppression of OT-I T cells

It seems likely that sensing of *S. epidermidis* by OT-I T cells induces the suppressive signalling cascade. To further support this hypothesis and to study if TLR-dependent activation of BMDCs by *S. epidermidis* is required for the suppression of OT-I T cells, co-cultures with MyD88$^{-/-}$ and TRIF$^{-/-}$ BMDCs were prepared. MyD88 and TRIF are two important adaptor proteins in TLR signalling and deficiency for these proteins prevents TLR signalling. TLR3 and TLR4 are dependent on TRIF signalling, while the signals of all other TLRs run via MyD88 (Sameer and Nissar 2021; Duan et al. 2022). The experimental setup of the co-cultures was the same as already described in co-cultures with other KO BMDCs (compare section 3.9.3 and 3.10.2).

Before setting up co-cultures with the two KO BMDC lines and the WT BMDCs, they were analysed for similarity in CD11b/CD11c expression and their maturity and activation state (Figure 51). Exemplary dot plots for the gating are depicted in Figure 51A. Cell debris was excluded by size gating (SSC-A, FSC-A) followed by the determination of the viable cell population. Live cells were gated on CD11b+CD11c+ cells. Moreover, for the evaluation of the maturation state a gate was put on CD86+ MHC class II+ cells. Results of the analysis are shown in Figure 51B. The expression of the lineage markers CD11b and CD11c were approximately equal in MyD88$^{-/-}$, TRIF$^{-/-}$ and WT BMDCs. Only the expression in MyD88$^{-/-}$ BMDCs was slightly lower than in the WT BMDCs regarding 100 CFU/BMDC stimulation. MFIs of the co-stimulatory marker CD86 showed no differences between TRIF$^{-/-}$ and WT BMDCs and *S. epidermidis* upregulated the expression. In MyD88$^{-/-}$ BMDCs the expression of CD86 was not upregulated by *S. epidermidis*. There were no significant differences in the expression levels of the antigen-presenting MHC class II between knockout and WT BMDCs. In MyD88$^{-/-}$ BMDCs MHC class II seemed to be slightly lower than in the other two BMDC types. The percentage of mature BMDCs, indicated by the CD86+ MHC class II+ population, was similar for all genotypes. In MyD88$^{-/-}$ BMDCs, however, the frequency appeared to be a bit lower than in the other two BMDC types.

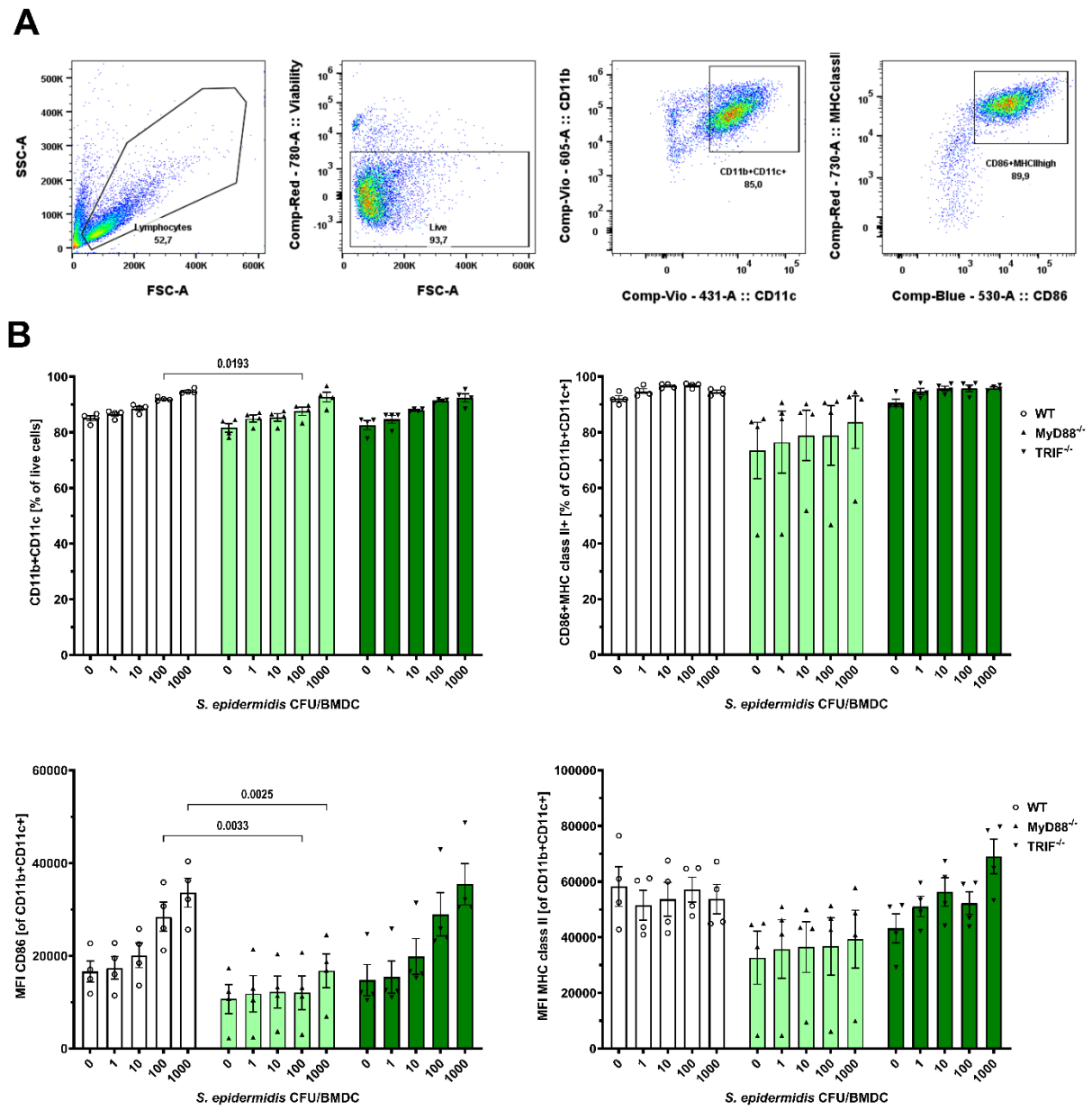

Figure 51: Comparison of MyD88$^{-/-}$ BMDCs and TRIF$^{-/-}$ BMDCs with WT BMDCs.

Day 9 BMDCs generated from WT, MyD88$^{-/-}$ and TRIF$^{-/-}$ mice were examined to see if they had a comparable phenotype before they were used in the co-cultures. **(A)** Representative dot plots of the gating strategy after FACS analysis (unstimulated WT BMDCs). **(B)** Proportion of CD11b+CD11c+ cells, maturation state (CD86+ MHC class II+) and MFI of CD86 and MHC class II expression of unstimulated BMDCs and BMDCs treated for 24 h with UV-attenuated *S. epidermidis* strain 614.
Bars represent means ± SEM of n = 4 BMDC donor mice for each genotype. Biological replicates are illustrated in symbols. Ordinary two-way ANOVA with Dunnett's multiple comparison test was performed to obtain p values. Only p values < 0.05 are shown.

In the following, the WT and KO BMDCs were used in co-cultures to investigate whether TLR-dependent signalling in BMDCs induced by *S. epidermidis* is required for the suppression of OT-I T cells. Counts and frequencies of proliferating OT-I T cells in co-culture with WT, MyD88$^{-/-}$ or TRIF$^{-/-}$ BMDCs are depicted in Figure 52. Compared to the unstimulated condition, counts of proliferating OT-I T cells were increased by OVA stimulation in MyD88$^{-/-}$ BMDC co-cultures. They

were also increased in the co-cultures with the other two BMDC types, albeit not significant. *S. epidermidis* reduced the OVA-induced proliferation in all three co-cultures. Regarding the counts, this was significant at 10 and 100 CFU/BMDC *S. epidermidis* in the MyD88$^{-/-}$ co-cultures. In terms of frequency, 10, 100 and 1000 CFU/BMDC *S. epidermidis* diminished the proliferation of OT-I T cells in MyD88$^{-/-}$ and TRIF$^{-/-}$ co-cultures. OT-I T cell proliferation in WT BMDC co-cultures seemed to be also reduced by *S. epidermidis* at 10 and 100 CFU/BMDC, although not significant. Stimulation with 10000 CFU/BMDC *S. epidermidis* increased counts and frequencies of proliferating OT-I T cells compared to the respective 0 CFU/BMDC condition in WT BMDC and TRIF$^{-/-}$BMDC co-cultures.

The comparisons of the counts and frequencies of proliferating OT-I T cells between the KO BMDC co-cultures and the WT control were calculated between identical stimulation concentrations, but no significant differences were detected (statistics not shown; Ordinary two-way ANOVA; Dunnett's multiple comparisons test).

In summary, no differences were detected between the WT BMDC co-cultures and the MyD88$^{-/-}$ and TRIF$^{-/-}$ BMDC co-cultures regarding the suppression of OVA-specific OT-I T cells proliferations by the addition of *S. epidermidis*.

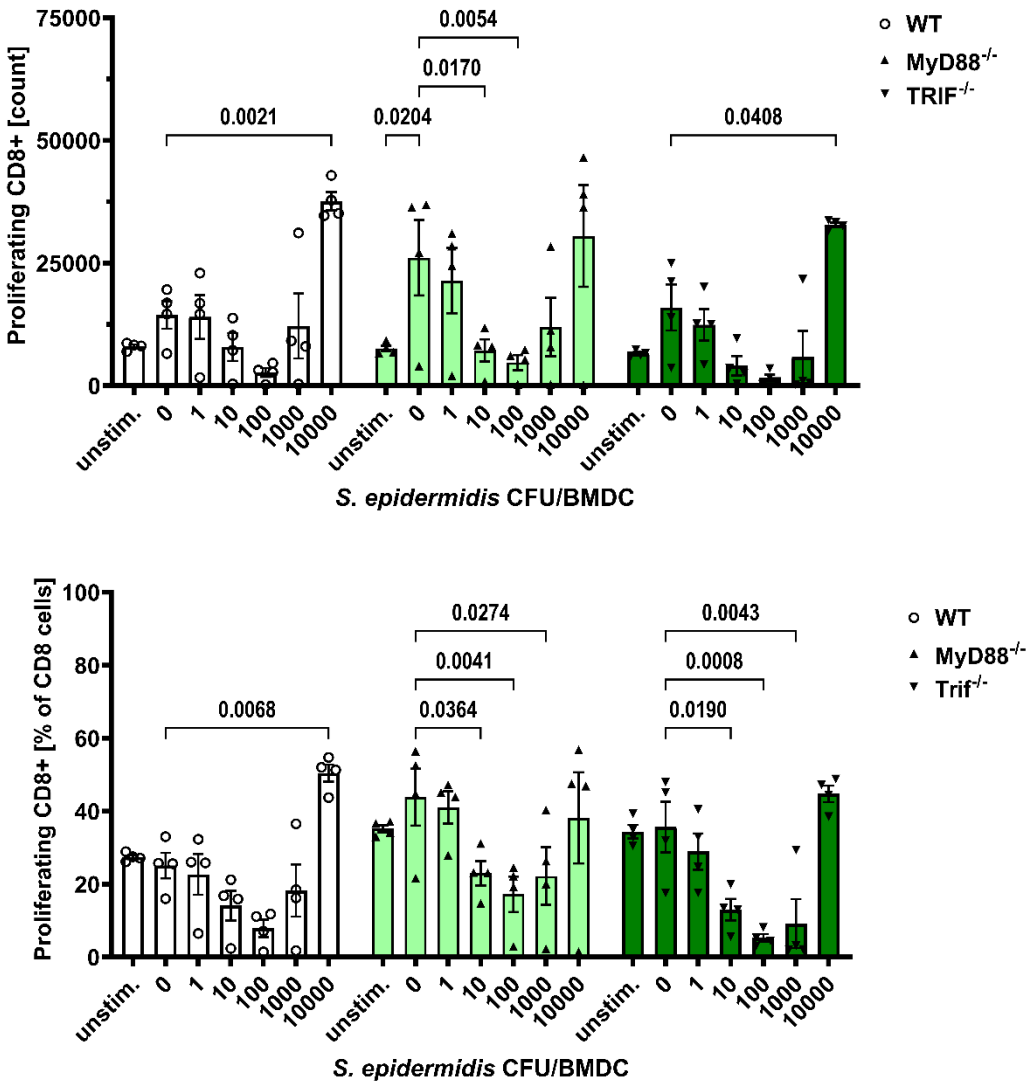

Figure 52: Proliferation of OT-I T cells in co-culture with BMDCs, generated from WT, MyD88$^{-/-}$ or TRIF$^{-/-}$ mice.

Co-cultures of CFSE-labelled OT-I T cells with BMDCs, generated from WT, MyD88$^{-/-}$ or TRIF$^{-/-}$ mice, were stimulated with OVA protein and treated with UV-attenuated *S. epidermidis* strain 614. OT-I T cell proliferation was analysed by detection of the CFSE intensity in FACS after 72 h of incubation. Counts of proliferating OT-I T cells and their frequencies among all OT-I T cells were compared to the respective 0 *S. epidermidis* CFU/BMDC value within a genotype.
Bars represent means ± SEM of n = 4 BMDC donor mice for each genotype. Replicates are illustrated in symbols. Ordinary two-way ANOVA with Dunnett's multiple comparisons test was performed to obtain p values. Only p values < 0.05 are shown.

3.14 The induced suppression of the OT-I T cell proliferation is not exclusive to *S. epidermidis*

In order to investigate whether the attenuation of OVA-specific OT-I T cell proliferation is specifically triggered by *S. epidermidis* or whether it is a more widespread mechanism of gram-positive bacteria, some of the experiments were performed with *Lactobacillus rhamnosus* (*L. rhamnosus*). Co-cultures of OT-I T cells and BMDCs were stimulated with OVA protein to induce proliferation of OT-I T cells. Further co-cultures were treated with different concentrations of *S. epidermidis* or *L. rhamnosus*. Counts of proliferating OT-I T cells are shown in Figure 53. In both co-cultures, the stimulation with OVA resulted in higher OT-I T cell counts than in the unstimulated condition. As already observed in previous experiments, the addition of *S. epidermidis* reduced the OVA-induced proliferation of OT-I T cells. Compared to 0 CFU/BMDC *S. epidermidis* (OVA only control), significantly less counts were detected in co-cultures stimulated with 100, 1000 and 10000 CFU/BMDC *S. epidermidis* (see Figure 53A). The addition of 1, 10 and 100 CFU/BMDC *L. rhamnosus* also reduced the counts of proliferating OT-I T cells in comparison to the respective 0 CFU/BMDC (OVA only) control (see Figure 53B).

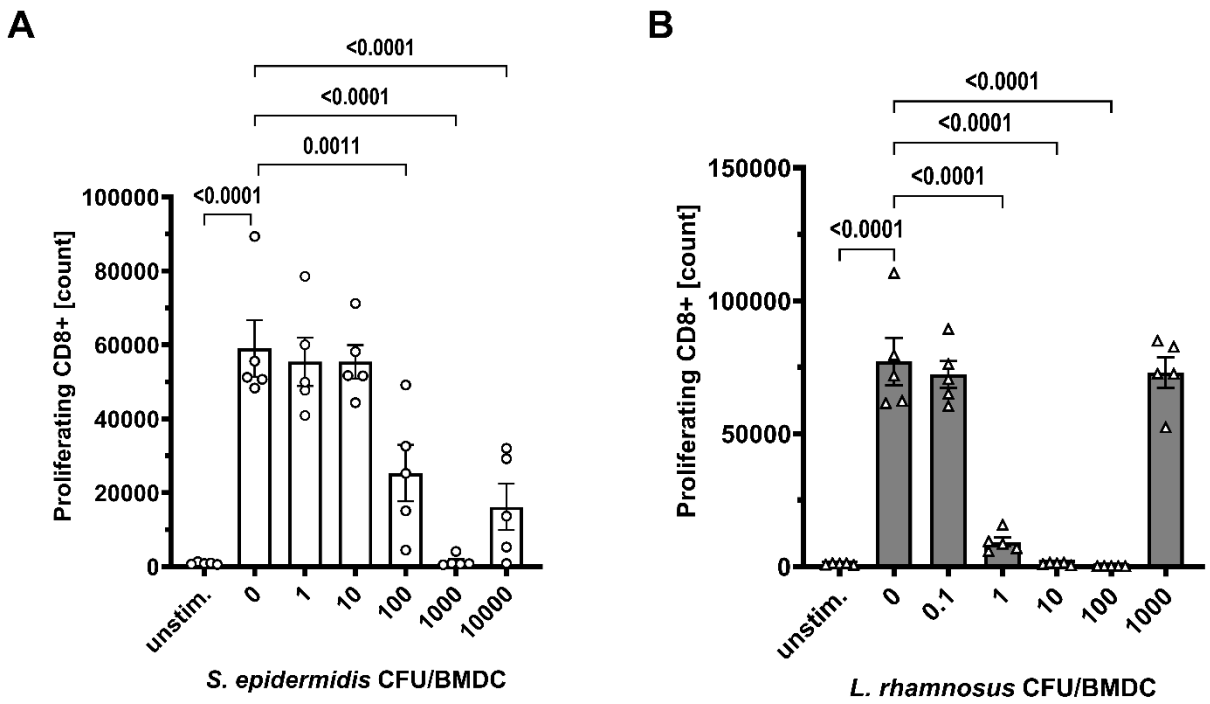

Figure 53: Proliferation of OT-I T cells and BMDC co-cultures after stimulation with OVA and treatment with *S. epidermidis* or *L. rhamnosus*.

CFSE-labelled OT-I T cells were co-cultured with BMDCs and were stimulated with OVA protein and treated with UV-attenuated *S. epidermidis* or UV-attenuated *L. rhamnosus*. OT-I T cell proliferation was analysed by detection of the CFSE intensity in FACS after 72 h of incubation. Counts of proliferating OT-I T cells and their frequencies among all OT-I T cells were compared to the respective 0 *S. epidermidis* CFU/BMDC condition. **(A)** Co-cultures were incubated with *S. epidermidis*. **(B)** Co-cultures were incubated with *L. rhamnosus*.
Bars represent means ± SEM of n = 5 BMDC donor mice. Replicates are illustrated in symbols. Ordinary one-way ANOVA with Dunnett's multiple comparisons test was performed to obtain p values. Only p values < 0.05 are shown.

The following experiments were carried out to investigate whether IFNγ also plays a role in *L. rhamnosus*-suppressed OT-I T cell proliferation, as is the case with *S. epidermidis* (see chapter 3.9). In Figure 54, a neutralising antibody against IFNγ was used in the co-cultures in addition to stimulation with OVA and the treatment with *L. rhamnosus*. The experimental setup is comparable to Figure 29 were *S. epidermidis* was used. Compared to the unstimulated condition, stimulation with OVA only (cf. 0 CFU/BMDC) induced the proliferation of OT-I T cells indicated by the elevated counts in all three co-cultures (Figure 54A). In co-cultures without antibody (w/o Ab) and the isotype control (Iso-IFNγ), the addition of *L. rhamnosus* to the OVA stimulation reduced the counts again. Compared to 0 CFU/BMDC, counts were significantly reduced in w/o Ab co-cultures at 0.1, 1, 10, 100 CFU/BMDC and in Iso-IFNγ co-cultures at 0.1, 1, 10 and 1000 CFU/BMDC. In anti-IFNγ-treated co-cultures, counts of proliferating OT-I T cells were only reduced at 1000 CFU/BMDC *L. rhamnosus* when compared to the 0 CFU/BMDC condition. The addition of *L. rhamnosus* even led to higher counts in the 1 and 10 CFU/BMDC condition than in the 0 CFU/BMDC control.

Comparing the proliferation of OT-I T cells between the Iso-IFNγ and the anti-IFNγ co-culture, significantly higher counts were detected in the anti-IFNγ than in the Iso-IFNγ group at all conditions, except the unstimulated one (Figure 54B).

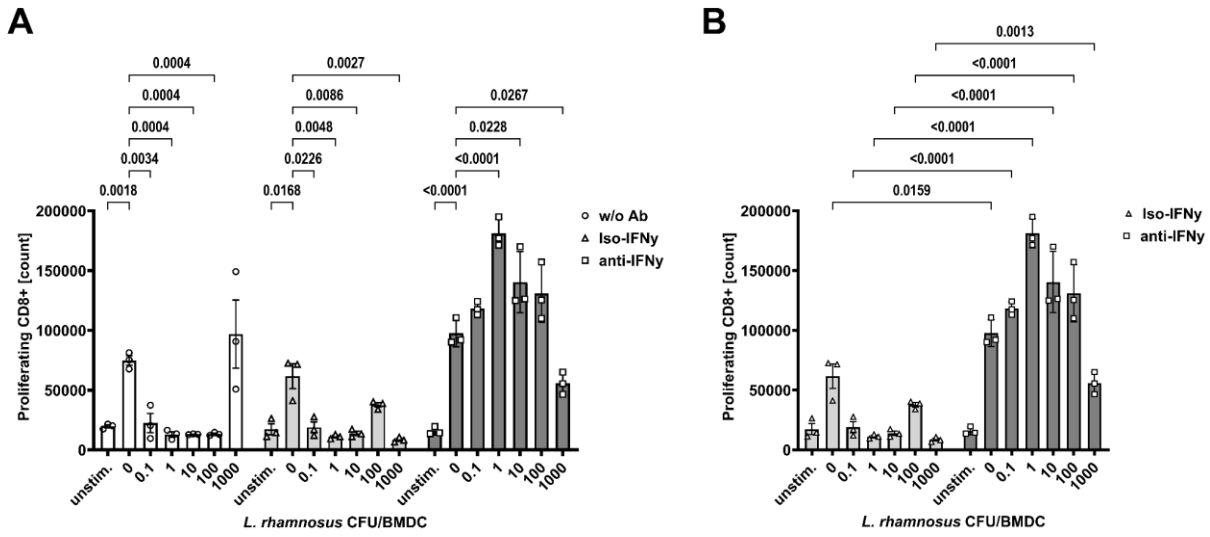

Figure 54: Counts of proliferating OT-I T cells in co-cultures with BMDCs, *L. rhamnosus* and neutralising anti-IFNγ antibody.

Co-cultures of CFSE-labelled OT-I T cells with BMDCs were stimulated with OVA protein and treated with UV-attenuated *L. rhamnosus*. Moreover, neutralising anti-IFNγ (anti-IFNγ) or an appropriate isotype control (Iso-IFNγ) was added to the co-cultures or they remained without antibody treatment (w/o Ab). OT-I T cell proliferation was analysed by detection of the CFSE profile in FACS after 72 h of incubation. **(A)** Counts of proliferating OT-I T cells compared to the respective 0 *L. rhamnosus* CFU/BMDC concentration within a group are depicted. **(B)** Counts of proliferating OT-I T cells in co-cultures with neutralising anti-IFNγ were compared to the ones in co-cultures containing the isotype at the related conditions.

Bars represent means ± SEM of n = 3 BMDC donor mice. Replicates are illustrated in symbols. Ordinary two-way ANOVA was performed to obtain p values. Dunnett's multiple comparisons test was applied for the comparison of 0 *S. epidermidis* CFU/BMDC to the other concentrations within a group. Tukey's multiple comparisons test was applied to compare the related *S. epidermidis* CFU/BMDC conditions between anti-IFNγ and Iso-IFNγ groups. Only p values < 0.05 are shown.

As described for *S. epidermidis* stimulation in section 3.9.3, co-cultures of OT-I T cells with WT as well as IFNγR$^{-/-}$ BMDCs were set up, to investigate if the IFNγ signalling in BMDCs is also involved in the dampening of OT-I T cell proliferation after addition of *L. rhamnosus* (Figure 55). Compared to the unstimulated condition, counts as well as frequencies of proliferating OT-I T cells were increased in OVA-stimulated co-cultures (cf. 0 CFU/BMDC) of both BMDC genotypes respectively. In the control co-culture with WT BMDCs, counts were reduced significantly at 10 CFU/BMDC *L. rhamnosus* and frequencies at 1, 10 and 100 CFU/BMDC in comparison to the 0 CFU/BMDC condition. In IFNγR$^{-/-}$ BMDC co-cultures, counts of proliferating OT-I T cells were not altered between the *L. rhamnosus*-treated and the OVA only (0 CFU/BMDC) condition. Regarding the frequency of proliferating OT-I T cells, only addition of 1 CFU/BMDC *L. rhamnosus* slightly reduced the proliferation in comparison to the 0 CFU/BMDC control.

Levels of secreted IFNγ detected in the supernatants of the co-cultures are depicted in Figure 56. In the WT BMDC co-culture, IFNγ levels raised in correlation with the concentration of *L. rhamnosus* and were significantly higher at 10, 100 and 1000 *L. rhamnosus* CFU/BMDC conditions than in the 0 CFU/BMDC condition. In IFNγR$^{-/-}$ BMDC co-cultures, the addition of *L. rhamnosus* increased the amount of detected IFNγ, too. Addition of 10, 100 and 1000 CFU/BMDC resulted in significantly higher levels of IFNγ than stimulation with OVA only (0 CFU/BMDC). The comparison of IFNγ levels at the same condition between the two BMDC types showed no differences except at 1000 CFU/BMDC. Here, the IFNγ level was lower in the IFNγR$^{-/-}$ co-cultures than in the WT co-cultures (statistics not shown; $p < 0.0001$; Ordinary two-way ANOVA with Šidák's multiple comparisons test).

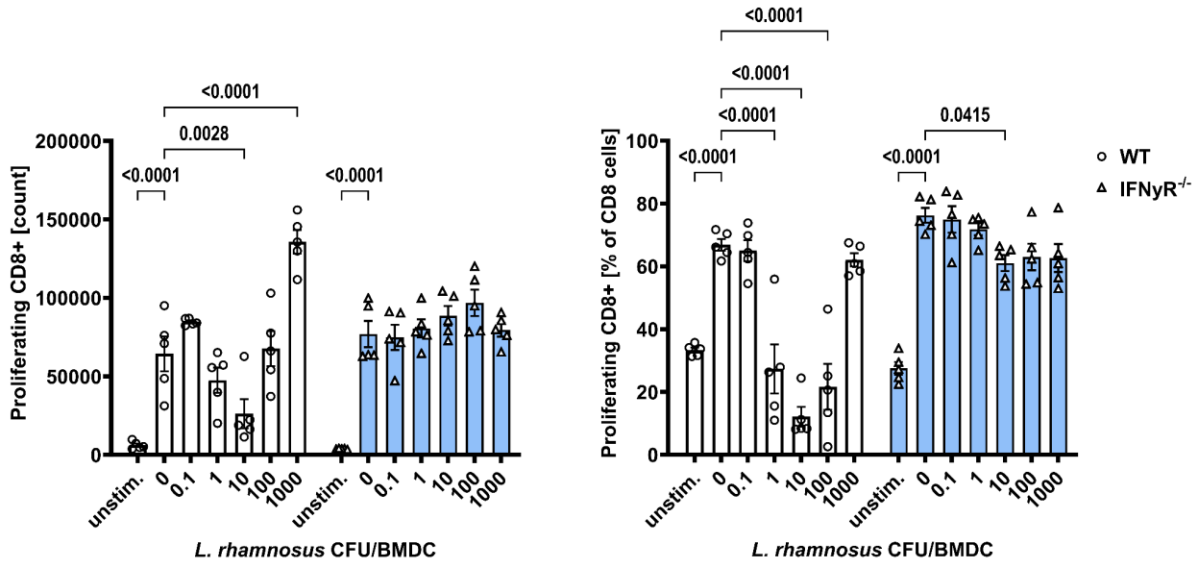

Figure 55: Proliferation of OT-I T cells in co-culture with OVA, *L. rhamnosus* and BMDCs, generated from WT and IFNγR$^{-/-}$ mice.

Co-cultures of CFSE-labelled OT-I T cells with BMDCs, generated from WT and IFNγR$^{-/-}$ were stimulated with OVA protein and exposed to UV-attenuated *L. rhamnosus*. OT-I T cell proliferation was analysed by detection of the CFSE intensity in FACS after 72 h of incubation. Counts of proliferating OT-I T cells and their frequencies among all OT-I T cells were compared to the respective 0 *L. rhamnosus* CFU/BMDC value within a genotype.
Bars represent means ± SEM of n = 5 BMDC donor mice for each genotype. Replicates are illustrated in symbols. Ordinary two-way ANOVA with Dunnett's multiple comparisons test was performed to obtain p values. Only p values < 0.05 are shown.

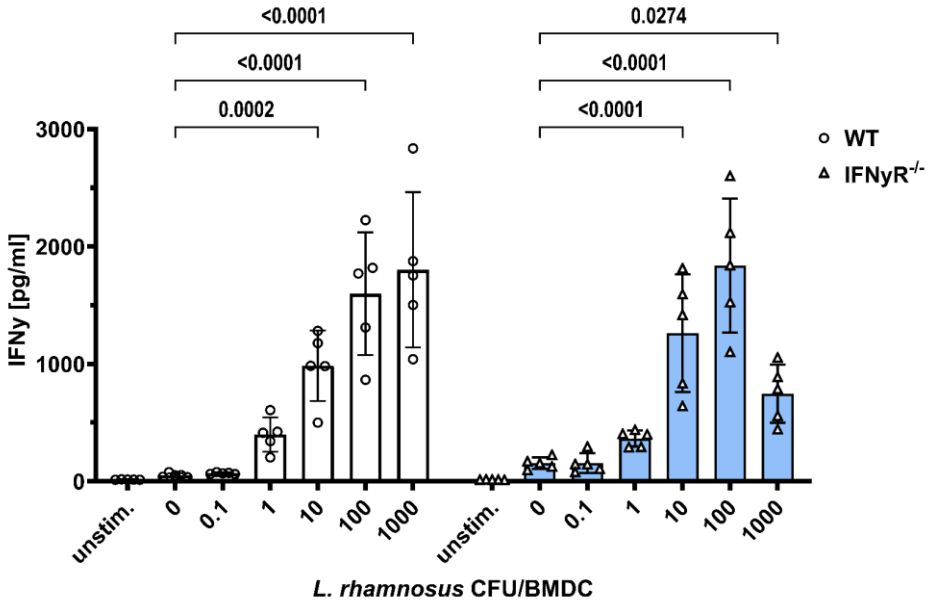

Figure 56: IFNγ levels in co-cultures of OT-I T cells, OVA, *L. rhamnosus* and BMDCs, generated from WT and IFNγR$^{-/-}$ mice.

Co-cultures of CFSE-labelled OT-I T cells with BMDCs, generated from WT and IFNγR$^{-/-}$ mice, were stimulated with OVA protein and exposed to UV-attenuated *L. rhamnosus*. Supernatants were collected after 72 h of incubation. IFNγ levels in supernatants of the co-cultures were compared to the respective 0 *L. rhamnosus* CFU/BMDC value within each group.
Bars represent means ± SEM of n = 5 BMDC donor mice for each genotype. Replicates are illustrated in symbols. Ordinary two-way ANOVA with Dunnett's multiple comparisons test was performed to obtain p values. Only p values < 0.05 are shown.

In Figure 57, the nitrite levels in supernatants of BMDC and OT-I T cell co-cultures are depicted. The co-cultures were stimulated with OVA protein and exposed to *L. rhamnosus* for 72 h. The nitrite level of the unstimulated condition as well as each *L. rhamnosus* concentration were compared to the 0 CFU/BMDC condition for each BMDC type respectively. In the co-culture with WT BMDCs, the unstimulated as well as the 0.1 and 1 *L. rhamnosus* CFU/BMDC conditions showed no significant difference compared to the 0 CFU/BMDC. At 10,100 and 1000 CFU/BMDC, significantly higher levels of nitrite were detected than in the 0 CFU/BMDC condition. No nitrite was detected in the IFNγR$^{-/-}$ BMDC co-cultures, irrespective of the condition. Comparing the related conditions between the two co-cultures showed that the nitrite levels were significantly higher in the WT than the IFNγR$^{-/-}$ co-cultures at 10, 100 and 1000 *L. rhamnosus* CFU/BMDC (statistics not shown; p = 0.0001 at 10 CFU/BMDC and p < 0.0001 at 100 and 1000 CFU/BMDC; Ordinary two-way ANOVA with Šidák's multiple comparisons test).

In conclusion, the use of *L. rhamnosus* instead of *S. epidermidis* in the co-cultures showed that the induction of OT-I T cell suppression is not specific for *S. epidermidis* but can also be induced by other bacteria such as *L. rhamnosus*. This was shown by reduced OT-I T cell proliferation, and the induction of IFNγ and NO in the presence of *L. rhamnosus*.

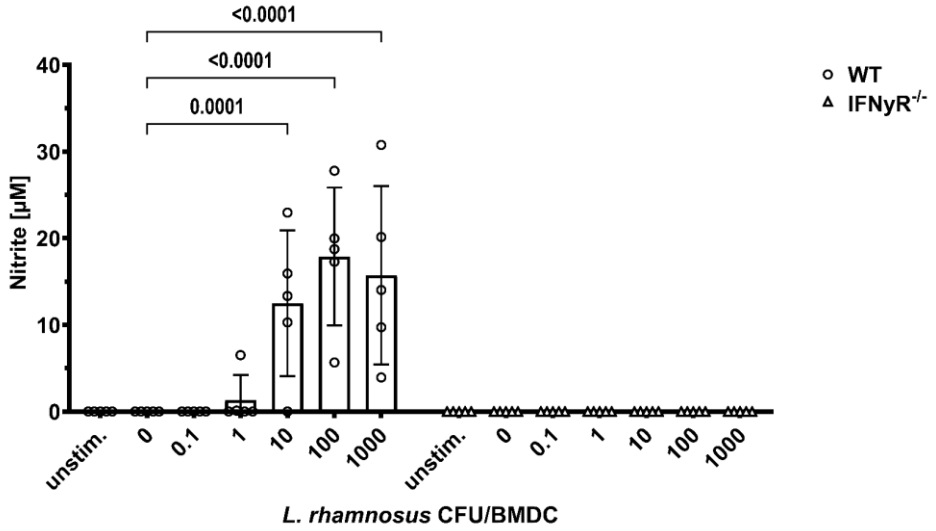

Figure 57: Nitrite levels in co-cultures of OT-I T cells, OVA, *L. rhamnosus* and BMDCs, generated from WT and IFNγR$^{-/-}$ mice.

Co-cultures of CFSE-labelled OT-I T cells with BMDCs, generated from WT and IFNγR$^{-/-}$ mice, were stimulated with OVA protein and exposed to UV-attenuated *L. rhamnosus*. Supernatants were collected after 72 h of incubation. Nitrite levels in supernatants of the co-cultures were compared to the respective 0 *L. rhamnosus* CFU/BMDC value within each group.
Bars represent means ± SEM of n = 5 BMDC donor mice for each genotype. Replicates are illustrated in symbols. Ordinary two-way ANOVA with Dunnett's multiple comparisons test was performed to obtain p values. Only p values < 0.05 are shown.

4 Discussion

4.1 Variance of the genome and antibiotic resistance of the *S. epidermidis* strains used

The different strains showed a certain basic variance in terms of genome and antibiotic resistance. The genomes of the different used *S. epidermidis* strains largely coincide in terms of the presence and absence of predicted genes. However, there are also many variable regions that appear to be partly specific to certain strains. This was true for strain 918, which was isolated from a patient with chronic infections, as well as the isolates from healthy subjects such as strain 912 or general clinical isolates (strains 614, 617, 618). Therefore, not only pathogenic strains carry specific variable gene clusters. Instead, all strains appear to differ essentially. Studies showed that this diversity of *S. epidermidis* strains not only develops between host individuals but also within a host. Different *S. epidermidis* strains have preferences for different skin regions and niches such as the foot environment. However, the heterogeneous composition of *S. epidermidis* strains could be positive for skin homeostasis, as the mixture of *S. epidermidis* strains inhibits the expression of virulence factors among the strains through quorum sensing and furthermore, it can prevent colonization by new strains (Kong and Oh 2022; Zhou et al. 2020).

Among the selected strains in our study, the two strains 614 and 617 were still relatively sensitive to antibiotics. The other three strains already carried multiple resistances and were only sensitive to a few antibiotics. The antibiotics that were still effective against the multi-resistant strains were mainly so-called reserve antibiotics such as fosfomycin and linezolid, which should be held back for emergencies (Zanichelli et al. 2023). Both strain 912, isolated from a healthy person, and strain 918, isolated from the blood of a patient suffering from chronic infections, showed a high rate of antibiotic resistance. Our results of the antibiogram are also consistent with those in the study by Chabi and Momtaz, where samples were collected from hospital infections. All identified *S. epidermidis* strains had at least three antibiotic resistances. Almost 17 % were even resistant to more than seven antibiotics. The fact that 46 % of these samples were positive for *S. epidermidis* also shows that the development of alternative treatment methods for infections with opportunistic commensals is of great importance (Chabi and Momtaz 2019). Lee and colleagues were able to show that the number of antibiotic resistances in *S. epidermidis* continues to increase and is even spreading globally (J. Y. H. Lee et al. 2018). The intraspecific and even interspecific exchange of genetic elements, such as the resistance genes, as can occur between *S. epidermidis* and the pathogen *S. aureus*, aggravates the situation even more (Méric et al. 2015; Su et al. 2020).

4.2 *S. epidermidis* induced the maturation and activity of BMDCs

The viability of immature BMDCs was not affected by incubation with *S. epidermidis*. Contact of relatively mature BMDCs with high concentrations of *S. epidermidis* slightly reduced viability, but lower concentrations did not. In general, *S. epidermidis* appears to have a rather activating effect on BMDCs, which is shown by the increased expression of markers such as CD86 and MHC class II after incubation with *S. epidermidis*. It is known from the literature that the increased expression of co-stimulatory molecules such as CD86 and antigen-presenting molecules such as MHC class II indicate maturation and activation of DCs (Xing et al. 2011; Dudek et al. 2013). It has also been shown that gram-positive bacteria can activate DCs. Saito and Quadery showed that *S. aureus* and its lipoproteins activate BMDCs and increase the expression of CD86 and MHC class II (Saito and Quadery 2018). Compared to *S. aureus*, there is less data on *S. epidermidis* treatment of DCs or BMDCs, but it has been shown in vitro and in vivo that *S. epidermidis* can activate DCs indicated by the upregulation of CD86, CD80 and MHC class II (Brescó et al. 2017). The described increase of these markers is consent with our observations for the incubation of BMDCs with *S. epidermidis*. Further, the comparison of *S. epidermidis* and *S. aureus* showed that they equally enhance the expression of maturation markers such as CD86 of DCs although if they are phagocytised differently well (Balraadjsing et al. 2020).

In our study, the secretion of the mainly pro-inflammatory acting cytokines IL-6, IL-12p40, CCL2, CXCL10 and TNFα was induced at lower concentrations of *S. epidermidis* than the secretion of the anti-inflammatory IL-10. Pro-inflammatory cytokines were already induced at 10 or 100 CFU/BMDC whereas IL-10 was only induced at 1000 CFU/BMDC. In addition, RNAseq analysis showed increased TPMs for genes encoding cytokines such as Il6, Cxcl10 and Tnf. The induction of pro-inflammatory cytokines is consistent with other studies. For example, the expression of IL-6 and TNFα was induced in moDCs that were incubated with *S. aureus* or *S. epidermidis* (Laborel-Préneron et al. 2015).
In the case of IL-10, however, there are contradictory data on the influence of *S. epidermidis* on its induction on DCs. Stimulated BMDCs release only small amounts whereas moDCs secrete large amounts of IL-10 after treatment with *S. epidermidis* (Brescó et al. 2017). According to our data, BMDCs did not express IL-10 when exposed to *S. epidermidis*, except at high concentrations.

Interestingly, a study by Saito et al. (2020) showed that LTA alone does not activate BMDCs. LTA is a cell wall component of all Gram-positive bacilli and a ligand for TLR2. On the contrary, it even suppresses LPS-induced secretion of TNFα as well as the activation of BMDCs, in the form of upregulation of CD86 and MHC class II. However, in this study they used LTA from *S. aureus*. In a previous study, they also found that this immunosuppressive mechanism of *S aureus*-derived LTA appears to be dose-dependent. Low doses suppressed inflammatory immune responses

whereas high doses reversed this suppression via the CLR (C-type lectin receptor) pathway (Saito, Lin, and Wu 2019; Saito et al. 2020). It is important to note that LTA from *S. epidermidis* and *S. aureus* partially differed in their stimulatory effect, as for example in an atopic dermatitis (AD) model. There, the secretion of IL-6 and IL-12p40 was induced by both LTAs, but more strongly by *S. aureus* LTA. The expression of IL-10 was similarly induced. Measured by the IL-10/IL-12p70 ratio, however, *S. epidermidis* LTA led to a more immunoregulatory phenotype while *S. aureus* LTA showed a pro-inflammatory effect. TNFα was induced equally by both LTAs, with higher doses leading to more TNFα (Volz et al. 2018).

Therefore, it cannot be generalised that *S. epidermidis* causes pro- or anti-inflammatory reactions in DCs. Rather this seems to depend on the context and also on the DC subtype concerned. Therefore, the effects of each model should be carefully considered in advance to avoid misguided interpretations. In our study, however, *S. epidermidis* had an activating effect on BMDCs, based on the analysed expression of surface markers such as CD86 and cytokines such as TNFα. This should allow BMDCs to present antigens and activate OT-I T cells in the co-culture system in an antigen-specific manner.

4.3 Inhibition of OT-I T cell proliferation is dependent on simultaneous incubation with BMDCs and *S. epidermidis*

In co-cultures of OT-I T cells and BMDCs, the incubation with *S. epidermidis* resulted in suppressed OT-I T cell proliferation. Normally, OT-I T cells are stimulated to proliferate upon presentation of OVA (or SIINFEKL) via MHC class I of BMDCs in this setting. Thus, *S. epidermidis* appears to be able to intervene in an antigen-specific immune response and to suppress it.

In literature reports, a proliferation-inducing effect of *S. epidermidis* on T cells is described. Many of the data focuses on the effect of *S. epidermidis* on CD4 T cells. In a study by Balraadjsing et al., DCs were pre-incubated with *S. epidermidis* for 48 h, washed and co-cultured with CD4 T cells. This induced moderate proliferation, of the CD4 T cells but not a suppression as seen in our experiments with OT-I T cells. However, *S. aureus*-stimulated DCs induced a strong proliferation of the CD4 T cells, but only if the *S. aureus* strain secreted super antigens. Otherwise, the proliferation level was similar to *S. epidermidis* stimulation (Balraadjsing et al. 2020). The authors suggested that such a boost in T cell proliferation as seen for *S. aureus* treatment is absent due to a lack of super antigens in *S. epidermidis* stimulations. However, BMDCs here already had a 48 h incubation with *S. epidermidis* before contact with the CD4 T cells. This is different to our study where *S. epidermidis* was present during the whole incubation period and BMDCs, OT-I T cells and *S. epidermidis* get in contact at the same time. Furthermore, the proliferation in Balraadjsing's experiments was specific to the bacterium itself and not to a second

antigen such as OVA as in our experiments (Balraadjsing et al. 2020). However, the setting used by Balraadjsing corresponds more to the uptake of a commensal antigen by APCs followed by migration into the lymph nodes in a physiological context. The *S. epidermidis*-exposed DCs then encounter T cells after a time delay, in example in the skin-draining lymph node. The experimental setting of simultaneous exposure used in our study, however, is expected to mimic the situation at the skin itself. Here, tissue-resident T_{RM} cells and APCs such as Langerhans cells or dDCs encounter commensals or their antigens relatively simultaneously. Similarly, in the case of a device-related infection with *S. epidermidis* or a bloodstream infection, simultaneous contact of APCs and T cells with *S. epidermidis* would be conceivable. Thus, two different physiological situations can be considered here.

In the intestine of mice, the presentation of commensal antigens by CD103+ DCs promoted a commensal antigen-specific proliferation of CD4+ as well as CD8+ T cells (Gehlhaar et al. 2022). A suppressed antigen-specific CD4 T cell response was demonstrated in relation to *S. aureus* by Lee et al. He observed that although the infection is combated, the establishment of an immune memory in the skin is prevented by *S. aureus*-derived α-toxin (B. Lee et al. 2020). Interestingly, high levels of *S. aureus* LTA can suppress T cell activation and proliferation in a TLR-2 independent mechanism. However, this is a reversible effect that is cancelled by the removal of LTA (Kaesler et al. 2016). The group of Volz et al. also detected an increased proliferation of OVA-specific CD4+ T cells when co-cultured with BMDCs that were primed with OVA and *S. epidermidis*-LTA simultaneously. However, they washed the BMDCs prior co-culture with CD4 T cells, thus no contact of T cells and *S. epidermidis* was possible (Volz et al. 2018). This could explain the different influence of *S. epidermidis* on T cell proliferation in their co-culture setting compared to our co-cultures.

Why proliferation is induced again at very high concentrations of *S. epidermidis*, from approximately 10000 CFU/BMDC in our data, is not known yet. One speculation is that this is a dose-dependent effect of *S. epidermidis* or one of its components or antigens on OT-I T cells or BMDCs. Such a dose-dependency was observed, for example by Saito et al., for the use of LTA of *S. aureus*. Low doses of LTA had an immunosuppressive effect on BMDCs and CD4 T cells by suppression of pro-inflammatory cytokines via TLR2 activation, whereas higher doses caused inflammation again and cancelled the suppression (Saito, Lin, and Wu 2019). In contrast to our study, they pulsed the BMDCs with OVA and LTA and therefore investigated the influence of LTA on BMDCs and their ability to induce T cell responses. Our data suggest a direct influence of *S. epidermidis* on OT-I T cells rather than BMDCs in the simultaneous presence of an antigen-specific stimulus by the BMDCs. However, such a dose-dependent effect of *S. epidermidis* or its antigens could also apply to T cells.

4.4 Direct influence of *S. epidermidis* on OT-I T cell proliferation only occurs in the presence of BMDCs

The use of different media controls showed that the presence of *S. epidermidis* itself in the co-cultures is necessary to suppress OT-I T cell proliferation. The clear suppression of OT-I T cell proliferation at 100 and 1000 CFU/BMDC *S. epidermidis* was only observed in co-cultures incubated with UV-attenuated *S. epidermidis*, but not by stimulation with equivalent volumes of media controls. On the one hand, this experiment ensured that the suppressive effect was not an artefact due to carry-over contamination in the production process of *S. epidermidis*. On the other hand, we showed that *S. epidermidis* itself and not parts of its secretome, consisting of expressed factors or metabolic products, is involved in the inhibition of OT-I T cell proliferation.

Another important observation in our experiments is that the proliferation of OT-I T cells could only be reduced by *S. epidermidis* in the presence of BMDCs. The addition of *S. epidermidis* to pure OT-I T cell cultures in which proliferation was induced by either anti-CD3/CD28 beads or the OVA peptide SIINFEKL did not affect proliferation. In both experiments, co-cultivation with BMDCs under otherwise constant conditions led to the collapse of OT-I T cell proliferation in a dose-dependent manner in *S. epidermidis*-treated conditions. A partially restored OVA-specific OT-I T cell proliferation due to the depletion of CD11c-DTR BMDCs in co-cultures after 24 h supports the assumption that BMDCs are crucial for the suppression of OT-I T cells. Consistent with our observations, literature reports that CD11c-BMDCs cannot be depleted by 100 %, may explaining, that there is still a slight reduction in OT-I T cell proliferation after incubation with *S. epidermidis* compared to the pure OVA stimulus (Dennis et al. 2002; Shaw and Starnbach 2006). In the experiments of our study, about 93 % of CD11c-DTR BMDCs could be depleted by DT administration. Maybe an earlier depletion could improve the restoration of the T cell proliferation, as we assume that BMDC-derived NO mediates the suppression (described below). With depletion after 24 hours, NO has very probably already been released, as in our kinetic experiment the expression of NO starts between 14 h and 24 h after stimulation. However, further NO secretion is prevented by depletion of BMDCs, meaning that depletion results in lower amounts of NO than in non-depleted co-cultures and thus in a weakened suppression of OT-I T cell proliferation.

4.5 Released cytokines rather than a *S. epidermidis*-altered BMDC phenotype are responsible for suppression of T cells

The transfer of untreated or heat-inactivated supernatants from *S. epidermidis*-treated co-cultures into new co-cultures, replacing *S. epidermidis*, brought up the suggestion that the suppressive effect is mediated by cytokines. Transfer of the supernatant from the 100 - 10000 *S. epidermidis* CFU/BMDC-treated co-cultures significantly reduced the OVA-specific OT-I T cell proliferation in the new co-culture. The presence of suppression together with the absence of *S. epidermidis* in the new co-culture strongly suggests the involvement of secreted factors, that are transferred along with the supernatant. Furthermore, the heat-inactivation of the supernatants before use in the co-cultures abolished their suppressive character. This suggests that cytokines mediate the inhibition of OT-I T cell proliferation, as they are proteins and proteins can be denatured by heat, resulting in a loss of function (J.-M. Zhang and An 2007; Kim et al. 2000).

The transfer of supernatants from pure BMDC or pure OT-I T cell cultures that were exposed to *S. epidermidis* for 72 h should show whether the source of a potential cytokine can be restricted to one of the two cell types. The transfer of the supernatant from *S. epidermidis*-treated BMDCs into a new co-culture slightly reduced the percentage of proliferating cells, but the absolute values were not affected, whereas the transfer of the supernatant from *S. epidermidis*-treated pure OT-I T cell cultures induced a decrease in OT-I T cell proliferation in the new co-cultures, both in counts and percentages. Supernatants from pure OT-I T cells incubated with higher concentrations of *S. epidermidis* thereby inhibited the proliferation of OT-I T cells in the new co-culture more strongly. In addition, the pattern of suppression with the OT-I T cell supernatants was more similar to the supernatants deriving from a *S. epidermidis*-treated co-culture. In summary, the suspicion was confirmed that a cytokine that is involved in the suppression of OVA-specific OT-I T cell proliferation has to be expressed by OT-I T cells themselves.

IFNγ and TNFα are among the typical cytokines produced by classical cytotoxic CD8 T cells (Tc1 subset). Moreover, memory Tc1 cells keep the ability to rapidly produce IFNγ after antigen reencounter. Other subtypes of CD8 T cells, such as Tc9, can also produce IFNγ (Koh et al. 2023). IFNγ can exert positive effects on CD8 T cells such as promotion of T cell migration, but it may also induce apoptosis and reduce proliferation (Bhat et al. 2017). TNFα is also known to activate CD8 T cells and promote proliferation as well as induce apoptosis (Mehta, Gracias, and Croft 2018; Bertrand et al. 2016). Therefore, we decided to investigate a possible involvement of these two cytokines in the suppression of the OVA-specific OT-I T cell proliferation by neutralizing them in the co-cultures through the addition of specific antibodies. That neutralization of IFNγ by antibodies restored OT-I T cell proliferation confirmed our assumption. This drew attention to IFNγ as a major cytokine involved in the suppression of OT-I T cell proliferation in the presence of *S. epidermidis* and BMDCs. Interestingly, the suppression was not only abrogated, but actually

improved, by the neutralisation of IFNγ. For the sake of completeness, neutralisation of TNFα did not mediate the OT-I T cell proliferation, compared to the control co-cultures.

The finding of slightly enhanced OT-I T cell proliferation is reminiscent of the data described above in which T cells were stimulated with *S. epidermidis* in the absence of BMDCs. A slight increase in proliferation was observed with certain amounts of *S. epidermidis*, too. In view of this data, one could conclude that BMDCs are also involved in the suppression of OT-I T cells in the context of IFNγ. Whether the BMDCs are the source or the target of IFNγ signalling and how IFNγ could contribute to suppression is discussed in more detail in the following section.

The fact that the addition of recombinant IFNγ to co-cultures of BMDCs, OT-I T and OVA attenuated OT-I T cell proliferation further demonstrated that IFNγ contributes to the suppression of OT-I T cells.

4.6 Identification of IFNγ-induced NO secretion by BMDCs as driver of *S. epidermidis*-mediated suppression of OT-I T cells

4.6.1 Increased IFNγ expression of memory OT-I T cells in the presence of *S. epidermidis*

By the use of neutralizing antibodies and rmIFNγ, we identified IFNγ as an essential cytokine that is involved in the suppression of OT-I T cells in co-cultures with BMDCs and *S. epidermidis*. That CD4+ as well as CD8+ T cells are a potential sources of IFNγ is widely known (Koh et al. 2023; Schoenborn and Wilson 2007). Myeloid cells are more likely to be the target of IFNγ while data on the ability of myeloid cells to produce IFNγ are contradictory (Bogdan and Schleicher 2006). Since there is the possibility that IFNγ could originate from BMDCs, we first looked for the cellular source of IFNγ. In the co-culture setting of our study, various experiments were used to exclude BMDCs as a source of IFNγ and to identify OT-I T cells as its origin. The use of IFNγ$^{-/-}$ BMDCs in the co-cultures showed no differences to the co-culture with WT BMDCs regarding the reduced proliferation of OT-I T cells after exposure to *S. epidermidis*. In addition, analysis of supernatants of co-cultures with WT BMDC and IFNγ$^{-/-}$ BMDC did not reveal any differences in the IFNγ levels between them. Thus, BMDCs could be excluded as source of sufficient amounts of IFNγ.

By exclusion procedure, only the OT-I T cells remain as a possible IFNγ source in our co-cultures. Stimulation of OT-I T cells with anti-CD3/CD28 beads induced the expression of IFNγ and thus confirmed the hypothesis. By separating naive (CD44- CD62L+) and memory (CD44+) OT-I T cells, the memory fraction could be identified as the main IFNγ-producing cell type in our co-cultures. Further, the use of the separated OT-I T cell fractions in the co-culture assay confirmed that memory OT-I T cells must be the source of IFNγ, indicated by the suppression of proliferation. In co-cultures with memory T cells, their proliferation was suppressed depending on the amount of *S. epidermidis* used, as was also the case in the control co-culture with unseparated OT-I T

cells. The capacity of memory OT-I T cells to be potent producers of IFNγ is shown already in literature (Koh et al. 2023). Moreover, skin resident memory CD8+ T cells were shown to produce IFNγ upon cognate antigen stimulation (Wu et al. 2018).
Our data suggest that the secretion of IFNγ is induced very early after contact with BMDCs and *S. epidermidis* in the co-cultures. Valid amounts of IFNγ were already measured after 6 h, suggesting that secretion must have started within the first 6 h of the co-culture.

4.6.2 Are OT-I T cells able to recognise *S. epidermidis*?

The combination of several observations brings up the interesting suggestion that OT-I T cells can recognise *S. epidermidis* and that the secretion of IFNγ is increased depending on the bacterial concentration. Firstly, in pure OT-I T cell cultures, the bead-induced secretion of IFNγ was dose-dependently increased by the presence of *S. epidermidis*. Thus, secretion of IFNγ was increased in OT-I T cells by the simultaneous activation of TCR and presence of *S. epidermidis*, particularly in the memory fraction. Secondly, different amounts of IFNγ were detected in the co-cultures depending on the amount of *S. epidermidis* used.

A reaction to bacteria is enabled by the recognition of PAMPs by PRRs. As already mentioned in the introduction, PRRs include various classes of receptors. The main groups include TLRs, RLRs, NLRs, CLRs and ALRs (Li and Wu 2021). The gram-positive bacterium *S. epidermidis* has various molecular structures that are categorised as PAMPs. LTA, PGN (peptidoglycan) and lipoproteins are common PAMPs among gram-positive bacteria that can activate TLR2. TLR1/2 heterodimers recognise triacyl lipopeptides whereas TLR2/6 heterodimers recognise diacyl lipopeptides and LTA (Otto 2009; Mogensen 2009). Small molecules and lipopeptides of *S. epidermidis* were also shown to influence innate immunity in a TLR3-dependent manner (Severn and Horswill 2022). In the case of PGN, however, it is still controversial whether it can really activate TLR2. However, it has been confirmed that PGN or its degraded fragments are recognized by cytosolic NLRs. This applies to NOD1, NOD2, NLRP1 and NLRP3 (Wolf and Underhill 2018). Further, muramyl dipeptide (MDP), a PGN-derivative can activate NOD2 and NLRP1. As a last example, TLR9 can bin bacterial CpG DNA (Mogensen 2009).

In order to be able to react to *S. epidermidis* themselves, we assume that OT-I T cells must express PRRs. Compared to myeloid cells such as DCs and BMDCs, the data on PRRs on T cells is relatively limited, but there is evidence for the expression in literature. For example, TLR1, TLR2 and TLR6 expression at mRNA and protein levels in mouse CD8 T cells. In human CD8 T cells, this is only the case for TLR2. In addition, there is also functional evidence of TLR2 expression in both murine and human CD8 T cells (Nouri, Weinkove, and Perret 2021). Own RNAseq data of OT-I T cells isolated from co-cultures after 72 h incubation showed that there is a possibility that OT-I T cells express PRRs such as NOD1, TLR1 and TLR 6 enabling them to sense *S. epidermidis*. This is in line with literature, where the expression of TLR1, TLR2 and TLR6 mRNA expression in naive CD8 T cells as well as activated cytotoxic CD8 T cells was

observed in B6 mice (Rahman, Taylor, and Turka 2009). However, the mere presence of RNA does not mean that a protein is ultimately synthesised, but Rahman et al. detected TLR2 protein by flow cytometry on the aforementioned CD8+ T cells. Further, TCR stimulation and activation of murine CD8 T cells could increase the expression of TLR2 (Rahman, Taylor, and Turka 2009). However, TLR2 needs to form heterodimers with TLR1 or TLR6 to enable ligand-specific recognition (Oliveira-Nascimento, Massari, and Wetzler 2012). Staining of the respective receptors or their stimulation by the use of agonists could provide definitive certainty about their expression on OT-I T cells in the case of our study. Very preliminary experiments have already been carried out by our group and are still ongoing. By these, it was possible to detect signals in the FACS for TLR1 and TLR2 on the OT-I T cells. Furthermore, the amount of IFNγ was increased by the simultaneous stimulation of OT-I T cells with anti-CD3/CD28 beads and the TLR2/6 agonist Pam2Csk4 compared to the sole bead stimulation. Caution is still required with the preliminary data in this experiments as the OT-I T cells were purified only via MACS. Therefore, the use of FACS sorted, very pure OT-I T cells is absolutely essential in the following experiments in order to exclude false signals due to contamination of myeloid cells. However, the results still need to be repeated in higher numbers of biological replicates to allow a reliable conclusion to be drawn. Nonetheless, these are promising preliminary data that would show that OT-I T cells can recognise *S. epidermidis* and respond with increased IFNγ production. This would also fit in very well with already known literature data. There are also findings in the literature that IFNγ expression in mouse Th1 and activated CD8+ T cells can be induced by activation of TLR2 (Imanishi and Saito 2020).

Our observations of varying immune responses, in example in the levels of released IFNγ, dependent on the different amounts of *S. epidermidis* may be explainable by findings in other studies, where different concentrations of LTA or PAMPs resulted in converse immune responses. Saito and colleagues observed that low dose LTA (*S. aureus*-derived) stimulation of BMDCs, with a dominant recognition of LTA via TLR2, did not result in pro-inflammatory cytokine production and suppressed the generation of effector T cells. In contrast, high dose LTA treatment overwrote the suppressive effect due to TLR2- induced upregulation of CLRs expression and TNFα induction (Saito, Lin, and Wu 2019). Interestingly, such a dose-dependent effect of LTA (*S. aureus*-derived) was the other way around in the priming of neutrophils. Here, low doses of LTA induced inflammatory responses, whereas high doses of LTA induced a tolerogenic phenotype in neutrophils, indicated by enhanced IL-10 expression and downregulation of pro-inflammatory cytokines (Lajqi et al. 2022). In another report, TLR2-expressing effector CD4+ T cell proliferation could be suppressed by LTA (*S. aureus*-derived) treatment. It must be noted that these effector CD4+ T cells originate from co-cultures with *S. aureus*-pulsed monocyte-derived DCs (Son 2013). In contrast, in our study OT-I T cells are simultaneously exposed to BMDCs, which mediate the TCR stimulus, and *S. epidermidis*, which can mediate the PRR stimulus. In addition, we did not use pre-activated cells when incubating OT-I T cells with TCR-stimulated

anti-CD3/CD28 beads and *S. epidermidis*. Whether LTA has a suppressive or activating effect seems to depend on the temporal context, the affected cell type and the bacterium from which LTA originates.

In our experiments, the stimulation of the TCR and potential PRRs of the OT-I T cells should occur synchronized or in a relatively overlapping time window, as all components were united simultaneously at the start of the co-cultures. The exposure to TCR as well as PRR stimuli acted synergistically and increased IFNγ production of OT-I T cells, dose-dependently of *S. epidermidis*, which is thought to stimulate PRRs. That PRRs, especially TLRs, are able to function as a co-stimulatory signal in CD8 T cells is already described. In human as well as murine CD8 T cells, co-stimulation via TLR2 or TLR3 in the presence of TCR signalling improved CD8+ T cell proliferation and cytokine production such as IFNγ. Further, TLR2 co-stimulation is suggested to have an influence in the maintenance and induction of CD8 memory T cell formation (Nouri, Weinkove, and Perret 2021). Interestingly, investigations by Cottalorda detected increased WT CD8 T cell proliferation using the TLR1/2 ligand Pam3CYSK4 and anti-CD3. This fits very well with our data that showed the increased IFNγ expression of OT-I T cells by simultaneous treatment with anti-CD3/CD28 beads and *S. epidermidis*. Cottalorda further showed that stimulation of CD8 T cells from F5 TCR-transgenic mice with NP68, which specifically activates this T cells, and co-stimulation with Pam3CYSK4 increased their proliferation. We also observed increased proliferation of OT-I T cells when incubated with SIINFEKL and *S. epidermidis*, albeit not significant. Similar to our studies, simultaneous stimulation of F5 TCR-transgenic CD8 T cells with NP68-pulsed DCs increased the amount of secreted IFNγ. In our co-cultures, IFNγ secretion from OT-I T cells was also increased by the addition of *S. epidermidis* in the presence of the antigen-specific OVA stimulus. Unfortunately, Cottalorda et al. did not show whether the proliferation of T cells in their co-cultures with BMDCs was affected after 72 h. They only showed that the number of IFNγ+ CD8 T cells was higher due to Pam3CYSK4 co-stimulation after 48 h (Cottalorda et al. 2009). This would have been an interesting comparison. Despite increased IFNγ production, we were able to detect reduced OT-I T cell proliferation. Further, exposure of CD8 T cells to *S. epidermidis* alone was not sufficient to induce IFNγ levels, supporting the assumption that synergistic signalling is necessary to induce a suppression of T cell proliferation via IFNγ and that a possible TLR2 engagement by *S. epidermidis* has a co-stimulatory effect on OT-I T cells.

The possibility that *S. epidermidis* directly inhibits OT-I T cell proliferation through PRR-induced signalling on the OT-I T cells naturally existed. However, several of our data clearly speak against this opportunity. For example, the addition of *S. epidermidis* to anti-CD3/CD28 bead-stimulated OT-I T cells did not negatively affect their proliferation. Therefore, it is also unlikely, that specific products of *S. epidermidis* directly impair OT-I T cells. As for example observed for alpha-toxin of *S. aureus,* that could inhibit CD8 T cell functions and even lead to their cell death (Blümel et al. 2020). Moreover, the observation that at very high concentrations of 10,000 CFU/BMDC

S. epidermidis proliferation is present again in most experiments compared to 100 or 1000 CFU/BMDC *S. epidermidis* speaks against a direct inhibition. Finally, the occurrence of OT-I T cell proliferation in co-cultures with BMDCs and stimulation by rmIFNγ in the absence of *S. epidermidis* suggests that on the one hand *S. epidermidis* does not directly inhibit the OT-I T cells and on the other hand that IFNγ mediates the suppression.
Of course there is the possibility of a TLR-independent mechanism. For example, Kaesler et al. showed that LTA (S. *aureus*-derived) can induce transient T_H2 cell paralysis in a TLR2-independent pathway and supress T cell proliferation by the induction of cell cycle arrest (Kaesler et al. 2016). In our study, this seems rather unlikely, because proliferation of OT-I T cells is present again at 10000 *S. epidermidis* CFU/BMDC treatment in our co-cultures.

All together, we suggest that elevated levels of OT-I T cell-derived IFNγ in response to synchronised TCR and PRR signalling mediate the reduction in OT-I T cell proliferation in a dose-dependent manner regarding *S. epidermidis*.

4.6.3 BMDCs as target of IFNγ and subsequent source of NO

Based on published data, two possibilities existed how the T cell-derived IFNγ could be involved in the suppression of OT-I T cell proliferation. The first opportunity is that IFNγ acts autocrine on the T cells. Suppressive effects in connection with IFNγ on different subtypes of T cells are suggested in literature (Bhat et al. 2017; Wood and Sawitzki 2006; De Araujo-Souza, Hanschke, and Viola 2015). The second opportunity is that IFNγ induces the suppression by affecting the BMDCs. There are some indications that the second option applies in our settings. As discussed above, several experiments showed that the presence of BMDCs is essential to observe a suppression of OT-I T cell proliferation in the context of *S. epidermidis* and IFNγ. In order to verify the responsible mode of action, co-cultures with WT-BMDCs and IFNγR$^{-/-}$ BMDCs were set up. Co-cultures consisted of OT-I T cell, OVA protein, ranging concentrations of *S. epidermidis* and one of the respective BMDC genotypes. This experiment clearly revealed that IFNγ must act on BMDCs to affect OT-I T cell proliferation. The measured amounts of IFNγ were relatively similar in the two co-cultures, regardless of the BMDC genotype present. Therefore, if OT-I T cells would have been directly affect by IFNγ a reduction in OT-I T cell proliferation would have been observed in both co-cultures irrespective of the used BMDC type. However, only the co-culture with WT BMDCs showed a suppressed OT-I T cell proliferation after the addition of *S. epidermidis*. No suppression was observed in the co-culture with IFNγR$^{-/-}$ BMDCs. Thus, BMDCs are the estimated target of IFNγ, which in turn means that further BMDC-derived components are required in the cascade of OT-I T cell suppression.

Based on literature search, we hypothesised that NO could be produced by BMDCs in response to IFNγ in our co-cultures, as already described for BMDCs by Lu et al. and in general by Aktan

et al. (Lu et al. 1996; Aktan 2004). It is known that NO can inhibit proliferation of T cells. In one study, DC-derived NO reduced proliferation of co-cultured T cells by inhibition of mitochondrial activity and attenuation of proliferation. Also mesenchymal stem-cell-derived NO suppressed CD4 and CD8 T cell proliferation (Thwe and Amiel 2018; Hoffman et al. 2002; Sato et al. 2007). To investigate the suspicion that IFNγ induced NO in BMDCs, we measured nitrite levels in supernatants of different co-cultures and OT-I T cell proliferation was analysed in co-cultures with iNOS$^{-/-}$ as well as Arg1$^{-/-}$ BMDCs. Nitrite is a product of NO oxidation and can be used to detect expression of the short-lived NO (Lundberg and Weitzberg 2022).

In co-cultures of OT-I T cells and BMDCs that were stimulated with rmIFNγ, nitrite levels were detected in dependency of the used rmIFNγ concentration. This indicated that NO is released as response to IFNγ. In the afore mentioned co-culture approach with WT, IFNγ$^{-/-}$ and IFNγR$^{-/-}$ BMDCs, nitrite levels were detected in WT BMDC and IFNγ$^{-/-}$ BMDC co-cultures but were hardly detectable in IFNγR$^{-/-}$ BMDC co-cultures. Together with the observed restored OT-I T cell proliferation in IFNγR$^{-/-}$ BMDC co-cultures and the fact that IFNγ was present in similar levels in all three co-cultures, this confirmed the presumption, that IFNγ-induced NO production by BMDCs is involved in the suppression of OT-I T cells. To support our findings, we analysed OT-I T cell proliferation and IFNγ as well as nitrite levels for co-cultures with iNOS$^{-/-}$ and Arg1$^{-/-}$ BMDCs. BMDCs that are deficient for iNOS are not able to produce NO due to iNOS induction. Arginase 1 is a more indirect part of the NO cycle, as it competes with iNOS for the common substrate L-arginine. Therefore, deficiency for Arg1 results in more substrate for iNOS. Besides the substrate competition, products of the Arg1 pathway is for example known to promote proliferation and repair functions of macrophages (Rath et al. 2014). We observed that OT-I T cell proliferation was suppressed in co-cultures with WT and Arg1$^{-/-}$ BMDCs in dependency of *S. epidermidis*, whereas in iNOS$^{-/-}$ BMDC co-cultures, OT-I T cell suppression was not reduced. However, IFNγ levels in supernatants of all three co-cultures were similar, excluding different IFNγ levels as a reason for differences in OT-I T cell proliferation. The detection of nitrite levels confirmed the iNOS deficiency in BMDCs and showed that NO originates from the BMDCs and is crucial in the mediation of OT-I T cell suppression.

We investigated the temporal resolution of IFNγ and NO expression by the performance of a kinetic experiment in which the supernatants from co-cultures containing OT-I T cells, BMDCs, *S. epidermidis* and OVA protein were analysed after specific incubation times. Here we could show that the expression of IFNγ took place relatively early after the start of incubation. This is in accordance with the above suggested induction of IFNγ by synergistic TCR and PRR signalling in T cells, as TCR stimulation via SIINFEKL-MHC class I complex and PRR stimulation via *S. epidermidis* can occur shortly after co-culture start. According to literature, BMDCs can take up and process OVA within minutes (Balneger et al. 2022). TCR stimulation was therefore possible shortly after the start of the co-culture. The early detection of IFNγ after approximately 6

h of OT-I T cell stimulation is consistent with the literature, where IFNγ was induced in antigen-experienced memory CD8 T cells by TLR2 stimulation and could already be detected after a few hours (Salerno et al. 2016). In the kinetic experiment we detected nitrite levels with a time delay to IFNy, which further supports the assumption that NO is induced by IFNγ.

In summary, memory OT-I T cell derived IFNγ was identified as inducer of NO release by BMDCs, which seems to be the last link in the chain of suppressed OT-I T cell proliferation. However, we planned experiments in which co-cultures as well as pure OT-I T cell cultures will be treated with a NO-donor in the absence of *S. epidermidis*, to investigate whether NO is for sure the effector molecule that affects OT-I T cells and their OVA-specific proliferation.

4.7 Possible effects of NO on OT-I T cells

Due to its known diverse effects on T cells, NO could actually be the responsible molecule that causes the suppression of OT-I T cells in our setting. Low NO levels due to eNOS and high NO levels due to iNOS usually result in different effects on T cells. For example, low concentrations of NO can prevent T cells from apoptosis by the S-nitrosylation of caspase 3, while high levels of NO can trigger activation-induced cell death through mechanisms such as the production of reactive oxygen and nitrogen species (García-Ortiz and Serrador 2018). Data from literature support the assumption that NO is the relevant molecule that ultimately mediated suppressed OT-I T cell proliferation in co-cultures of our study. Levels of NO in the micromolar range, as observed in our co-cultures, are suggested to induce oxidative and nitrosative stress for cells and are thought to favour apoptosis, senescence and cell cycle arrest (Wood and Sawitzki 2006; Napoli et al. 2013). Regarding the cell cycle arrest, NO can inhibit the G1/S transition, resulting in a G1 arrest, as shown in different cell types including T cells. This can be mediated via targeting of cell cycle proteins, mitogenic receptors and apoptosis factors (Napoli et al. 2013; Villalobo 2006). In other studies, NO was recognised to induce DNA damage and p53 activation in OT-I T cells in co-culture with DCs and MDSCs, resulting in T cell apoptosis. In addition, peroxynitrite, which can be formed by a reaction of NO and superoxide, was proposed to inhibit T cells by the nitrosylation of TCR and CD8 (Cartwright et al. 2021).

One possible explanation for the suppressed OT-I T cell proliferation, observed in our study, is that NO induced an exhaustion-like T cell state. In RNAseq analysis of OT-I T cells that were isolated from co-cultures after 72 h incubation, selected markers that are associated with exhaustion of T cells were upregulated in *S. epidermidis* treated conditions compared to the control condition with OVA only. Eomes, Tcf7, Foxo1 and Lag3 expression are some genes that are associated with exhaustion or dysfunctional CD8+ T cells (Jenkins et al. 2023; Z. Zhang et al. 2020). Cblb was shown to be upregulated in exhausted CD8+ T cells and its depletion reversed

exhaustion in CAR T cell experiments (Kumar et al. 2021; Gumber and Wang 2022). Last CD39, encoded by Entpd1, was identified in exhausted CD8+ T cells (Gupta et al. 2015). However, these are only selected genes from ongoing analyses of the RNAseq data. The data must still be analysed in depth in order to be able to make reliable and more concrete statements. Other mechanisms mediated by NO, as mentioned above, could be involved in the suppression of OT-I T cells in the co-culture setting as well.

4.8 An altered antigen presentation of BMDCs can be excluded as the cause of the suppressed OT-I T cell proliferation

An impaired or deteriorated forming of the immunological synapse and the antigen presentation could also be a reason for a reduced T cell proliferation. Weak TCR signalling can further be linked with T cell anergy or cell death (Shah et al. 2021). Our data from co-cultures consisting of OT-I T cells, BMDCs, anti-CD3/CD28 beads and *S. epidermidis* argue against the assumption that a change in antigen presentation by BMDCs is primarily responsible for the reduced OT-I T cell proliferation. In this experiment, anti-CD3/CD28 beads and not BMDCs induced the OT-I T cell proliferation because no OVA protein was present. Thus, antigen processing and presentation were not involved in induction of the OT-I T cell proliferation and their possible modulation would not result in effects on OT-I T cell proliferation. Nevertheless, in the presence of BMDCs, OT-I T cell proliferation was significantly reduced by the addition *S. epidermidis* compared to cultures without BMDCs. This clearly speaks in favour of the involvement of BMDCs in the suppression of OT-I T cells, but not in dependence on antigen processing and presentation. The observation that the induction of proliferation by beads was not as strong in co-cultures with BMDCs as in pure OT-I T cell cultures compared to the unstimulated condition could be explained by the phagocytation of beads by BMDCs. With the addition of *S. epidermidis*, the proliferation of OT-I T cells in the co-cultures even increases compared to the pure bead stimulus, which could be explained by the increased availability of beads, as BMDCs are now also phagocytised *S. epidermidis*.

Of course, an influence on antigen presentation by *S. epidermidis* cannot be completely ruled out. It is quite possible that several mechanisms are intertwined in the suppression of OT-I T cells. However, the observations strongly suggest that the suppression is primarily mediated by the secretion of IFNγ and subsequently NO in response to *S. epidermidis*.

4.9 Suppression of OT-I T cells by the induction of IFNγ and NO is not specific for *S. epidermidis*

The use of *L. rhamnosus* in certain experiments should shed light on whether the induction of IFNγ and NO is a specific mechanism of *S. epidermidis* to suppress antigen-specific OT-I T cell proliferation or whether it is a more conserved mechanism among gram-positive bacteria. *L. rhamnosus* is a gram-positive, anaerobic or facultative anaerobic bacterium and mainly colonises human genitourinary and gastro-intestinal tracts (Albarillo et al. 2020). Lactobacilli are also detected in the human skin microbiome, but are not among its most common representatives. However, it is assumed that they are already transmitted during birth and are thus among the first colonizers of neonatal skin (Lebeer et al. 2022; Fijan et al. 2019; Delanghe et al. 2021). This is therefore similar to *S. epidermidis* (Brescó et al. 2017). Lactobacilli have been studied as a probiotic treatment due to the ability to support the skin barrier and to modulate immunity. It is the most frequently used probiotic bacterium and among Lactobacilli, *L. rhamnosus* is one of the most investigated representatives (Gao et al. 2023; Lebeer et al. 2022; Xie et al. 2023). For *L. rhamnosus* GG it could be observed that it inhibits toxic effects of *S. aureus* on keratinocytes, promotes re-epithelialization and tight-junctions (Lebeer et al. 2022). In another study, *L. rhamnosus* HN001 was observed to reduce prevalence of atopic dermatitis (Xie et al. 2023).
In our study, the use of *L. rhamnosus* in co-cultures, in the IFNγ neutralisation experiment, or in co-cultures with IFNγR$^{-/-}$ BMDCs resulted in similar outcomes as previously observed with *S. epidermidis*. Also IFNγ and nitrite levels in supernatants from co-cultures with WT BMDCs or IFNγR$^{-/-}$ BMDCs showed that IFNγ as well as nitrite must be involved in the suppression of OT-I T cell proliferation after exposure to *L. rhamnosus*. The shift in the required CFU of *L. rhamnosus* compared to *S. epidermidis* to mediate the suppression of OT-I T cell proliferation may be due to the size difference between the two bacteria. *L. rhamnosus* is a rod shaped bacterium with a length of 2.0 – 4.0 and a width of 0.8 – 1.0 µm (Collins, Phillips, and Zanoni 1989). *S. epidermidis* has a spherical shape with a diameter of 0.5 to 1.0 µm and is hence smaller than *L. rhamnosus* (Schleifer and Kloos 1975). A CFU-dependent effect could be shifted due to the difference in size and therefore the concentration of a potential PAMP that enhances the secretion of IFNγ in OT-I T cells in a potential PRR-related manner. Thus, PAMPs could be present in higher amounts in *L. rhamnosus* than in *S. epidermidis* with the use of same CFUs due to the size difference.

The consistency of the results according to *L. rhamnosus* and *S. epidermidis* exposure suggests that the suppression of OT-I T cell proliferation due to IFNy and NO must be a more general mechanism that can be triggered by gram-positive bacteria. However, in order to narrow down the range of bacteria capable of inducing such immunosuppression, it is necessary to precisely identify the responsible PAMP and the cognate receptor. A more specific statement about the bacteria that are able to induce the suppression can then be made on the basis of the identified

PAMP, as some PAMPS are exclusive to gram-negative or gram-positive bacteria, while others are more widespread. In example, LTA and LPS are exclusive in gram-positive and gram-negative bacteria respectively, whereas PGN is present in both (Cavaillon 2017; Dickson and Lehmann 2019)

Results from very preliminary studies in our group indicate that PAMPS that bind to TLR2/6 could be involved in the suppression of OT-I T cell proliferation, as simultaneous stimulation of OT-I T cells with anti-CD3/CD28 beads and the synthetic lipopeptide Pam2CSK4 increased IFNγ expression compared to beads alone. TLR2/6 binds diacyl lipopeptides in general. Possible ligands for TLR2/6 are LTA and PGN (Li and Wu 2021; Oliveira-Nascimento, Massari, and Wetzler 2012). Soluble secreted components of bacteria, such as PSM of *S. epidermidis* are alternative ligands for TLR2/6 (Brescó et al. 2017). The fact that we observed OT-I T cell suppression in the presence of *S. epidermidis*, but not with media controls suggests that solid components of the bacteria such as LTA or PGN and not secreted components such as PSM enhance IFNγ production of OT-I T cells.
The identification of a responsible PAMP and the classification of bacteria that can trigger such a mechanism could be a complicated task. For example, although gram-positive bacteria have in common that they express LTA, such a PAMP can differ structurally and have different effects on immune responses. This is true between and within species. The comparison of LTA from four *Lactiplantibacillus plantarum* strains showed differences in its structure and also triggered different immune responses such as the amount of induced TNFα .The authors suggested that the different immune responses can be attributed to varying binding abilities due to structural differences of LTA (Jung, Kim, and Chung 2022). Similar findings were also observed in a study of two *Streptococcus pneumoniae* strains (Draing et al. 2006). Furthermore, differences were found in the suppressive effect of LTA on TLR3-induced immune responses depending on its structure and bacterial origin (Lai et al. 2009). Also the LTA derived from *S. aureus* and *S. epidermidis*, partially differed in the stimulation of DCs and subsequent CD4 T cell activation, as already described above (Volz et al. 2018).

4.10 Possible transfer of the suppression of OT-I T cells into a physiological context

After antigen uptake and processing, APCs can migrate into lymph nodes to prime antigen-specific T cells. These T cells then migrate to the target tissues and exert effector functions (Egawa and Kabashima 2011; Clark 2010). In this pathway, the activation of the T cells via TCR and a possible activation of PRRs by bacteria are normally decoupled. The constellation of co-cultures in our study lead to a relatively simultaneous activation of TCR and possible PRRs on

the OT-I T cells. Transferred to in vivo situations, this could be the case for example in the skin in general or after barrier disruption. In skin, LCs and CD8 T_{RM} cells are mainly located in the epidermis, the skin layer which is closest to the microbiome (Nestle et al. 2009; Kabashima et al. 2019; C. Zhang et al. 2022). Interaction of epidermal CD8 T cells is also enabled by the fact that bacteria not only reside on the surface of the epidermis, but bacterial products such as RNA, DNA and antigens were detected in the epidermis, dermis and hypodermis (Lunjani et al. 2021; Nakatsuji et al. 2013). It therefore seems quite conceivable that PAMPs from commensals bind to PRRs of CD8 T_{RM} cells while TCR and costimulatory signalling by APCs such as LCs takes place at the same time. Thus, the possibility of synchronous activation of the receptors is also given under physiological conditions. All the prerequisites for the induction of IFNγ and NO that involved in the hypothesis of the suppressive cascade in our study are present in the epidermis as well as the dermis. T cells, in particular T_{RM} cells, are capable of producing large amounts of IFNγ after stimulation (Koh et al. 2023; Wu et al. 2018). In memory CD4+ T cells and CD8+ T cells, the co-stimulation of TCR and TLRs could increase IFNγ production (Rahman, Taylor, and Turka 2009; Nouri, Weinkove, and Perret 2021). LCs and other dDCs, macrophages and keratinocytes are sources of NO (Lundberg and Weitzberg 2022; Coleman 2001; Xue et al. 2018; Moura et al. 2018; Sugita et al. 2010). Induction of NO production by IFNγ has also been demonstrated (Negishi, Taniguchi, and Yanai 2018; Lu et al. 1996). The suppression of the CD8+ T_{RM} cells as well as other T cells and immune cells that reside in the skin, which normally lead to rapid inflammatory responses after renewed antigen contact, could be assessed as positive from the point of view of both commensals and the host with regard to skin homeostasis. Such a suppressive mechanism would be advantageous for commensals to evade immune responses. However, the suppression of T cells could also be an unintended side effect due to NO release by immune cells as a response to infections. For example, the antimicrobial effects of NO can support the control of staphylococcal infections by mediating their virulence as shown by Urbano and colleagues (Urbano et al. 2018). From the host's point of view, however, a non-induced immune response towards commensals could be positive as it prevents chronic inflammation against skin commensals.

Nevertheless, suppression of immune cells in the skin can lead to problems barrier disruption or in the case of device-related infections. There, inhibition of immune responses in the skin can be a serious issue. However, it is also conceivable that such suppression mechanisms as observed in our study occur in skin-draining lymph nodes when specific PAMPs enter there. Studies showed that antigens can reach lymph nodes by diffusion via the lymph even without active transport by APCs, if they are present in sufficient concentration in the tissue and are smaller than 200 nm in diameter (Eisenbarth 2019). The suppression of T cells would allow the bacteria to spread unhindered and cause serious infections. A possible rescue mechanism depending on the bacterial concentration would be conceivable here. This may occur when PRR signalling exceeds a threshold value as seen for LTA, where low doses did not induce skin inflammation whereas

high doses did. Low doses showed a suppression in pro-inflammatory cytokine secretion and the high dose of LTA restored this effect (Saito, Lin, and Wu 2019). One could speculate that a kind of rescue mechanism is also present in our investigations. Lower concentrations of *S. epidermidis* in the range of 10 - 1000 CFU induced the suppressive effect in OT-I T cell proliferation, while proliferation was mostly restored at 10000 CFU. In addition, expression of pro-inflammatory cytokines and co-stimulatory molecules increased in BMDCs along with the concentration of *S. epidermidis*. This may allow to overwrite the suppressive effect of NO in OT-I T cells by enhanced co-stimulatory signalling or by inactivation of NO (Lundberg and Weitzberg 2022). Another hypothesis would be that the PRR signalling in OT-I T cells itself prevents the suppression in the T cells when the signal exceeds a certain threshold in a dose-dependent manner regarding *S. epidermidis*. The above already mentioned varying immune responses to different LTA concentrations are an example for this hypothesis (Saito, Lin, and Wu 2019). The experiments in which supernatants were transferred from a *S. epidermidis*-treated co-culture into a new co-culture (without *S. epidermidis*) could also indicate the presence of a PRR-dependent rescue mechanism. In the *S. epidermidis*-treated co-culture, proliferation was still restored at 10000 *S. epidermidis* CFU/BMDC*.* In the new co-culture, however, OT-I T cell proliferation was still strongly suppressed for the supernatant of this condition. That the responsible cytokines IFNγ and eventually also NO are transferred, but *S. epidermidis* is no longer present in the second culture could be an explanation for this. Thus, a strong activation of PRRs on OT-I T cells would not be possible any longer to induce a rescue mechanism. However, it seems unlikely that a feedback loop acts on IFNγ production and NO production to restore proliferation as the levels of cytokines were not very different between 10000 CFU//BMDC and e.g. 100 CFU/BMDC.

4.11 Current limitations and future direction

As far as such a modulation of the antigen-specific immune response of OT-I T cells is concerned, a number of questions still needs to be clarified in order to fully decipher the mechanism involved. The expression of a responsible PRR on OT-I T cells must be identified and its involvement must be confirmed. This can be determined via the specific activation and inhibition of the identified receptor using specific agonists and antagonists. The use of OT-I T cells with a corresponding deficiency for the receptor or subsequent signalling molecules such as MyD88$^{-/-}$ in the co-culture setting would also provide further information. It is important to identify the responsible PAMP that enhanced IFNγ expression by OT-I T cells. For proof of concept, an identified PAMP should then be tested separately for its suppressive capacity. Furthermore, knowing which ligand is involved would allow to narrow down which bacteria are capable of supressing T cells or immune responses in this context.

In fact, the identification of involved receptor-ligand pairs would allow modulating or exploiting the mechanism in order to utilise it for therapeutic approaches. This would be conceivable in the case of skin diseases or autoimmune diseases caused by misdirected T cell responses. CD4+ and CD8+ T cells are connected to T cell driven inflammatory skin diseases, such as psoriasis, atopic dermatitis and vitiligo, but also to cutaneous T-cell lymphoma. Often the unnatural activation of T_{RM}s cells causes the disease and the reprogramming of these T cells could help to cure or efficiently treat the diseases. In many cases, an altered microbiome also contributes to the development of the diseases or worsens them, as observed for increased *S. aureus* colonization. However, the specific function of T_{RM} cells seems to depend on the disease (Roediger and Schlapbach 2022; Kortekaas Krohn et al. 2022; Tokura et al. 2021). Suppression of T cell activity by administration of an identified ligand could help to improve the symptoms. It is assumed that tumors and their microenvironment can also be colonized by bacteria, viruses and fungi. *S. aureus* and *S. epidermidis* are assumed to be present in lung cancer, melanoma and breast cancer (Schorr et al. 2023). For example, *S. aureus* alpha toxin was shown to inhibit CD8 T cell cytotoxicity in cutaneous T cell lymphoma and thus favours tumor progression (Blümel et al. 2020). It is also assumed that memory T cells, including CD8+ T_{RM} cells, are necessary for a permanent immune response against tumors (Han et al. 2020). It is therefore quite conceivable that the simultaneous activation of TCR and PRR by bacteria in the vicinity of a tumor also leads to the suppression of T cell proliferation and as a consequence to tumor growth.

If such a suppressive mechanism induced by the IFNγ production of CD8 T cells is present in skin, its blockade could also help to fight infections with opportunistic bacteria locally such as device-related infections and thus could support medical treatments and the immune response itself.

4.12 Conclusion

This study investigated whether skin commensals, such as *S. epidermidis* are able to modulate antigen-specific immune responses of CD8 T cells. An antigen-specific proliferation of OT-I T cells, induced by the presentation of processed OVA via MHC class I by BMDCs, was suppressed in the presence of *S. epidermidis*. The proposed sequence of induction of OT-I T cell suppression is shown in Figure 58. The presence of *S. epidermidis* enhanced the expression of IFNγ by memory OT-I T cells in a dose-dependent manner. IFNγ in turn induced iNOS in BMDCs and thus the release of NO by BMDCs, which ultimately led to suppression of the OT-I T cell proliferation. The presented data clearly demonstrate that, BMDCs, OT-I T cells, *S. epidermidis* and the specific antigen OVA must be present at the same time to suppress the OT-I T cell proliferation. We assume that PAMPs of commensals can be recognised by PRRs of OT-I T cells. We further suggest that the suppression is initialised by a relatively simultaneous activation of TCR as well as co-stimulatory signals by BMDCs and PRR activation by *S. epidermidis* on memory OT-I T cells.

The described prerequisites for the initiation of T cell suppression in our co-cultures are present in a similar manner in the skin. In the epidermal and dermal region, antigen-presenting immune cells such as LCs and dDCs, CD8 T_{RM} cells capable of producing IFNγ, and bacteria or bacterial products are present. We therefore assume that the signalling cascade observed in this study can also take place in the skin.

Even if the initial receptor-ligand pair between T cells and bacteria still needs to be precisely identified, there is evidence to suggest the existence of the suppressive cascade. The cancellation of this suppressive mechanism could support the treatment of infections with resistant skin commensals. The induced inhibition of T cell proliferation in T cell-mediated skin diseases such as psoriasis and atopic dermatitis would be conceivable in order to treat them by exploiting this suppressive signalling cascade.

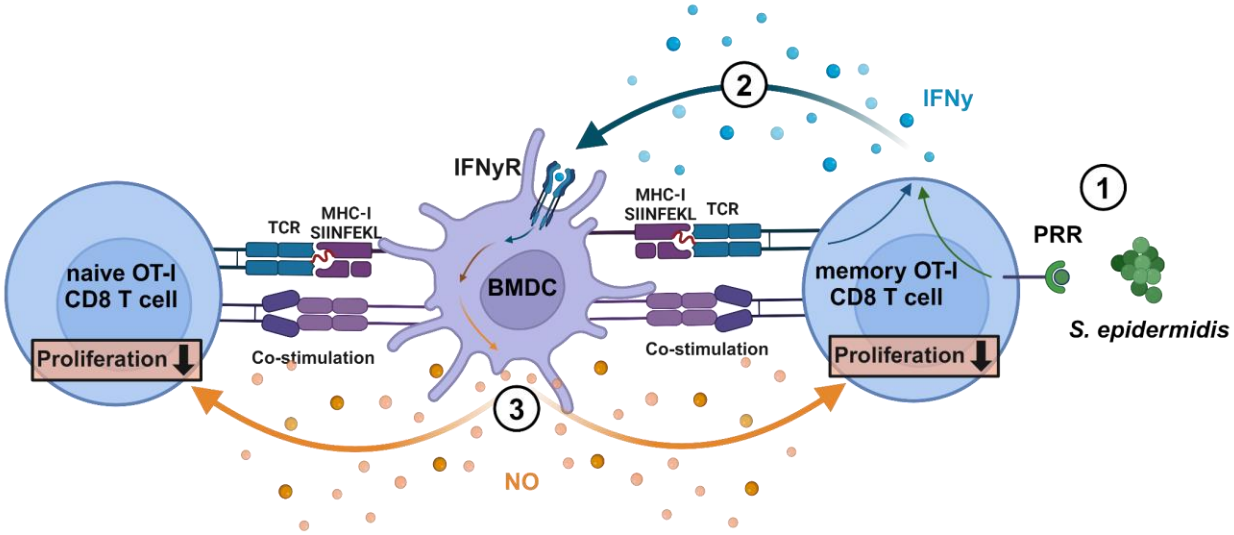

Figure 58: Graphical summary.

The figure illustrates the sequence of the suppressive mechanism identified in this thesis as acting on OT-I T cell proliferation. The co-culture setting of BMDCs, OVA protein, *S. epidermidis* and OT-I T cells consisting of the memory and naive population is shown. The OVA protein can be taken up and processed by BMDCs, resulting in the presentation of the OVA peptide sequence SIINFEKL via MHC class I. Presentation of the SIINFEKL MHC class I complex by BMDCs together with co-stimulatory signals induces OT-I T cell proliferation. In the first step, a relatively simultaneous stimulation of OT-I T cells by BMDCs and exposure to *S. epidermidis* leads to an increased release of IFNy by memory OT-IT cells. It is assumed that the memory OT-I T cells can recognize *S. epidermidis* via PRRs. In the second step, activation of the IFNγR on BMDCs by IFNγ induces iNOS, resulting in the production of NO. In the third step, the released NO has a suppressive effect on the OVA-specific proliferation of both memory and naive OT-I T cells. Created with BioRender.

Abbreviations

ACK-lysis buffer	Ammoniochloride-potassium-lysis buffer
ALR	Absent in melanoma-2-like receptor
AMP	Antimicrobial peptide
ANOVA	Analysis of variance
APC	Antigen-presenting cell
Arg1	Arginase 1
BMDC	Bone marrow-derived dendritic cell
BMDM	Bone marrow-derived macrophage
CCL	C-C motif chemokine ligand
CD	Cluster of differentiation
cDC	Conventional dendritic cell
cf.	Confer
CFSE	Carboxyfluorescein succinimidyl ester
CFU	Colony forming unit
CLR	C-type lectin receptor
CoNS	Coagulase-negative staphylococci
CTLA-4	Cytotoxic T lymphocyte-associated protein 4
CTV	Cell trace violet
DC	Dendritic cell
dDC	Dermal dendritic cell
DNA	Deoxyribonucleic acid
DT	Diphtheria toxin
DTR	Diphtheria toxin receptor
eNOS	Endothelia nitric oxide synthase
FACS	Fluorescence activated cell sorting
FCS	Fetal calf serum
GM-CSF	Granulocyte-macrophage colony-stimulating factor
HSV	Herpes simplex virus
HTS	High Throughput Sampler
ICOS	Inducible T cell co-stimulator
IFN	Interferon
IFNγ	Interferon gamma
IFNγR	Interferon gamma receptor
IL	Interleukin
ILC	Innate lymphoid cell

IMHR	Institute of Clinical Microbiology and Hygiene at the University Hospital Regensburg
iNOS	Inducible nitric oxide synthase
IRF	IFN regulatory factor
iSALT	Inducible skin-associated lymphoid tissue
JAK	Janus kinase
KO	Knockout
L. rhamnosus	*Lactobacillus rhamnosus*
LB	Lysogeny broth
LC	Langerhans cell
LPS	Lipopolysaccharide
LTA	Lipoteichoic acid
MACS	Magnetic cell separation
MFI	Median fluorescence intensity
MHC	Major histocompatibility complex
moDC	Monocyte-derived dendritic cell
MyD88	Myeloid differentiation primary response 88
NaCl	Sodium chloride
NLR	Nod-like receptor
nNOS	Neuronal nitric oxide synthase
NO	Nitric oxide
OD	Optical density
OVA	Ovalbumin
PAMP	Pathogen-associated molecular pattern
PBS	Dulbeccos's phosphate-buffered saline
pDC	Plasmacytoid dendritic cell
PGN	Peptidoglycan
PRR	Pattern recognition receptor
PSM	Phenol-soluble modulin
RLR	RIG-I-like receptor
RLT	RNA lysis buffer
rmGM-CSF	Recombinant murine granulocyte-macrophage colony-stimulating factor
RNA	Ribonucleic acid
RNAseq	Ribonucleic acid sequencing
RPMI	Roswell park memorial institute
RT	Room temperature
S. aureus	*Staphylococcus aureus*

S. epidermidis	*Staphylococcus epidermidis*
SALT	Skin associated lymphoid tissue
SEM	Standard error of the mean
SN	Supernatant
SPF	Specific pathogen-free
STAT	Signal transducers and activators of transcription
TCR	T cell receptor
T_H cell	T helper cell
TIP DC	Tumor necrosis factor and inducible nitric oxide synthase producing dendritic cell
TLR	Toll-like receptor
TNF	Tumor necrosis factor
T_{reg} cell	Regulatory T cell
TRIF	TIR domain-containing adaptor protein inducing interferon beta
T_{RM} cell	Resident memory T cell
TSB	Tryptic soy broth
UV	Ultraviolet
WT	Wild type
WTA	Wall teichoic acid

List of figures

List of tables

References

Abdallah, Florence, Lily Mijouin, and Chantal Pichon, 2017, “Skin Immune Landscape: Inside and Outside the Organism,” Mediators Inflamm. **2017**.

Aktan, Fugen, 2004, “INOS-Mediated Nitric Oxide Production and Its Regulation,” Life Sci. **75**, 639–653.

Albarillo, Fritzie, Ushma Shah, Cara Joyce, and David Slade, 2020, “Lactobacillus Rhamnosus Infection: A Single-Center 4-Year Descriptive Analysis,” J. Glob. Infect. Dis. **12**, 119–123.

Alliliche, Wael, Christine Renaud, Jean Michel Cros, and Zhi Qiang Feng, 2023, “Numerical Simulation of Mechanical Tests on a Living Skin Using Anisotropic Hyperelastic Law,” J. Mech. Behav. Biomed. Mater. (Elsevier Ltd) **141**, 105755, https://doi.org/10.1016/j.jmbbm.2023.105755.

Alloatti, Andrés, Fiorella Kotsias, Joao Gamelas Magalhaes, and Sebastian Amigorena, 2016, “Dendritic Cell Maturation and Cross-Presentation: Timing Matters!,” Immunol. Rev. **272**, 97–108.

Annunziato, Francesco, Chiara Romagnani, and Sergio Romagnani, 2015, “The 3 Major Types of Innate and Adaptive Cell-Mediated Effector Immunity,” J. Allergy Clin. Immunol. (Elsevier Ltd) **135**, 626–635, http://dx.doi.org/10.1016/j.jaci.2014.11.001.

Bäckhed, Fredrik, Josefine Roswall, Yangqing Peng, Qiang Feng, Huijue Jia, Petia Kovatcheva-Datchary, Yin Li, et al., 2015, “Dynamics and Stabilization of the Human Gut Microbiome during the First Year of Life,” Cell Host Microbe **17**, 690–703.

Balneger, N., L. A.M. Cornelissen, M. Wassink, S. J. Moons, T. J. Boltje, Y. E. Bar-Ephraim, K. K. Das, J. N. Søndergaard, C. Büll, and G. J. Adema, 2022, “Sialic Acid Blockade in Dendritic Cells Enhances CD8+ T Cell Responses by Facilitating High-Avidity Interactions,” Cell. Mol. Life Sci. (Springer International Publishing) **79**, 1–15, https://doi.org/10.1007/s00018-021-04027-x.

Balraadjsing, Payal P., Esther C. de Jong, Willem J.B. van Wamel, and Sebastian A.J. Zaat, 2020, “Dendritic Cells Internalize Staphylococcus Aureus More Efficiently than Staphylococcus Epidermidis, but Do Not Differ in Induction of Antigen-Specific t Cell Proliferation,” Microorganisms **8**.

Baroni, Adone, Elisabetta Buommino, Vincenza De Gregorio, Eleonora Ruocco, Vincenzo Ruocco, and Ronni Wolf, 2012, “Structure and Function of the Epidermis Related to Barrier Properties,” Clin. Dermatol. (Elsevier B.V.) **30**, 257–262, http://dx.doi.org/10.1016/j.clindermatol.2011.08.007.

Battaglia, Michael, and Lee Ann Garrett-Sinha, 2023, “Staphylococcus Xylosus and Staphylococcus Aureus as Commensals and Pathogens on Murine Skin,” Lab. Anim. Res. **39**, 1–13.

Bedoui, Sammy, Paul G. Whitney, Jason Waithman, Liv Eidsmo, Linda Wakim, Irina Caminschi, Rhys S. Allan, et al., 2009, “Cross-Presentation of Viral and Self Antigens by Skin-Derived CD103+ Dendritic Cells,” Nat. Immunol. **10**, 488–495.

Belheouane, Meriem, Marie Vallier, Aleksa Čepić, Cecilia J. Chung, Saleh Ibrahim, and John F. Baines, 2020, “Assessing Similarities and Disparities in the Skin Microbiota between Wild and Laboratory Populations of House Mice,” ISME J.

Belkaid, Yasmine, and Oliver J. Harrison, 2017, “Homeostatic Immunity and the Microbiota,” Immunity (Elsevier Inc.) **46**, 562–576, http://dx.doi.org/10.1016/j.immuni.2017.04.008.

Belkaid, Yasmine, and Julia A. Segre, 2014, “Dialogue between Skin Microbiota and Immunity,” Science (80-.). **346**, 954–959.

Belkaid, Yasmine, and Samira Tamoutounour, 2016, “The Influence of Skin Microorganisms on Cutaneous Immunity,” Nat. Rev. Immunol. (Nature Publishing Group) **16**, 353–366.

Bertrand, Florie, Julia Rochotte, Céline Colacios, Anne Montfort, Nathalie Andrieu-Abadie, Thierry Levade, Hervé Benoist, and Bruno Ségui, 2016, “Targeting TNF Alpha as a Novel Strategy to Enhance CD8+ T Cell-Dependent Immune Response in Melanoma?,” Oncoimmunology **5**, 8–10.

Bhat, Purnima, Graham Leggatt, Nigel Waterhouse, and Ian H. Frazer, 2017, “Interferon-γ Derived from Cytotoxic Lymphocytes Directly Enhances Their Motility and Cytotoxicity,” Cell Death Dis. (Nature Publishing Group) **8**, 1–11, http://dx.doi.org/10.1038/cddis.2017.67.

Biosciences, Bd, 2009, “An Introduction to Compensation for Multicolor Assays on Digital Flow Cytometers,” BD Biosci. Tech. Bull., 1–12.

Bitschar, Katharina, Birgit Sauer, Jule Focken, Hanna Dehmer, Sonja Moos, Martin Konnerth, Nadine A. Schilling, et al., 2019, “Lugdunin Amplifies Innate Immune Responses in the Skin in Synergy with Host- and Microbiota-Derived Factors,” Nat. Commun. (Springer US) **10**, http://dx.doi.org/10.1038/s41467-019-10646-7.

Blümel, Edda, Shamaila Munir Ahmad, Claudia Nastasi, Andreas Willerslev-Olsen, Maria Gluud, Simon Fredholm, Tengpeng Hu, et al., 2020, "Staphylococcus Aureus Alpha-Toxin Inhibits CD8+ T Cell-Mediated Killing of Cancer Cells in Cutaneous T-Cell Lymphoma," Oncoimmunology (Taylor & Francis) **9**, https://doi.org/10.1080/2162402X.2020.1751561.

Bogdan, Christian, 2001, "Nitric Oxide and the Immune Response NO Production in the Immune System," Nat. Immunol. **2**, 907–916, http://immunol.nature.xn--com-up0a.

Bogdan, Christian, 2015, "Nitric Oxide Synthase in Innate and Adaptive Immunity: An Update," Trends Immunol. (Elsevier Ltd) **36**, 161–178, http://dx.doi.org/10.1016/j.it.2015.01.003.

Bogdan, Christian, and Ulrike Schleicher, 2006, "Production of Interferon-γ by Myeloid Cells - Fact or Fancy?," Trends Immunol. **27**, 282–290.

Bomar, Lindsey, Silvio D. Brugger, Brian H. Yost, Sean S. Davies, and Katherine P. Lemon, 2016, "Corynebacterium Accolens Releases Antipneumococcal Free Fatty Acids from Human Nostril and Skin Surface Triacylglycerols," MBio **7**.

Brescó, Marina Sabaté, Llinos G. Harris, Keith Thompson, Barbara Stanic, Mario Morgenstern, Liam O'Mahony, R. Geoff Richards, and T. Fintan Moriarty, 2017, "Pathogenic Mechanisms and Host Interactions in Staphylococcus Epidermidis Device-Related Infection," Front. Microbiol. **8**.

Brewig, Nancy, Adrien Kissenpfennig, Bernard Malissen, Alexandra Veit, Thomas Bickert, Bernhard Fleischer, Sven Mostbo, and Uwe Ritter, 2013, "Leishmaniasis Is Initiated by Different Dendritic Cell."

Cartwright, Adam N.R., Shengbao Suo, Soumya Badrinath, Sushil Kumar, Johannes Melms, Adrienne Luoma, Archis Bagati, et al., 2021, "Immunosuppressive Myeloid Cells Induce Nitric Oxide–Dependent DNA Damage and P53 Pathway Activation in CD8+ T Cells," Cancer Immunol. Res. **9**, 470–485, https://aacrjournals.org/cancerimmunolres/article/9/4/470/666156/Immunosuppressive-Myeloid-Cells-Induce-Nitric.

Cavaillon, Jean-Marc, 2017, "Pathogen-Associated Molecular Patterns," in *Inflammation - From Molecular and Cellular Mechanisms to the Clinic* (Wiley-VCH Verlag GmbH & Co. KGaA, Weinheim, Germany), pp. 17–56, https://onlinelibrary.wiley.com/doi/10.1002/9783527692156.ch2.

Chabi, Roya, and Hassan Momtaz, 2019, "Virulence Factors and Antibiotic Resistance Properties of the Staphylococcus Epidermidis Strains Isolated from Hospital Infections in Ahvaz, Iran," Trop. Med. Health (Tropical Medicine and Health) **47**, 1–9.

Chaplin, David D., 2010, "Overview of the Immune Response," J. Allergy Clin. Immunol. (Elsevier Ltd) **125**, S3–S23, http://dx.doi.org/10.1016/j.jaci.2009.12.980.

Cheung, Gordon Y.C., and Michael Otto, 2010, "Understanding the Significance of Staphylococcus Epidermidis Bacteremia in Babies and Children," Curr. Opin. Infect. Dis. **23**, 208–216.

Clark, Rachael A., 2010, "Skin-Resident T Cells: The Ups and Downs of On Site Immunity," J. Invest. Dermatol. (Elsevier Masson SAS) **130**, 362–370, http://dx.doi.org/10.1038/jid.2009.247.

Coates, Margaret, Sarah Blanchard, and Amanda S. MacLeod, 2018, "Innate Antimicrobial Immunity in the Skin: A Protective Barrier against Bacteria, Viruses, and Fungi," PLoS Pathog. **14**, 1–7.

Coates, Margaret, Min Jin Lee, Diana Norton, and Amanda S. MacLeod, 2019, "The Skin and Intestinal Microbiota and Their Specific Innate Immune Systems," Front. Immunol. **10**, 1–11.

Cogen, Anna L., Kenshi Yamasaki, Katheryn M. Sanchez, Robert A. Dorschner, Yuping Lai, Daniel T. MacLeod, Justin W. Torpey, et al., 2010, "Selective Antimicrobial Action Is Provided by Phenol-Soluble Modulins Derived from Staphylococcus Epidermidis, a Normal Resident of the Skin," J. Invest. Dermatol. (Elsevier Masson SAS) **130**, 192–200, http://dx.doi.org/10.1038/jid.2009.243.

Coleman, John W., 2001, "Nitric Oxide in Immunity and Inflammation," Int. Immunopharmacol. **1**, 1397–1406.

Coligan, John E., and Stefanie N. Vogel, 2008, "Innate Immunity," Curr. Protoc. Immunol., 57–64.

Collins, M.D. Matthew D, B.A. Brian A Phillips, and Paolo Zanoni, 1989, "Deoxyribonucleic Acid Homology Studies of Lactobacillus Casei ," Int. J. Syst. Bacteriol. **39**, 105–108.

Conlan, Sean, Lilia A. Mijares, Jesse Becker, Robert W. Blakesley, Gerard G. Bouffard, Shelise Brooks, Holly Coleman, et al., 2012, "Staphylococcus Epidermidis Pan-Genome Sequence Analysis Reveals Diversity of Skin Commensal and Hospital Infection-Associated Isolates," Genome Biol. **13**.

Cottalorda, Anne, Blandine C. Mercier, Florentin M. Mbitikon-Kobo, Christophe Arpin, Denise Y.L. Teoh, Andrew McMichael, Jacqueline Marvel, and Nathalie Bonnefoy-Bérard, 2009, "TLR2 Engagement on Memory CD8+ T Cells Improves Their Cytokine-Mediated Proliferation and IFN-γ Secretion in the Absence of Ag," Eur. J. Immunol. **39**, 2673–2681.

Cox, Maureen A., Laurie E. Harrington, and Allan J. Zajac, 2011, “Cytokines and the Inception of CD8 T Cell Responses,” Trends Immunol. **32**, 180–186, https://www.ncbi.nlm.nih.gov/pmc/articles/PMC3624763/pdf/nihms412728.pdf.

Datta, Sandip K., Vanessa Redecke, Kiley R. Prilliman, Kenji Takabayashi, Maripat Corr, Thomas Tallant, Joseph DiDonato, et al., 2003, “A Subset of Toll-Like Receptor Ligands Induces Cross-Presentation by Bone Marrow-Derived Dendritic Cells,” J. Immunol. **170**, 4102–4110.

De Araujo-Souza, Patrícia S., Steffi C.H. Hanschke, and Joaõ P.B. Viola, 2015, “Epigenetic Control of Interferon-Gamma Expression in CD8 T Cells,” J. Immunol. Res. **2015**.

Del Rio, Maria Luisa, Günter Bernhardt, Jose Ignacio Rodriguez-Barbosa, and Reinhold Förster, 2010, “Development and Functional Specialization of CD103+ Dendritic Cells,” Immunol. Rev. **234**, 268–281.

Delanghe, Lize, Irina Spacova, Joke Van Malderen, Eline Oerlemans, Ingmar Claes, and Sarah Lebeer, 2021, “The Role of Lactobacilli in Inhibiting Skin Pathogens,” Biochem. Soc. Trans. **49**, 617–627.

Dennis, Megan K, Angela S Field, Ritwik Burai, Chinnasamy Ramesh, K Whitney, Cristian G Bologa, Tudor I Oprea, et al., 2002, “In Vivo Depletion of CD11c+ Dendritic Cells Abrogates Priming of CD8+ T Cells by Exogenous Cell-Associated Antigens,” Immunity **17**, 221–220.

Dickson, Kayle, and Christian Lehmann, 2019, “Inflammatory Response to Different Toxins in Experimental Sepsis Models,” Int. J. Mol. Sci. **20**.

Ding, Huihui, Gongfu Wang, Zhen Yu, Huimin Sun, and Lu Wang, 2022, “Role of Interferon-Gamma (IFN-γ) and IFN-γ Receptor 1/2 (IFNγR1/2) in Regulation of Immunity, Infection, and Cancer Development: IFN-γ-Dependent or Independent Pathway,” Biomed. Pharmacother. (Elsevier Masson SAS) **155**, 113683, https://doi.org/10.1016/j.biopha.2022.113683.

Donlan, Rodney M., and J. William Costerton, 2002, “Biofilms: Survival Mechanisms of Clinically Relevant Microorganisms,” Clin. Microbiol. Rev. **15**, 167–193.

Draing, Christian, Markus Pfitzenmaier, Sebastiana Zummo, Giuseppe Mancuso, Armin Geyer, Thomas Hartung, and Sonja Von Aulock, 2006, “Comparison of Lipoteichoic Acid from Different Serotypes of Streptococcus Pneumoniae,” J. Biol. Chem. (Â© 2006 ASBMB. Currently published by Elsevier Inc; originally published by American Society for Biochemistry and Molecular Biology.) **281**, 33849–33859, http://dx.doi.org/10.1074/jbc.M602676200.

Dréno, B., E. Araviiskaia, E. Berardesca, G. Gontijo, M. Sanchez Viera, L. F. Xiang, R. Martin, and T. Bieber, 2016, “Microbiome in Healthy Skin, Update for Dermatologists,” J. Eur. Acad. Dermatology Venereol. **30**, 2038–2047.

Dress, Regine J., Alicia Y.W. Wong, and Florent Ginhoux, 2018, “Homeostatic Control of Dendritic Cell Numbers and Differentiation,” Immunol. Cell Biol. **96**, 463–476.

Du, Xin, Jesper Larsen, Min Li, Axel Walter, Christoph Slavetinsky, Anna Both, Patricia M. Sanchez Carballo, et al., 2021, “Staphylococcus Epidermidis Clones Express Staphylococcus Aureus-Type Wall Teichoic Acid to Shift from a Commensal to Pathogen Lifestyle,” Nat. Microbiol. (Springer US) **6**, 757–768, http://dx.doi.org/10.1038/s41564-021-00913-z.

Duan, Tianhao, Yang Du, Changsheng Xing, Helen Y. Wang, and Rong Fu Wang, 2022, “Toll-Like Receptor Signaling and Its Role in Cell-Mediated Immunity,” Front. Immunol. **13**, 1–22.

Dudek, Aleksandra M., Shaun Martin, Abhishek D. Garg, and Patrizia Agostinis, 2013, “Immature, Semi-Mature, and Fully Mature Dendritic Cells: Toward a DC-Cancer Cells Interface That Augments Anticancer Immunity,” Front. Immunol. **4**, 1–14.

Egawa, Gyohei, and Kenji Kabashima, 2011, “Skin as a Peripheral Lymphoid Organ: Revisiting the Concept of Skin-Associated Lymphoid Tissues,” J. Invest. Dermatol. (Elsevier Masson SAS) **131**, 2178–2185, http://dx.doi.org/10.1038/jid.2011.198.

Egawa, Gyohei, and Kenji Kabashima, 2016, “Multifactorial Skin Barrier Deficiency and Atopic Dermatitis: Essential Topics to Prevent the Atopic March,” J. Allergy Clin. Immunol. (Elsevier Inc.) **138**, 350-358.e1, http://dx.doi.org/10.1016/j.jaci.2016.06.002.

Eisenbarth, S. C., 2019, “Dendritic Cell Subsets in T Cell Programming: Location Dictates Function,” Nat. Rev. Immunol. (Springer US) **19**, 89–103, http://dx.doi.org/10.1038/s41577-018-0088-1.

Erin Chen, Y., Michael A. Fischbach, and Yasmine Belkaid, 2018, “Skin Microbiota-Host Interactions,” Nature (Nature Publishing Group) **553**, 427–436.

Eyerich, Stefanie, Kilian Eyerich, Claudia Traidl-Hoffmann, and Tilo Biedermann, 2018, “Cutaneous Barriers and Skin Immunity: Differentiating A Connected Network,” Trends Immunol. (Elsevier Ltd) **39**, 315–327, http://dx.doi.org/10.1016/j.it.2018.02.004.

Fijan, Sabina, Anita Frauwallner, Tomaž Langerholc, Bojan Krebs, Jessica A. Ter Haar, Adolf Heschl, Dušanka Mičetić Turk, and Irena Rogelj, 2019, “Efficacy of Using Probiotics with Antagonistic Activity against Pathogens of Wound Infections: An Integrative Review of Literature,” Biomed Res. Int. **2019**.

Foster, Timothy J., 2020, “Surface Proteins of Staphylococcus Epidermidis,” Front. Microbiol. **11**.

Gallo, Richard L., 2017, “Human Skin Is the Largest Epithelial Surface for Interaction with Microbes,” J. Invest. Dermatol. **137**, 1213–1214.

Gao, Ting, Xiaoyu Wang, Yixuan Li, and Fazheng Ren, 2023, “The Role of Probiotics in Skin Health and Related Gut–Skin Axis: A Review,” Nutrients **15**.

García-Ortiz, Almudena, and Juan M. Serrador, 2018, “Nitric Oxide Signaling in T Cell-Mediated Immunity,” Trends Mol. Med. **24**, 412–427.

Gebhardt, Thomas, Paul G. Whitney, Ali Zaid, Laura K. MacKay, Andrew G. Brooks, William R. Heath, Francis R. Carbone, and Scott N. Mueller, 2011, “Different Patterns of Peripheral Migration by Memory CD4+ and CD8+ T Cells,” Nature (Nature Publishing Group) **477**, 216–219.

Gehlhaar, Arne, Ashwin Inala, Dhana Llivichuzhca-Loja, Tatiana N. Silva, Comfort Y. Adegboye, Amy E. O’connell, and Liza Konnikova, 2022, “Insights into the Role of Commensal-Specific T Cells in Intestinal Inflammation,” J. Inflamm. Res. **15**, 1873–1887.

Gill, Steven R., Derrick E. Fouts, Gordon L. Archer, Emmanuel F. Mongodin, Robert T. DeBoy, Jacques Ravel, Ian T. Paulsen, et al., 2005, “Insights on Evolution of Virulence and Resistance from the Complete Genome Analysis of an Early Methicillin-Resistant Staphylococcus Aureus Strain and a Biofilm-Producing Methicillin-Resistant Staphylococcus Epidermidis Strain,” J. Bacteriol. **187**, 2426–2438.

Grice, Elizabeth A., Heidi H. Kong, Sean Conlan, Clayton B. Deming, Joie Davis, Alice C. Young, Gerard G. Bouffard, et al., 2009, “Topographical and Temporal Diversity of the Human Skin Microbiome,” Science (80-.). **324**, 1190–1192.

Grice, Elizabeth A., and Julia A. Segre, 2011, “The Skin Microbiome,” Nat. Rev. Microbiol. **9**, 244–253.

Guilliams, Martin, Charles Antoine Dutertre, Charlotte L. Scott, Naomi McGovern, Dorine Sichien, Svetoslav Chakarov, Sofie Van Gassen, et al., 2016, “Unsupervised High-Dimensional Analysis Aligns Dendritic Cells across Tissues and Species,” Immunity **45**, 669–684.

Gumber, Diana, and Leo D. Wang, 2022, “Improving CAR-T Immunotherapy: Overcoming the Challenges of T Cell Exhaustion,” eBioMedicine (Elsevier B.V.) **77**, 103941, https://doi.org/10.1016/j.ebiom.2022.103941.

Gupta, Prakash K., Jernej Godec, David Wolski, Emily Adland, Kathleen Yates, Kristen E. Pauken, Cormac Cosgrove, et al., 2015, “CD39 Expression Identifies Terminally Exhausted CD8+ T Cells,” PLoS Pathog. **11**, 1–21.

Han, Jichang, Nikhil Khatwani, Tyler G. Searles, Mary Jo Turk, and Christina V. Angeles, 2020, “Memory CD8+ T Cell Responses to Cancer,” Semin. Immunol. (Elsevier Ltd) **49**, 101435, https://doi.org/10.1016/j.smim.2020.101435.

Hansen, Steffi, and Claus Michael Lehr, 2014, “Transfollicular Delivery Takes Root: The Future for Vaccine Design?,” Expert Rev. Vaccines **13**, 5–7.

Helft, Julie, Jan Böttcher, Probir Chakravarty, Santiago Zelenay, Jatta Huotari, Barbara U. Schraml, Delphine Goubau, and Caetano Reis e Sousa, 2015, “GM-CSF Mouse Bone Marrow Cultures Comprise a Heterogeneous Population of CD11c+MHCII+ Macrophages and Dendritic Cells,” Immunity **42**, 1197–1211.

Hirai, Toshiro, Sarah K. Whitley, and Daniel H. Kaplan, 2020, “Migration and Function of Memory CD8+ T Cells in Skin,” J. Invest. Dermatol. (The Authors) **140**, 748–755, https://doi.org/10.1016/j.jid.2019.09.014.

Hoffman, Rosemary A., Raja S. Mahidhara, Amanda S. Wolf-Johnston, Lina Lu, Angus W. Thomson, and Richard L. Simmons, 2002, “Differential Modulation of CD4 and CD8 T-Cell Proliferation by Induction of Nitric Oxide Synthesis in Antigen Presenting Cells,” Transplantation **74**, 836–845.

Hogquist, Kristin A., Stephen C. Jameson, William R. Heath, Jane L. Howard, Michael J. Bevan, and Francis R. Carbone, 1994, “T Cell Receptor Antagonist Peptides Induce Positive Selection,” Cell **76**, 17–27.

Honda, Tetsuya, Gyohei Egawa, and Kenji Kabashima, 2019, “Antigen Presentation and Adaptive Immune Responses in Skin,” Int. Immunol. **31**, 423–429.

Honda, Tetsuya, and Kenji Kabashima, 2016, “Novel Concept of ISALT (Inducible Skin-Associated Lymphoid Tissue) in the Elicitation of Allergic Contact Dermatitis,” Proc. Japan Acad. Ser. B Phys. Biol. Sci. **92**, 20–28.

Imanishi, Takayuki, and Takashi Saito, 2020, “T Cell Co-Stimulation and Functional Modulation by Innate Signals,” Trends Immunol. (Elsevier Ltd) **41**, 200–212, https://doi.org/10.1016/j.it.2020.01.003.

Jenkins, Edward, Toby Whitehead, Martin Fellermeyer, Simon J. Davis, and Sumana Sharma, 2023, “The Current State and Future of T-Cell Exhaustion Research,” Oxford Open Immunol. **4**.

Jensen, Simon S., and Monika Gad, 2010, “Differential Induction of Inflammatory Cytokines by Dendritic Cells Treated with Novel TLR-Agonist and Cytokine Based Cocktails: Targeting Dendritic Cells in Autoimmunity,” J. Inflamm. **7**, 1–12.

Jung, Bong Jun, Hangeun Kim, and Dae Kyun Chung, 2022, “Differential Immunostimulatory Effects of Lipoteichoic Acids Isolated from Four Strains of Lactiplantibacillus Plantarum,” Appl. Sci. **12**.

Kabashima, Kenji, Tetsuya Honda, Florent Ginhoux, and Gyohei Egawa, 2019, “The Immunological Anatomy of the Skin,” Nat. Rev. Immunol. (Springer US) **19**, 19–30, http://dx.doi.org/10.1038/s41577-018-0084-5.

Kaesler, Susanne, Yuliya Skabytska, Ko Ming Chen, Wolfgang E. Kempf, Thomas Volz, Martin Köberle, Florian Wölbing, et al., 2016, “Staphylococcus Aureus–Derived Lipoteichoic Acid Induces Temporary T-Cell Paralysis Independent of Toll-like Receptor 2,” J. Allergy Clin. Immunol. **138**, 780-790.e6.

Kak, Gunjan, Mohsin Raza, and Brijendra K. Tiwari, 2018, “Interferon-Gamma (IFN-γ): Exploring Its Implications in Infectious Diseases,” Biomol. Concepts **9**, 64–79.

Kim, T. D., Hyun Jeong Ryu, Hyun Il Cho, C. H. Yang, and J. Kim, 2000, “Thermal Behavior of Proteins: Heat-Resistant Proteins and Their Heat-Induced Secondary Structural Changes,” Biochemistry **39**, 14839–14846.

Kobayashi, Tetsuro, Martin Glatz, Keisuke Horiuchi, Hiroshi Kawasaki, Haruhiko Akiyama, Daniel H. Kaplan, Heidi H. Kong, Masayuki Amagai, and Keisuke Nagao, 2015, “Dysbiosis and Staphyloccus Aureus Colonization Drives Inflammation in Atopic Dermatitis,” Immunity (Elsevier Inc.) **42**, 756–766, http://dx.doi.org/10.1016/j.immuni.2015.03.014.

Kogame, Toshiaki, Kenji Kabashima, and Gyohei Egawa, 2021, “Putative Immunological Functions of Inducible Skin-Associated Lymphoid Tissue in the Context of Mucosa-Associated Lymphoid Tissue,” Front. Immunol. **12**, 1–10.

Koh, Choong Hyun, Suyoung Lee, Minkyeong Kwak, Byung Seok Kim, and Yeonseok Chung, 2023, “CD8 T-Cell Subsets: Heterogeneity, Functions, and Therapeutic Potential,” Exp. Mol. Med. (Springer US) **55**, 2287–2299.

Kong, Heidi H., and Julia Oh, 2022, “State of Residency: Microbial Strain Diversity in the Skin,” J. Invest. Dermatol. (The Authors) **142**, 1260–1264, https://doi.org/10.1016/j.jid.2021.10.005.

Kong, Heidi H., Julia Oh, Clay Deming, Sean Conlan, Elizabeth A. Grice, Melony A. Beatson, Effie Nomicos, et al., 2012, “Temporal Shifts in the Skin Microbiome Associated with Disease Flares and Treatment in Children with Atopic Dermatitis,” Genome Res. **22**, 850–859.

Kong, Heidi H., and Julia A. Segre, 2017, “The Molecular Revolution in Cutaneous Biology: Investigating the Skin Microbiome,” J. Invest. Dermatol. (The Authors) **137**, e119–e122, http://dx.doi.org/10.1016/j.jid.2016.07.045.

Konjar, Špela, Xenia Ficht, Matteo Iannacone, and Marc Veldhoen, 2022, “Heterogeneity of Tissue Resident Memory T Cells,” Immunol. Lett. **245**, 1–7.

Kortekaas Krohn, Inge, Joeri L. Aerts, Karine Breckpot, Cleo Goyvaerts, Edward Knol, Femke Van Wijk, and Jan Gutermuth, 2022, “T-Cell Subsets in the Skin and Their Role in Inflammatory Skin Disorders,” Allergy Eur. J. Allergy Clin. Immunol. **77**, 827–842.

Kubo, Akiharu, Keisuke Nagao, Mariko Yokouchi, Hiroyuki Sasaki, and Masayuki Amagai, 2009, “External Antigen Uptake by Langerhans Cells with Reorganization of Epidermal Tight Junction Barriers,” J. Exp. Med. **206**, 2937–2946.

Kumar, Jitendra, Ritesh Kumar, Amir Kumar Singh, Elviche L. Tsakem, Mahesh Kathania, Matthew J. Riese, Arianne L. Theiss, Marco L. Davila, and K. Venuprasad, 2021, “Deletion of Cbl-b Inhibits CD8 + T-Cell Exhaustion and Promotes CAR T-Cell Function,” J. Immunother. Cancer **9**, 1–6.

Laborel-Préneron, Emeline, Pascale Bianchi, Franck Boralevi, Philippe Lehours, Frédérique Fraysse, Fanny Morice-Picard, Motoyuki Sugai, et al., 2015, “Effects of the Staphylococcus Aureus and Staphylococcus Epidermidis Secretomes Isolated from the Skin Microbiota of Atopic Children on CD4+ T Cell Activation,” PLoS One **10**, 1–16.

Lai, Yuping, Anna Di Nardo, Teruaki Nakatsuji, Anke Leichtle, Yan Yang, Anna L. Cogen, Zi Rong Wu, et al., 2009, “Commensal Bacteria Regulate Toll-like Receptor 3-Dependent Inflammation after Skin Injury,” Nat. Med. **15**, 1377–1382.

Lajqi, Trim, David Frommhold, Christian Gille, and Hannes Hudalla, 2022, “Induction of Memory-like Adaptive Responses in Murine Neutrophils in Vitro,” Cell. Immunol. **376**.

Le, Katherine Y., Matthew D. Park, and Michael Otto, 2018, “Immune Evasion Mechanisms of Staphylococcus Epidermidis Biofilm Infection,” Front. Microbiol. **9**, 1–8.

Lebeer, Sarah, Eline F.M. Oerlemans, Ingmar Claes, Tim Henkens, Lize Delanghe, Sander Wuyts, Irina Spacova, et al., 2022, “Selective Targeting of Skin Pathobionts and Inflammation with Topically Applied Lactobacilli,” Cell

Reports Med. (The Authors) **3**, 100521, https://doi.org/10.1016/j.xcrm.2022.100521.

Lebre, Maria C., Angelic M.G. Van Der Aar, Lisa Van Baarsen, Toni M.M. Van Capel, Joost H.N. Schuitemaker, Martien L. Kapsenberg, and Esther C. De Jong, 2007, "Human Keratinocytes Express Functional Toll-like Receptor 3, 4, 5, and 9," J. Invest. Dermatol. (Elsevier Masson SAS) **127**, 331–341, http://dx.doi.org/10.1038/sj.jid.5700530.

Lee, Brandon, Reuben Olaniyi, Jakub M. Kwiecinski, and Juliane Bubeck Wardenburg, 2020, "Staphylococcus Aureus Toxin Suppresses Antigen-Specific T Cell Responses," J. Clin. Invest. **130**, 1122–1127, https://www.jci.org/articles/view/130728.

Lee, Eun Gang, and Ji Eun Oh, 2024, "From Neglect to Spotlight: The Underappreciated Role of B Cells in Cutaneous Inflammatory Diseases," Front. Immunol. **15**, 1–13.

Lee, Hyun Ji, and Miri Kim, 2022, "Skin Barrier Function and the Microbiome," Int. J. Mol. Sci. **23**.

Lee, Jean Y.H., Ian R. Monk, Anders Gonçalves da Silva, Torsten Seemann, Kyra Y.L. Chua, Angela Kearns, Robert Hill, et al., 2018, "Global Spread of Three Multidrug-Resistant Lineages of Staphylococcus Epidermidis," Nat. Microbiol. **3**, 1175–1185.

Leech, John M., Miqdad O. Dhariwala, Margaret M. Lowe, Kevin Chu, Geil R. Merana, Clémence Cornuot, Antonin Weckel, et al., 2019, "Toxin-Triggered Interleukin-1 Receptor Signaling Enables Early-Life Discrimination of Pathogenic versus Commensal Skin Bacteria," Cell Host Microbe **26**, 795-809.e5.

Lerman, Irina, Drew C. Mitchell, and Christopher T. Richardson, 2021, "Human Cutaneous B Cells: What Do We Really Know?," Ann. Transl. Med. **9**, 440–440.

Li, Danyang, and Minghua Wu, 2021, "Pattern Recognition Receptors in Health and Diseases," Signal Transduct. Target. Ther. (Springer US) **6**, 1–24, http://dx.doi.org/10.1038/s41392-021-00687-0.

Linehan, Jonathan L., Oliver J. Harrison, Seong Ji Han, Allyson L. Byrd, Ivan Vujkovic-Cvijin, Alejandro V. Villarino, Shurjo K. Sen, et al., 2018, "Non-Classical Immunity Controls Microbiota Impact on Skin Immunity and Tissue Repair," Cell (Elsevier Inc.) **172**, 784-796.e18, https://doi.org/10.1016/j.cell.2017.12.033.

Lu, L, C A Bonham, F G Chambers, S C Watkins, R A Hoffman, R L Simmons, and A W Thomson, 1996, "Induction of Nitric Oxide Synthase in Mouse Dendritic Cells by IFN-Gamma, Endotoxin, and Interaction with Allogeneic T Cells: Nitric Oxide Production Is Associated with Dendritic Cell Apoptosis.," J. Immunol., 3577–3586.

Lundberg, Jon O., and Eddie Weitzberg, 2022, "Nitric Oxide Signaling in Health and Disease," Cell (The Author(s)) **185**, 2853–2878, https://doi.org/10.1016/j.cell.2022.06.010.

Lunjani, Nonhlanhla, Sinead Ahearn-Ford, Felix S. Dube, Carol Hlela, and Liam O'Mahony, 2021, "Mechanisms of Microbe-Immune System Dialogue within the Skin," Genes Immun. (Springer US) **22**, 276–288, http://dx.doi.org/10.1038/s41435-021-00133-9.

Lutz, Manfred B., Nicole Kukutsch, Alexandra L.J. Ogilvie, Susanne Rößner, Franz Koch, Nikolaus Romani, and Gerold Schuler, 1999, "An Advanced Culture Method for Generating Large Quantities of Highly Pure Dendritic Cells from Mouse Bone Marrow," J. Immunol. Methods **223**, 77–92.

Mackay, Laura K., Angus T. Stock, Joel Z. Ma, Claerwen M. Jones, Stephen J. Kent, Scott N. Mueller, William R. Heath, Francis R. Carbone, and Thomas Gebhardt, 2012, "Long-Lived Epithelial Immunity by Tissue-Resident Memory T (TRM) Cells in the Absence of Persisting Local Antigen Presentation," Proc. Natl. Acad. Sci. U. S. A. **109**, 7037–7042.

Maseda, Damian, Silvio Manfredo-Vieira, and Aimee S Payne, 2023, "T Cell and Bacterial Microbiota Interaction at Intestinal and Skin Epithelial Interfaces," Discov. Immunol. **2**, 1–12.

Matejuk, Agata, 2018, "Skin Immunity," Arch. Immunol. Ther. Exp. (Warsz). (Springer International Publishing) **66**, 45–54.

Matsui, Takeshi, and Masayuki Amagai, 2015, "Dissecting the Formation, Structure and Barrier Function of the Stratum Corneum," Int. Immunol. **27**, 269–280.

McKinnon, Katherine M., 2018, "Flow Cytometry: An Overview," Curr. Protoc. Immunol. **120**, 5.1.1-5.1.11, https://currentprotocols.onlinelibrary.wiley.com/doi/10.1002/cpim.40.

Mehta, Amit K., Donald T. Gracias, and Michael Croft, 2018, "TNF Activity and T Cells," Cytokine (Elsevier Ltd) **101**, 14–18, https://doi.org/10.1016/j.cyto.2016.08.003.

Merad, Miriam, Priyanka Sathe, Julie Helft, Jennifer Miller, and Arthur Mortha, 2013, "The Dendritic Cell Lineage: Ontogeny and Function of Dendritic Cells and Their Subsets in the Steady State and the Inflamed Setting," Annu. Rev. Immunol. **31**, 563–604.

Méric, Guillaume, Leonardos Mageiros, Johan Pensar, Maisem Laabei, Koji Yahara, Ben Pascoe, Nattinee Kittiwan, et al., 2018, "Disease-Associated Genotypes of the Commensal Skin Bacterium Staphylococcus Epidermidis,"

Nat. Commun. **9**, 1–11.

Méric, Guillaume, Maria Miragaia, Mark De Been, Koji Yahara, Ben Pascoe, Leonardos Mageiros, Jane Mikhail, et al., 2015, "Ecological Overlap and Horizontal Gene Transfer in Staphylococcus Aureus and Staphylococcus Epidermidis," Genome Biol. Evol. **7**, 1313–1328.

Mogensen, Trine H., 2009, "Pathogen Recognition and Inflammatory Signaling in Innate Immune Defenses," Clin. Microbiol. Rev. **22**, 240–273.

Mohamed, Sarah A., and Rachel Hargest, 2022, "Surgical Anatomy of the Skin," Surg. (United Kingdom) (Elsevier Ltd) **40**, 1–7, https://doi.org/10.1016/j.mpsur.2021.11.021.

Moran, Josephine C., Jamal A. Alorabi, and Malcolm J. Horsburgh, 2017, "Comparative Transcriptomics Reveals Discrete Survival Responses of S. Aureus and S. Epidermidis to Sapienic Acid," Front. Microbiol. **8**, 1–12.

Moura, Ana Karina Alves, Fernanda Guedes, Maria Cecília Rivitti-Machado, and Mirian N. Sotto, 2018, "Inate Immunity in Rosacea. Langerhans Cells, Plasmacytoid Dentritic Cells, Toll-like Receptors and Inducible Oxide Nitric Synthase (INOS) Expression in Skin Specimens: Case-Control Study," Arch. Dermatol. Res. (Springer Berlin Heidelberg) **310**, 139–146, http://dx.doi.org/10.1007/s00403-018-1806-z.

Mueller, Scott N., Thomas Gebhardt, Francis R. Carbone, and William R. Heath, 2013, "Memory T Cell Subsets, Migration Patterns, and Tissue Residence," Annu. Rev. Immunol. **31**, 137–161.

Murphy, Kenneth, and Casey Weaver, 2018, *Janeway Immunologie* (Springer Berlin Heidelberg, Berlin, Heidelberg), http://link.springer.com/10.1007/978-3-662-56004-4.

Naik, Shruti, Nicolas Bouladoux, Jonathan L. Linehan, Seong-Ji Han, Oliver J. Harrison, Christoph Wilhelm, Sean Conlan, et al., 2015a, "Commensal–Dendritic-Cell Interaction Specifies a Unique Protective Skin Immune Signature," Nature **520**, 104–108, https://www.nature.com/articles/nature14052.

Naik, Shruti, Nicolas Bouladoux, Jonathan L. Linehan, Seong Ji Han, Oliver J. Harrison, Christoph Wilhelm, Sean Conlan, et al., 2015b, "Commensal-Dendritic-Cell Interaction Specifies a Unique Protective Skin Immune Signature," Nature **520**, 104–108.

Naik, Shruti, Nicolas Bouladoux, Christoph Wilhelm, Michael J Molloy, Rosalba Salcedo, Sean Spencer, Jason A Hall, Amiran Dzutsev, Heidi Kong, and Daniel J Campbell, 2012, "Compartmentalized Control of Skin Immunity by Resident Commensals," Science **337**, 1115–1120.

Nakagawa, Yujin, Gyohei Egawa, Toshiya Miyake, Saeko Nakajima, Atsushi Otsuka, Takashi Nomura, Akihiko Kitoh, et al., 2022, "A Phenotypic Analysis of Involucrin–Membrane-Bound Ovalbumin Mice after Adoptive Transfer of Ovalbumin-Specific CD8+ T Cells," JID Innov. (The Authors) **2**, 100127, https://doi.org/10.1016/j.xjidi.2022.100127.

Nakamura, Kouki, Michael R. Williams, Jakub M. Kwiecinski, Alexander R. Horswill, and Richard L. Gallo, 2021, "Staphylococcus Aureus Enters Hair Follicles Using Triacylglycerol Lipases Preserved through the Genus Staphylococcus," J. Invest. Dermatol. **141**, 2094–2097.

Nakatsuji, Teruaki, Tiffany H. Chen, Saisindhu Narala, Kimberly A. Chun, Aimee M. Two, Tong Yun, Faiza Shafiq, et al., 2017, "Antimicrobials from Human Skin Commensal Bacteria Protect against Staphylococcus Aureus and Are Deficient in Atopic Dermatitis," Sci. Transl. Med. **9**, S205–S206, https://www.science.org/doi/10.1126/scitranslmed.aah4680.

Nakatsuji, Teruaki, Joyce Y. Cheng, and Richard L. Gallo, 2021, "Mechanisms for Control of Skin Immune Function by the Microbiome," Curr. Opin. Immunol. (Elsevier Ltd) **72**, 324–330, https://doi.org/10.1016/j.coi.2021.09.001.

Nakatsuji, Teruaki, Hsin I. Chiang, Shangi B. Jiang, Harish Nagarajan, Karsten Zengler, and Richard L. Gallo, 2013, "The Microbiome Extends to Subepidermal Compartments of Normal Skin," Nat. Commun. (Nature Publishing Group) **4**, 1–8.

Napoli, Claudio, Giuseppe Paolisso, Amelia Casamassimi, Mohammed Al-Omran, Michelangela Barbieri, Linda Sommese, Teresa Infante, and Louis J. Ignarro, 2013, "Effects of Nitric Oxide on Cell Proliferation: Novel Insights," J. Am. Coll. Cardiol. **62**, 89–95.

Negishi, Hideo, Tadatsugu Taniguchi, and Hideyuki Yanai, 2018, "The Interferon (IFN) Class of Cytokines and the IFN Regulatory Factor (IRF) Transcription Factor Family," Cold Spring Harb. Perspect. Biol. **10**.

Nestle, Frank O., Paola Di Meglio, Jian Zhong Qin, and Brian J. Nickoloff, 2009, "Skin Immune Sentinels in Health and Disease," Nat. Rev. Immunol. (Nature Publishing Group) **9**, 679–691.

Nguyen, Thuan H., Matthew D. Park, and Michael Otto, 2017, "Host Response to Staphylococcus Epidermidis Colonization and Infections," Front. Cell. Infect. Microbiol. **7**, 1–7.

Nguyen, Alan V., and Athena M. Soulika, 2019, "The Dynamics of the Skin's Immune System," Int. J. Mol. Sci. **20**, 1–53.

Nouri, Yasmin, Robert Weinkove, and Rachel Perret, 2021, “T-Cell Intrinsic Toll-like Receptor Signaling: Implications for Cancer Immunotherapy and CAR T-Cells,” J. Immunother. Cancer **9**.

Oh, Julia, Allyson L. Byrd, Morgan Park, Heidi H. Kong, and Julia A. Segre, 2016, “Temporal Stability of the Human Skin Microbiome,” Cell **165**, 854–866.

Oliveira-Nascimento, Laura, Paola Massari, and Lee M. Wetzler, 2012, “The Role of TLR2 Ininfection and Immunity,” Front. Immunol. **3**, 1–17.

Ono, Sachiko, and Kenji Kabashima, 2015, “Novel Insights into the Role of Immune Cells in Skin and Inducible Skin-Associated Lymphoid Tissue (ISALT),” Allergo J. Int. **24**, 170–179.

Otto, Michael, 2008, “Staphylococcal Biofilms,” in *Gram-Positive Pathogens* (ASM Press, Washington, DC, USA), pp. 207–228, http://doi.wiley.com/10.1128/9781683670131.ch43.

Otto, Michael, 2009, “Staphylococcus Epidermidis - The ‘accidental’ Pathogen,” Nat. Rev. Microbiol. **7**, 555–567.

Ozato, Keiko, Prafullakumar Tailor, and Toru Kubota, 2007, “The Interferon Regulatory Factor Family in Host Defense: Mechanism of Action,” J. Biol. Chem. (Â© 2007 ASBMB. Currently published by Elsevier Inc; originally published by American Society for Biochemistry and Molecular Biology.) **282**, 20065–20069, http://dx.doi.org/10.1074/jbc.R700003200.

Paludan, Søren R., Thomas Pradeu, Seth L. Masters, and Trine H. Mogensen, 2021, “Constitutive Immune Mechanisms: Mediators of Host Defence and Immune Regulation,” Nat. Rev. Immunol. (Springer US) **21**, 137–150, http://dx.doi.org/10.1038/s41577-020-0391-5.

Park, Jin, Nicole H. Schwardt, Jay Hyun Jo, Zhiwei Zhang, Valentina Pillai, Sheila Phang, Sheila M. Brady, et al., 2022, “Shifts in the Skin Bacterial and Fungal Communities of Healthy Children Transitioning through Puberty,” J. Invest. Dermatol. (The Authors) **142**, 212–219, https://doi.org/10.1016/j.jid.2021.04.034.

Park, Young Joon, Chae Won Kim, and Heung Kyu Lee, 2019, “Interactions between Host Immunity and Skin-Colonizing Staphylococci: No Two Siblings Are Alike,” Int. J. Mol. Sci. **20**.

Park, Young Joon, and Heung Kyu Lee, 2018, “The Role of Skin and Orogenital Microbiota in Protective Immunity and Chronic Immune-Mediated Inflammatory Disease,” Front. Immunol. **8**, 1–13.

Pasparakis, Manolis, Ingo Haase, and Frank O. Nestle, 2014, “Mechanisms Regulating Skin Immunity and Inflammation,” Nat. Rev. Immunol. (Nature Publishing Group) **14**, 289–301.

Prescott, Susan L., Danica Lea Larcombe, Alan C. Logan, Christina West, Wesley Burks, Luis Caraballo, Michael Levin, et al., 2017, “The Skin Microbiome: Impact of Modern Environments on Skin Ecology, Barrier Integrity, and Systemic Immune Programming,” World Allergy Organ. J. (World Allergy Organization Journal) **10**, 1–16.

Pritchard, Gretchen Harms, Eric W. Cross, Marjorie Strobel, Stephen C. Jameson, Ross M. Kedl, Kristin A. Hogquist, and Christopher A. Hunter, 2016, “Spontaneous Partial Loss of the OT-I Transgene,” Nat. Immunol. **17**, 471.

Quaresma, Juarez Antonio Simões, 2019, “Organization of the Skin Immune System and Compartmentalized Immune Responses in Infectious Diseases,” Clin. Microbiol. Rev. **32**, 1–35.

Rahman, Adeeb H., Devon K. Taylor, and Laurence A. Turka, 2009, “The Contribution of Direct TLR Signaling to T Cell Responses,” Immunol. Res. **45**, 25–36.

Rath, Meera, Ingrid Müller, Pascale Kropf, Ellen I. Closs, and Markus Munder, 2014, “Metabolism via Arginase or Nitric Oxide Synthase: Two Competing Arginine Pathways in Macrophages,” Front. Immunol. **5**.

Refaeli, Yosef, Luk Van Parijs, Stephen I. Alexander, and Abul K. Abbas, 2002, “Interferon γ Is Required for Activation-Induced Death of T Lymphocytes,” J. Exp. Med. **196**, 999–1005.

Riera Romo, Mario, Dayana Pérez-Martínez, and Camila Castillo Ferrer, 2016, “Innate Immunity in Vertebrates: An Overview,” Immunology **148**, 125–139.

Roediger, Ben, and Christoph Schlapbach, 2022, “T Cells in the Skin: Lymphoma and Inflammatory Skin Disease,” J. Allergy Clin. Immunol. (The Authors) **149**, 1172–1184, https://doi.org/10.1016/j.jaci.2022.02.015.

Rojas, Carolina, Felipe Gálvez-Jirón, Javiera De Solminihac, Cristina Padilla, Ignacio Cárcamo, Natalia Villalón, Mónica Kurte, and Karina Pino-Lagos, 2022, “Crosstalk between Body Microbiota and the Regulation of Immunity,” J. Immunol. Res. **2022**.

Ruddle, Nancy H, 2020, *Inducible Lymphoid Organs*, Edited by Kenji Kabashima and Gyohei Egawa, *Current Topics in Microbiology and Immunology*, Current Topics in Microbiology and Immunology (Springer International Publishing, Cham), Vol. 426, http://link.springer.com/10.1007/978-3-030-51747-2.

Rutter, Nicholas, 2000, “The Dermis,” Semin. Neonatol. **5**, 297–302.

Saito, Lin, and Wu, 2019, “The Unique Immunoregulatory Function of Staphylococcus Aureus Lipoteichoic Acid in

Dendritic Cells," J **2**, 326–339.

Saito, Suguru, Alato Okuno, Duo Yao Cao, Zhenzi Peng, Hui Ya Wu, and Shu Hui Lin, 2020, "Bacterial Lipoteichoic Acid Attenuates Toll-like Receptor Dependent Dendritic Cells Activation and Inflammatory Response," Pathogens **9**, 1–14.

Saito, Suguru, and Ali F. Quadery, 2018, "Staphylococcus Aureus Lipoprotein Induces Skin Inflammation, Accompanied with IFN-γ-Producing T Cell Accumulation through Dermal Dendritic Cells," Pathogens **7**, 1–17.

Salerno, Fiamma, Aurelie Guislain, Dilay Cansever, and Monika C. Wolkers, 2016, "TLR-Mediated Innate Production of IFN-γ by CD8+ T Cells Is Independent of Glycolysis," J. Immunol. **196**, 3695–3705.

Sameer, Aga Syed, and Saniya Nissar, 2021, "Toll-Like Receptors (TLRs): Structure, Functions, Signaling, and Role of Their Polymorphisms in Colorectal Cancer Susceptibility," Biomed Res. Int. **2021**.

Sanford, James A., and Richard L. Gallo, 2013, "Functions of the Skin Microbiota in Health and Disease," Semin. Immunol. (Elsevier Ltd) **25**, 370–377, http://dx.doi.org/10.1016/j.smim.2013.09.005.

Sato, Kazuya, Katsutoshi Ozaki, Iekuni Oh, Akiko Meguro, Keiko Hatanaka, Tadashi Nagai, Kazuo Muroi, and Keiya Ozawa, 2007, "Nitric Oxide Plays a Critical Role in Suppression of T-Cell Proliferation by Mesenchymal Stem Cells," Blood **109**, 228–234.

Scharschmidt, Tiffany C., 2017, "Establishing Tolerance to Commensal Skin Bacteria: Timing Is Everything," Dermatol. Clin. **35**, 1–9.

Scharschmidt, Tiffany C., Kimberly S. Vasquez, Mariela L. Pauli, Elizabeth G. Leitner, Kevin Chu, Hong An Truong, Margaret M. Lowe, et al., 2017, "Commensal Microbes and Hair Follicle Morphogenesis Coordinately Drive Treg Migration into Neonatal Skin," Cell Host Microbe (Elsevier Inc.) **21**, 467-477.e5, http://dx.doi.org/10.1016/j.chom.2017.03.001.

Scharschmidt, Tiffany C., Kimberly S. Vasquez, Hong An Truong, Sofia V. Gearty, Mariela L. Pauli, Audrey Nosbaum, Iris K. Gratz, et al., 2015, "A Wave of Regulatory T Cells into Neonatal Skin Mediates Tolerance to Commensal Microbes," Immunity (Elsevier Inc.) **43**, 1011–1021, http://dx.doi.org/10.1016/j.immuni.2015.10.016.

Scheib, Nils, Jessica Tiemann, Christian Becker, Hans Christian Probst, Verena Katharina Raker, and Kerstin Steinbrink, 2022, "The Dendritic Cell Dilemma in the Skin: Between Tolerance and Immunity," Front. Immunol. **13**, 1–15.

Schilcher, Katrin, and Alexander R. Horswill, 2020, "Staphylococcal Biofilm Development: Structure, Regulation, and Treatment Strategies," Microbiol. Mol. Biol. Rev. **84**, https://journals.asm.org/doi/10.1128/MMBR.00026-19.

Schleifer, K. H., and W. E. Kloos, 1975, "Isolation and Characterization of Staphylococci from Human Skin. I. Amended Descriptions of Staphylococcus Epidermidis and Staphylococcus Saprophyticus and Descriptions of Three New Species: Staphylococcus Cohnii, Staphylococcus Haemolyticus, and Staphylo," Int. J. Syst. Bacteriol. **25**, 50–61.

Schlitzer, Andreas, Naomi McGovern, and Florent Ginhoux, 2015, "Dendritic Cells and Monocyte-Derived Cells: Two Complementary and Integrated Functional Systems," Semin. Cell Dev. Biol. (Elsevier Ltd) **41**, 9–22, http://dx.doi.org/10.1016/j.semcdb.2015.03.011.

Schoenborn, Jamie R., and Christopher B. Wilson, 2007, "Regulation of Interferon-γ During Innate and Adaptive Immune Responses," Adv. Immunol. **96**, 41–101.

Schorr, Lena, Marius Mathies, Eran Elinav, and Jens Puschhof, 2023, "Intracellular Bacteria in Cancer—Prospects and Debates," npj Biofilms Microbiomes (Springer US) **9**.

Serbina, Natalya V., Thais P. Salazar-Mather, Christine A. Biron, William A. Kuziel, and Eric G. Pamer, 2003, "TNF/INOS-Producing Dendritic Cells Mediate Innate Immune Defense against Bacterial Infection," Immunity **19**, 59–70.

Severn, Morgan M., and Alexander R. Horswill, 2022, "Staphylococcus Epidermidis and Its Dual Lifestyle in Skin Health and Infection," Nat. Rev. Microbiol. (Springer US) **21**.

Sfriso, R., M. Egert, M. Gempeler, R. Voegeli, and R. Campiche, 2020, "Revealing the Secret Life of Skin - with the Microbiome You Never Walk Alone," Int. J. Cosmet. Sci. **42**, 116–126.

Shah, Kinjal, Amr Al-Haidari, Jianmin Sun, and Julhash U. Kazi, 2021, "T Cell Receptor (TCR) Signaling in Health and Disease," Signal Transduct. Target. Ther. (Springer US) **6**.

Shaw, Christine A., and Michael N. Starnbach, 2006, "Stimulation of CD8+ T Cells Following Diphtheria Toxin-Mediated Antigen Delivery into Dendritic Cells," Infect. Immun. **74**, 1001–1008.

Smythe, Paisleigh, and Holly N. Wilkinson, 2023, "The Skin Microbiome: Current Landscape and Future Opportunities," Int. J. Mol. Sci. **24**.

Son, Young Min, 2013, "Lipoteichoic Acid Suppresses Effector T Cells Induced by Staphylococcus Aureus-Pulsed

Dendritic Cells," J. Microbiol. Biotechnol. **23**, 1023–1030, http://www.jmb.or.kr/journal/viewJournal.html?year=2013&vol=23&num=7&page=1023.

Spiliopoulou, Anastasia I., Fevronia Kolonitsiou, Maria I. Krevvata, Michalis Leontsinidis, Thomas S. Wilkinson, Dietrich Mack, and Evangelos D. Anastassiou, 2012, "Bacterial Adhesion, Intracellular Survival and Cytokine Induction upon Stimulation of Mononuclear Cells with Planktonic or Biofilm Phase Staphylococcus Epidermidis," FEMS Microbiol. Lett. **330**, 56–65.

Steinbrink, K., and V. Raker, 2016, "SALT (»skin-Associated Lymphoid Tissue«)," in *Allergologie* (Springer Berlin Heidelberg, Berlin, Heidelberg), Vol. 80, pp. 127–135, http://link.springer.com/10.1007/978-3-642-37203-2_12.

Stinson, Lisa F., Mary C. Boyce, Matthew S. Payne, and Jeffrey A. Keelan, 2019, "The Not-so-Sterile Womb: Evidence That the Human Fetus Is Exposed to Bacteria Prior to Birth," Front. Microbiol. **10**, 1–15.

Su, Fei, Rui Tian, Yi Yang, Hexin Li, Gaoyuan Sun, Ying Li, Bingqing Han, et al., 2020, "Comparative Genome Analysis Reveals the Molecular Basis of Niche Adaptation of Staphylococcus Epidermidis Strains," Front. Genet. **11**, 1–11.

Suffia, Isabelle J., Stacie K. Reckling, Ciriaco A. Piccirillo, Romina S. Goldszmid, and Yasmine Belkaid, 2006, "Infected Site-Restricted Foxp3+ Natural Regulatory T Cells Are Specific for Microbial Antigens," J. Exp. Med. **203**, 777–788.

Sugita, Kazunari, Kenji Kabashima, Ryutaro Yoshiki, Atsuko Ikenouchi-Sugita, Masato Tsutsui, Jun Nakamura, Nobuyuki Yanagihara, and Yoshiki Tokura, 2010, "Inducible Nitric Oxide Synthase Downmodulates Contact Hypersensitivity by Suppressing Dendritic Cell Migration and Survival," J. Invest. Dermatol. (Elsevier Masson SAS) **130**, 464–471.

Tamura, Tomohiko, Hideyuki Yanai, David Savitsky, and Tadatsugu Taniguchi, 2008, "The IRF Family Transcription Factors in Immunity and Oncogenesis," Annu. Rev. Immunol. **26**, 535–584.

Thwe, Phyu M., and Eyal Amiel, 2018, "The Role of Nitric Oxide in Metabolic Regulation of Dendritic Cell Immune Function," Cancer Lett. (Elsevier B.V.) **412**, 236–242, https://doi.org/10.1016/j.canlet.2017.10.032.

Tokura, Yoshiki, Pawit Phadungsaksawasdi, Kazuo Kurihara, Toshiharu Fujiyama, and Tetsuya Honda, 2021, "Pathophysiology of Skin Resident Memory T Cells," Front. Immunol. **11**, 1–19.

Tordesillas, Leticia, Daniel Lozano-Ojalvo, David Dunkin, Lucie Mondoulet, Judith Agudo, Miriam Merad, Hugh A. Sampson, and M. Cecilia Berin, 2018, "PDL2+ CD11b+ Dermal Dendritic Cells Capture Topical Antigen through Hair Follicles to Prime LAP+ Tregs," Nat. Commun. (Springer US) **9**, http://dx.doi.org/10.1038/s41467-018-07716-7.

Uebele, Julia, Katharina Habenicht, Olga Ticha, and Isabelle Bekeredjian-Ding, 2020, "Staphylococcus Aureus Protein A Induces Human Regulatory T Cells Through Interaction With Antigen-Presenting Cells," Front. Immunol. **11**, 1–12.

Urbano, Rodolfo, Joyce E. Karlinsey, Stephen J. Libby, Paschalis Thomas Doulias, Harry Ischiropoulos, Helen I. Warheit-Niemi, Denny H. Liggitt, Alexander R. Horswill, and Ferric C. Fang, 2018, "Host Nitric Oxide Disrupts Microbial Cell-to-Cell Communication to Inhibit Staphylococcal Virulence," Cell Host Microbe (Elsevier Inc.) **23**, 594-606.e7, https://doi.org/10.1016/j.chom.2018.04.001.

Villalobo, Antonio, 2006, "Nitric Oxide and Cell Proliferation," FEBS J. **273**, 2329–2344.

Volz, Thomas, Susanne Kaesler, Christian Draing, Thomas Hartung, Martin Röcken, Yuliya Skabytska, and Tilo Biedermann, 2018, "Induction of IL-10-Balanced Immune Profiles Following Exposure to LTA from Staphylococcus Epidermidis," Exp. Dermatol. **27**, 318–326.

Volz, Thomas, Yuliya Skabytska, Emmanuella Guenova, Ko Ming Chen, Julia Stefanie Frick, Carsten J. Kirschning, Susanne Kaesler, Martin Röcken, and Tilo Biedermann, 2014, "Nonpathogenic Bacteria Alleviating Atopic Dermatitis Inflammation Induce IL-10-Producing Dendritic Cells and Regulatory Tr1 Cells," J. Invest. Dermatol. **134**, 96–104.

Vuong, Cuong, Jovanka M. Voyich, Elizabeth R. Fischer, Kevin R. Braughton, Adeline R. Whitney, Frank R. DeLeo, and Michael Otto, 2004, "Polysaccharide Intercellular Adhesin (PIA) Protects Staphylococcus Epidermidis against Major Components of the Human Innate Immune System," Cell. Microbiol. **6**, 269–275.

Wakim, Linda M, Jason Waithman, Nico van Rooijen, William R. Heath, and Francis R. Carbone, 2008, "Dendritic Cell-Induced Memory T Cell Activation in Nonlymphoid Tissues," Science (80-.). **319**, 198–202, https://www.science.org/doi/10.1126/science.1151869.

Wang, Jinhai, Gregory Roderiquez, and Michael A. Norcross, 2012, "Control of Adaptive Immune Responses by Staphylococcus Aureus through IL-10, PD-L1, and TLR2," Sci. Rep. **2**, 1–11.

Wayne Streilein, J., 1983, "Skin-Associated Lymphoid Tissues (SALT): Origins and Functions," J. Invest. Dermatol. (Elsevier Masson SAS) **80**, S12–S16, https://doi.org/10.1038/jid.1983.4.

Widerström, Micael, 2016, “Significance of Staphylococcus Epidermidis in Health Care-Associated Infections, from Contaminant to Clinically Relevant Pathogen: This Is a Wake-up Call!,” J. Clin. Microbiol. **54**, 1679–1681.

Williams, Michael R., Stephen K. Costa, Livia S. Zaramela, Shadi Khalil, Daniel A. Todd, Heather L. Winter, James A. Sanford, et al., 2019, “Quorum Sensing between Bacterial Species on the Skin Protects against Epidermal Injury in Atopic Dermatitis,” Sci. Transl. Med. **11**.

Wolf, Andrea J., and David M. Underhill, 2018, “Peptidoglycan Recognition by the Innate Immune System,” Nat. Rev. Immunol. (Nature Publishing Group) **18**, 243–254, http://dx.doi.org/10.1038/nri.2017.136.

Wood, Kathryn J., and Birgit Sawitzki, 2006, “Interferon γ: A Crucial Role in the Function of Induced Regulatory T Cells in Vivo,” Trends Immunol. **27**, 183–187.

Wu, Xuejie, Pin Wu, Yifei Shen, Xiaodong Jiang, and Feng Xu, 2018, “CD8+Resident Memory T Cells and Viral Infection,” Front. Immunol. **9**.

Xie, Anni, Ailing Chen, Yuqing Chen, Zichen Luo, Shanyu Jiang, Daozhen Chen, and Renqiang Yu, 2023, “Lactobacillus for the Treatment and Prevention of Atopic Dermatitis: Clinical and Experimental Evidence,” Front. Cell. Infect. Microbiol. **13**, 1–20.

Xing, Feiyue, Jiongkun Wang, Mingqian Hu, Yu Yu, Guoliang Chen, and Jing Liu, 2011, “Comparison of Immature and Mature Bone Marrow-Derived Dendritic Cells by Atomic Force Microscopy,” Nanoscale Res. Lett. **6**, 1–9.

Xu, Yuekang, Yifan Zhan, Andrew M Lew, Shalin H Naik, and Michael H Kershaw, 2007, “Differential Development of Murine Dendritic Cells by GM-CSF versus Flt3 Ligand Has Implications for Inflammation and Trafficking,” J. Immunol. **179**, 7577–7584, https://journals.aai.org/jimmunol/article/179/11/7577/81203/Differential-Development-of-Murine-Dendritic-Cells.

Xue, Qingjie, Yingchun Yan, Ruihua Zhang, and Huabao Xiong, 2018, “Regulation of INOS on Immune Cells and Its Role in Diseases,” Int. J. Mol. Sci. **19**.

Zanichelli, Veronica, Michael Sharland, Bernadette Cappello, Lorenzo Moja, Haileyesus Getahun, Carmem Pessoa-Silva, Hatim Sati, et al., 2023, “The WHO AWaRe (Access, Watch, Reserve) Antibiotic Book and Prevention of Antimicrobial Resistance,” Bull. World Health Organ. **101**, 290–296, https://www.ncbi.nlm.nih.gov/pmc/articles/PMC10042089/pdf/BLT.22.288614.pdf.

Zhang, Chenlu, Geil R. Merana, Tamia Harris-Tryon, and Tiffany C. Scharschmidt, 2022, “Skin Immunity: Dissecting the Complex Biology of Our Body’s Outer Barrier,” Mucosal Immunol. (Â© Society for Mucosal Immunology) **15**, 551–561.

Zhang, Jun-Ming, and Jianxiong An, 2007, “Cytokines, Inflammation, and Pain,” Int. Anesthesiol. Clin. **45**, 27–37, https://journals.lww.com/00004311-200704520-00004.

Zhang, Yumeng, Lucia Seminario-Vidal, Leah Cohen, Mohammad Hussaini, Jiqiang Yao, David Rutenberg, Youngchul Kim, Anna Giualiano, Lary A. Robinson, and Lubomir Sokol, 2022, “‘Alterations in the Skin Microbiota Are Associated With Symptom Severity in Mycosis Fungoides,’” Front. Cell. Infect. Microbiol. **12**, 1–10.

Zhang, Zhen, Shasha Liu, Bin Zhang, Liang Qiao, Yi Zhang, and Yi Zhang, 2020, “T Cell Dysfunction and Exhaustion in Cancer,” Front. Cell Dev. Biol. **8**.

Zheng, Danping, Timur Liwinski, and Eran Elinav, 2020, “Interaction between Microbiota and Immunity in Health and Disease,” Cell Res. (Springer US) **30**, 492–506, http://dx.doi.org/10.1038/s41422-020-0332-7.

Zhou, Wei, Michelle Spoto, Rachel Hardy, Changhui Guan, Elizabeth Fleming, Peter J. Larson, Joseph S. Brown, and Julia Oh, 2020, “Host-Specific Evolutionary and Transmission Dynamics Shape the Functional Diversification of Staphylococcus Epidermidis in Human Skin,” Cell (Elsevier Inc.) **180**, 454-470.e18, https://doi.org/10.1016/j.cell.2020.01.006.

Zipperer, Alexander, Martin C. Konnerth, Claudia Laux, Anne Berscheid, Daniela Janek, Christopher Weidenmaier, Marc Burian, et al., 2016, “Human Commensals Producing a Novel Antibiotic Impair Pathogen Colonization,” Nature (Nature Publishing Group) **535**, 511–516.